Exercise training on the regulation of inhibitory extracellular modulators of plasticity in the central nervous system.

Natalie Ellen Doody

PhD Thesis

Submitted in accordance with the requirements for the degree of
Doctor of Philosophy

The University of Leeds
School of Biomedical Sciences

January 2022

Intellectual property rights

The candidate confirms that the work submitted is her own and that appropriate credit has been given where reference has been made to the work of others.

Declaration

The candidate confirms that the work submitted is her own. The candidate confirms that appropriate credit has been given within the thesis where reference has been made to the work of others.

Throughout this thesis all animal training, behavioural assessments, experiments, and analyses were conducted by Natalie Doody unless stated below.

Chapter 3: Fresh dissection of central nervous system tissue and skeletal muscle dissection were performed by Natalie Doody with the assistance of Nicole Smith. Gene expression experiments were conducted by Natalie Doody under the supervision of Dr Elizabeth Akam at Loughborough University.

Chapter 4: Transcardial perfusions were performed by Natalie Doody with the assistance of Nicole Smith. Tile scan images were obtained by Dr Sally Boxall and Dr Ruth Hughes as a service by Faculty of Biomedical Sciences (FBS) Bioimaging facility. Immunohistochemistry experiments for PNNs in the motor cortex were performed and analysed by Tim McDonald as work completed for his Master of Research degree.

Chapter 5: Stereotaxic surgeries were performed by Natalie Doody with the assistance of Nicole Smith. Fresh dissection of central nervous system tissue was performed by Natalie Doody and transcardial perfusions were performed by Dr Varinder Lall.

All experiments have been designed and conducted by Natalie Ellen Doody, with supervision by Professor Ronaldo Ichiyama, Dr Jessica Kwok, and Dr Graham Askew.

Acknowledgements

In Leeds…

To Professor Ronaldo Ichiyama, thank you for welcoming me into your lab and for the opportunity to be part of a great community of scientists. Thank you for your trust and confidence in my scientific abilities, and allowing me to grow as an independent researcher. Thank you for your enthusiasm for my project, for the great emotional support when life gets tough, and for always providing the best snacks at lab meetings and social gatherings.

Dr Jessica Kwok, thank you for always helping me to move forward and to improve as a scientist. Thank you for the meaningful chats, whether scientific, therapeutic, or joyfully shared over a glass of wine. I really appreciate you trying to keep my busy brain happy with creative side projects and public engagement.

Dr Graham Askew, thank you for sharing your expertise, for always supporting my DIY lab projects, and for letting me loose in the lab with a tool box.

As a supervisory team, thank you for your support throughout this PhD. I have learnt so much and I am proud of the science I have produced with your guidance.

Thank you to the other half of the dream team, Nicole Smith. Together we have experienced the extreme highs and lows of two PhDs. You are the most memorable lab partner, and I am so proud of what we have each achieved throughout these last four years. Thank you for making surgeries, D-Days, and the full PhD rollercoaster a whole lot easier. Here we are at the other side of it all, and I cannot wait to graduate with you.

To Dr Varinder Lall and Dr Sîan Irvine, firstly, thank you for everything that you have taught me. You are admirable women in science, and I am appreciative of everything that I have learnt from you in my time at Leeds. Secondly, thank you for your friendship and for being such lovely humans. Thank you for sharing my values, humour, and colour in wardrobe.

Thank you to Professor Stuart Egginton and Dr Roger Kissane for always providing captivating scientific conversation and for sharing such breadth of knowledge and lab skills. Thank you for supporting me throughout my PhD and academic development.

Thank you to Dr Sally Boxall and Dr Ruth Hughes for helping get the most beautiful scientific images, and for helping my project to continue through the difficulties of the pandemic. From CBS, thank you to Neil, Stan, Scott, Andy, and Khawar for all of the friendly chats, advice, and for helping make this project a success.

Nicole, V, and Ben, the three of you deserve a special mention. Thank you for helping me throughout the final study that seemed to have never-ending obstacles to face. Thank you for being the spare pairs of hands when I really needed them and for keeping my spirits up until the finish line.

Speaking of keeping spirits up, thank you to my dearest Maddie/Maddog/Mandy English. Thank you for the instalments of Monday Night Madness, Treat Yourself Thursdays', hilarity with Henrietta, and for a friendship full of fun, falls, and spilling drinks up walls.

To Nicole, Maddie, V, Sîan, Dani, and Rachel, thank you for the coffee dates, crosswords, bottomless brunches, and the covid catchup calls. I am so glad to have shared my Leeds experience with all of you.

Rachel Brown, thank you for being our 'work mum', for the afterwork debriefs, for the legendary biscuit deliveries, and for bringing the best out of my Yorkshire accent.

Thank you to the rest of the amazing people I have worked with during my PhD, including Alex Evans, Pierce Mullen, Scott Dixon, Peter Tickle, Agnès Lewden, Jordan Balaban, Molly Baldwin, Sylvain Gigout, Charley Rodgers, Tim McDonald, Jack Simm, and Ben Stevens.

To the Ash girls, Nicole, Jess, and Maddie, I am glad we shared our PhD experiences being fellow grandmas on the sofa, for our lockdown hobbies, and for endless family dinners. Thank you for being such wholesome housemates.

There is not much during a PhD that cannot be solved when you are surrounded by such a great bunch of people. Though if in doubt, Gorilla tape or a trip to Caffè Nero will do the trick.

"Thank you, Leeds."

Out of Leeds…

Dr Liz Akam, thank you for recognising my potential, for nurturing my love for science, and for teaching me a skillset that prepared me so well to complete a PhD. You have been such a great role model, mentor, and friend throughout my academic journey.

Mum and Dad, thank you for your constant support throughout all my years of studying. There are so many qualities I have learnt from both of you that have helped to get me here. Mum thank you for sharing your intelligence and being the best thesaurus. Dad, thank you for teaching me how to be practical and for helping me make the apparatus used in this project. Thank you both for believing in me in every adventure, I owe so much to both of you.

To Auntie Elaine and Uncle Jules, thank you for the support you give me in everything I do, for never letting me forget how proud you are, and for always taking an interest and trying to understand the complicated science bits. You are very special people in my life.

To Jess, who will forever be my number one cheer leader. Thank you for your loyalty, friendship, and belief that I can do anything. From being babies in prams, to radio stars, to twenty-somethings yawning our heads off after long days of sergeanting and science, you have always been the best fan girl in all of my endeavours. Thank you for always keeping me going. Thank you to you and Dan for making my final study and the four hour commute to Leeds feel more possible.

Finally, to Juniper, thank you for your unwavering support throughout the day to day challenges of PhD life. Thank you for the virtual office facetimes that made working from home all the more successful. Thank you for your honesty, altruism, and your incredible judge of character. Your friendship has been my pillar of strength throughout the PhD whirlwind.

Abstract

Exercise training is well established to enhance neural plasticity and improve learning and memory, which is associated with enhanced neurotrophic factor expression. However, much less is known regarding the modulation of molecules that restrict neural plasticity following exercise training. We hypothesised that exercise training would downregulate the expression of genes involved in the RhoA/ROCK pathway, which is known to restrict neurite outgrowth and dendritic spine plasticity. Adult male Wistar rats underwent six weeks of moderate intensity continuous training (MICT) or high intensity interval training (HIIT) on a motorised treadmill and were compared to sedentary control animals. MICT and HIIT downregulated aggrecan and Nogo-receptor 2 mRNA expression in the hippocampus. Aggrecan is a component of perineuronal nets (PNNs): lattice-like structures that enwrap subsets of neurons, restrict plasticity, and are implicated in learning and memory. PNNs were fluorescently labelled with anti-aggrecan and *Wisteria floribunda agglutinin* to visualise aggrecan core protein and chondroitin sulphate glycosaminoglycan (CS-GAG) chains, respectively. MICT induced a shift towards a higher proportion of PNNs that expressed aggrecan without WFA labelling, suggesting that MICT modulated CS-GAG expression in hippocampal PNNs. Given these findings, we hypothesised that overexpression of *Chst11*, a chondroitin 4-sulfotransferase that makes CS-GAGs more inhibitory to plasticity, would impair memory and thus could be used to investigate the causal link between exercise-induced CS-GAG modulation and memory improvements. Hippocampal *Chst11* overexpression impaired short-term object recognition memory, which was attenuated by 24 hours in animals that had completed MICT. These results show that exercise training improves recognition memory by modulating CS-GAG expression in hippocampal PNNs. This study provides evidence that exercise training is a non-invasive method of manipulating PNN composition and alleviating cognitive deficits. These adaptations induced by exercise training may have therapeutic value in neurological conditions that display PNN abnormalities, such as Alzheimer's disease, schizophrenia, epilepsy, and CNS injuries.

Table of contents

List of tables

List of figures

List of equations

Abbreviations

ACAN	Aggrecan
ASPA	Animals Scientific Procedures Act
BCAN	Brevican
BDNF	Brain-derived neurotrophic factor
BRAL2	Brain-specific link protein 2
C4S	Sulphation at position carbon 4 of GalNAc residues
C4STs	Chondroitin 4-O-sulfotransferases
C6S	Sulphation at position carbon 6 of GalNAc residues
C6ST	Chondroitin 6-O-sulfotransferase
CA	Cornu Ammonis
CDK5	Cyclin-dependent kinase 5
CFL1	Cofilin 1
CHST11	Chondroitin 4-O-sulfotransferase 1
CHST12	Chondroitin 4-O-sulfotransferase 2
CHST13	Chondroitin 4-O-sulfotransferase 3
CHST15	GalNAc 4-sulphate 6-O-sulfotransferase
CHST3	Chondroitin 6-O-sulfotransferase 1
CNS	Central nervous system
CO_2	Carbon dioxide
CON	Sedentary control
CRMP2	Collapsin response mediator protein 2
CRTL1	Cartilage link protein 1
CS-A	Chondroitin sulphate disaccharide with GalNAc 4-O-sulphation
CS-C	Chondroitin sulphate disaccharide with GalNAc 6-O-sulphation
CS-D	Chondroitin sulphate disaccharide with 2-O-sulphation of GlcA and 6-O-sulphation of GalNAc
CS-E	Chondroitin sulphate disaccharide with GalNAc 4-O and 6-O-sulphation
CS-GAGs	Chondroitin sulphate glycosaminoglycan chains
CS-O	Sulphate free chondroitin sulphate disaccharide

CSPGs	Chondroitin sulphate proteoglycans
DEGs	Differentially expressed genes
DG	Dentate gyrus
dH_20	Distilled water
DTNB	5,5′-Dithiobis 2- nitrobenzoic acid
EDL	Extensor digitorum longus
EFNB3	Ephrin-B3
EPHA4	Ephrin A4
Ex-Chst11	Exercise group that received hippocampal Chst11 injections
Ex-GFP	Exercise group that received hippocampal GFP injections
G13	G protein 13
GABA	Gamma-aminobutyric acid
GalNAc	N-acetylgalactosamine
GDNF	Glial cell line-derived neurotrophic factor
GDP	Guanosine diphosphate
GEFs	Guanine exchange factors
GFP	Green fluorescent protein
GlcA	Glucuronic acid
GlcNAc	N-Acetylglucosamine
GTP	Guanosine triphosphate
HAPLN	Hyaluronan and proteoglycan binding link proteins
HAS	Hyaluronan synthase
HIIT	High intensity interval training
IGF1	Insulin-like growth factor 1
IU	International units
LARG	Rho guanine nucleotide exchange factor 12
LIMK1	LIM domain kinase 1
LINGO-1	Leucine rich repeat and Ig domain containing 1
LOTUS	Lateral olfactory tract usher substance
LSD	Least significant difference
LTP	Long term potentiation

M1	Primary motor cortex
MAG	Myelin-associated glycoprotein
MGV	Mean gray value
MICT	Moderate intensity continuous training
MLC2	Myosin light chain 2
NCAN	Neurocan
NDS	Normal donkey serum
NEP1-40	NOGO extracellular peptide, residues 1 to 40
NGF	Nerve growth factor
NgR1	Nogo receptor 1
NgR2	Nogo receptor 2
NgR3	Nogo receptor 3
NT-3	Neurotrophin-3
O_2	Oxygen
OCT	Optimum cutting temperature
OMGp	Oligodendrocyte myelin glycoprotein
$p75^{NTR}$	p75 neurotrophin receptor
PB	Sodium phosphate buffer
PBS	Phosphate buffered saline
PBST	Phosphate buffered saline with Triton X
PFA	Paraformaldehyde
PNNs	Perineuronal nets
PTEN	Phosphatase and tensin homolog
PTPRF	Leukocyte antigen-related tyrosine phosphatase (LAR)
PTPRS	Protein tyrosine phosphatase receptor type S (PTPσ)
RhoA	Ras homolog family member A
ROCK	Rho-associated coiled-coil containing protein kinase
ROI	Region of interest
RTN4	Reticulon 4 (Nogo-A)
RT-qPCR	Reverse transcription quantitative polymerase chain reaction
S1PR2	Sphingosine-1 phosphate receptor 2

SD	Standard deviation
Sed-Chst11	Sedentary group that received hippocampal Chst11 injections
Sed-GFP	Sedentary group that received hippocampal GFP injections
SEM	Standard error of the mean
SEMA3A	Semaphorin-3A
SEMA4D	Semaphorin-4D
Shh	Sonic hedgehog
TNS	Tris non-saline
TrkB	Tropomyosin receptor kinase B
TROY	Tumour necrosis factor receptor superfamily, member 19
VCAN	Versican
VEGF	Vascular endothelial growth factor
WFA	*Wisteria floribunda agglutinin*

Chapter 1 General introduction

The central nervous system (CNS), consisting of the brain and spinal cord, is constantly changing in response to interaction with external stimuli and experience. These changes occur throughout the lifetime including during development and learning, and can also be maladaptive e.g. in ageing and disease (Cramer *et al.*, 2011). Exercise training is known to promote neuroplasticity and enhance learning and memory (Cotman, Berchtold and Christie, 2007; Cassilhas, Tufik and de Mello, 2015). However, how exercise training modulates plasticity inhibiting pathways is not completely understood. Inhibitory extracellular modulators of plasticity may be the missing piece to the puzzle of how exercise enhances plasticity and exerts neuroprotective effects. Understanding how inhibitory, extracellular modulators of plasticity respond to exercise in the CNS of healthy adults will provide a fundamental understanding that may be manipulated to benefit cognition, delay age-related memory loss, and be used in neurorehabilitation.

1.1 Neural plasticity

Neural plasticity is a multifaceted phenomenon allowing the CNS to adapt in response to its internal and external environment (Mateos-Aparicio and Rodríguez-Moreno, 2019). However, it was previously thought that the adult CNS was hardwired and void of regenerative capacity, with Santiago Ramón y Cajal once describing neural pathways as ‘fixed’ and ‘immutable’ (Cajal, 1928). Neural plasticity was conceptualised throughout the 20th century, aided by the Konorski (1948) hypothesis that the formation of new synapses underlie plastic changes that support learning (Konorksi, 1948). Konorski theorised that the level of plasticity was associated with the amount of stimulation experienced (Konorksi, 1948). This was supported by Hebb (1949) who postulated that synapse

formation occurs in response to increased neural activity, providing the basis for changes in synaptic transmission (Hebb, 1949). Hebb also hypothesised that repeated simultaneous neuronal activity of two cells would result in these cells becoming associated with each other, forming the premise that ‘neurons that fire together, wire together’ (Hebb, 1949).

It was later shown that following lesions within the septal nuclei, new synaptic connections could be formed in the brain to compensate for synapses lost in response to the injury (Raisman, 1969). Further synaptic changes were observed in 1971, where it was demonstrated that rats reared in an enriched environment containing toys and mazes had an increased mean length and thickness of synapses in comparison to rats that were housed in social isolation (Møllgaard *et al.*, 1971). Together, these studies demonstrated that the CNS could adapt to different experiences and that there was potential for recovery after neural injury.

The term ‘neural plasticity’ now encompasses a multitude of structural and functional changes in the CNS including: neurogenesis, altered dendritic morphology, synaptic efficacy, and the rewiring of neuronal circuitry (Galván, 2010). These changes drive development, support learning and memory formation, and are fundamental for the central nervous system to recover from injury (Cramer *et al.*, 2011). Plasticity declines throughout adulthood and into senescence, however, the adult CNS retains the capacity for experience-driven plasticity (Oberman and Pascual-Leone, 2013; Hübener and Bonhoeffer, 2014). Identifying lifestyle interventions to enhance experience-driven plasticity (e.g. exercise training) can therefore be advantageous for treating conditions such as age-related cognitive decline and pathophysiological deficits in learning and memory. Exercise is already used as a treatment for several conditions such as

depression and Alzheimer's disease (Carek, Laibstain and Carek, 2011; De la Rosa *et al.*, 2020), however, our understanding of the underlying mechanisms remains incomplete. Further elucidating how exercise training exerts neuroprotective effects may help identify novel interventions for treating neurological conditions.

1.2 Exercise-induced plasticity

Exercise is a form of experience that enhances neural plasticity (Cooper, Moon and Van Praag, 2018). Exercise training has been observed to reduce neuronal activity in brain areas involved in cardiorespiratory control including the diencephalon (hypothalamic locomotor region), the midbrain (mesencephalic locomotor region and periaqueductal gray), and the brain stem (rostral ventrolateral medulla and nucleus tractus solitarius) (Ichiyama et al., 2002). Further experiments revealed that the decline in neuronal activity reported in cardiorespiratory brain areas was accompanied by reduced dendritic fields (Nelson *et al.*, 2005, 2010). In contrast, dendritic complexity has been reported to increase in the hippocampus (dentate gyrus) following exercise training (Eadie, Redila and Christie, 2005; Dostes *et al.*, 2016). Furthermore, acrobatic training in the form of an obstacle course increased the number of synapses in the motor cortex and on Purkinje cells in the cerebellar cortex (Black *et al.*, 1990; Kleim *et al.*, 1996, 1997). In addition to structural changes in neural circuitry, exercise training has also been shown to enhance angiogenesis, the sprouting of new microvasculature, in several brain regions including the hippocampus, motor cortex, striatum, and cerebellum (Black *et al.*, 1990; Kleim, Cooper and VandenBerg, 2002; Swain *et al.*, 2003; Ekstrand, Hellsten and Tingström, 2008; Clark *et al.*, 2009; Van Der Borght *et al.*, 2009).

These results demonstrate that exercise training induces widespread changes throughout numerous brain regions, although most of the research exploring the effect of exercise training on neural plasticity has focused on the hippocampus.

1.2.1 Exercise training and the hippocampus

The hippocampus is a highly plastic brain region that contains a neurogenic niche (the subgranular zone of the dentate gyrus) and is sensitive to activity-dependent plasticity (Leuner and Gould, 2010). It is well documented that voluntary wheel running and forced treadmill training enhance neurogenesis, the synthesis of new neurons from neural stem cells, in the rodent hippocampus (Van Praag *et al.*, 1999; Kim *et al.*, 2002; Farmer *et al.*, 2004; Pereira *et al.*, 2007; Bednarczyk *et al.*, 2009; Clark *et al.*, 2009; Van Der Borght *et al.*, 2009; Ferreira *et al.*, 2011; Patten *et al.*, 2013; Inoue, Hanaoka, *et al.*, 2015; Inoue, Okamoto, *et al.*, 2015; Nokia *et al.*, 2016). Additionally, exercise training increases hippocampal dendritic spine density (Eadie, Redila and Christie, 2005; Stranahan, Khalil and Gould, 2007; Lin *et al.*, 2012; Brockett, LaMarca and Gould, 2015), and enhances long-term potentiation (LTP) (Van Praag *et al.*, 1999; Farmer *et al.*, 2004; O'Callaghan, Ohle and Kelly, 2007; Patten *et al.*, 2013; Radahmadi, Hosseini and Alaei, 2016).

The dorsal hippocampus is associated with spatial memory, recognition memory, and contextual fear learning (Kim and Fanselow, 1992; Moser *et al.*, 1995; Broadbent, Squire and Clark, 2004; Pothuizen *et al.*, 2004; Fanselow and Dong, 2010). The types of plasticity induced by exercise (neurogenesis, dendritic spine density and synaptic plasticity) have been associated with memory improvements (Moser, Trommald and Andersen, 1994; Stuchlik, 2014). Mice exposed to a stress model displayed a reduction in dendritic spines in the hippocampal CA3

region which coincided with impaired object recognition memory (Chen *et al.*, 2010). These cognitive deficits were alleviated after the loss of dendritic spines was rescued by blocking the receptor for corticotropin-releasing hormone (Chen *et al.*, 2010), demonstrating a causal link between dendritic spine density hippocampal-related memory. Furthermore, blocking adult hippocampal neurogenesis was shown to impair both spatial memory and object recognition memory (Dupret *et al.*, 2008; Jessberger *et al.*, 2009). Additionally, neurogenesis induced by exercise training improved fear memory extinction in rats, which was not observed in trained rats that received temozolomide to block neurogenesis (Scott *et al.*, 2021).

Many treadmill training paradigms have improved spatial memory (Ang *et al.*, 2006; Cassilhas *et al.*, 2012; Silva *et al.*, 2012; Cetinkaya *et al.*, 2013; Inoue, Hanaoka, *et al.*, 2015), and object recognition memory in healthy adult rats (O'Callaghan, Ohle and Kelly, 2007; Bechara and Kelly, 2013). Furthermore, voluntary wheel running has also been shown to improve spatial memory (Lee *et al.*, 2012; Cetinkaya *et al.*, 2013).

1.2.2 Neurotrophic factors

Neurotrophic factors are a family of molecules that facilitate neural plasticity including neurotrophin-3 (NT-3), brain-derived neurotrophic factor (BDNF), nerve growth factor (NGF), glial cell line-derived neurotrophic factor (GDNF), insulin-like growth factor 1 (IGF1) and vascular endothelial growth factor (VEGF) (Huang and Reichardt, 2001; Mattson, 2008; Calvo, Pastor and De La Cruz, 2018). Neurotrophic factors are important for the differentiation (Ghosh and Greenberg, 1995; Vicario-Abejón *et al.*, 1995; Arsenijevic and Weiss, 1998; Liu *et al.*, 2014) and survival of neuronal populations (Alderson *et al.*, 1990; Kirschenbaum,

Goldman and Purpura, 1995; Nonner, Barrett and Barrett, 1996; Catapano *et al.*, 2001). Furthermore, neurotrophic factors have been shown to be chemoattractive during axon guidance (Gundersen and Barrett, 1980; Ming, Lohof and Zheng, 1997; Paves and Saarma, 1997; Chen *et al.*, 2013) and regulate myelination in the CNS (Cellerino *et al.*, 1997; Xiao *et al.*, 2010; Fletcher *et al.*, 2018).

The neural adaptations prompted by exercise training have in part been ascribed to the exercise-induced increases in neurotrophic factors. The most potent neurotrophic factor proposed to enhance exercise-induced plasticity is BDNF, which drives neurogenesis, synaptogenesis, synaptic plasticity, and changes in dendritic morphology (Tong *et al.*, 2001; Ferreira *et al.*, 2011). BDNF expression was enhanced in the rodent hippocampus via voluntary wheel running of either an acute manner (6 – 12 hours) or longer term training (one week to eight months) (Neeper *et al.*, 1996; Oliff *et al.*, 1998; Tong *et al.*, 2001; Russo-Neustadt *et al.*, 2004; Vaynman, Ying and Gómez-Pinilla, 2004; Berchtold *et al.*, 2005; Kobilo *et al.*, 2011; Abel and Rissman, 2013). Moreover, treadmill training also increased hippocampal BDNF expression (Soya *et al.*, 2007; Griffin *et al.*, 2009; Cassilhas *et al.*, 2012). BDNF has a high affinity to the tropomyosin receptor kinase B (TrkB) (Yamada and Nabeshima, 2003). Blocking BDNF-TrkB signalling abolished the improvements in spatial memory induced by voluntary wheel running (Vaynman, Ying and Gomez-Pinilla, 2004; Gomez-Pinilla, Vaynman and Ying, 2008), evidencing the importance of neurotrophic factors in exercise-induced functional plasticity. Furthermore, upregulated expression of BDNF, TrkB, and IGF1 has been observed in the hippocampus of rodents with enhanced memory performance following exercise training (O'Callaghan, Ohle and Kelly, 2007; Cassilhas *et al.*, 2012; Bechara and Kelly, 2013; Cetinkaya *et al.*, 2013).

1.2.3 Exercise paradigms used in neural plasticity research

The majority of exercise-induced plasticity research has utilised voluntary wheel running, a paradigm in which rodents are housed with a running wheel to allow *ad libitum* running. The volume of running can accumulate up to 18 km and exceed durations of 250 minutes per day in Wistar rats (Ruegsegger *et al.*, 2017). Such high volumes of exercise are rare in human behaviour, thus, shorter bouts of treadmill training may be more translatable and achievable for human health. Traditional exercise recommendations encourage moderate intensity continuous training (MICT), however, high intensity interval training (HIIT) is a form of exercise deemed to provide equivalent or sometimes superior physiological adaptations. MICT involves exercising non-stop at a moderate intensity, usually for longer periods of time (≥30 minutes), whereas, HIIT alternates short intervals of high intensity exercise with intervals of rest or active recovery periods for shorter durations (≤30 minutes) (Jiménez-Maldonado *et al.*, 2018). The American College of Sports Medicine recommends that adults should partake in a minimum of either 30 minutes of moderate exercise five days per week, or 20 minutes of intense exercise three times a week (Piercy and Troiano, 2018).

There is considerable variation in the experimental design of studies that compare MICT and HIIT within the following exercise parameters: duration of training sessions; length of study; presence of warm ups/cool downs; number and duration of intervals for HIIT; exercise speeds; treadmill incline; fixed protocol or progressive overload; and whether MICT and HIIT protocols are matched for energy expenditure or use unequal training volumes. Despite inconsistencies in methodology, there is evidence to support that HIIT is superior to MICT for enhancing BDNF and TrkB expression in the rodent CNS (Afzalpour *et al.*, 2015;

Naghibzadeh *et al.*, 2019; Constans *et al.*, 2021; Okamoto *et al.*, 2021). However, Okamoto *et al*., (2021) reported that improvements in spatial memory and increased adult hippocampal neurogenesis were comparable between MICT and HIIT. Additionally, another study observed that HIIT did not increase neurogenesis in comparison to sedentary control animals, despite the distance ran throughout the protocol being positively correlated with the number of new neurons (Nokia *et al.*, 2016).

Debate also exists regarding which exercise intensities of continuous training are more successful for enhancing plasticity. Treadmill training at a higher intensity (18 $m.min^{-1}$) for 30 min/day for seven days produced a significantly higher increase in BDNF than low intensity training (12 $m.min^{-1}$) (Cefis *et al.*, 2019). However, lower intensity treadmill training (15 $m.min^{-1}$) was more favourable for enhancing hippocampal neurogenesis and spatial memory than a higher intensity group (40 $m.min^{-1}$) (treadmill training provided 60 min/day for six weeks) (Inoue, Hanaoka, *et al.*, 2015). Spatial memory was also improved following eight weeks (30 min/day) of lower intensity continuous exercise (up to 10 $m.min^{-1}$), whereas, higher intensity continuous exercise (up to 22 $m.min^{-1}$) impaired spatial memory (Wu *et al.*, 2020). The lower exercise intensity employed by Wu *et al.* (2020) upregulated *BDNF* mRNA, whereas the higher intensity exercise downregulated *BDNF* mRNA, supporting that spatial memory performance is associated with BDNF expression. This suggests that exercise intensity follows the dose-response relationship on the inverted-U hormetic model (Calabrese, 2004), e.g. moderate doses of exercise may be beneficial whilst higher doses of exercise may have adverse effects (Pietrelli *et al.*, 2018).

Overall, research regarding cerebral adaptations to MICT and HIIT in rodents is limited and the durations, speeds, and intervals used are extremely variable. Further research is required to ascertain the role of treadmill training and exercise parameters in the CNS, though the aforementioned studies provide evidence that moderate intensity exercise is better than implementing higher intensity training for improving memory.

1.3 Balance between neurotrophic and inhibitory factors

It is well established that exercise training enhances the expression of BDNF, which facilitates structural plasticity (neurogenesis and dendritic spine density) and functional plasticity (LTP and cognition) (Farmer *et al.*, 2004; Vaynman, Ying and Gómez-Pinilla, 2004; O'Callaghan, Ohle and Kelly, 2007; Gomez-Pinilla, Vaynman and Ying, 2008; Cassilhas *et al.*, 2012; Lin *et al.*, 2012; Bechara and Kelly, 2013; Inoue, Hanaoka, *et al.*, 2015; Wu *et al.*, 2020). However, there is a fine balance between mechanisms that promote and inhibit neural adaptations to achieve optimum plasticity and maintain normal physiological functions (Oberman and Pascual-Leone, 2013). It is possible that there are dual effects of exercise training, essentially 'taking a foot off the inhibitory brakes' and facilitating the 'acceleration' of neurotrophic factors to create a more permissive, plastic environment, though this is yet to be investigated. Fully understanding the intrinsic mechanisms of exercise-induced plasticity may expand the therapeutic potential of exercise and be beneficial for improving cognition, neuroprotection, and neurorehabilitation.

1.4 Inhibitory modulators of plasticity

Within this document, the terms ‘inhibitory modulators of neuroplasticity’ or ‘inhibitory molecules’ refer to molecules within the CNS with the ability to restrict neurite outgrowth, induce growth cone collapse, negatively regulate dendritic spine formation, and stabilise/prevent reorganisation of synapses (Lai and Ip, 2013; Baldwin and Giger, 2015; Sorg *et al.*, 2016; Boghdadi, Teo and Bourne, 2018). These terms do not refer to inhibitory neurotransmitters such as gamma-aminobutyric acid (GABA).

Most of our knowledge of inhibitory modulators of plasticity pertains to their role in closing the critical period (Pizzorusso *et al.*, 2002; Nowicka *et al.*, 2009; Mirzadeh *et al.*, 2019), where experience drives the maturation of neural circuitry during postnatal development, and preventing regeneration in the injured adult CNS (Akbik, Cafferty and Strittmatter, 2012). However, inhibitory modulators of plasticity are expressed in the healthy, adult CNS, regulating cytoskeletal/anatomical rearrangements and limiting experience-dependent plasticity (Akbik, Cafferty and Strittmatter, 2012). These inhibitory modulators of plasticity in the CNS are classified into three subtypes: myelin-associated inhibitors, chondroitin sulphate proteoglycans (CSPGs), and guidance molecules (Giger, Hollis and Tuszynski, 2010).

1.4.1 Myelin-associated inhibitors

Myelin in the CNS contains three main myelin-associated inhibitors: Nogo, myelin associated glycoprotein (MAG), and oligodendrocyte myelin glycoprotein (OMGp). The myelin-associated inhibitors are expressed in oligodendrocytes and

some neurons, and are mainly implicated in the inhibition of neurite outgrowth (Fujita and Yamashita, 2014).

MAG is produced by oligodendrocytes and is part of the SIGLEC family (Crocker, Paulson and Varki, 2007). It is localised on the peri-axonal membrane, and although MAG only constitutes to 1% of CNS myelin, it plays an important role in myelin-axon stability and axon cytoskeleton regulation (Schnaar and Lopez, 2009). Nogo is the fourth member of the reticulon family (RTN4) and contains three protein products: Nogo-A, Nogo-B, and Nogo-C. Whilst all three Nogo proteins are expressed in the CNS, Nogo-B and Nogo-C also have widespread expression in peripheral tissue (Oertle and Schwab, 2003). Nogo-A contains two distinct regions: the Nogo-A specific region, Nogo-Δ20, and the 66 amino acid loop region, Nogo-66 (Schwab, 2010). Both Nogo-A regions have been observed to activate Ras homolog family member A (RhoA) signalling and its downstream effector rho-associated coiled-coil containing protein kinase (ROCK) (Schwab, 2010) *(discussed further in Section 1.4.4).* OMGp is part of the leucine-rich repeat family and is expressed in oligodendrocytes and many adult neurons in the adult CNS (Wang *et al.*, 2002; Raiker *et al.*, 2010). The three myelin-associated inhibitors have collectively been shown to inhibit neurite outgrowth *in vitro* and prevent axonal regeneration following CNS injury (Boghdadi, Teo and Bourne, 2018).

Myelin associated inhibitors bind to a family of Nogo receptors: Nogo receptor 1 (NgR1), Nogo receptor 2 (NgR2), and Nogo receptor 3 (NgR3). The Nogo-66 region of Nogo-A, MAG, and OMGp ligands all bind to NgR1 (Domeniconi *et al.*, 2002; Liu *et al.*, 2002; Wang *et al.*, 2002). NgR1 also works within a receptor complex alongside the p75 neurotrophin receptor ($p75^{NTR}$) and leucine rich repeat

and Ig domain containing 1 (LINGO-1) that binds Nogo-A, MAG, and OMGp (Mi *et al.*, 2004). $p75^{NTR}$ may also be replaced by the receptor tumour necrosis factor receptor superfamily, member 19 (TROY) within this complex. Both the NgR1/$p75^{NTR}$/LINGO-1 complex and NgR1/TROY/LINGO-1 complex can induce RhoA activation and inhibitory signalling in the CNS (Park *et al.*, 2005). Nogo-Δ20 binds to a separate receptor, sphingosine-1 phosphate receptor 2 (S1PR2) (Kempf *et al.*, 2014). The receptors NgR2 and NgR3 are named after NgR1 due to their structural homology (Barton *et al.*, 2003), however, they exhibit different binding profiles to NgR1. NgR2 selectively binds MAG (Venkatesh *et al.*, 2005) and NgR3 is actually reported to bind with CSPGs instead of myelin-associated inhibitors (Dickendesher *et al.*, 2012). Despite the differences in Nogo receptor binding partners, NgR1, NgR2, and NgR3 are all known to restrict the formation of synapses *in vitro* (Wills *et al.*, 2012).

The therapeutic effect of targeting myelin associated inhibitors has been trialled in several pathophysiological models in the CNS. Nogo-A activity has been suppressed using the antibodies IN-1 (Fouad, Dietz and Schwab, 2001) and 11C7 (Liebscher *et al.*, 2005; Maier *et al.*, 2009; Chen *et al.*, 2017) which improved axonal regeneration and locomotor function in rat models of spinal cord injury. There is also evidence that the IN-1, 11C7, and anti-MAG antibodies improve recovery following strokes in rodents (Irving *et al.*, 2005; Seymour *et al.*, 2005; Tsai *et al.*, 2011). Nogo-A/B, MAG, and OMGp have also been genetically targeted in a triple knockout model resulting in enhanced axonal regeneration in a dorsal hemisection spinal cord injury model (Cafferty *et al.*, 2010). However, a triple knockout model for Nogo-A/B/C, MAG, and OMGp, which also included

Nogo-C, did not improve axonal regeneration in a similar dorsal hemisection injury (Lee *et al.*, 2010).

In addition to neutralising myelin associated ligands, modulating Nogo receptor activity has also benefited neurorehabilitation. Blocking NgR1 activity with NOGO extracellular peptide, residues 1 to 40 (NEP1-40) promoted recovery following spinal cord injury and stroke models, and enhanced plasticity in the visual cortex following monocular deprivation (Wang *et al.*, 2007; Luo *et al.*, 2011; Xu *et al.*, 2017). Additionally, another NgR1 antagonist, lateral olfactory tract usher substance (LOTUS), prevented growth cone collapse *in vitro* and enhanced axonal regeneration and motor recovery in spinally injured mice (Kurihara and Takei, 2015; Hirokawa *et al.*, 2017).

During postnatal development, Nogo-A is involved in axon guidance, the negative regulation of dendritic branching, and has been shown to be inhibitory to axon growth and sprouting in both the developing and non-injured adult CNS (Schmandke, Schmandke and Schwab, 2014). Moreover, shifts in ocular dominance following monocular deprivation are only normally observed in postnatal development. However, mice lacking Nogo-A and NgR1 still display shifts in ocular dominance during adulthood (McGee *et al.*, 2005), providing evidence that Nogo-A also plays a role in restricting neural plasticity in the CNS of mature rodents that are not injured.

1.4.2 Chondroitin sulphate proteoglycans (CSPGs)

CSPGs include a family of lecticans (aggrecan (ACAN), brevican (BCAN), neurocan (NCAN), and versican (VCAN)) which are expressed loosely in the extracellular matrix, and are integral components of structures in the CNS called

perineuronal nets that restrict plasticity (Sorg *et al.*, 2016) (Figure 1.1A). Lecticans consist of a core protein which is covalently bonded to chondroitin sulphate – glycosaminoglycan side chains (CS-GAGs). CSPGs are highly heterogeneous, with variations in the number of CS-GAG chains and the length of the region on the core protein in which they attach (Kwok *et al.*, 2011). Out of the lecticans, aggrecan has the highest number of CS-GAGs, (Galtrey and Fawcett, 2007), making it highly negatively charged (Roughley and Mort, 2014). The biosynthesis of CS-GAGs has been reported in depth (Kwok, Warren and Fawcett, 2012; Mikami and Kitagawa, 2013). Briefly, CSPG core proteins act as a scaffold to which a GAG protein linkage region is attached to a serine residue. The GAG protein linkage region is a tetrasaccharide that is assembled through the step-by-step addition of four monosaccharides: xylose, two galactose residues, and one glucuronic acid (GlcA) residue. This is achieved by the enzymes xylosyltransferase; β1,4-galactosyltransferase; β1,3-galactosyl-transferase II; and β1,3-glucuronyltransferase I. The synthesis of the chondroitin backbone of CS-GAGs is then triggered by the transfer of the first *N*-acetylgalactosamine (GalNAc) residue to GlcA by GalNAc transferase I. Elongation of the chondroitin backbone occurs through the repetitive addition of GlcA alternated with GalNac via the enzymes GlcA transferase II and GalNAc transferase II, respectively, creating a disaccharide chain. For a simplified schematic of CS-GAGs see Figure 1.1B.

CSPGs were shown to inhibit neurite extension *in vitro* in a range of cell types including dorsal root ganglia, retinal ganglion cells, PC12D cells, and neuroblastoma cells (Snow *et al.*, 1990; Oohira, Matsui and Katoh-Semba, 1991; Hynds and Snow, 1999; Inatani *et al.*, 2001). Following CNS injury, reactive

astrocytes secrete CSPGs into the extracellular matrix which contributes to the formation of the glial scar (McKeon, Jurynec and Buck, 1999; Jones, Margolis and Tuszynski, 2003). Using explant cultures of glial scar cells harvested from neonate and adult rats, (McKeon *et al.*, 1991) showed that the level of neurite inhibition was higher when cultured on glial scar tissue from adult rats that expressed CSPGs, in comparison to the neonate tissue that did not express CSPGs. *In vivo,* the glial scar forms a physical obstacle to regeneration in which the inhibitory nature of CSPGs prevents axons from migrating through CNS lesions (Bradbury *et al.*, 2002; Cafferty *et al.*, 2007).

Furthermore, the CSPG receptors protein tyrosine phosphatase receptor type S (PTPRS - also known as PTPσ), and leukocyte antigen-related tyrosine phosphatase (PTPRF - also known as LAR) activate RhoA signalling, consequently inhibiting neurite outgrowth (Ohtake *et al.*, 2016). Additionally, CSPGs are reported to bind with NgR1 and NgR3 which are also receptors involved in the RhoA/ROCK signalling pathway (Section 1.4.4-Figure 1.2) (Dickendesher *et al.*, 2012).

The inhibitory influence of CSPGs can be attenuated by administering chondroitinase ABC, a bacterial enzyme that cleaves CS-GAG chains from the core protein. The enzymatic digestion of CSPGs in glial scars enhances axonal regeneration, and promotes functional recovery following brain and spinal cord injury (Bradbury and Carter, 2011; Koh, Pronin and Hughes, 2018).

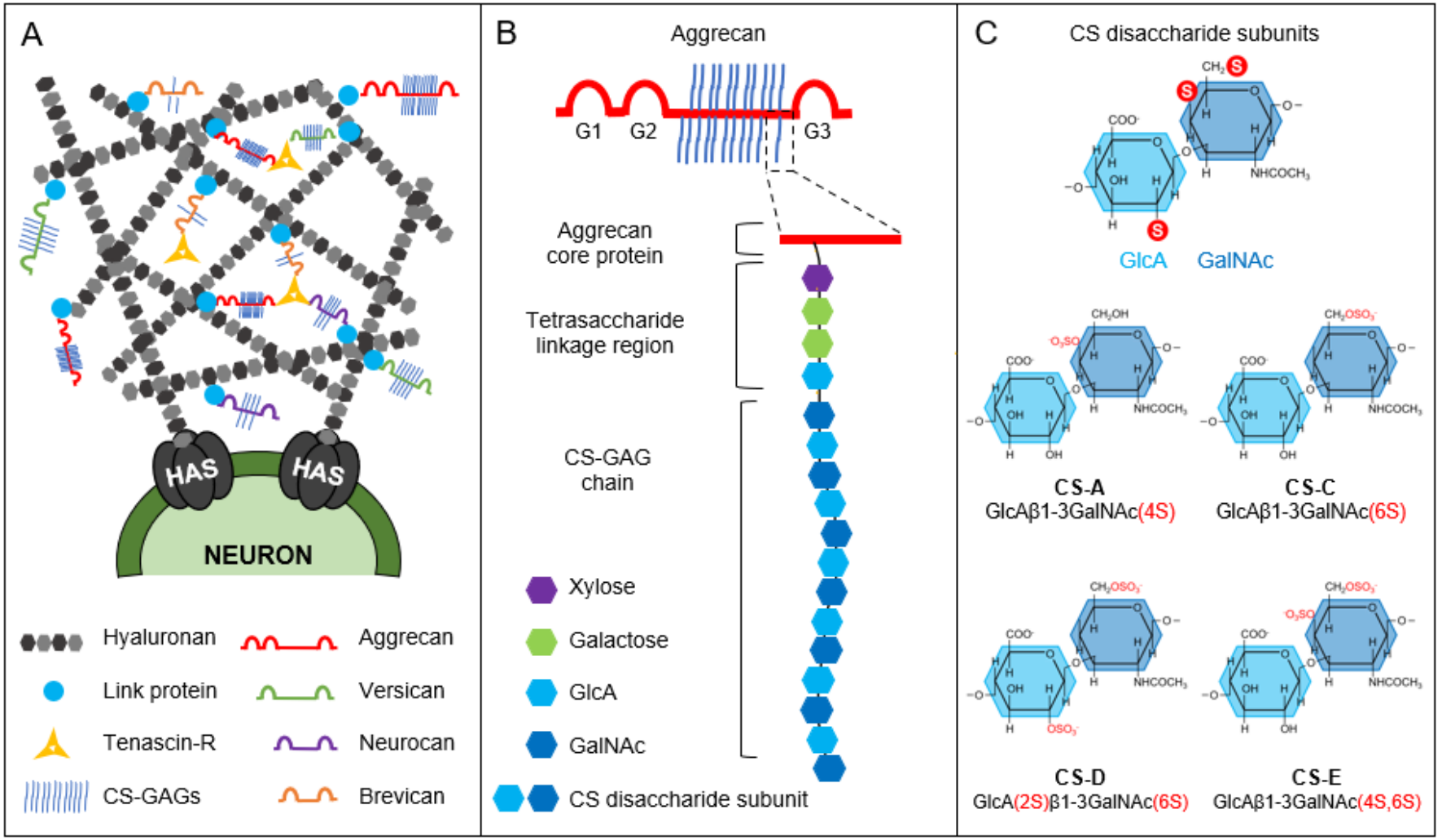

Figure 1.1. Structure of PNNs, CSPGs, and CS-GAGs.

A. On perineuronal net (PNN) bearing neurons a plasma membrane enzyme, hyaluronan synthase (HAS), produces a hyaluronan backbone that forms the PNN scaffold. Chondroitin sulphate proteoglycans (CSPGs) of the lectican family bind to the hyaluronan backbone via link proteins at their N terminal domains. Lectican CSPGs include aggrecan, versican, neurocan, and brevican, which vary in the number of chondroitin sulphate – glycosaminoglycans (CS-GAG) chains and the length of the CS-GAG attachment region. Up to three lecticans can be crosslinked in the PNN structure at their C terminal domains by tenascin-R.

B. All lecticans have a G1 domain at the N-terminal and a G3 domain at the C-terminal, whilst aggrecan has an extra G2 domain located after G1. CS-GAG chains covalently attach to serine residues in the lectican core protein by a tetrasaccharide linkage region containing xylose, two galactose residues, and glucuronic acid (GlcA). The chondroitin sulphate (CS) chain is then extended with repeating disaccharide subunits of GlcA and *N*-acetylgalactosamine (GalNAc).

C. CS disaccharide units (GlcA and GalNAc) can be sulphated at several positions denoted by the red circles labelled ‘S’. Variations in sulphation patterns results in five different CS subunits that can be incorporated into CS-GAGs in any combination. CS-O has no sulphation (not included in the figure). CS-A has GalNAc sulphation at position C4. CS-C has GalNAc sulphation at position C6. CS-D has GlcA sulphation at position C2 and GalNAc sulphation at position C6. CS-E has GalNAc sulphation at positions C4 and C6.

Figure adapted from (Kwok *et al.*, 2011; Kwok, Warren and Fawcett, 2012; Mikami and Kitagawa, 2013).

The inhibitory nature of CSPGs can also be modified by altering sulphation patterns of CS-GAGs (Duncan, Foster and Kwok, 2019). Sulfotransferases transfer sulphate groups to sulphation sites of GalNAc residues resulting in either 4-O-sulphation (C4S) or 6-O-sulphation (C6S). C4S is catalysed by chondroitin 4-O-sulfotransferases (C4STs) including C4ST1, C4ST2, and C4ST3 (also known as CHST11, CHST12 and CHST13, respectively). Likewise, C6S is catalysed by chondroitin 6-O-sulfotransferase (C6ST), also known as CHST3. Another enzyme, GalNAc 4-sulphate 6-O-sulfotransferase (CHST15), produces disulphated chondroitin disaccharides, in which C6S is transferred to a GalNAc residue already containing C4S (Mikami and Kitagawa, 2013). The variation in GalNAc sulphation results in several possible disaccharide units that can be present in CS-GAGs: CS-A (4-O-sulphation), CS-C (6-O-sulphation), and CS-E (4-O-sulphation and 6-O-sulphation) (Kwok, Warren and Fawcett, 2012) (Figure 1.1C). Additionally, CS-O disaccharide units are sulphate-free, and CS-D contains 2-O-sulphation of the GlcA residue and 6-O-sulphation of GalNAc.

CS-A (with C4S) is known to be inhibitory, whereas CS-C (with C6S) is more permissive to axonal regeneration (Wang *et al.*, 2008; Lin *et al.*, 2011). Throughout the lifespan, CS-GAGs transition to becoming more inhibitory and thus more restrictive to neural plasticity. During embryonic development there is a higher level of C6S resulting in a lower C4S:C6S ratio; as C6S declines throughout maturation the C4S:C6S ratio increases (Kitagawa *et al.*, 1997). C6S expression continues to decline whilst C4S increases during postnatal development, further increasing the ratio of C4S:C6S (Miyata *et al.*, 2012). Heightened ratios of C4S:C6S during postnatal development coincide with the closure of critical periods and the restriction of plasticity (Miyata *et al.*, 2012). CS-

A is the predominant disaccharide in the mature CNS, and C4S and C6S simultaneously increase and decrease, respectively, throughout adulthood (Foscarin *et al.*, 2017). The inhibitory environment resultant of high C4S:C6S ratios can be attenuated by overexpressing C6ST1, which can delay the closure of critical periods, enhance plasticity, and rescue age-related memory deficits (Miyata *et al.*, 2012; Yang *et al.*, 2021).

1.4.3 Negative guidance molecules

Negative guidance molecules use chemo-repulsive signals to help migrating axons navigate to their targets and form synapses (Stoeckli, 2018). Migrating axons contain tips called growth cones that house actin-based machinery for motility, and also the sensory capacity to screen the extracellular environment for guidance cues (Omotade, Pollitt and Zheng, 2017). CNS oligodendrocytes express the repulsive guidance molecules semaphorin-4D (SEMA4D) and ephrin-B3 (EFNB3) (Moreau-Fauvarque *et al.*, 2003; Benson *et al.*, 2005). SEMA4D is upregulated following spinal cord injury, and has been shown to repel mature axons *in vitro* (Moreau-Fauvarque *et al.*, 2003). SEMA4D can also induce growth cone collapse and reduce dendritic outgrowth through its receptor, plexin-B1 (Ito *et al.*, 2006; Oinuma *et al.*, 2010; Tasaka, Negishi and Oinuma, 2012). Similar to SEMA4D, EFNB3 induces growth cone collapse and restricts axonal outgrowth (Kullander *et al.*, 2001; Benson *et al.*, 2005). EFNB3 mediates inhibition in the CNS through the receptor ephrin A4 (EPHA4) (Kullander *et al.*, 2001). Both EPHA4 and SEMA4D/PLEXIN-B1 signalling regulate RhoA activation in the CNS (Shamah *et al.*, 2001; Swiercz *et al.*, 2002). Other repulsive guidance molecules include class-3 semaphorins, Slits, and sonic hedgehog (Shh) (Stoeckli, 2018), although they are beyond the scope of this thesis.

1.4.4 RhoA/ROCK signalling pathway

The aforementioned inhibitory modulators of plasticity are ligands in the RhoA/ROCK signalling pathway that alters neuronal morphology (Figure 1.2). The inhibitory molecules bind to membrane receptors including a family of Nogo receptors (NgR1, NgR2, NgR3); a receptor complex containing NgR1, LINGO1, and TROY; CSPG receptors (LPAR1, PTPRF, PTPRS); and the semaphorin and ephrin receptors PLEXIN-B1 and EPHA4, respectively (Kullander *et al.*, 2001; Bashaw and Klein, 2010; Liu, Gao and Wang, 2015; Sami, Selzer and Li, 2020). These membrane receptors converge to activate the RhoA/ROCK signalling pathway which regulates actin cytoskeleton dynamics, dendritic spine morphology, and inhibits neurite outgrowth via growth cone collapse (Fujita and Yamashita, 2014; Spence and Soderling, 2015).

Upon binding to the membrane receptors, these inhibitory factors activate molecules called guanine exchange factors (GEFs) which convert guanosine diphosphate (GDP) to guanosine triphosphate (GTP), allowing the activation of the Rho small GTPase, RhoA (Fujita and Yamashita, 2014). Additionally, Nogo-Δ20 signalling through the S1PR2 receptor activates G protein 13 (G13), followed by rho guanine nucleotide exchange factor 12 (LARG), resulting in RhoA GTP activation (Fujita and Yamashita, 2014; Kempf *et al.*, 2014). LARG-induced activation of RhoA GTP is also mediated by SEMA4D/PLEXIN-B1 signalling (Swiercz *et al.*, 2002).

There are two isoforms of ROCK: ROCK 2 is the dominant isoform in CNS, cardiac, and skeletal muscle tissue, whereas ROCK 1 is prevalent is the lungs, liver, blood, and immune system (Koch *et al.*, 2018). When RhoA is in its GTP-bound form, it activates ROCK 2 which triggers a cascade of downstream

effectors including LIM domain kinase 1 (LIMK1), myosin light chain 2 (MLC2), phosphatase and tensin homolog (PTEN), collapsin response mediator protein 2 (CRMP2) and cofilin 1 (CFL1); which regulate actin depolymerisation, growth cone collapse, neurite outgrowth inhibition, and dendritic spine dynamics (Amano, Nakayama and Kaibuchi, 2010; Liu, Gao and Wang, 2015; Woolfrey and Srivastava, 2016).

The RhoA/ROCK signalling pathway is involved in CNS pathophysiology including spinal cord injury, strokes, and traumatic brain injury (Kubo *et al.*, 2008; Mulherkar and Tolias, 2020). As there are numerous inhibitory ligands to RhoA/ROCK signalling, targeting the common effectors RhoA or ROCK is a common way to remediate neurite outgrowth inhibition and the restriction of plasticity for neurorehabilitation. RhoA activity can be blocked with the enzyme C3 transferase, which enhanced neurite extension following optic nerve crush and spinal cord injury models (Lehmann *et al.*, 1999; Dergham *et al.*, 2002; Fischer *et al.*, 2004). Neuroregeneration has also been achieved by using the ROCK inhibitors Y-27632 and Fasudil in rodents. Following cortical traumatic brain injury, Y-27632 improved motor performance and prevented the degeneration of cortical neurons (Bye *et al.*, 2016). Similarly, Fasudil alleviated motor and cognitive impairments following cortical injury, alongside suppressing the loss of mature dendritic spines (Mulherkar *et al.*, 2017).

Enhanced axonal outgrowth subsequent to Y-27632 treatment was demonstrated on cryosections of injured rat spinal cords, dorsal root ganglia and retinal ganglion cell explants (Borisoff *et al.*, 2003; Monnier *et al.*, 2003). Additionally, the *in vivo* application of Y-27632 after spinal cord injury improved axonal sprouting and motor recovery, and reduced disruption of the blood-spinal cord barrier (Dergham

et al., 2002; Chan *et al.*, 2005; Chang and Cao, 2021). Improvements in motor recovery were also reported in spinally injured rats following Fasudil treatment (Nishio *et al.*, 2006; Fu *et al.*, 2016).

These studies show that obstructing the main effectors, RhoA and ROCK, enhances plasticity and has therapeutic value in the CNS. However, the RhoA/ROCK pathway is involved in other physiological systems beyond the CNS, and its inactivation can induce adverse side effects such as systemic vasodilation, hypotension, and renal impairment (Koch *et al.*, 2018). These side effects could exacerbate complications following CNS injuries in which homeostatic regulation is already hindered (Partida *et al.*, 2016; Price and Trbovich, 2018). Thus, identifying components of the RhoA/ROCK pathway that can be intrinsically regulated, *e.g.* by exercise, may enable a more specific activation profile of RhoA/ROCK signalling to enhance neural plasticity with reduced side effects.

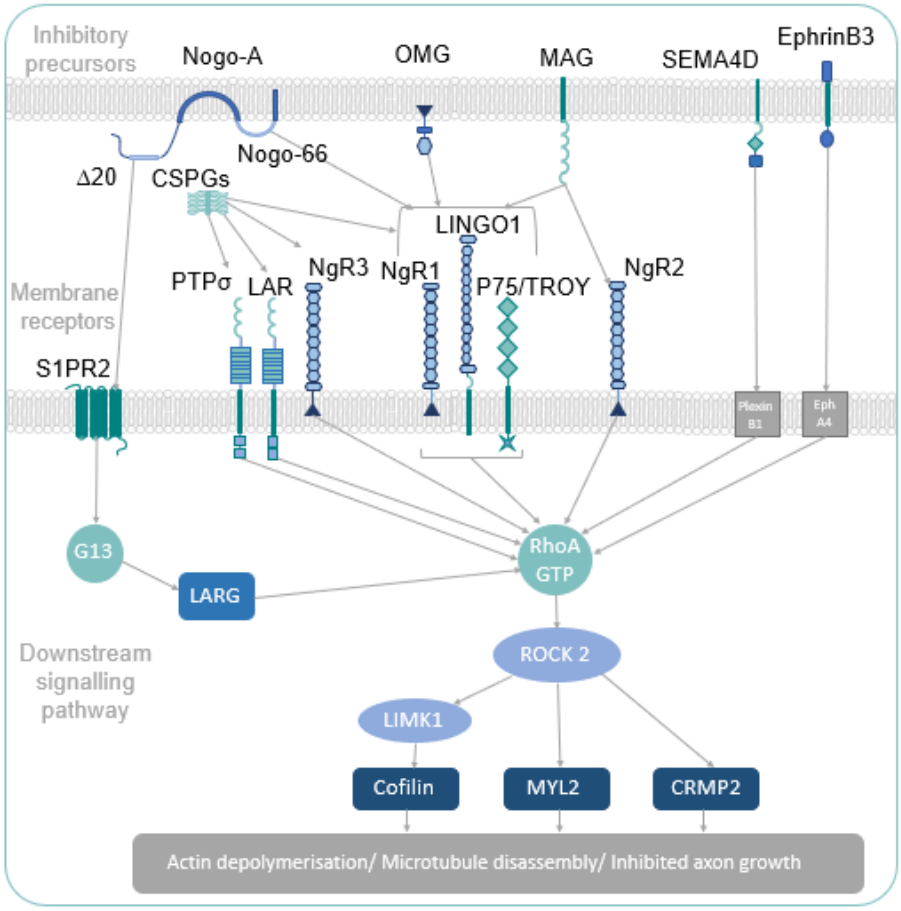

Figure 1.2. RhoA/ROCK signalling pathway.

Several inhibitory molecules in the CNS bind to membrane receptors that trigger the activation of the RhoA/ROCK signalling pathway, leading to neurite outgrowth inhibition and restricted dendritic spine plasticity. Inhibitory precursors include: Nogo-A; Myelin-associated glycoprotein (MAG); Oligodendrocyte-myelin glycoprotein (OMGp); Semaphorin-4D (SEMA4D); Ephrin-B3; and Chondroitin sulphate proteoglycans (CSPGs – aggrecan, brevican, neurocan, and versican). Membrane receptors include: Sphingosine-1 phosphate receptor 2 (S1PR2) – a transmembrane G protein-coupled receptor; the transmembrane receptors protein tyrosine phosphatase receptor type S (PTPσ) and leukocyte antigen-related tyrosine phosphatase (LAR) that have intracellular domains; the GPI-anchored cell surface receptors - Nogo receptors 1-3 (NgR1, NgR2, NgR3); the transmembrane receptor Leucine rich repeat and Ig domain containing 1 (LINGO-1); the transmembrane p75 neurotrophin receptor (p75NTR)/Tumour necrosis factor receptor superfamily, member 19 (TROY) which have an intracellular domain; Plexin-B1; and Ephrin-A4 (EphA4). Downstream signalling molecules include RhoA; Rho-associated coiled-coil containing protein kinase 2 (ROCK 2); Guanine nucleotide binding protein, alpha 13 (GNA13); Rho guanine nucleotide exchange factor 12 (LARG); LIM domain kinase 1 (LIMK1); Cofilin; Myosin light chain 2 (MYL2 also known as MLC2); and Collapsin response mediator protein 2 (CRMP2).

1.4.5 Perineuronal nets

In addition to the inhibitory ligands that modulate plasticity via RhoA/ROCK activation, pericellular structures called perineuronal nets (PNNs) also restrict plasticity in the mature CNS. PNNs present as a reticular structure (Figure 1.3) which surround the soma and proximal dendrites of subsets of neurons in the CNS, stabilising synaptic connections (Bosiacki *et al.*, 2019). Immunohistochemical experiments have identified a variety of neuronal subtypes that bare PNNs throughout the CNS (van't Spijker and Kwok, 2017). The most commonly used PNN marker is *Wisteria floribunda agglutinin* (WFA), a lectin that labels the GalNAc units of CS-GAGs (Brückner *et al.*, 1996).

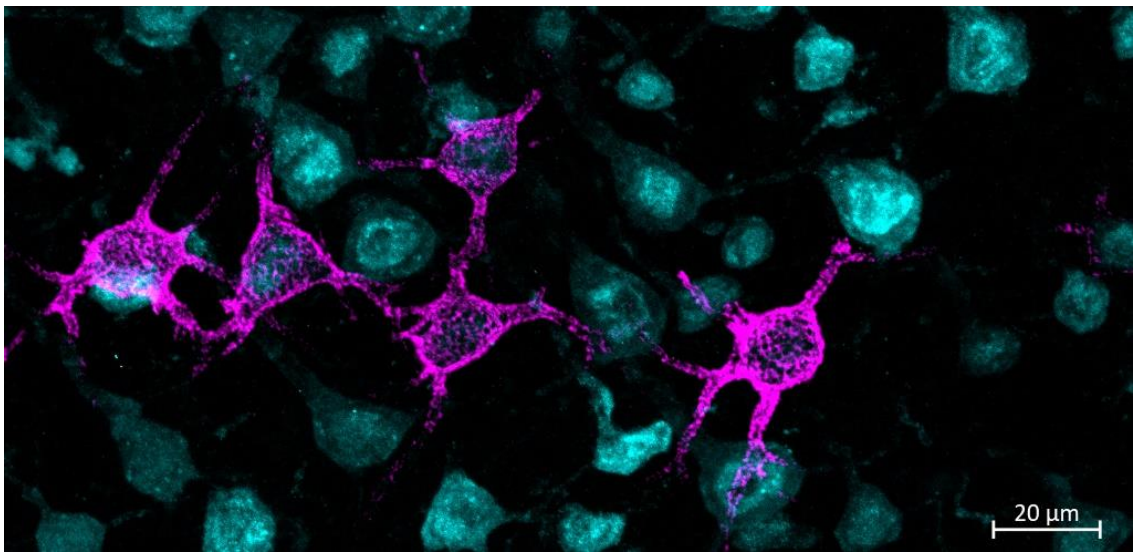

Figure 1.3. Perineuronal nets surrounding cortical neurons.

Perineuronal nets (magenta - stained by Wisteria floribunda agglutinin) surrounding neurons in the cerebral cortex (cyan – stained by NeuN). 3D z stack reconstruction – imaged with a Zeiss LSM880 confocal microscope.

In the cerebral cortex, PNNs are predominantly expressed around parvalbumin-positive GABAergic inhibitory interneurons, that modulate pyramidal neurons (Härtig, Brauer and Brückner, 1992; Baig, Wilcock and Love, 2005). Though, weaker staining of PNNs is also observed to surround some cortical pyramidal

cells (Alpár *et al.*, 2006). PNNs are prevalent throughout cortical layers 2-5 and densely populate the motor- and sensory- cortices (Brückner *et al.*, 1999).

Within the hippocampus, PNNs are localised in the Cornu Ammonis (CA) regions 1-3 and the dentate gyrus. WFA labelled sparse, yet distinct, PNNs in the CA1 region, whilst the pyramidal layer of the CA2 and CA3 regions, and granular cell layer of the dentate gyrus displayed more diffuse WFA staining of PNNs around the tightly compacted neuronal cells (Lensjø, Christensen, *et al.*, 2017). PNNs in the hippocampus were observed to enwrap parvalbumin-positive basket cells and bistratified cells (subtypes of interneuron) in the stratum pyramidale layer, and around interneurons in the stratum oriens layer (Yamada and Jinno, 2015). Though, PNNs have also been noted on hippocampal pyramidal cells, especially in the CA2 region (Carstens *et al.*, 2016).

In the cerebellar cortex, PNNs are strongly expressed around excitatory Golgi neurons, whilst weaker, less compact WFA staining is expressed around granule and purkinje cells (Mabuchi *et al.*, 2001; Carulli *et al.*, 2006). PNNs are also observed around the large excitatory deep cerebellar nuclei (fastigial, interpositus, and dentate) (Carulli *et al.*, 2006, 2020; Mueller *et al.*, 2014; Blosa *et al.*, 2016).

PNNs within the spinal cord envelop alpha motor neurons in the ventral horn, large neurons in the dorsal horn, and interneurons on the intermediate zone (Galtrey *et al.*, 2008; Smith *et al.*, 2015; Irvine and Kwok, 2018). The regional and neuronal variations associated with PNNs supports that these extracellular structures are involved in diverse CNS functions.

1.4.5.1 PNN components and structure

The densely aggregated PNN structure is assembled out of four main components (Figure 1.1A): a hyaluronan backbone - the structural scaffold of PNNs, CSPGs, link proteins, and tenascins (Bucher *et al.*, 2021). PNN-bearing neurons express hyaluronan synthase (HAS) enzymes, which synthesise hyaluronan GAG chains and keep them anchored to the neuronal cell surface (Kwok, Carulli and Fawcett, 2010; Fowke *et al.*, 2017). The hyaluronan chains consist of repeating disaccharide units of GlcA and N-Acetylglucosamine (GlcNAc) (Ghiselli, 2017). The hyaluronan backbone forms a scaffold for the attachment of other PNN components (van't Spijker and Kwok, 2017). CSPGs, including the lectican family (aggrecan, brevican, neurocan, and versican) bind to the hyaluronan back bone by their N-terminal globular domains (Yamaguchi, 2000; Su *et al.*, 2019). A family of hyaluronan and proteoglycan binding link proteins (HAPLN), including HAPLN1 (also known as cartilage link protein 1 (CRTL1)) and HAPLN4 (brain-specific link protein 2 (BRAL2)), stabilise the interaction between the hyaluronan chains and CSPGs (Frischknecht and Seidenbecher, 2008; Kwok, Carulli and Fawcett, 2010; Bosiacki *et al.*, 2019). Tenascin molecules (tenascin-R and tenascin-C) further stabilise the PNN structure by crosslinking CSPGs at their C-terminals (Aspberg *et al.*, 1997; Day *et al.*, 2004; Morawski *et al.*, 2014). Each of these components are required for mature PNN development. Hyaluronan and aggrecan have been shown to be fundamental for PNN formation (Giamanco, Morawski and Matthews, 2010; Kwok, Carulli and Fawcett, 2010; Rowlands *et al.*, 2018). Additionally, CTRL1 and tenascin-R are integral to the stability and densely aggregated structure of PNNs, as without these components, neurons display vestigial PNNs (Carulli *et al.*, 2010; Morawski *et al.*, 2014).

The basic structure of PNNs (hyaluronan, CPSGs, link proteins, and tenascins) is similar throughout the CNS, however, PNN composition is highly heterogeneous due to different combinations of isoforms, or family members, of the four main components (Dauth *et al.*, 2016). There are three HAS isoforms: HAS-1, HAS-2 and HAS-3 in the mammalian CNS (Itano and Kimata, 2002). Cortical neurons developing *in vitro* express all three HAS isoforms, whereas *in vivo*, PNNs associated with neurons in the spinal cord express HAS-1 and HAS-3, and cerebellar PNNs contain HAS-2 and HAS-3 (Carulli *et al.*, 2006; Galtrey *et al.*, 2008; Fowke *et al.*, 2017). All four lecticans (aggrecan, brevican, neurocan, and versican) were expressed in the extracellular matrix of brain and spinal cord homogenates (Deepa *et al.*, 2006). Although, differential spatial expression of CSPGs has been identified in the CNS. Aggrecan and brevican were shown to be highly expressed in the hippocampus, however, aggrecan labelled individual PNNs whilst brevican was mainly expressed in the extracellular matrix (Dauth *et al.*, 2016). In contrast, the caudate and putamen displayed many PNNs that expressed both aggrecan and brevican, and also PNNs that only expressed brevican (Dauth *et al.*, 2016). PNNs enveloping neurons in deep cerebellar nuclei, and spinal motor neurons have been shown to express all of the lectican CSPGs (Carulli *et al.*, 2006; Vitellaro-Zuccarello *et al.*, 2007; Irvine and Kwok, 2018). WFA was once considered a ‘universal’ PNN marker, however, PNN structures labelled with CSPG core proteins that lack WFA expression have been visualised in the CNS (Vitellaro-Zuccarello *et al.*, 2007; Yamada and Jinno, 2017; Irvine and Kwok, 2018). This supports that PNNs exhibit variation in the expression of CS-GAGs as well as CSPG core proteins. Furthermore, the morphology of PNNs differs in CNS regions. Cerebral PNNs are mainly discrete and individually distinguishable, whilst PNNs in the spinal cord show higher staining intensity of

the extracellular matrix, almost forming an uninterrupted PNN around many neurons (Carulli *et al.*, 2006; Vitellaro-Zuccarello *et al.*, 2007). Together, these studies demonstrate that PNN composition is highly heterogeneous in the CNS, yet, the functional importance of this is yet to be fully determined.

1.4.5.2 PNN function

PNNs are established in the CNS towards the end of critical periods during postnatal development (Pizzorusso *et al.*, 2002; Nowicka *et al.*, 2009; Mirzadeh *et al.*, 2019). At the closure of critical periods, PNN accumulation is associated with the maturation of parvalbumin-positive interneurons that inhibit excitatory pyramidal cells (Fawcett, Oohashi and Pizzorusso, 2019). PNNs develop around the soma and proximal dendrites of neurons, and transition from having immature, punctate staining, to a contiguous reticular-net structure (Sigal *et al.*, 2019). The holes in the mature perforated structure contain synapses that are secured in place by the PNN (Sigal *et al.*, 2019). This helps to consolidate the neuronal connections that develop from exposure to new sensory experiences during the critical period (Hensch, 2004). The PNN also forms a barrier around the neuron that prevents new synaptic connections from being formed (Sorg *et al.*, 2016). This compact barrier structure harbours inhibitory molecules such as CSPGs and semaphorin 3A that can induce growth cone collapse of approaching neurites, thus further restricting new synapse formation (Sorg *et al.*, 2016; van't Spijker and Kwok, 2017). Additionally, PNNs restrict the mobility of AMPA receptors upon the surface of neurons (Frischknecht *et al.*, 2009). This prevents the exchange of redundant AMPA receptors for new functional ones, reducing synaptic plasticity (Frischknecht *et al.*, 2009).

PNNs predominantly ensheath neurons with fast-spiking activity that colocalise with parvalbumin, a calcium binding protein, and the Kv3.1b subunit of voltage-gated potassium channels (Härtig *et al.*, 1999; Carulli *et al.*, 2006; Vitellaro-Zuccarello *et al.*, 2007). These neurons have distinct electrophysiological properties that enable them to sustain fast-spiking activity. For example, they have low input resistance (high conductance with open membrane channels) and high resting membrane potentials, which facilitates the rapid firing of neurons (Härtig *et al.*, 1999; Okaty *et al.*, 2009). High firing action potentials are dependent on efficient sodium influx and potassium efflux (Carter and Bean, 2009). The presence of Kv3 potassium channels allows for the high speed membrane repolarisation following action potentials (Okaty *et al.*, 2009). Moreover, since PNN aggregates are anionic (containing many negatively charged ions), it is suggested that PNNs act as a buffer/reservoir for cations (positively charged ions) such as calcium, sodium, and potassium (Härtig *et al.*, 1999; Carulli and Verhaagen, 2021). Therefore, PNNs may provide a microenvironment that supports high sodium and potassium currents, and facilitate the activity of fast-spiking neurons.

1.4.5.3 PNN modulation in neural plasticity

As PNNs restrict plasticity, they have become therapeutic targets in order to reinstate plasticity, improve cognitive function, and facilitate neurorehabilitation. PNN formation coincides with the closure of the critical period (Pizzorusso *et al.*, 2002). Rearing animals in the dark during postnatal development deprives them of visual sensory experience. This dark rearing prolongs the duration of developmental plasticity and delays the emergence of PNNs in the visual cortex, which was counteracted by reintroducing animals into normal light living

conditions (Fagiolini *et al.*, 1994; Pizzorusso *et al.*, 2002). Further visual experiments have shown that following monocular deprivation (suppressing the use of one eye), there is a shift in ocular dominance to the non-deprived eye (Fagiolini *et al.*, 1994; Pizzorusso *et al.*, 2002). However, this plastic adaptation is only observed during development and does not occur in the mature CNS. In adult rats, the digestion of CSPGs with chondroitinase ABC reinstated the developmental-like capacity to shift ocular dominance to the non-deprived eye (Pizzorusso *et al.*, 2002; Lensjø, Lepperød, *et al.*, 2017). The chondroitinase ABC-induced plasticity in the visual cortex of adult rats was also shown to have comparable electrophysiological properties to juvenile plasticity, e.g. increased spiking variability and reduced neural activity of inhibitory neurons (Lensjø, Lepperød, *et al.*, 2017). Similar results have been observed in an aggrecan knockout model, where PNNs were ablated, there was a shift in ocular dominance, and juvenile-like plasticity was reinstated (Rowlands *et al.*, 2018).

The aforementioned visual experiments show that PNNs can be modulated in an experience-dependent (e.g. dark rearing) or pharmaceutical manner (e.g. chondroitinase ABC or aggrecan knockout). Eye blink conditioning is another experience (or activity) demonstrating the capacity to modulate PNNs. Eye blink conditioning entails synchronising light and air puff stimulation to the eye. The air puff causes the eye to blink, and with training animals become conditioned to blink at the presence of the light without air puff stimulation. It is well established that eye blink conditioning is dependent on cerebellar circuitry, including: excitatory collaterals of mossy fibres from the basilar pontine nuclei, climbing fibres from the inferior olive, purkinje cells in the cerebellar cortex, and the anterior interpositus nucleus which eventually projects to the facial motor nucleus

to initiate eye blinking (Freeman and Steinmetz, 2011; Carulli *et al.*, 2020). Throughout the learning period of eye blink conditioning, the staining intensity of WFA and aggrecan within PNNs in the deep cerebellar nuclei was downregulated, which was also associated with more conditioned eye blink responses (Carulli *et al.*, 2020). The downregulation of WFA was not maintained when learning plateaued, suggesting that PNNs were strengthened as the memory of eye blink conditioning was consolidated. This was supported as application of chondroitinase ABC in the deep cerebellar nuclei improved the acquisition of eye blink conditioning, whereas it impaired memory retention (Hirono *et al.*, 2018; Carulli *et al.*, 2020).

Supporting the role of PNNs in memory processes, PNNs have been implicated in fear memory (Gogolla *et al.*, 2009; Banerjee *et al.*, 2017; Thompson *et al.*, 2018; Shi *et al.*, 2019). Animals can be conditioned to fear an innocuous stimulus, e.g. a sound, if exposed to it with a simultaneous aversive stimulus such as an electric shock (LeDoux, 2000). The fear of the innocuous stimulus can then be counteracted by subsequent exposure to the innocuous stimulus without the presence of the aversive stimulus, known as fear extinction. Juvenile mice, which lacked WFA staining in the amygdala, demonstrated better fear extinction than older mice in which WFA-positive PNNs had developed (Gogolla *et al.*, 2009). Fear extinction was re-established in adult rodents that were treated with chondroitinase ABC in the amygdala (Gogolla *et al.*, 2009). Removing PNNs with chondroitinase ABC in the auditory cortex prevented fear learning in a paradigm that used sound as the innocuous stimulus (Banerjee *et al.*, 2017). However, chondroitinase ABC treatment in the hippocampus and visual cortex in studies that used sound and light stimuli, respectively, impaired the recall of fear memory

without affecting memory acquisition (Thompson *et al.*, 2018; Shi *et al.*, 2019). These results demonstrate that cells ensheathed by PNNs may have varying functions associated with fear memory throughout different CNS regions.

The ablation of PNNs was also shown to be beneficial for improving object recognition memory (Romberg *et al.*, 2013; Rowlands *et al.*, 2018). Novel object recognition experiments let rodents explore two identical objects, prior to exposure to a new pair of objects: a familiar object (identical to the first pair) and one completely novel object. The animals should remember the familiar object and spend more time exploring the novel object (Lueptow, 2017). The modulation of PNNs via chondroitinase ABC or CTRL1 knockout in the perirhinal cortex was documented to improve object recognition memory (Romberg *et al.*, 2013). Likewise, object recognition memory was improved in an aggrecan knockout model (Rowlands *et al.*, 2018).

In summary, the removal of PNNs in the mature CNS can open a window of plasticity similar to the critical period in postnatal development (Gogolla *et al.*, 2009; Lensjø, Lepperød, *et al.*, 2017; Rowlands *et al.*, 2018). PNNs can be regulated enzymatically, genetically, and by experience/activity. It will be beneficial to further elucidate how PNNs can be regulated and how this alters CNS function in order to maximise the potential of therapeutically targeting PNNs. The function of PNNs appears to vary throughout regions of the CNS. How PNNs have the capacity to contribute to diverse neuronal functions is likely due to heterogeneity in their composition (Sorg *et al.*, 2016).

1.5 Exercise and inhibitory modulators of plasticity

As discussed in the previous section, inhibitory modulators of plasticity are present in the mature CNS, mediating plasticity of actin-rich structures such as neurites and dendritic spines, and stabilising synapses. Voluntary wheel running downregulated the expression of Nogo-A and MAG in the hippocampus of both intact rats and rats that received a traumatic brain injury (Chytrova, Ying and Gomez-Pinilla, 2008). Furthermore, treadmill training reduced the expression of Nogo-A in the rat striatum and cortex following ischaemic stroke (Zhang *et al.*, 2013).

In the intact CNS, voluntary wheel running downregulated the expression of Nogo-A and MAG in the cortex and spinal cord, respectively (Ghiani *et al.*, 2007; Stehle *et al.*, 2021). Additionally, PNNs were downregulated in the hippocampus and upregulated in the spinal cord following voluntary wheel running (Smith *et al.*, 2015). Overall, there is some evidence that exercise training can modulate the expression of inhibitory molecules in the mature CNS, however, this research is extremely limited. This thesis aims to provide a novel insight into how exercise training regulates the expression of inhibitory modulators of plasticity. Understanding how inhibitory modulators are affected by training is the first step to understand how inhibitory and neurotrophic factors cooperate to control exercise-induced plasticity. Understanding this relationship and the resultant structural and functional changes may be pivotal in determining how we can harness the intrinsic response of the CNS following exercise for therapeutic benefit.

1.6 Aims and objectives of thesis

1.6.1 Determining whether exercise training alters the expression of molecules associated with the inhibition of plasticity within the CNS.

Exercise training is known to enhance neural plasticity (Van Praag *et al.*, 1999; Farmer *et al.*, 2004; Eadie, Redila and Christie, 2005; Patten *et al.*, 2013; Nokia *et al.*, 2016). However, there is limited research investigating whether exercise can modulate the expression of inhibitory molecules within the CNS. The first experimental chapter *(Chapter 3: The regulation of inhibitory modulators of plasticity following exercise training)* was intended to be an exploratory study to identify inhibitory candidates that could be investigated throughout the rest of this thesis. The expression of 25 genes involved in the RhoA/ROCK signalling pathway, including inhibitory ligands, membrane receptors, and downstream signalling molecules, were analysed in the hippocampus, cortex, and lumbar regions of the CNS following treadmill training.

The objectives of Chapter 3 were to address:

a) Does treadmill training alter the expression of genes involved in the RhoA/ROCK signalling pathway?

   As exercise training enhances neural plasticity, it was hypothesised that MICT and HIIT would reduce the expression of molecules within the RhoA/ROCK pathway that is known to restrict plasticity. Alterations in the expression of RhoA/ROCK pathway components were expected to be more profound in the hippocampus as it is a highly plastic region of the CNS.

b) Does HIIT downregulate the expression of RhoA/ROCK pathway components to a greater extent than MICT?

HIIT training was previously shown to be superior to MICT for upregulating the expression of the neurotrophic factor BDNF (Afzalpour *et al.*, 2015). Therefore, it was hypothesised that HIIT would also modulate the expression of inhibitory factors (RhoA/ROCK pathway components) to a greater extent than MICT.

1.6.2 Characterising the modulation of PNNs following exercise training.

Voluntary wheel running has previously been shown to downregulate the number and thickness of WFA-positive PNNs in the hippocampus (Smith *et al.*, 2015). Chapter 4 *(Characterising adaptations to perineuronal nets following exercise training)*, investigated whether treadmill training (MICT and HIIT) could also reduce the expression of PNNs within the hippocampus. Aggrecan is a main component of PNNs that is important for PNN formation (Rowlands *et al.*, 2018). Thus, in Chapter 4, PNNs were visualised using immunohistochemistry to label the aggrecan core protein using an aggrecan antibody, and CS-GAG chains using the lectin WFA. To further characterise the effect of exercise training on PNNs, the expression of genes that are involved in the sulphation of CS-GAGs were analysed.

The objectives of Chapter 4 were to address:

a) Does treadmill training (MICT and HIIT) modulate PNN expression in the hippocampus?

   It was hypothesised that MICT and HIIT, like voluntary wheel running, would reduce the number and thickness of PNNs in the hippocampus.

b) Does treadmill training alter the expression of CS-GAG sulphation genes?

   As exercise training is known to enhance plasticity, it was hypothesised that treadmill training would reduce the expression of genes that add the inhibitory sulphation pattern (C4S), and increase the expression of genes that add the plasticity-promoting sulphation pattern (C6S) to CS-GAGs.

1.6.3 Investigating whether exercise enhances memory through the modulation of hippocampal PNNs.

CS-GAG chains can be sulphated at position C4 by the sulfotransferase Chst11, making CS-GAG chains more inhibitory to CNS plasticity (Miyata *et al.*, 2012; Mikami and Kitagawa, 2013). Chapter 5 *(The effect of exercise and hippocampal Chst11 overexpression on object recognition memory)* was the first known study to use AAVs to overexpress *Chst11* in the rodent hippocampus and investigate whether the sulphation patterns of hippocampal CS-GAGs play a role in object recognition memory.

Furthermore, exercise training has been shown to reduce the number and thickness of WFA positive PNNs in the hippocampus (Smith *et al.*, 2015). WFA labels the GalNAc residues of CS-GAG chains (Brückner *et al.*, 1996) which are sulphated by *Chst11*. The degradation of CS-GAGs using chondroitinase ABC has been demonstrated to improve object recognition memory (Romberg *et al.*, 2013; Yang *et al.*, 2015). Thus, Chapter 5 investigated whether exercise training (MICT) improved object recognition memory via the modulation of hippocampal CS-GAGs.

The objectives of Chapter 5 were to address:

a) Does overexpression of *Chst11* in the hippocampus impair novel object recognition memory?

   The overexpression of *Chst11* in the hippocampus was intended to upregulate sulphation at the position of carbon 4 in the GalNAc residues of CS-GAG chains, thus increasing the inhibitory sulphation pattern of CS-GAGs within PNNs. The upregulation of C4S was hypothesised to

increase the level of restriction on hippocampal plasticity and impair novel object recognition.

b) Is there a causal relationship between exercise training, CS-GAG modulation, and improved object recognition memory performance?

It was hypothesised that exercise training would modulate CS-GAG chains that contained the inhibitory C4-sulphation, and therefore attenuate memory-impairments induced by overexpression of hippocampal *Chst11*.

Chapter 2 General materials and methods

2.1 Animals

Adult male Wistar rats (200-250 g) were obtained from Charles River Laboratories (Canterbury, UK, *n*=44) and Central Biomedical Services (University of Leeds, UK, *n*=12). Animals were housed four to a cage with *ad libitum* access to food and water, at 20 ± 1 °C, and under a 12 hour light/dark cycle at Central Biomedical Services (University of Leeds, UK). All procedures were conducted during the light cycle, complied with the UK Animals (Scientific Procedures) Act 1986 (ASPA), and were approved by the University of Leeds Animal Welfare and Ethical Review Committee (Home Office Project license numbers 70/8085 and P7DD7EE20 held by Professor Ronaldo Ichiyama).

2.2 Exercise training protocols

For all chapters, animals were familiarised on a motorised treadmill (Figure 2.1) for five days before being allocated into three experimental groups: CON, MICT, and HIIT. The rats were subjected to their experimental conditions once a day, five days a week, for six weeks (30 days in total). The day after the last day of training, animals were overdosed with an intraperitoneal injection of pentobarbital and tissue was collected.

Figure 2.1. Motorised treadmill apparatus.

A rat running in the custom built treadmill chamber on a motorised treadmill at 5° incline.

2.2.1 Treadmill familiarisation

Animals were familiarised on a motorised treadmill (Panlab, Harvard apparatus, UK) for five minutes over five consecutive days. The treadmill speed was gradually increased from 0 $cm.s^{-1}$ to 50 $cm.s^{-1}$ throughout the week (Table 2.1). If animals faced towards the back of the treadmill the speed was lowered to enable them to return to forward facing. Treats (marshmallows and Cheerios) and mirrors were used to attract the animals to the front of the treadmill. From day three of familiarisation and during training, short bursts of air aimed at the hind limbs were administered through a hole in the door at the back of the treadmill and nudges with a wooden dowel were used to encourage the animals to run. Positive running behaviour was also reinforced with treats.

Table 2.1. Treadmill familiarisation speeds.

Minutes	Day 1	Day 2	Day 3	Day 4	Day 5
0-1	0 $cm.s^{-1}$	20 $cm.s^{-1}$	25 $cm.s^{-1}$	25 $cm.s^{-1}$	25 $cm.s^{-1}$
1-2	0 $cm.s^{-1}$	25 $cm.s^{-1}$	30 $cm.s^{-1}$	30 $cm.s^{-1}$	30 $cm.s^{-1}$
2-3	20 $cm.s^{-1}$	30 $cm.s^{-1}$	35 $cm.s^{-1}$	35 $cm.s^{-1}$	35 $cm.s^{-1}$
3-4	20 $cm.s^{-1}$	35 $cm.s^{-1}$	40 $cm.s^{-1}$	40 $cm.s^{-1}$	40 $cm.s^{-1}$
4-4:30	25 $cm.s^{-1}$	40 $cm.s^{-1}$	45 $cm.s^{-1}$	45 $cm.s^{-1}$	45 $cm.s^{-1}$
4:30-5	25 $cm.s^{-1}$	40 $cm.s^{-1}$	50 $cm.s^{-1}$	50 $cm.s^{-1}$	50 $cm.s^{-1}$

2.2.2 Experimental group allocation (Chapters 3 and 4)

Each day during familiarisation the animals were given a performance rating: good runner (maintained continuous running) – two points; okay runner (some turning/hanging back) – one point; and bad runner (mostly refusing to run) – zero points. Each animal was given a total score out of 10 to measure familiarisation compliance, and ranked by performance (1 the best, 12 the worst). The performance rankings were divided into quartiles. One animal from each quartile was randomly allocated to each experimental group (CON, MICT, or HIIT).

2.2.3 Treadmill conditions

The CON animals remained sedentary throughout the six-week training period. MICT and HIIT animals ran for a total of 33 minutes on the treadmill at 5° inclination, five days a week, for six weeks. MICT and HIIT protocols are presented in Table 2.2. The first three minutes of each treadmill protocol served as a warm up at 25 $cm.s^{-1}$. Following the warm up, MICT animals ran for 30

minutes at 32 $cm.s^{-1}$. HIIT animals ran for 30 minutes with alternating three minute intervals of running at 50 $cm.s^{-1}$ and three minutes walking at 15 $cm.s^{-1}$. The MICT and HIIT protocols were matched for duration and total vertical distance ran.

Table 2.2. Exercise training treadmill protocols.

Protocol	Incline	Warm up	Training duration	Running speed
MICT	5°	3 minutes at 25 $cm.s^{-1}$	30 minutes	32 $cm.s^{-1}$
HIIT	5°	3 minutes at 25 $cm.s^{-1}$	30 minutes (3 minute intervals)	Alternating between 50 $cm.s^{-1}$ and 15 $cm.s^{-1}$

MICT: Moderate intensity continuous training, HIIT: High intensity interval training.

Chapter 3 The regulation of inhibitory modulators of plasticity following exercise training.

3.1 Introduction

For structural and functional plasticity to occur in the CNS, the mechanisms that promote plasticity must outweigh the mechanisms that restrict plasticity. Exercise training is well known to enhance the expression of factors that promote neural plasticity including BDNF, GDNF, and IGF1 (Neeper *et al.*, 1996; Oliff *et al.*, 1998; Tong *et al.*, 2001; Vaynman, Ying and Gómez-Pinilla, 2004; Russo-Neustadt *et al.*, 2004; Berchtold *et al.*, 2005; O'Callaghan, Ohle and Kelly, 2007; Kobilo *et al.*, 2011; Cassilhas *et al.*, 2012; Bechara and Kelly, 2013; Cetinkaya *et al.*, 2013; Afzalpour *et al.*, 2015). However, it is possible that exercise also affects factors that inhibit neural plasticity. Molecules that are known to restrict plasticity such as myelin-associated inhibitors, negative guidance molecules, and CSPGs, are expressed in the mature CNS. These inhibitory ligands are known to trigger RhoA/ROCK signalling that restricts neurite outgrowth and dendritic spine plasticity (Bashaw and Klein, 2010; Giger, Hollis and Tuszynski, 2010; Dickendesher *et al.*, 2012; Fujita and Yamashita, 2014; Liu, Gao and Wang, 2015; Spence and Soderling, 2015; Sami, Selzer and Li, 2020). In the non-injured CNS, there is limited evidence to show that exercise training reduced the expression of the myelin-associated inhibitors Nogo-A and MAG in the hippocampus (Chytrova, Ying and Gomez-Pinilla, 2008). Exercise training has also been shown to reduce the number and thickness of hippocampal PNNs, structures that contain CSPGs, in healthy adult rats (Smith *et al.*, 2015). The aforementioned studies use voluntary wheel running as an exercise paradigm, which lacks translatability to human health due to the high volumes of running involved. It is therefore more suitable to investigate how lower volumes of exercise training, such as MICT and HIIT, modulate the expression of molecules

that restrict plasticity in the CNS. A more complete understanding of how exercise training modulates the factors that both promote and restrict plasticity is fundamental for maximising the therapeutic potential of exercise e.g. for neurorehabilitation or improving cognition.

3.2 Aims

There is a lack of current research investigating the role of exercise training on the regulation of inhibitory molecules in the CNS. Therefore, this first experimental chapter was an exploratory study to identify novel candidates in the field.

This study aimed to determine whether inhibitory molecules involved in the RhoA/ROCK signalling pathway were susceptible to modulation following exercise training (MICT and HIIT) within the hippocampus, cortex, striatum, cerebellum, and lumbar regions of the CNS. Additionally, this study sought to identify whether there were differences between MICT and HIIT on the gene expression of RhoA/ROCK components. It was hypothesised that exercise training would downregulate the expression of genes involved in the RhoA/ROCK pathway, particularly in the hippocampus which is known to be a highly plastic region of the CNS. As previous research has shown that HIIT training was superior to MICT for enhancing BDNF expression, it was expected that greater alterations in the gene expression of RhoA/ROCK pathway components would be observed following HIIT in comparison to MICT.

Alongside assessing transcriptional changes in the CNS following exercise training, this study aimed to investigate the physiological response to MICT and HIIT in the periphery (skeletal muscle) using a citrate synthase assay. It was hypothesised that citrate synthase activity would increase in skeletal muscle following exercise training, as a result of increased oxidative capacity.

3.3 Methods

3.3.1 Study overview

Male Wistar rats (200-250 g) were habituated on a motorised treadmill for five days before being allocated to their experimental groups and completing their exercise protocols once a day, 5 days a week, for six weeks (timeline in Figure 3.1). The experimental groups were: sedentary control (CON); moderate intensity continuous training (MICT); and high intensity interval training (HIIT). For in-depth details of training protocols see General Methods Section 2.2. Animals were euthanised and tissue was collected following the last day of training. Fresh CNS tissue from the hippocampus, cortex, and lumbar region was dissected and snap frozen for use in gene expression experiments (*n*=4 per experimental group). Skeletal muscles (EDL and soleus) were dissected for use in enzymatic assays and fibre typing histology (*n*=8 per experimental group).

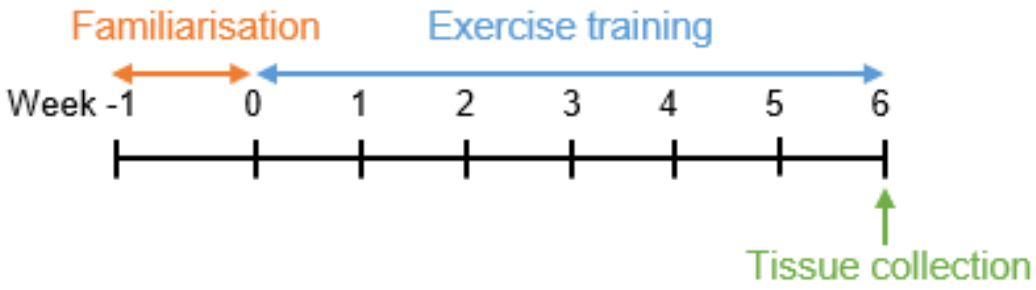

Figure 3.1. Study timeline for experiments in Chapter 3.

Adult male Wistar rats were familiarised on a treadmill over five days before completing six weeks of either a moderate intensity or high intensity interval training protocol (once a day, 5 days a week, for six weeks). One group remained completely sedentary. Tissue was collected following the final day of training for CNS gene expression experiments, muscle enzymatic assays, and muscle histology.

3.3.2 Exercise and physiological assessments

3.3.2.1 Body mass change throughout training

Body mass (g) was measured before each training session throughout the six-week training period. Body mass change throughout the training period was calculated using Equation 3.1.

Equation 3.1. Change in body mass

$$Change\ in\ body\ mass\ (g) =$$

$$Body\ mass\ on\ training\ day\ 30\ (g)\ - Body\ mass\ on\ training\ day\ 1\ \ (g)$$

3.3.2.2 Assessment of aerobic capacity ($\dot{V}O_{2\ max}$)

To assess aerobic capacity, the animals ran on the treadmill whilst the levels of oxygen (O_2) and carbon dioxide (CO_2) where constantly measured from within the treadmill chamber. The $\dot{V}O_{2\ max}$ testing protocol was modified from (Kemi *et al.*, 2002). Animals ran at 20 $cm.s^{-1}$, 25 $cm.s^{-1}$ and 30 $cm.s^{-1}$ for five minutes at each level (25° inclination), followed by an increase of 3 $cm.s^{-1}$ every two minutes until the end of the test. All $\dot{V}O_{2\ max}$ tests were terminated when the rat was incapable, or resistant, of maintaining pace with the treadmill.

$\dot{V}O_{2\ max}$ testing was optimised in a pilot study (*n*=4). Ultimately, it was not possible to assess $\dot{V}O_{2\ max}$ within our experimental set up. The animals were unwilling to comply with exercise at speeds required to elicit $\dot{V}O_{2\ max}$, likely due to this study not using electric shocks to encourage exercise compliance . Additionally, as we did not have access to a metabolic treadmill we had to modify the treadmill chamber to be suitable for respirometry experiments. It was not possible to detect increases in oxygen consumption throughout the $\dot{V}O_{2\ max}$ protocols, likely due to

air leakage around the treadmill belt as were we unable to completely seal the treadmill chamber whilst keeping the treadmill functional.

Thus, estimated total work (J) was calculated at the end of the training study. More detailed information regarding the respirometry system is included in Appendix 1.

3.3.2.3 Estimated total work

Estimated total work was calculated using Equation 3.2 as described in (Constans *et al.*, 2021). Body mass was measured daily prior to each training session. The treadmill grade (8.75%) and exercise duration remained constant throughout the exercise protocols. Treadmill speed was dependent on experimental group (Section 2.2).

Equation 3.2. Estimated total work

$$Estimated\ energy\ expenditure\ (J) = body\ mass\ (kg)\ \times\ treadmill\ speed\ (m.min^{-1}) \times treadmill\ grade\ (\%) \times exercise\ duration\ (minutes)\ \times 9.81$$

3.3.2.4 Citrate synthase assay

Citrate synthase activity was quantified for the extensor digitorum longus (EDL) (fast twitch) and soleus (slow twitch) hindlimb muscles as described in (Eigentler, 2020). Briefly, the proximal and distal portions of each muscle were snap frozen (See section 2.5.3). Approximately 30 mg of tissue was homogenised in 1 mL of RIPA lysis buffer (Sodium chloride 150 mM; Nonidet P-40 1%; Sodium deoxycholate 0.5%; SDS 0.1%; Tris 25 mM) using a bead mill with 7 mm ball bearings (Qiagen, TissueLyser LT) to isolate mitochondria. The RIPA lysis buffer also contained one cOmplete™ EDTA-free Protease Inhibitor Cocktail tablet

(Roche) per 10 mL lysis buffer before being aliquoted for tissue homogenisation. A Pierce™ BCA Protein Assay Kit (ThermoFisher, UK) was used to determine the protein concentration of homogenised samples. For the citrate synthase assay 1 µL of muscle sample was added to 200 µL of reaction buffer (per approximately 1 mL: 900 µL of distilled water (dH_20); 100 µL 5,5′-Dithiobis 2-nitrobenzoic acid (DTNB); and 25 µL acetyl-CoA). Oxaloacetate (10 µL) was injected into the reaction and the absorbance was measured at 412 nm using a Varioskan Flash plate reader (ThermoScientific, UK). The total reaction volume was 211 µL and absorbance readings were taken every 30 seconds for 10 minutes. Two wells containing the reaction reagents with no muscle sample were ran as a negative control. Citrate synthase activity was calculated as described by (Eigentler, 2020).

3.3.2.5 Skeletal muscle fibre typing

Cryostat sections of EDL tissue (10 µm) were cut at -20 °C, collected onto polysine coated slides, and stored at -20 °C. For on-slide immunohistochemistry, slides were left to thaw for 30 minutes at room temperature before a seal was drawn around the sections using a PAP pen (#L4197M, Agar Scientific). Slides were rinsed with 1 M phosphate buffered saline (PBS) to rehydrate the tissue. Slides were then incubated for one hour in 1 M PBS and 5% goat serum containing the primary antibody BA-D5 to label Type I fibres (oxidative) (1:250, Developmental Studies Hybridoma Bank, University of Iowa). Slides were washed with 0.5 % PBST (1 M PBS and 0.5% Triton X-100) and then incubated for one hour with the secondary antibody goat-anti mouse IgG2b Cross-Adsorbed (1:500, A-21242, Alexa Fluor® 647, Invitrogen) diluted in 1M PBS and 12% goat serum. Slides were washed and then incubated for one hour with the primary

antibody SC-71 to label Type IIa fibres (fast oxidative glycolytic) (1:250, Developmental Studies Hybridoma Bank, University of Iowa) diluted in 1 M PBS and 5% goat serum. Slides were then washed and incubated for one hour with the secondary antibody goat anti-Mouse IgG1 Cross-Adsorbed (1:500, A-21121, Alexa Fluor® 488, Invitrogen) diluted in 1M PBS and 12% goat serum. Slides were washed and then incubated for 10 minutes in *Wheat Germ Agglutinin* (1:1000, RL-1022-5, Rhodamine, Vector Labs) diluted in 1 M PBS to distinguish muscle fibre boundaries. Slides were washed and then incubated for one hour with *Griffonia simplicifolia* conjugated with fluorescein to label capillaries (1:200, FL-1101-2, 2B Scientific) diluted in 1 M PBS and 5% goat serum. Slides were washed for a final time and cover slipped using CC/Mount™ tissue mounting medium (C9368, Sigma-Aldrich. Glycolytic Type IIb fibres were left unstained. Tile scans of muscle cross sections were imaged at 20X magnification on an Axio Scan Z1 slide scanner (Zeiss, UK).

3.3.3 Tissue collection

24 hours after the final day of treadmill training, animals were overdosed with an intraperitoneal injection of sodium pentobarbital (200 mg/kg) to induce deep anaesthesia. Once the blink and pedal reflexes were absent, rats were decapitated and fresh dissection of the brain and spinal cord were performed rapidly. The hippocampus, cortex (directly above the hippocampus), cerebellum, striatum, and lumbar region of the spinal cord were snap frozen in Eppendorfs using liquid nitrogen and later stored at −80°C. Skeletal muscle dissections were performed following fresh CNS dissection. The femoral artery was clamped and the left EDL and soleus muscles were dissected and weighed. The muscles were cut with razor blades into three sections. The proximal and distal sections were

stored in Eppendorf tubes and snap frozen in liquid nitrogen. The middle sections were mounted onto cork disks with optimum cutting temperature (OCT, FSC 22 Frozen Section Media, Leica Biosystems) and frozen with isopentane cooled with liquid nitrogen. All muscle tissue was then stored at −80°C. Snap frozen EDL and soleus muscles were used for citrate synthase assays. Corked EDL muscles were used for muscle fibre typing experiments.

3.3.4 Reverse transcription quantitative polymerase chain reaction (RT-qPCR)

Fresh CNS regions (hippocampus, cortex, striatum, cerebellum, lumbar) were homogenised for 10 minutes in 700 µL of TRIzol® using 7 mm stainless steel ball bearings and a TissueLyser LT bead mill (Qiagen, Germany). RNA was extracted using TRIzol® and the PureLink® RNA Mini Kit with On-column PureLink® DNase Treatment (ThermoFisher Scientific, UK). RNA concentration and purity were determined with a NanoDrop™ ND-2000 spectrophotometer. RNA was diluted to 200 ng/µl using ultra-pure nuclease free water.

cDNA was reverse transcribed from 2 µg of RNA using the Precision nanoScript TM2 Reverse Transcription kit (PrimerDesign, UK). cDNA was diluted to 5 ng/µl using ultra-pure nuclease free water. Custom TaqMan® Array Plates were used to quantify the relative gene expression of 25 genes within the RhoA/ROCK signalling pathway of neurite outgrowth inhibition. The wells of the TaqMan® Array Plates were pre-loaded with dried-down TaqMan™ Gene Expression Assays with PCR efficiencies of 100% (see Table 3.1 for gene assay list). The plates were briefly centrifuged before adding the cDNA-master mix. Each 20 µL reaction contained 10 µL of cDNA at 2 ng/µL (total cDNA per reaction: 20 ng) and 10 µL of TaqMan™ Fast Advanced Master Mix (ThermoFisher Scientific, UK).

Plates were sealed with optical adhesive film, briefly centrifuged, and loaded on a CFX96 Touch™ Real-Time PCR Detection System (Bio-Rad, UK). The thermal protocol included a UNG incubation at 50°C for two minutes, an enzyme activation period at 95°C for 20 seconds, and 40 cycles of a one second denaturing step at 95°C and a 20 second anneal/extension step at 60°C. Each sample was ran in duplicate for no template control wells and for each gene expression assay. Gene expression experiment were informed by the MIQE guidelines (Bustin *et al.*, 2009).

3.3.5 Data processing

Relative quantification of target genes was calculated using the $2^{-\Delta\Delta CT}$ method. Relative gene expression was normalised using the reference genes 18s and Cyclophilin A. Data were excluded if the Cq value was above cycle 35 or outside two standard deviations from the mean. Gene expression data within the cerebellum and striatum was either too low to be detected or was excluded due to the above exclusion criteria. Therefore, the cerebellum and striatum could not be analysed. Group sizes for each gene after exclusions were applied are presented in Table 3.2. Heatmaps to visualise relative fold change of target genes were produced in Morpheus, using Euclidean distance and averaging for hierarchical clustering (https://software.broadinstitute.org/morpheus). Statistical tests were performed to identify statistically significant differentially expressed genes (DEGs). As all genes analysed were part of the RhoA/ROCK pathway, smaller gene changes that were not deemed statistically significant individually may still be of biological relevance when observed as a full pathway. Thus, relative fold change cut off values of ≤0.75 and ≥1.5 were used to further explore

the gene expression profiles of the RhoA/ROCK pathway (Hori *et al.*, 2015; Kubo *et al.*, 2015; Yook *et al.*, 2016; Schmidt, Roessler and Schumann, 2018).

Venn diagrams of DEGs were created using InteractiVenn (Heberle *et al.*, 2015) (http://www.interactivenn.net/). The STRING online tool (Version 11.0) was used to generate a protein interaction network of the gene expression profiles created with the cut off values, and to extend the network by predicting a further 10 functional protein interactions (https://string-db.org/). Enrichment analysis was performed by the STRING online tool using the KEGG and Reactome databases. The STRING network was imported into Cytoscape 3.7.2 (Shannon *et al.*, 2003) using the STRINGapp (Doncheva *et al.*, 2019) to visualise and prepare the network for figures.

Table 3.1. TaqMan™ gene expression assay information (RhoA/ROCK pathway).

Gene name	Gene type	TaqMan gene symbol	TaqMan assay ID	Amplicon length
18s	Reference	18s rRNA	Hs99999901_s1	
Cyclophilin A (CyPA)	Reference	Ppia	Rn00690933_m1	
Nogo-A	Target	Rtn4	Rn00582903_m1	90
Myelin-associated glycoprotein (MAG)	Target	Mag	Rn01457782_m1	56
Oligodendrocyte-myelin glycoprotein (OMGp)	Target	Omg	Rn02533851_s1	131
Semaphorin-4D (SEMA4D)	Target	Sema4d	Rn01435039_m1	62
Ephrin-B3 (EFNB3)	Target	Efnb3	Rn01750591_g1	82
Aggrecan (ACAN)	Target	Acan	Rn00573424_m1	74
Versican (VCAN)	Target	Vcan	Rn01493755_m1	89
Neurocan (NCAN)	Target	Ncan	Rn00581331_m1	59
Brevican (BCAN)	Target	Bcan	Rn00563814_m1	71
Nogo receptor 1 (NgR1)	Target	Rtn4r	Rn00586061_s1	57
Nogo receptor 2 (NgR2)	Target	Rtn4rl2	Rn00710574_m1	63
Nogo receptor 3 (NgR3)	Target	Rtn4rl1	Rn01466695_m1	119
Tumour necrosis factor receptor superfamily, member 19 (TROY)	Target	Tnfrsf19	Rn01534699_m1	60
Leucine rich repeat and Ig domain containing 1 (LINGO-1)	Target	Lingo1	Rn03993618_s1	109
Lysophosphatidic acid receptor 1 (LPAR1)	Target	Lpar1	Rn00588435_m1	67
Protein tyrosine phosphatase, receptor type, F (PTPRF)	Target	Ptprf	Rn00695914_m1	70
Protein tyrosine phosphatase, receptor type, S (PTPRS)	Target	Ptprs	Rn00569511_m1	76
Rho-associated coiled-coil containing protein kinase 2 (ROCK2)	Target	Rock2	Rn00564633_m1	73
Guanine nucleotide binding protein, alpha 13 (GNA13)	Target	Gna13	Rn01461471_m1	106
Rho guanine nucleotide exchange factor 12 (LARG)	Target	Arhgef12	Rn01417838_m1	101
LIM domain kinase 1 (LIMK1)	Target	Limk1	Rn01499352_m1	69
Myosin light chain 2 (MYL2)	Target	Myl2	Rn01480558_g1	94
Phosphatase and tensin homolog (PTEN)	Target	Pten	Rn00477208_m1	73
Collapsin response mediator protein 2 (CRMP2)	Target	Dpysl2	Rn01534654_m1	73
Cofilin 1 (CFL1)	Target	Cfl1	Rn01501422_g1	77

Table 3.2. Gene expression group numbers after data exclusions.

Target gene	Hippocampus			Cortex			Lumbar		
	CON (*n*)	MICT (*n*)	HIIT (*n*)	CON (*n*)	MICT (*n*)	HIIT (*n*)	CON (*n*)	MICT (*n*)	HIIT (*n*)
ACAN	3	3	4	3	2	1	4	4	4
BCAN	4	4	4	4	3	4	4	4	4
CFL1	4	4	4	4	3	4	4	4	4
CRMP2	4	4	4	4	3	4	4	4	4
EFNB3	4	4	4	-	-	-	-	-	-
GNA13	4	4	4	4	3	4	4	4	4
LARG	4	4	4	4	3	4	4	4	4
LIMK1	2	2	3	4	3	4	4	4	4
LINGO1	4	4	4	4	3	4	4	4	4
LPAR1	4	4	4	4	3	4	4	4	4
MAG	4	4	4	4	3	4	4	4	4
MYL2	-	-	-	-	-	-	3	4	3
NCAN	4	4	4	4	3	4	4	4	4
NgR1	4	4	4	4	3	4	4	4	4
NgR2	4	2	4	3	3	4	-	-	-
NgR3	4	3	4	3	3	4	-	-	-
NOGO-A	4	4	4	4	3	4	4	4	4
OMGp	4	4	4	4	3	4	4	4	4
PTEN	4	4	4	4	3	4	4	4	4
PTPRF	2	2	4	2	2	1	3	3	3
PTPRS	3	-	1	3	3	2	-	-	-
ROCK2	4	4	4	4	3	4	4	4	4
SEMA4D	4	4	4	4	3	4	4	4	4
TROY	4	4	4	4	3	4	4	4	4
VCAN	4	4	4	4	3	4	4	4	4

3.3.6 Statistical analysis and experimental design

All statistical analysis was performed in IBM SPSS software version 26 (IBM, USA). Shapiro-Wilk tests determined normality prior to conducting statistical tests. Data are presented as means ± standard deviation (SD) unless otherwise

specified. The alpha level was set at 0.05 and statistical significance was denoted in figures with an asterisk (*p<0.05). If other symbols were used they were noted in the figure captions.

3.3.6.1 Exercise and physiological assessments

Data in bar charts are presented as the mean ± standard error of the mean (SEM). All group sizes were *n*=8. A one-way ANOVA followed by Bonferroni post hoc tests were used to determine changes in body mass throughout the six-week training period, and citrate synthase activity in the EDL and soleus muscles. An independent t-test was used to compare total estimated work between the MICT and HIIT groups.

3.3.6.2 RhoA/ROCK pathway RT-qPCR

Data in bar charts are presented as the mean relative fold change compared to the sedentary control group ± SEM. For target genes that were normally distributed, one-way ANOVAs followed by least significant difference (LSD) post hoc tests were used to determine significant differences in relative gene expression between experimental groups. For target genes that were not normally distributed, Kruskal–Wallis H tests followed by Dunn's multiple comparison tests and the Bonferroni correction were used. All statistical analyses were performed on Log2 transformed data. An *n*=4 animals were analysed per group. Table 3.2 specifies if any group sizes fell below *n*=3 after data exclusions were applied.

3.4 Results

To assess whether inhibitory molecules in the CNS were modulated by exercise training (MICT and HIIT) the gene expression of 25 components of the RhoA/ROCK signalling pathway of neurite sprouting inhibition were determined using RT-qPCR. Gene expression profiles of the inhibitory ligands, membrane receptors, and downstream signalling molecules of the RhoA/ROCK pathway following six weeks of treadmill training (33 minutes a day, five days a week) are presented in (Figure 3.2). In general, exercise reduced the expression of multiple genes that are involved in the inhibition of neurite outgrowth within the hippocampus. Whereas, the cortex and lumbar regions were less susceptible to changes in exercise-induced gene expression of RhoA/ROCK pathway components. Gene expression experiments were also performed for the cerebellum and striatum, however, the expression of target genes within these regions was either too low to be included in analysis, or not detected at all.

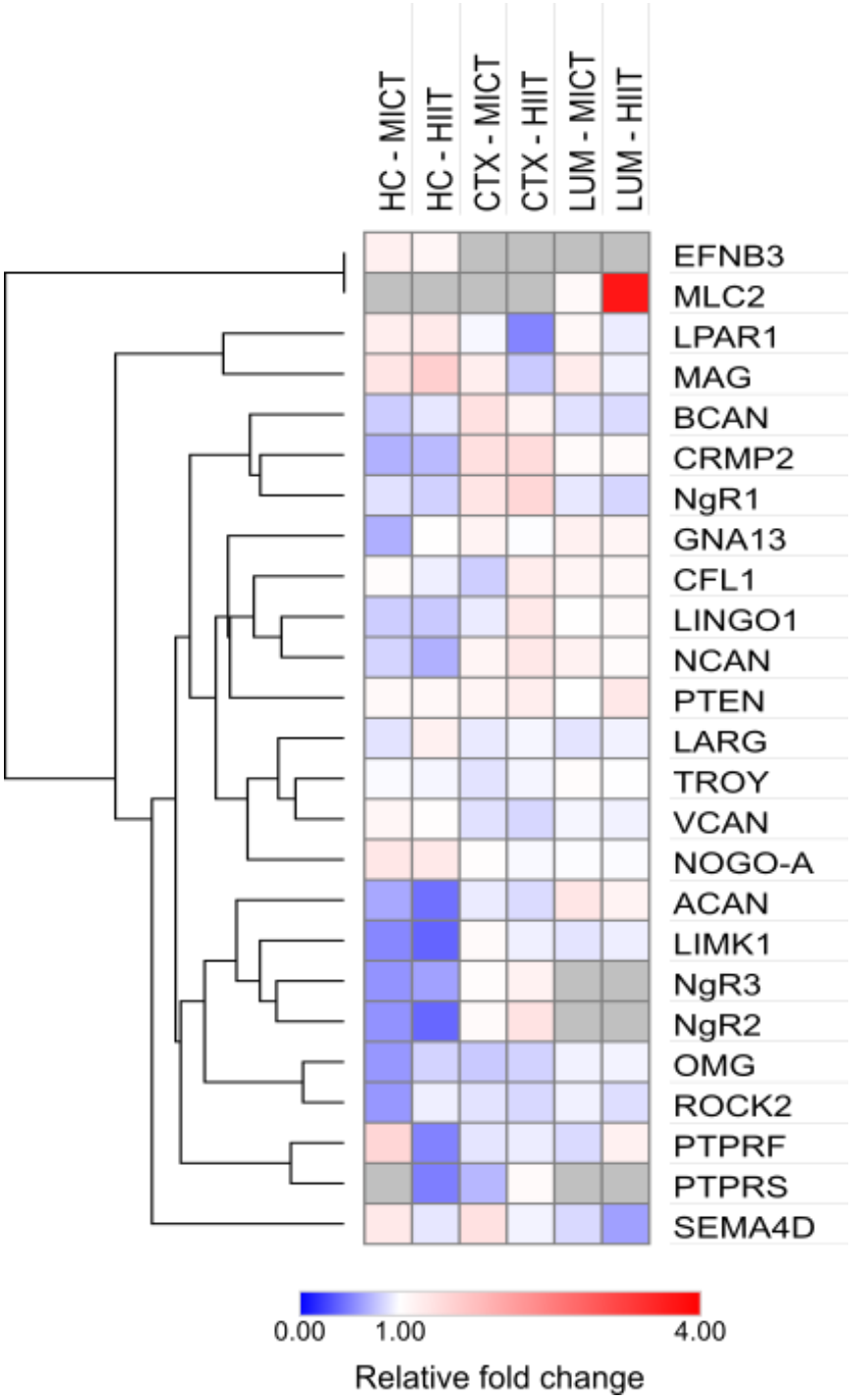

Figure 3.2. Effect of exercise training on the transcription of RhoA/ROCK signalling pathway components in the central nervous system.

Heatmaps presenting the relative fold change of genes involved in the RhoA/ROCK signalling pathway following six weeks of moderate intensity continuous training (MICT) or high intensity interval training (HIIT) in adult male Wistar rats compared to sedentary animals (relative fold change 1). Gene expression profiles were determined for the following CNS regions: hippocampus (HC – first two columns); cortex (CTX – middle two columns); and lumbar spinal cord (LUM – last two columns). Hierarchical clustering was performed using the Euclidean distance method.

3.4.1 Exercise downregulates aggrecan and NgR2 expression in the hippocampus.

Of the 25 genes analysed, two differentially expressed genes (DEGs) were identified following exercise training in comparison to sedentary animals. The relative mRNA expression of *Aggrecan* (a CSPG) was downregulated in the hippocampus following both exercise protocols (MICT: -0.6078 ± 0.17 Log2 FC, p=0.029; HIIT: -1.2057 Log2 FC, p=0.001) ($F(2,7)= 16.902$, p=0.002) (Figure 3.3). Figure 1.2 in the introduction chapter shows were these genes are involved in the RhoA/ROCK pathway. Additionally, HIIT significantly downregulated *Aggrecan* more than the MICT group (p=0.024). Furthermore, *NgR2* (a receptor for MAG) expression was shown to be significantly lower in the HIIT group than in sedentary controls (HIIT: -1.3752 Log2 FC, p=0.005) ($F(2,7)= 8.383$, p=0.014) (Figure 3.3). Hippocampal gene expression data for all target genes are presented in Table 3.3.

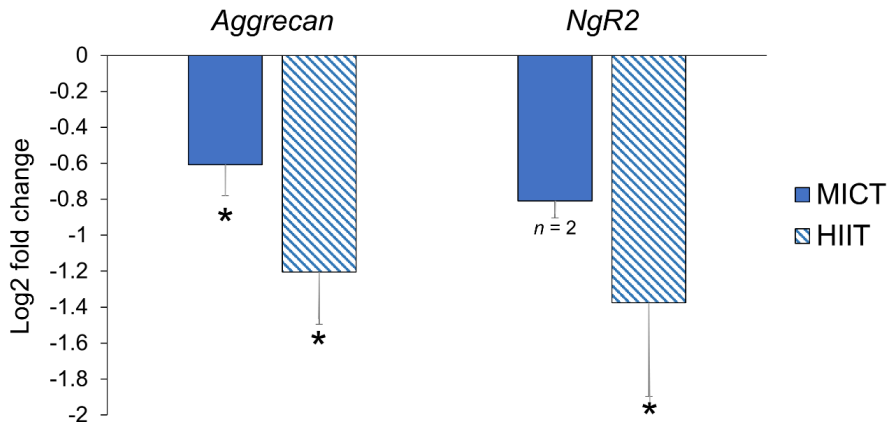

Figure 3.3. Downregulation of hippocampal aggrecan and NgR2 mRNA expression following six weeks of treadmill training.

Gene expression data presented as relative fold change to sedentary controls. Statistical significance determined using a one way ANOVA and LSD correction for multiple comparisons. * $p<0.05$ when compared to sedentary control. *n*=3 or 4 unless stated otherwise. MICT – Moderate intensity continuous training, HIIT – High intensity interval training, NgR2 – Nogo-receptor 2. Bars represent mean relative fold change ± SEM.

Table 3.3. Gene expression of RhoA/ROCK pathway components in the hippocampus following exercise training.

	Mean relative gene expression (Log2 FC) compared to sedentary control (±SD)		
Target gene	MICT	HIIT	Statistical analysis
ACAN	-0.6078 (0.1719) *	-1.2057 (0.2897) *	**F(2,7) = 16.902 p = 0.002**
BCAN	-0.4544 (0.7611)	-0.3540 (0.9175)	F(2,9) = 0.331 p = 0.727
CFL1	-0.0126 (0.4561)	-0.2186 (0.6823)	F(2,9) = 0.151 p = 0.862
CRMP2	-0.5966 (0.4854)	-0.5343 (0.5663)	H(2) = 2.000 p = 0.368
EFNB3	0.1808 (0.4605)	-0.0546 (0.8580)	F(2,9) = 0.134 p = 0.876
GNA13	-0.6927 (0.7413)	-0.1568 (0.7950)	H(2) = 2.808 p = 0.246
LARG	-0.2157 (0.4591)	0.2068 (0.2115)	F(2,9) = 1.619 p = 0.251
LINGO-1	-0.4201 (0.6351)	-0.6044 (1.0967)	F(2,9) = 0.693 p = 0.525
LPAR1	0.1274 (0.7306)	0.2858 (0.3698)	F(2,9) = 0.288 p = 0.757
MAG	0.2420 (0.7568)	0.5076 (0.7330)	F(2,9) = 0.659 p = 0.540
NCAN	-0.3074 (0.4003)	-0.6612 (0.6932)	H(2) = 1.885 p = 0.390
NgR1	-0.3368 (0.7758)	-0.3634 (0.5427)	F(2,9) = 0.303 p = 0.746
NgR2	-0.8084 (0.0950) #	-1.3752 (0.5226) *	**F(2,7) = 8.383 p = 0.014**
NgR3	-0.8081 (0.2445)	-0.8064 (0.7704)	F(2,8) = 2.220 p = 0.171
Nogo-A	0.3194 (0.3726)	0.3311 (0.0985)	F(2,9) = 1.589 p = 0.257
OMGp	-0.9671 (1.0012)	-0.2793 (0.1417)	F(2,9) = 2.694 p = 0.121
PTEN	0.0249 (0.5664)	0.0994 (0.2512)	F(2,9) = 0.069 p = 0.934
ROCK2	-0.9755 (0.9308)	-0.4699 (1.4542)	H(2) = 2.808 p = 0.246
SEMA4D	0.2554 (0.5620)	-0.1706 (0.3377)	F(2,9) = 0.600 p = 0.570
TROY	-0.1514 (0.6697)	-0.1419 (0.6121)	F(2,9) = 0.097 p = 0.909
VCAN	0.1001 (0.4484)	0.0156 (0.3292)	H(2) = 0.269 p = 0.874

Sedentary control Log2 FC = 0. Downregulated gene expression Log2 FC <0. Upregulated gene expression Log2 FC >0. F – one way ANOVA, H - Kruskal Wallis H, Bold text represents $p<0.05$ for difference testing. Statistical significance determined by post hoc tests denoted with * - $p<0.05$ compared to sedentary control, # $n<3$.

All of the genes analysed are involved in the RhoA/ROCK signalling pathway. Although only two DEGs were identified, the accumulation of smaller gene changes that are not classed as statistically significant alone may collectively impact the action of the signalling pathway. Therefore, relative fold change cut off values of ≤0.75 and ≥1.5 were applied to further explore the gene expression profiles of the RhoA/ROCK pathway.

After the cut off points were applied, a total of 11 genes were modulated by exercise training in the hippocampus. The expression profiles identified five commonly downregulated genes between the MICT and HIIT groups (Figure 3.4 A and B); *Acan* (a CSPG), *NgR2* and *NgR3* (two Nogo receptors), *Limk1* (a downstream signalling molecule of *Rock2*), and *Crmp2*, which controls microtubule dynamics (Sumi *et al.*, 2018).

MICT alone downregulated three genes; *Omgp*, a myelin associated inhibitory ligand, and the downstream signalling molecules *Gna13* and *Rock2*. HIIT independently downregulated *Ncan*, a CSPG, and *Ptprs*, a known CSPG receptor, and increased the expression of *Mag*, a myelin-associated inhibitor. These genes were identified by the cut off points and were not shown to be statistically significant individually unless stated earlier within this section.

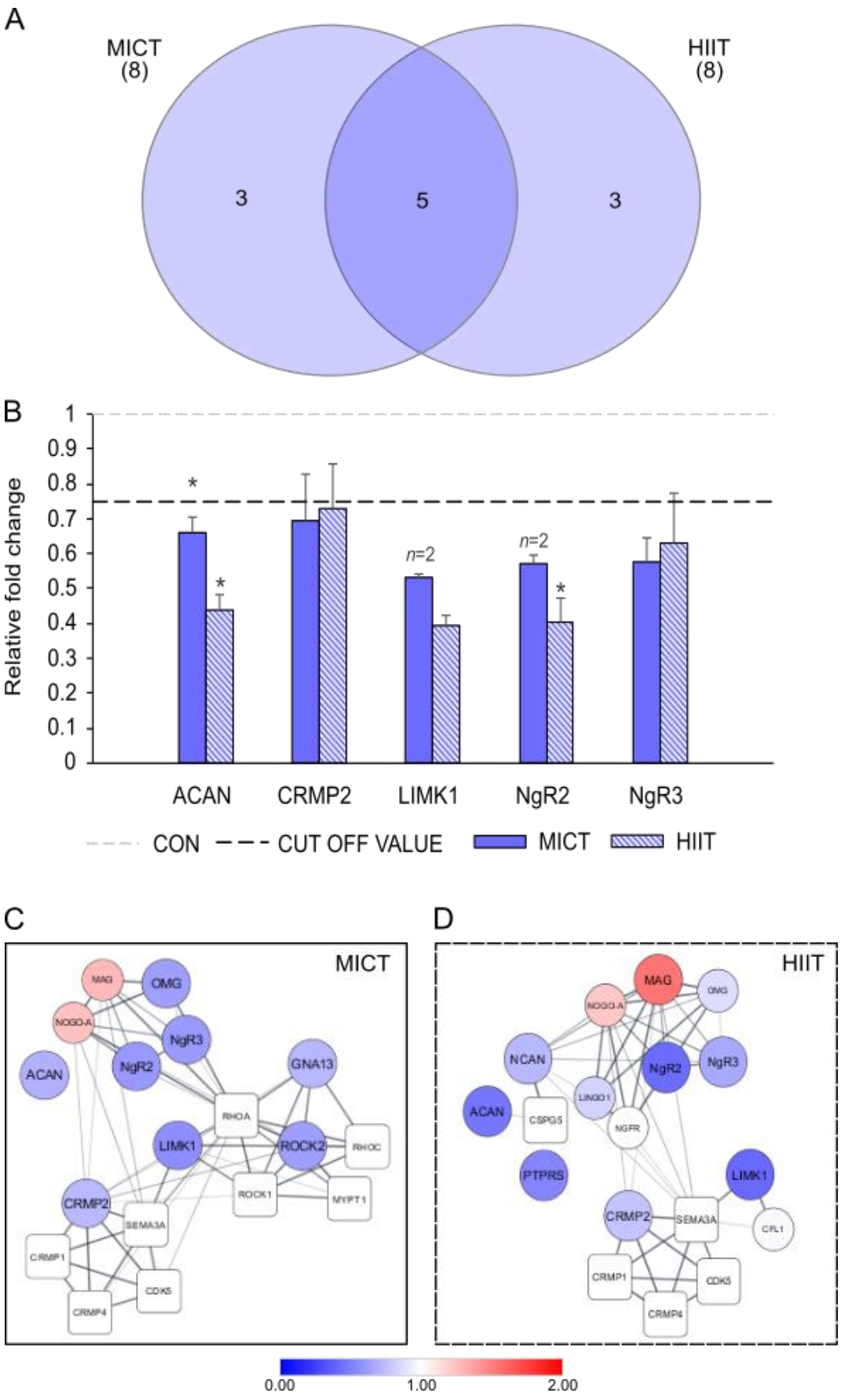

Figure 3.4. Exercise training reduced the expression of inhibitory molecules in the hippocampus.

A. Venn diagram showing the number of modulated genes outside of the cut off values following six weeks of moderate intensity continuous training (MICT) or high intensity interval training (HIIT) in adult male Wistar rats. Modulated genes were determined using ≤0.75 and ≥1.5 as the cut off points for relative fold change (RFC). B. The mean relative fold change of five commonly downregulated genes following MICT and HIIT in comparison to sedentary controls (RFC = 1). MICT significantly reduced the expression of *Acan*, whilst HIIT training significantly reduced the expression of *Acan* and *NgR2* (*=p<0.05). Error bars: mean relative fold change ± SEM. *n*=3 or 4 unless otherwise stated. One way ANOVAs were performed for each target gene separately. C and D. STRING networks showing protein interactions of the gene expression profiles for MICT and HIIT. The larger circles represent genes that were identified as modulated genes in each experimental group. The network was expanded by predicting the next 10 functional interactions. White squares represent the predicted protein interactions of genes that had not been analysed in this study. Smaller circles represent predicted protein interactions of genes that had been analysed in this study, but not identified outside of the cut off values. The colour of the circles represents the relative fold change of gene expression compared to sedentary controls (RFC = 1). Blue – downregulated, Red – upregulated.

3.4.2 Hippocampal STRING networks following exercise.

The online STRING database is an open access tool that scours online resources for known information regarding protein interactions (Szklarczyk *et al.*, 2019). It can be used to display a map of known interactions and functional associations of your candidates with other proteins. In this study, the STRING database was used to visualise the molecular networks of the genes identified by the cut off values, and to predict further protein-protein interactions to gain wider functional insight of the networks. STRING networks for the modulated genes following exercise in the hippocampus are presented in (Figure 3.4 C and D). The networks identified overlapping predicted interactions in the two exercise groups, stemming from the shared gene, *Crmp2*. CRMP2 protein was predicted to be functionally associated with two other members of the collapsin response mediator protein family (CRMP1 and CRMP4), cyclin-dependent kinase 5 (CDK5) and the guidance molecule, semaphorin 3A (SEMA3A).

To further interpret the expanded molecular networks, the STRING database conducted an enrichment analysis to align the gene lists to biological pathways classified by KEGG and Reactome databases. There were two KEGG pathways that were enriched in the MICT and HIIT: 'Axon guidance' and 'Regulation of actin cytoskeleton'. The enrichment of these pathways would be expected as the RhoA/ROCK signalling pathway was investigated in this study due to its role in actin depolymerisation, cytoskeleton disassembly, and thus neurite outgrowth inhibition. Additionally, the 'Alzheimer's disease' KEGG pathway and two Reactome pathways ('Axonal growth inhibition (RHOA activation)' and 'CRMPs in SEMA3A signalling') were commonly enriched in the MICT and HIIT networks. The CRMP family and SEMA3A are also implicated in growth cone collapse (Schmidt and Strittmatter, 2007).

3.4.3 Gene expression within the cortex and lumbar regions is relatively stable following exercise.

Although MICT and HIIT were potent stimuli of transcriptional changes in the hippocampus, the cortex and lumbar regions were much more resistant to exercise-induced changes in the expression of RhoA/ROCK pathway components (Figure 3.2). Treadmill training did not induce any statistically significant differences in relative gene expression in the cortex and lumbar tissue compared to the sedentary controls. However, after the cut off points were applied, one gene was reduced in each of MICT and HIIT, *Ptprs* and *Lpar1*, respectively (both CSPG receptors). In the lumbar region of the spinal cord, MICT did not regulate any genes, whereas HIIT reduced the expression *Sema4d*, a negative guidance molecule, and upregulated *Mlc2* (regulatory myosin light chain – also known as Myl2). STRING networks were not generated for cortical and

lumbar regions due to the low number of genes outside of the cut off values in response to exercise.

3.4.4 Distinct regional gene expression profiles in response to exercise training.

When comparing the cut off value gene expression profiles of each exercise protocol across the hippocampus, cortex and lumbar regions, there were no overlapping genes (Figure 3.5). The broadest transcriptional response to MICT was shown in the hippocampus with eight downregulated genes, including *Acan*, *Omg*, two NOGO receptors, and several downstream signalling molecules. However, in the cortex, MICT only downregulated *Ptprs*.

Similarly, there were no genes modulated by HIIT that appeared in all three regional expression profiles. The widest response occurred in the hippocampus (eight modulated genes), and only one gene was downregulated in the cortex (*Lpar1*). However, HIIT was the only exercise protocol with the capacity to regulate gene expression in the lumbar spinal cord (*Sema4d* and *Mlc2*).

When directly comparing MICT and HIIT, there was only a statistically significant difference in one target gene, with HIIT reducing *Acan* expression more than MICT. For the remaining 24 target genes, there were no statistically significant differences in expression between MICT and HIIT. This suggests that both MICT and HIIT provide comparable transcriptional responses, predominantly downregulating inhibitory genes in the hippocampus. This exercise-induced downregulation of genes that contribute to the inhibition of plasticity may create a more permissive environment for structural and functional changes to take place within the hippocampus.

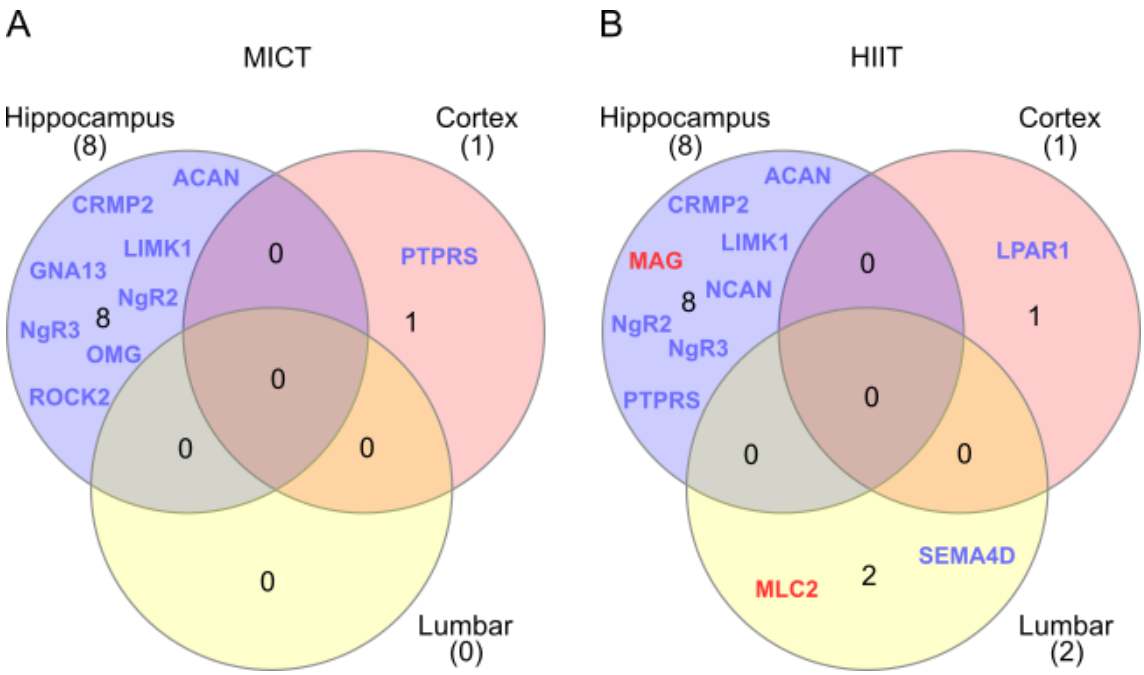

Figure 3.5. The hippocampus shows the largest transcriptional response of inhibitory molecules following exercise training.

Venn diagrams showing the number of modulated genes following six weeks of moderate intensity continuous training (MICT) (A) or high intensity interval training (HIIT) (B) in adult male Wistar rats. Modulated genes were determined using ≤0.75 and ≥1.5 as the cut off points for relative fold change. Blue text represents downregulated genes, and red text represents upregulated genes. There is no overlap in identified genes between any of the three CNS regions analysed: hippocampus, cortex, and lumbar spinal cord.

3.4.5 Physiological assessments following treadmill training.

Following the six week training protocols, the CON group had gained significantly more body mass (52.59 ± 7.10 g) than the MICT (43.11 ± 5.22 g, p=0.028) and HIIT groups (42.97 ± 7.36 g, p=0.026) ($F(2,21)= 5.536$, p=0.012). There was no statistically significant difference in gained body mass between MICT and HIIT (p=1.0), suggesting that each exercise protocol required comparable energy expenditure (Figure 3.6).

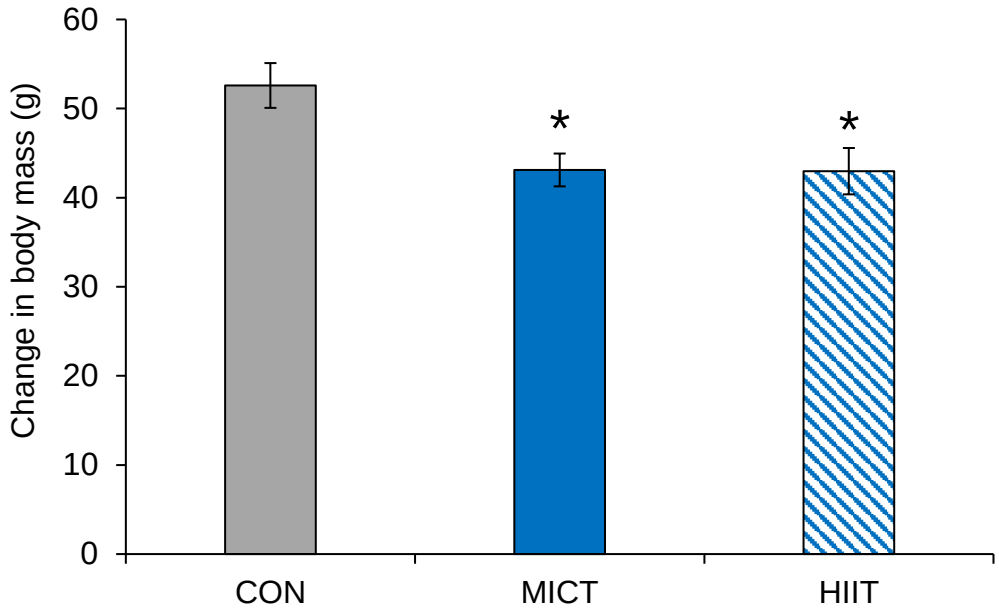

Figure 3.6. Change in body mass throughout six weeks of exercise training.

Exercised male Wistar rats gained less body mass during six weeks of training than sedentary controls. Change in body mass was calculated between training day one and training day 30. Bars represent mean change in body mass ± SEM. *p<0.05 compared to sedentary control. CON – sedentary control; MICT – moderate intensity continuous training; HIIT – high intensity interval training. *n*=8. Statistical significance determined with one way ANOVA and Bonferroni post hoc tests.

The exercise protocols, MICT and HIIT, were matched for duration, distance, and volume. To further characterise the nature of the training protocols, $\dot{V}O_2$ max tests were conducted during a pilot study to measure maximal oxygen uptake. Ultimately, the respirometry set up was not compatible for detecting changes in oxygen levels within our treadmill chamber (as discussed in the methods section). Instead, estimated total work was calculated at the end of the training study. There was no statistically significant difference in the mean total estimated work between the MICT (4726.55 ± 241.42 J) and HIIT groups (4417.17 ± 429.27 J) ($t(14)=1.776$ $p=0.097$) (Figure 3.7). This further supports that the MICT and HIIT protocols were matched for volume of training.

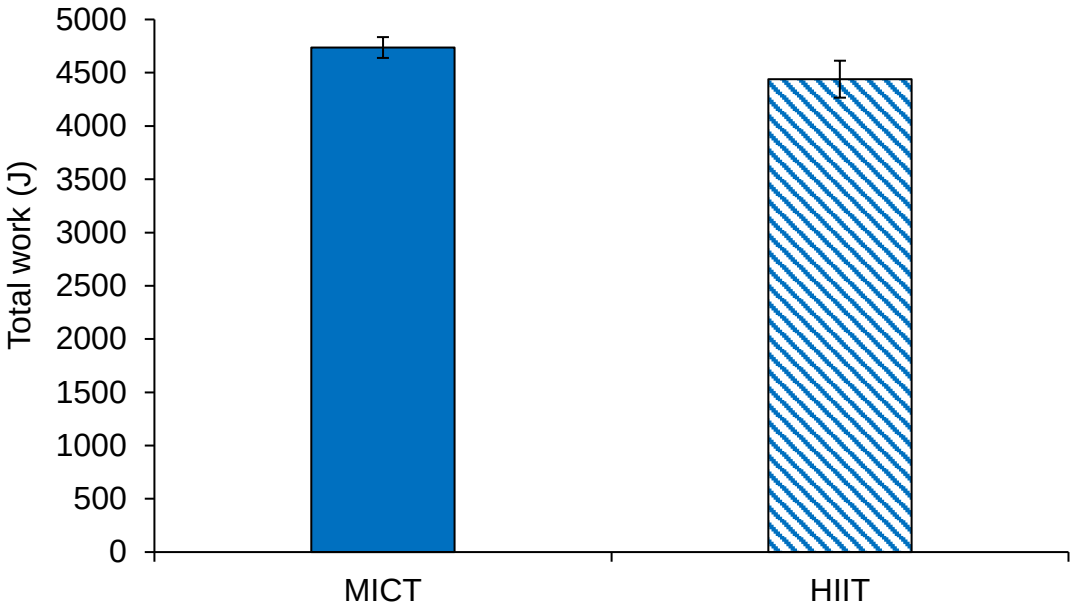

Figure 3.7. Total estimated work throughout six weeks of exercise training.

In adult male Wistar rats, the total estimated work (J) was comparable between both exercise protocols following six weeks of training. Bars represent mean total work ± SEM. *n*=8. MICT – moderate intensity continuous training; HIIT – high intensity interval training. Statistical analysis performed using independent t tests and an alpha level of $p<0.05$.

Since aerobic capacity could not be assessed with $\dot{V}O_2$ max tests, citrate synthase assays were performed in the EDL and soleus muscles. Citrate synthase activity is a marker of oxidative adaptation in skeletal muscle (Vigelsø, Andersen and Dela, 2014). Citrate synthase activity was comparable between all three experimental groups in the EDL (CON: 7.77 ± 2.54 IU; MICT: 5.71 ± 1.11 IU; HIIT: 6.80 ± 0.83 IU; $F(2,21)= 3.054$, $p=0.069$) (Figure 3.8). Similarly, there was no statistical difference in citrate synthase activity in the soleus (CON: 10.36 ± 4.24 IU; MICT: 8.69 ± 2.42 IU; HIIT 9.14 ± 1.69 IU; $F(2,21)= 0.672$, $p=0.521$).

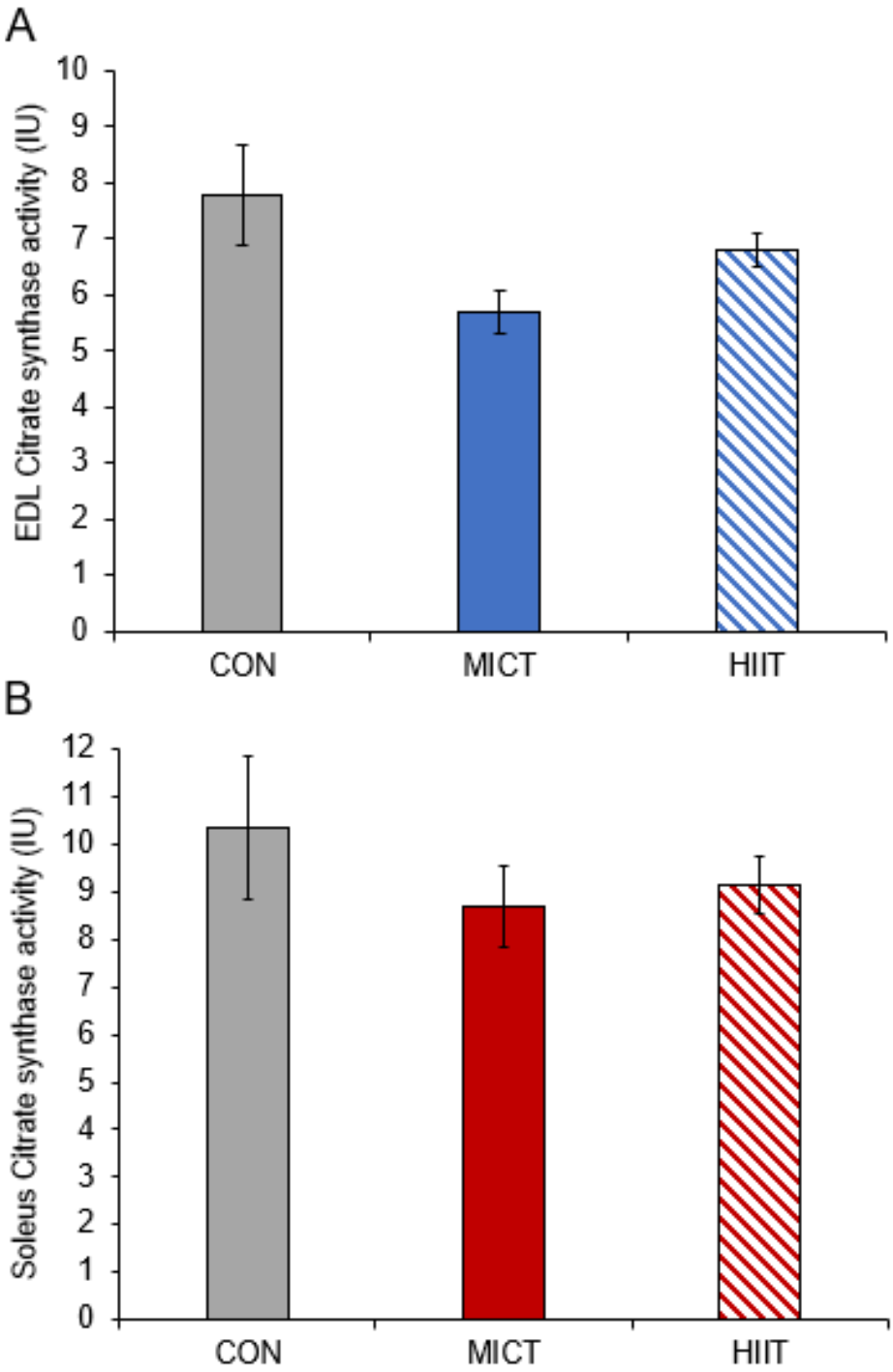

Figure 3.8. Citrate synthase activity.

Citrate synthase activity following six weeks of either moderate intensity continuous training (MICT) or high intensity interval training (HIIT) in adult male Wistar rats. A. Citrate synthase activity in the extensor digitorum longus (EDL). B. Citrate synthase activity in the soleus. Bars represent mean citrate synthase activity ± SEM. *n*=8. IU – international units. Statistical significance determined using a one way ANOVA and Bonferroni post hoc tests. Alpha level $p<0.05$.

3.5 Discussion

This study provided a novel insight into how exercise can be implemented to modulate the expression of inhibitory molecules within the healthy, adult CNS. Both modes of exercise (MICT and HIIT) showed the capacity to reduce the expression of inhibitory molecules within the hippocampus. The exercise-induced transcriptional changes were mainly observed within the hippocampus, whilst the gene expression of inhibitory modulators within the cortex and lumbar regions remained largely unaltered.

3.5.1 Exercise reduced aggrecan expression in the hippocampus.

Six weeks of MICT or HIIT (33 minutes/day, five days a week) significantly downregulated *Acan* mRNA in the hippocampus of male Wistar rats. *Acan* encodes the CSPG aggrecan, which is expressed in the dentate gyrus and CA regions of the hippocampus, and is a major constituent of PNNs (Matthews *et al.*, 2002; Dauth *et al.*, 2016). PNNs are condensed extracellular matrix structures which enwrap subsets of neurons and stabilise synaptic connections, thus limiting synaptic plasticity (Sorg *et al.*, 2016). Enzymatic removal of PNNs using chondroitinase ABC reopens a window of plasticity in the brain, similar to that observed in juvenile development (Pizzorusso *et al.*, 2002; Gogolla *et al.*, 2009; Banerjee *et al.*, 2017; Lensjø, Lepperød, *et al.*, 2017). However, these studies investigated the effect of cleaving the CS-GAG chains of CSPGs to degrade PNNs, and do not focus on the modulation of the CSPG aggrecan specifically.

Targeted *Acan* knockdown in the mouse brain resulted in the absence of PNNs in the adult cortex, and improved object recognition memory (Rowlands *et al.*, 2018). Improved object recognition memory was also observed following chondroitinase ABC removal of PNNs in the mouse perirhinal cortex (Romberg

et al., 2013), although the hippocampus is also an important brain region involved in object recognition memory (Broadbent *et al.*, 2010). Furthermore, the expression of aggrecan and PNNs is reduced during the acquisition of cerebellar motor-learning tasks, and learning is enhanced by targeted PNN degradation in the deep cerebellar nuclei (Carulli *et al.*, 2020). The staining intensity of PNNs in the dorsolateral hump of the deep cerebellar nuclei, measured by WFA and aggrecan, was negatively correlated with the degree of learning (Carulli *et al.*, 2020). There is also evidence that PNNs can be modulated by exercise, with six weeks of voluntary wheel running reducing the number and thickness of PNNs in the rat hippocampus (Smith *et al.*, 2015). Together, these results suggest that the exercise-induced downregulation of *Acan* observed in this study may be important in enhancing hippocampal related learning and memory.

3.5.2 Exercise training downregulated Nogo-receptor 2 in the hippocampus.

Additionally, the HIIT protocol significantly downregulated hippocampal *NgR2* expression. NgR2 belongs to a family of Nogo receptors alongside NgR1 and NgR3, which demonstrate binding of myelin-associated inhibitors (NOGO-A, MAG and OMGp) and CSPGs, and contribute to neurite outgrowth inhibition (Schwab, 2010; Dickendesher *et al.*, 2012). NgR2 was named due to its structural similarity to the first identified Nogo receptor, NgR1 (Pignot *et al.*, 2003). However, unlike NgR1, NgR2 was shown to selectively bind MAG, and no other myelin-associated inhibitors (Venkatesh *et al.*, 2005).

In hippocampal cultured neurons, the reduced expression of *NgR2* in either individual neurons using short hairpin RNA, or by harvesting cultures from *NgR2* knockdown mice, resulted in an increase in the number, size, and intensity of

postsynaptic excitatory synapses (Wills *et al.*, 2012). Moreover, Wills *et al.* (2012) demonstrated that the overexpression of *NgR2* significantly decreased the number of synapses, highlighting *NgR2* as a potent modulator of hippocampal synaptic formation.

In adult mice, *NgR2* knockdown resulted in no changes in dendritic density, length or complexity in the CA1 region; however, whilst dendritic structure remained unchanged, a shift towards more 'mushroom' shaped dendritic spines was observed (Borrie *et al.*, 2014). Increases in the number of mushroom dendritic spines have been observed to accompany increases in spine density following spatial learning (Mahmmoud *et al.*, 2015). The *NgR2* deficient mice showed no alterations in spatial learning and memory during Morris water maze assessments (Borrie *et al.*, 2014), though it would be valuable to explore whether activity-driven modulation of *Ngr2*, rather than genetic ablation, impacts hippocampal learning and memory.

Overall, this study shows that *Acan* and *NgR2* are novel candidates in exercise training related hippocampal plasticity. It is biologically plausible to suggest that the exercise-induced downregulation of *Acan* may lead to modulation of PNNs, thus lifting the degree of restriction they impose upon synaptic plasticity. Coupled with the reduction of *NgR2* expression, this may create a more permissive environment which facilitates synaptic remodelling, and potentially contribute to hippocampal learning and memory.

3.5.3 Exercise reduced the expression profile of inhibitory molecules within the hippocampus.

The accumulation of subtle changes in the expression of multiple genes within a biological pathway may considerably impact pathway function. Therefore, this

study applied cut off values of ≤0.75 and ≥1.5 for relative fold change of the target genes to further explore hippocampal gene expression profiles of the RhoA/ROCK pathway (Hori *et al.*, 2015; Kubo *et al.*, 2015; Yook *et al.*, 2016; Schmidt, Roessler and Schumann, 2018). Both MICT and HIIT reduced the expression of five RhoA/ROCK signalling pathway components: *Acan*, *NgR2*, *NgR3*, *Limk1* and *Crmp2*. RhoA signalling dynamically modulates the actin cytoskeleton and induces neuronal death, neurite retraction, and the loss of dendritic spines/synapses throughout development (Stankiewicz and Linseman, 2014). The RhoA/ROCK pathway remains functional in the adult CNS, restricting the remodelling of actin-rich dendritic spines; thus modulating structural and functional synaptic plasticity which is fundamental for learning and memory (Mulherkar and Tolias, 2020). Furthermore, inhibition of the RhoA/ROCK pathway can enhance neurite outgrowth and has been used to combat pathogeneses of CNS disorders including Alzheimer's disease and strokes, and to improve functional recovery in spinal cord injury models (Kubo *et al.*, 2008). It is possible that the exercise-induced downregulation of RhoA/ROCK pathway components may lead to increased plasticity within the hippocampus, and thus a more complex interplay exists between neurotrophic and inhibitory factors to tightly regulate activity-driven plasticity. It is important to note that the gene expression analysis within this study was limited to 25 genes that were implicated in the restriction of neural plasticity. There may be other candidates involved with plasticity inhibition in the CNS that change in response to exercise training that were not included in this thesis.

Previous research regarding the role of exercise in the modulation of RhoA/ROCK pathway components in the healthy CNS is meagre. However, the

protein expression of NOGO-A and MAG, two myelin-associated inhibitors that are ligands in the RhoA/ROCK pathway, was reduced in the hippocampus of sham rats in a traumatic brain injury model following one week of voluntary wheel running (Chytrova, Ying and Gomez-Pinilla, 2008). Furthermore, *MAG* mRNA and MAG protein expression was downregulated in the lumbar spinal cord of intact rats following seven and 28 days of voluntary wheel running (Ghiani *et al.*, 2007). Within this study, *Nogo-A* mRNA expression remained stable throughout the hippocampus, cortex and lumbar regions following exercise, and *Mag* remained stable in the lumbar enlargement. However, in the previous studies, the reduction in NOGO-A and MAG expression was proportional to the distance ran on running wheels (Ghiani *et al.*, 2007; Chytrova, Ying and Gomez-Pinilla, 2008). Those studies provided 24-hour access to the running wheels, resulting in considerably larger daily distances accrued when compared to treadmill training, which could contribute to the inconsistency of results. Moreover, our treadmill training was implemented across a longer timeline than the wheel running studies, and there is a possibility that earlier alterations in *Nogo-A* expression may have returned to baseline levels with the additional weeks of training. Interestingly, in the present investigation, *MAG* was identified as the only gene to be upregulated following HIIT in the hippocampus (after cut off values applied – no statistical significance individually). The trend in *MAG* upregulation was coupled with a statistically significant reduction in its receptor, *NgR2*. It is possible that the downregulation of *NgR2* may be a way for the CNS to compensate for the observed upregulation of *MAG*.

Although there is variability of results with different exercise paradigms and durations, the present study is the first to show that treadmill training can

significantly reduce the gene expression of *Acan* and *NgR2* in the rat hippocampus.

3.5.4 The hippocampus is the most plastic CNS region in response to exercise.

Following exercise training, the significant downregulation of *Acan* and *NgR2* was only observed in the hippocampus, whilst changes in gene expression in the cortex and lumbar regions were limited. This study specifically investigated genes involved in the inhibition of plasticity. Therefore, it is not surprising that the downregulation of inhibitory genes was reported within the hippocampus, noted as a highly plastic and vulnerable brain region (Dhikav and Anand, 2012).

Due to the paucity of literature pertaining to activity-driven modulation of CNS inhibitory molecules, it is difficult to expand upon these regional differences. However, similar patterns in distinct regional expression of BDNF, a neurotrophic factor that stimulates neurite outgrowth, were also observed in the hippocampus and cortex of exercised rats (Neeper *et al.*, 1996; Serra *et al.*, 2019). The expression of *BDNF* mRNA was significantly increased in the rat hippocampus following two, four and seven days of voluntary wheel running, yet not in the cortical areas that were also analysed in that study (Neeper *et al.*, 1996). The same exercise paradigm also increased *BDNF* mRNA expression in the lumbar enlargement, an area which remained relatively stable in the present study (Gómez-Pinilla *et al.*, 2002). Within the aforementioned studies, *BDNF* mRNA expression was positively correlated with the distance ran, which with 24-hour access to running wheels, accumulates to much further daily distances than what is achieved with treadmill training. Running distance was a controlled variable

between the two exercise protocols adopted in in this study, and thus could not be correlated with inhibitory factor expression.

Treadmill training in rats over 39 days also reported hippocampal increases in BDNF protein levels, which remained unchanged in the cerebral cortex (Serra *et al.*, 2019). That exercise paradigm was more similar to the MICT protocol implemented in this study, with speeds progressing to 30 $cm.s^{-1}$ for up 60 mins. Serra *et al.* (2019) also reported increases in dendritic length, dendritic bifurcations and the number of dendritic ends in cortical neurons following the treadmill training. However, hippocampal neurons remained constant in these measures following exercise, demonstrating yet another divergent, plastic response between the hippocampus and cerebral cortex. Although these hippocampal dendritic measures remained unchanged, Serra *et al.* (2019) did not investigate the number of dendritic spines or alterations in spine morphology; processes which are associated with *NgR2* expression without modifying dendritic structure in the hippocampus (Borrie *et al.*, 2014). Although this literature is not specifically focused on CNS inhibitory molecules, it provides further evidence that other plasticity related factors are being differentially regulated in CNS regions following the same exercise stimulus.

3.5.5 Is HIIT superior to MICT?

The present study is the first to compare different exercise protocols on the modulation of inhibitory molecules in the CNS. The gene expression profiles in this study were mainly similar for MICT and HIIT, although the HIIT protocol induced a greater downregulation of *Aggrecan* than the MICT group. HIIT has previously been shown to increase hippocampal BDNF protein (Freitas *et al.*, 2018), and to be superior to MICT in increasing the protein levels of neurotrophic

factors in the rat brain (Afzalpour *et al.*, 2015). As mentioned previously, *BDNF* mRNA was positively correlated with the distance ran in voluntary wheel running studies (Neeper *et al.*, 1996; Gómez-Pinilla *et al.*, 2002). However, Afzalpour *et al.* (2015) showed that significantly higher increases in BDNF protein levels were attained in six weeks of HIIT treadmill training in comparison to continuous training, despite only running for 40% of the duration, and 47% of the distance of the continuous training group. This suggests that whilst executing lower volumes of training, exercising at the higher intensities in HIIT training may contribute to the further elevation of BDNF protein in the rat brain.

Within the present study, the total duration, distance, and estimated mechanical work were controlled between MICT and HIIT. Thus, the only manipulated exercise parameters were the exercise intensity and the nature of the exercise training (continuous or interval). There were no statistically significant differences in the expression between MICT and HIIT in 24 out of the 25 genes analysed. However, it remains to be questioned whether the HIIT group were exercising at speeds that should be classed as 'high intensity'. Most HIIT studies determine their interval intensities by utilising speeds that correlate with a certain percentage of $\dot{V}O_{2\ max}$ (maximum oxygen uptake). The use of electric shock to encourage exercise compliance is not permitted in the UK. Therefore, it is not possible to exercise rats at speeds beyond their natural will, and true $\dot{V}O_{2\ max}$ measurements could not be measured in this study. Although the speed of 50 $cm.s^{-1}$ in the high intensity intervals is lower than routinely used in the literature, it was the maximum possible speed that the rats would comply with. In eight-week old, untrained, male Wistar rats, the speeds used in our MICT (32 $cm.s^{-1}$) and HIIT (50 $cm.s^{-1}$) protocols at 5° treadmill grade, corresponded to approximately 67%

and 86% $\dot{V}O_{2\ max}$, respectively (Qin *et al.*, 2020). Although the HIIT protocol elicited higher exercise intensities than MICT, 86% $\dot{V}O_{2\ max}$ is still lower than the 90-100% $\dot{V}O_{2\ max}$ bracket often used to characterise HIIT training. In future experiments, it would be advantageous to include physiological measurements such as blood lactate, stress hormones, and inflammatory markers to help classify the HIIT protocol.

3.5.6 Exercise did not induce oxidative adaptation in skeletal muscle.

As it was not possible to assess $\dot{V}O_{2\ max}$ in this study, citrate synthase assays were conducted in skeletal hindlimb muscle as marker of oxidative adaptation to exercise training (Vigelsø, Andersen and Dela, 2014). There were no differences observed in citrate synthase activity of the EDL or soleus muscles following MICT or HIIT. In this study, animals trained for 33 minutes, five days a week, for six weeks. Treadmill training at 15 $m.min^{-1}$, 30 minutes a day, for two weeks (which is slower than the MICT protocol in this study) increased the mRNA expression of citrate synthase in the soleus, whereas there was no change in citrate synthase mRNA at 25 $m.min^{-1}$ (a speed in between the MICT and HIIT protocols in this study) (Farenia *et al.*, 2019). Although this suggests that exercise intensity may influence citrate synthase activity, pooled results from human research showed that citrate synthase activity was not correlated with training intensity, though it was positively correlated with training volume (Bishop, Granata and Eynon, 2014). The latter is corroborated by several rodent studies that show endurance training with higher training volumes (ranging from one to 12 hours per day) increased citrate synthase activity in the soleus, plantaris, and gastrocnemius muscles (Schluter and Fitts, 1994; Inashima *et al.*, 2003; Siu *et al.*, 2003; Gallo *et al.*, 2008). Therefore, changes in citrate synthase activity may not have been

observed during this study due to relatively low training volumes (33 minutes per day).

Skeletal muscle adaptation to exercise can also be determined by analysing fibre type and the capillaries around muscle fibres. Muscle histology has been performed to visualise the different muscle fibre types and capillaries of the EDL muscle (Figure 3.9). However, due to the impact of COVID lab restrictions, data analysis for these images is yet to be completed. Future analysis of muscle fibre types, capillaries, and oxygen transport modelling will be conducted as outlined in (Al-Shammari *et al.*, 2018), to further establish the physiological adaptation to the MICT and HIIT protocols utilised in this study. It is important to note that even though physiological adaptations in the periphery have not yet been confirmed, significant changes within the CNS were still observed.

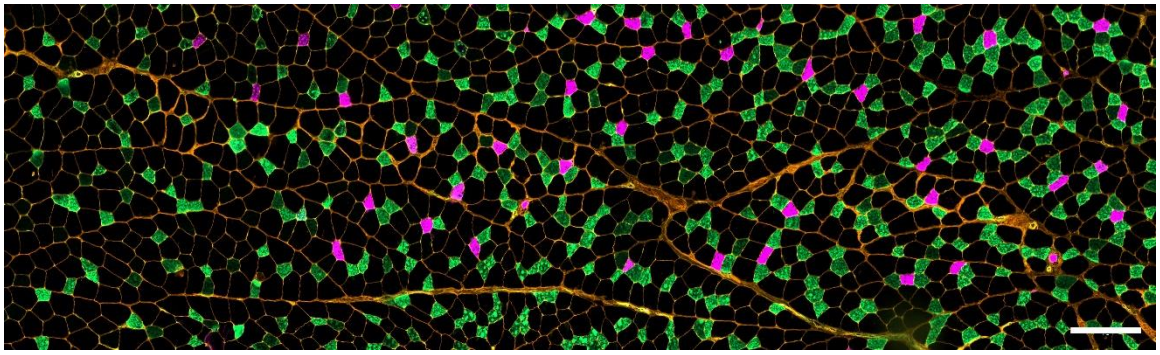

Figure 3.9. Skeletal muscle fibre types in the extensor digitorum longus.

The glycolytic to oxidative gradient of muscle fibre types in the male Wistar extensor digitorum longus. Muscle fibre boundaries (orange) were labelled with wheat germ agglutinin – rhodamine. Oxidative type 1 fibres (magenta) were labelled with BA-D5 and Alexa-Fluor 647 antibodies. Intermediate type 2a fibres (green) were labelled with SC-71 and Alexa-Fluor 488 antibodies. Glycolytic type 2b fibres (black) were left unstained. Scale bar: 200 μm.

3.5.7 Conclusions

To conclude, this study is the first to show that the relative gene expression of *Acan* and *NgR2* can be modulated by treadmill training in the hippocampus; highlighting these genes as novel candidates in exercise-induced hippocampal plasticity. Additionally, it is well known that exercise increases neurotrophic factors in the hippocampus. This study provides evidence to suggest that there are dual effects of exercise training in the hippocampus, essentially 'taking a foot off the inhibitory brakes' and facilitating the 'acceleration' of neurotrophic factors to create a more permissive, plastic environment.

It would be noteworthy to investigate whether the exercise-induced transcriptional changes are corroborated by alterations in protein expression, and whether these changes are localised to specific hippocampal regions. Furthermore, it would be advantageous to determine the functionality of these transcriptional alterations, and to ascertain whether they contribute to structural plasticity and behavioural outcomes such as hippocampal related learning and memory.

Chapter 4 Characterising adaptations to perineuronal nets following exercise training.

4.1 Introduction

In the previous experimental chapter, aggrecan mRNA was significantly downregulated in the hippocampus following six weeks of either MICT or HIIT. Aggrecan is a CSPG expressed in PNN structures throughout the hippocampal dentate gyrus and CA regions (Dauth *et al.*, 2016). PNNs are lattice-like aggregations in the extracellular matrix, that enwrap subsets of neurons in the CNS and restrict plasticity (Sorg *et al.*, 2016). Additionally, aggrecan is major component of PNNs that is essential for PNN formation (Giamanco, Morawski and Matthews, 2010; Rowlands *et al.*, 2018). Previous research has shown that six weeks of voluntary wheel running reduced the number and thickness of PNNs labelled by WFA in the hippocampus (Smith *et al.*, 2015). However, whether shorter durations of exercise training (such as MICT and HIIT that are more translatable interventions for humans) affect the protein expression of other PNN components, such as aggrecan, is yet to be investigated.

Throughout learning and memory processes, PNNs have been observed to be dynamically regulated. A cerebellar motor learning task was shown to reduce the expression of PNNs in the deep cerebellar nuclei, which were restored during memory consolidation (Carulli *et al.*, 2020). Furthermore, object recognition memory was improved by the specific removal of aggrecan in a brain-wide knockout model, and by the use of chondroitinase ABC and the knockout of the link protein, CTRL1, in the perirhinal cortex (Romberg *et al.*, 2013; Rowlands *et al.*, 2018). Exercise training has also been observed to improve spatial and object recognition memory in rodents (Ang *et al.*, 2006; O'Callaghan, Ohle and Kelly, 2007; Cassilhas *et al.*, 2012; Lee *et al.*, 2012; Silva *et al.*, 2012; Bechara and Kelly, 2013; Cetinkaya *et al.*, 2013; Inoue, Hanaoka, *et al.*, 2015). It is possible that the exercise-induced downregulation of aggrecan and PNNs may enhance

neural plasticity, and improve hippocampal-related memory. Determining the structural changes in PNNs following exercise training is the first step in elucidating whether the modulation of PNNs is a mechanism involved in exercise-induced memory improvements.

4.2 Aims

This chapter aimed to identify adaptations in PNNs using the general marker WFA and more specifically how aggrecan expression is modulated following six weeks of MICT or HIIT. Brain sections were immunohistochemically stained using anti-aggrecan and WFA to label aggrecan core protein and CS-GAG chains, respectively. Image analysis was conducted in the hippocampus and motor cortex to investigate whether MICT and HIIT had an effect on the staining intensity, number, and thickness of PNNs. It was hypothesised that treadmill training would reduce the expression of hippocampal PNNs in both number and thickness. Additionally, RT-qPCR was performed in hippocampal tissue to determine whether exercise training altered the expression of genes that are involved in CS-GAG chain sulphation. It was hypothesised that treadmill training would reduce the expression of genes that add the inhibitory sulphation pattern and increase the expression of genes that add the plasticity-promoting sulphation pattern to CS-GAGs, C4S and C6S, respectively.

4.3 Methods

4.3.1 Study overview

Male Wistar rats (200-250 g) were habituated on a motorised treadmill for five days before being allocated to their experimental groups and completing their exercise protocols once a day, 5 days a week, for six weeks (timeline in Figure 4.1). The experimental groups were: sedentary control (CON); moderate intensity continuous training (MICT); and high intensity interval training (HIIT). For in-depth details of training protocols see General Methods Section 2.2. Animals were transcardially perfused and brain tissue was collected following the last day of training. Fixed brain tissue was used in immunohistochemistry experiments (*n*=4 per experimental group). RNA samples from Chapter 3 were used for further gene expression experiments (*n*=4 per experimental group).

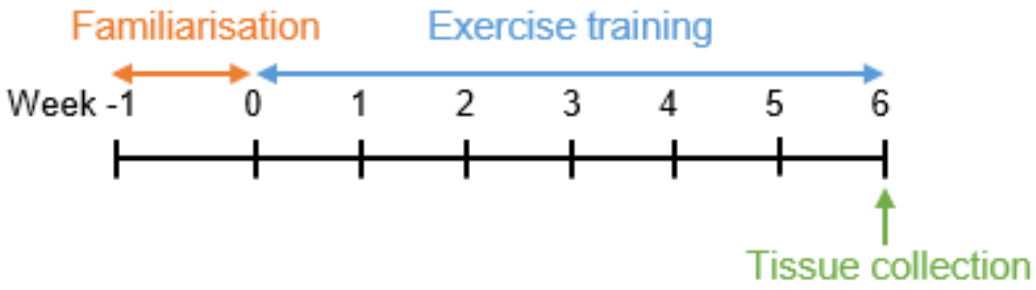

Figure 4.1. Study timeline for experiments in Chapter 4.

Adult male Wistar rats were familiarised on a treadmill over five days before completing six weeks of either a moderate intensity or high intensity interval training protocol (once a day, 5 days a week, for six weeks). One group remained completely sedentary. Tissue was collected following the final day of training for CNS immunohistochemistry and gene expression experiments.

4.3.2 Tissue collection

24 hours after the final day of treadmill training, animals were overdosed with an intraperitoneal injection of sodium pentobarbital (200 mg/kg) to induce deep anaesthesia. Once the blink and pedal reflexes were absent, rats were transcardially perfused (Gage, Kipke and Shain, 2012) with sodium phosphate buffer (1 M PB), followed by 4% paraformaldehyde (PFA), and a final rinse with 1 M PB. Brains were dissected out and post-fixed in 4% PFA overnight at 4°C. The tissue was then cryoprotected in a 30% sucrose solution with 1 M PB and stored at 4°C. Fixed brain tissue was used for immunohistochemistry experiments. Fresh CNS tissue collected in Chapter 3 was used for gene expression experiments.

4.3.3 Immunohistochemistry

4.3.3.1 Tissue preparation

The brain was cut into two coronal segments and mounted in OCT (FSC 22 Frozen Section Media; Leica Biosystems) before being frozen with dry ice and stored at −80°C. Before sectioning the tissue was moved to −20°C overnight to equilibrate to the temperature used within the cryostat chamber. Tissue was cut into 25 µm coronal sections using a cryostat (Leica CM1850; Leica Biosystems). Sections were collected into 24-well plates containing 1 M PBS to dissolve the OCT before being transferred into cryoprotectant and being stored at −20°C.

4.3.3.2 Immunohistochemical staining procedure

Free-floating sections were washed at room temperature, for three five-minute periods in 1 M PBS to remove the cryoprotectant. The sections were then blocked for two hours in 0.2% PBST (1 M PBS and 0.2% Triton X-100) and 3% normal donkey serum (NDS). The sections were then incubated overnight in 0.2% PBST

and 3% NDS, containing the primary antibodies at 4°C. The primary antibodies were the neuronal cell marker anti-NeuN (#MAB377, 1:500, Mouse, Millipore), anti-Aggrecan (#AB1031, 1:250, Rabbit, Millipore), and biotin-conjugated *Wisteria floribunda agglutinin* (WFA) (#L1766, 1:300, Sigma). Anti-Aggrecan and WFA bind to the PNN components of aggrecan core protein and the GalNAc residues of CS-GAG chains, respectively (Brückner *et al.*, 1996; Giamanco, Morawski and Matthews, 2010).

The tissue was then washed three times for 10 minutes in 1 M PBS before being incubated for two hours at room temperature in 1 M PBS containing the following secondary antibodies: donkey anti-mouse (1:1000, Alexa Fluor® 488, Invitrogen), donkey anti-rabbit (1:1000, Alexa Fluor® 555, Invitrogen) and streptavidin (1:250, Pacific Blue™, Invitrogen). The tissue was then washed three times for 10 minutes in 1 M PBS and washed twice for five minutes in tris non-saline (1 M TNS). Sections were mounted onto microscope slides (Superfrost Plus™, ThermoFisher Scientific) using mounting medium (VECTASHIELD® Antifade Mounting Medium, Vector Laboratories). Coverslips were added and sealed with clear nail varnish. Negative control tissue was incubated with only the secondary antibodies (no primary antibodies).

4.3.3.3 Image acquisition

Images were acquired in the Bio-Imaging Facility at the University of Leeds with the assistance of Dr Sally Boxall and Dr Ruth Hughes. Full tile scans of the dorsal hippocampus (between Bregma -3.14 and -3.80 mm) and the primary motor cortex (Bregma: 1.60) were taken at 20X magnification on an Axio Scan Z1 slide scanner (Zeiss, UK). Images were assigned a new code so that image analysis could be performed blinded to experimental groupings.

4.3.3.4 Image analysis

All image analysis was conducted in the software Fiji for ImageJ (Schindelin *et al.*, 2012). Group sizes of *n*=3 were used for histology experiments. Tissue sections between Bregma -3.14 and -3.80 mm that displayed the dorsal hippocampus were chosen for analysis. Five sections were imaged per animal to ensure that a minimum of three sections could be analysed. All analysis was performed bilaterally. The normalised results were averaged between the two hemispheres. The mean of normalised results were then calculated per animal (mean of 3-5 sections) and then per experimental group (mean of 3 animals). All custom written macro scripts are included in Appendix 2.

4.3.3.4.1 Regions of interest

For hippocampal analysis, 12 regions of interest (ROI) were manually drawn with the polygon tool covering the CA regions (1-4) and dentate gyrus of the hippocampus (Figure 4.2). For the primary motor cortex two ROIs were drawn representing the M1 region of each hemisphere (Figure 4.3). Hippocampal and cortical ROIs were outlined with reference to Bregma -3.30 mm and Bregma 1.60 mm, respectively, in the Rat Brain Atlas (Paxinos and Watson, 2013). Custom macro scripts were written to automate the renaming and saving process of ROIs (Appendix 2).

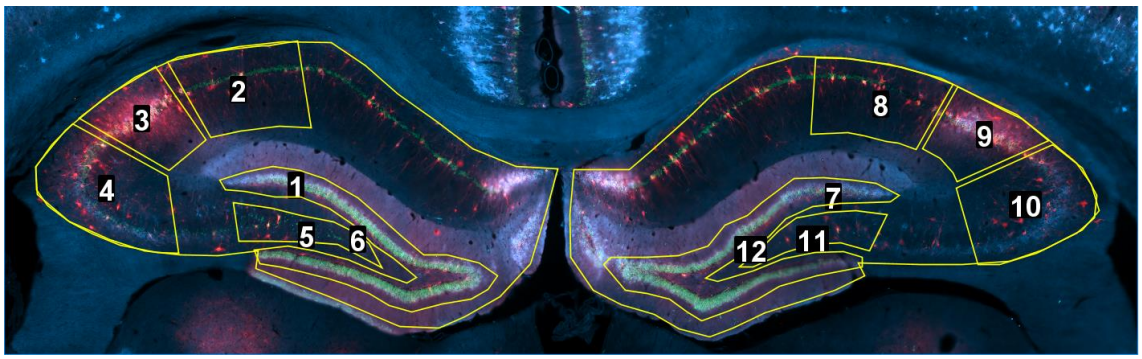

Figure 4.2. Hippocampal regions of interest.

Hippocampal regions of interest manually drawn using ImageJ. 1 – Left total hippocampus (the number label is in the middle of the whole outlined region); 2 – Left CA1; 3 – Left CA2; 4 – Left CA3; 5 – Left CA4; 6 – Left dentate gyrus; 7 - Right total hippocampus (the number label is in the middle of the whole outlined region); 8 – Right CA1; 9 – Right CA2; 10 – Right CA3; 11 – Right CA4; 12 – Right dentate gyrus. Regions outlined using Figure 33 (Bregma -3.30 mm) in the Rat Brain Atlas (Paxinos and Watson, 2013).

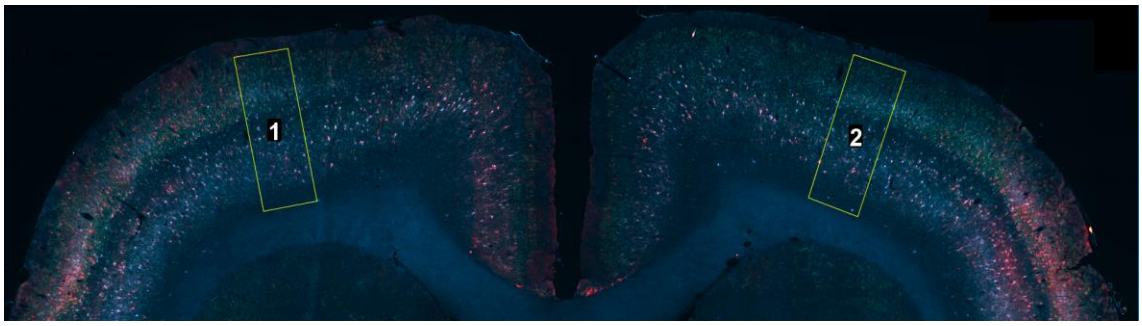

Figure 4.3. Motor cortex regions of interest.

Primary motor cortex (M1) regions of interest manually drawn using ImageJ. 1 – Left M1, 2 – Right M1. Regions outlined using Figure 12 (Bregma 1.60 mm) in the Rat Brain Atlas (Paxinos and Watson, 2013).

4.3.3.4.2 Staining intensity

The staining intensity of aggrecan and WFA (mean gray value), area, and integrated density were recorded for each ROI using a custom macro script (Appendix 2). Staining intensity was normalised by subtracting the mean gray value for the respective negative control from the experimental mean gray value. For each ROI, the normalised staining intensity was averaged between the two

hemispheres. The mean normalised staining intensity was then taken for all sections per animal and then for each animal per experimental group.

4.3.3.4.3 PNN counts

PNNs were counted using the Cell Counter plugin (Kurt de Vos; https://imagej.nih.gov/ij/plugins/cell-counter.html). Three different PNN phenotypes were counted: 1) PNNs that express both aggrecan and WFA (ACAN+ WFA+); 2) PNNs that express only aggrecan (ACAN+ WFA-); and 3) PNNs that express only WFA (ACAN- WFA+). PNN counts were normalised to the area of the ROI and converted from μm to mm (Equation 4.1). The total PNN count was calculated as the sum of all three phenotype counts.

Equation 4.1. Normalised PNN count.

$$Normalised\ PNN\ count\ (mm^2) = \left(\frac{Number\ of\ PNNs}{Area}\right) \times 1000$$

4.3.3.4.4 PNN thickness

PNN thickness was measured by drawing four intersecting lines for the outer distance of the PNN and four intersecting lines for the inner distance of the PNN (Figure 4.4). PNN thickness was then calculated using Equation 4.2. PNN thickness was analysed separately for aggrecan and WFA positive PNNs for each hippocampal region. All visible PNNs were included in analysis if the outer and inner edges of the PNN could be clearly defined.

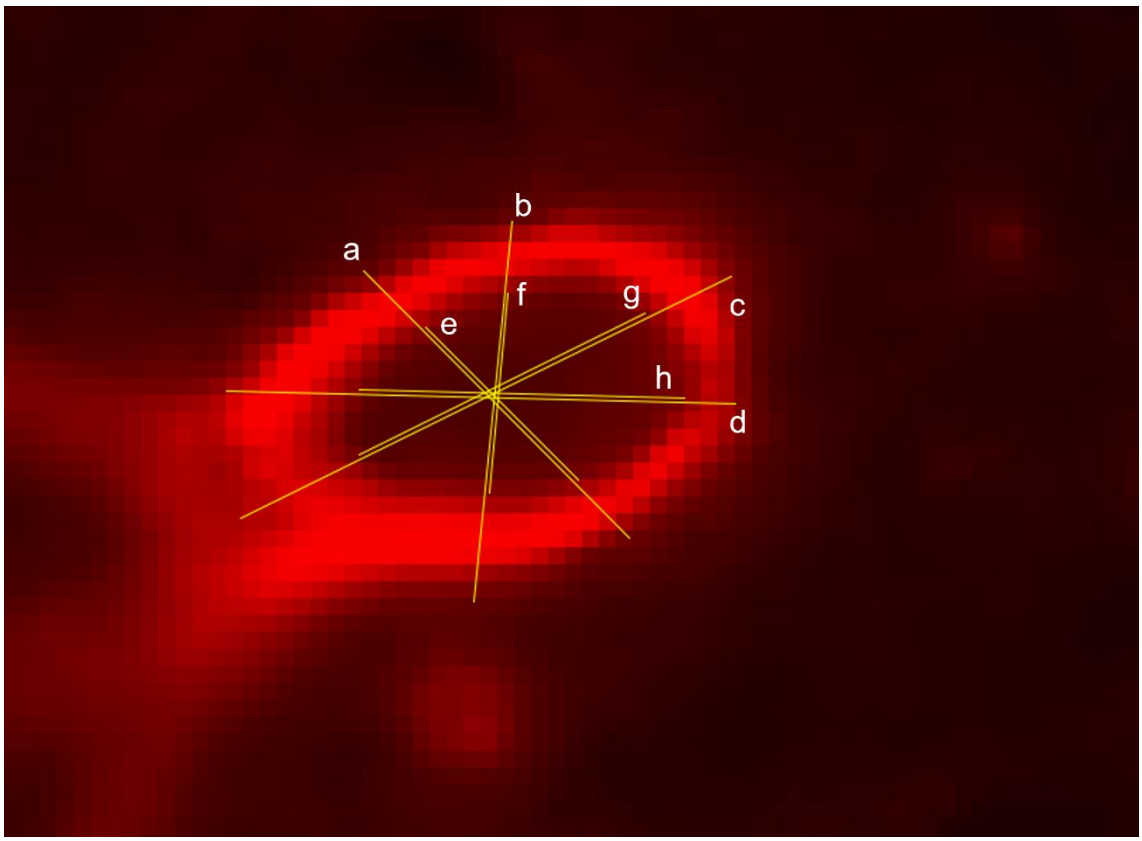

Figure 4.4. Analysing PNN thickness.

PNN thickness was calculated by subtracting the mean inner distance of the PNN (e-h) from the mean outer distance of the PNN (a-d) and divided by 2.

Equation 4.2. PNN thickness.

$$PNN\ thickness\ (\mu m) = \frac{(Mean\ outer\ PNN\ distance\ - Mean\ inner\ PNN\ distance)}{2}$$

4.3.4 RT-qPCR

The expression of CS-GAG sulphation genes (Table 4.1) was analysed in hippocampal tissue using RT-qPCR as outlined in Section 3.3.4. Gene expression was analysed using the $2^{-\Delta\Delta CT}$ method and normalised to the expression of the reference gene 18s.

Table 4.1. TaqMan™ gene expression assay information (CS-GAG sulphation).

Gene name	Gene type	TaqMan gene symbol	TaqMan assay ID	Amplicon length
18s	Reference	18s rRNA	Hs99999901_s1	
Carbohydrate (chondroitin 6) sulfotransferase 3 (CHST3)	Target	Chst3	Rn00584637_m1	100
Carbohydrate (N-acetylgalactosamine 4-0) sulfotransferase 8 (CHST8)	Target	Chst8	Rn01764506_m1	100
Carbohydrate (chondroitin 4) sulfotransferase 11 (CHST11)	Target	Chst11	Rn01509313_m1	81
Carbohydrate (chondroitin 4) sulfotransferase 12 (CHST12)	Target	Chst12	Rn01756351_m1	109
Carbohydrate (chondroitin 4) sulfotransferase 13 (CHST13)	Target	Chst13	Rn01426125_s1	76
Carbohydrate (N-acetylgalactosamine 4-sulfate 6-O) sulfotransferase 15 (CHST15)	Target	Chst15	Rn00597859_m1	72

4.3.5 Statistical analysis and experimental design

Data are presented as means ± standard deviation (SD) unless otherwise specified. The alpha level was set at 0.05 and statistical significance was denoted in figures with an asterisk (*p<0.05). If other symbols were used they were noted in the figure captions. Shapiro-Wilk tests determined normality prior to conducting statistical tests. All statistical analysis was performed in IBM SPSS software version 26 (IBM, USA).

4.3.5.1 PNN immunohistochemistry

Data in bar charts are presented as the mean ± SEM. A minimum of three sections per animal (*n*=3) were analysed for staining intensity, PNN counts, and PNN thickness. Differences in the mean staining intensity of aggrecan and WFA,

PNN counts, and PNN thickness were analysed using Kruskal–Wallis H tests, followed by Dunn's multiple comparison tests and the Bonferroni correction.

4.3.5.2 CS-GAG sulphation RT-qPCR

Data in bar charts are presented as the mean relative fold change in comparison to the sedentary control group ± (SEM). A one-way ANOVA determined differences in the relative gene expression between experimental groups followed by Bonferroni post hoc tests. Statistical analyses were performed on Log2 transformed data.

4.4 Results

4.4.1 Exercise does not alter the staining intensity of aggrecan and WFA in the hippocampus.

CSPGs are expressed in the loose extracellular matrix and in PNN structures, thus, intensity measurements were recorded for full hippocampal regions: CA1, CA2, CA3, CA4, and the dentate gyrus (outlined in Figure 4.5). Following six weeks of treadmill training, there were no statistically significant differences in the staining intensity of aggrecan or WFA in any hippocampal region (Figure 4.6, Statistical analyses reported in Table 4.2).

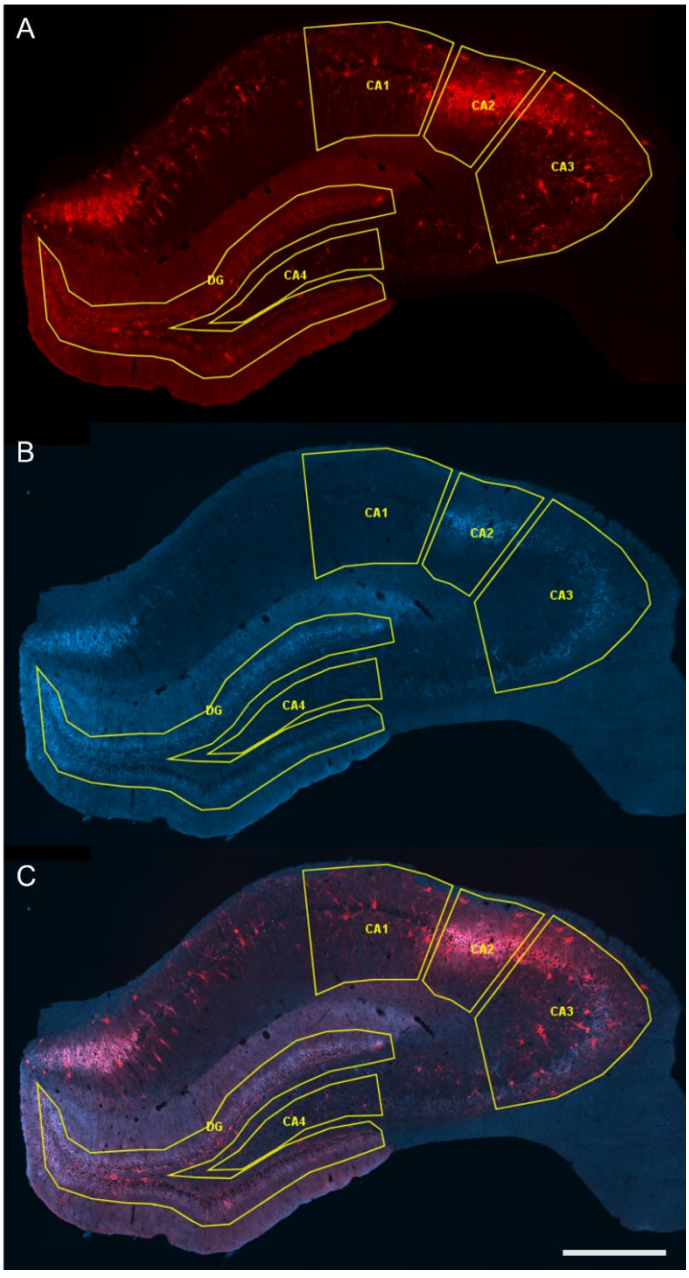

Figure 4.5. Hippocampal regions of interest.

Hippocampal regions of interest are outlined in yellow including CA1, CA2, CA3, CA4, and dentate gyrus (DG).

A. Hippocampal tiles scan labelled for aggrecan core protein.

B. Hippocampal tile scan labelled for CS-GAG chains with *Wisteria Floribunda Agglutinin* (WFA).

C. Merged hippocampal tile scan displaying both aggrecan (red) and WFA (blue) labelled perineuronal nets. Scale bar: 200 μm.

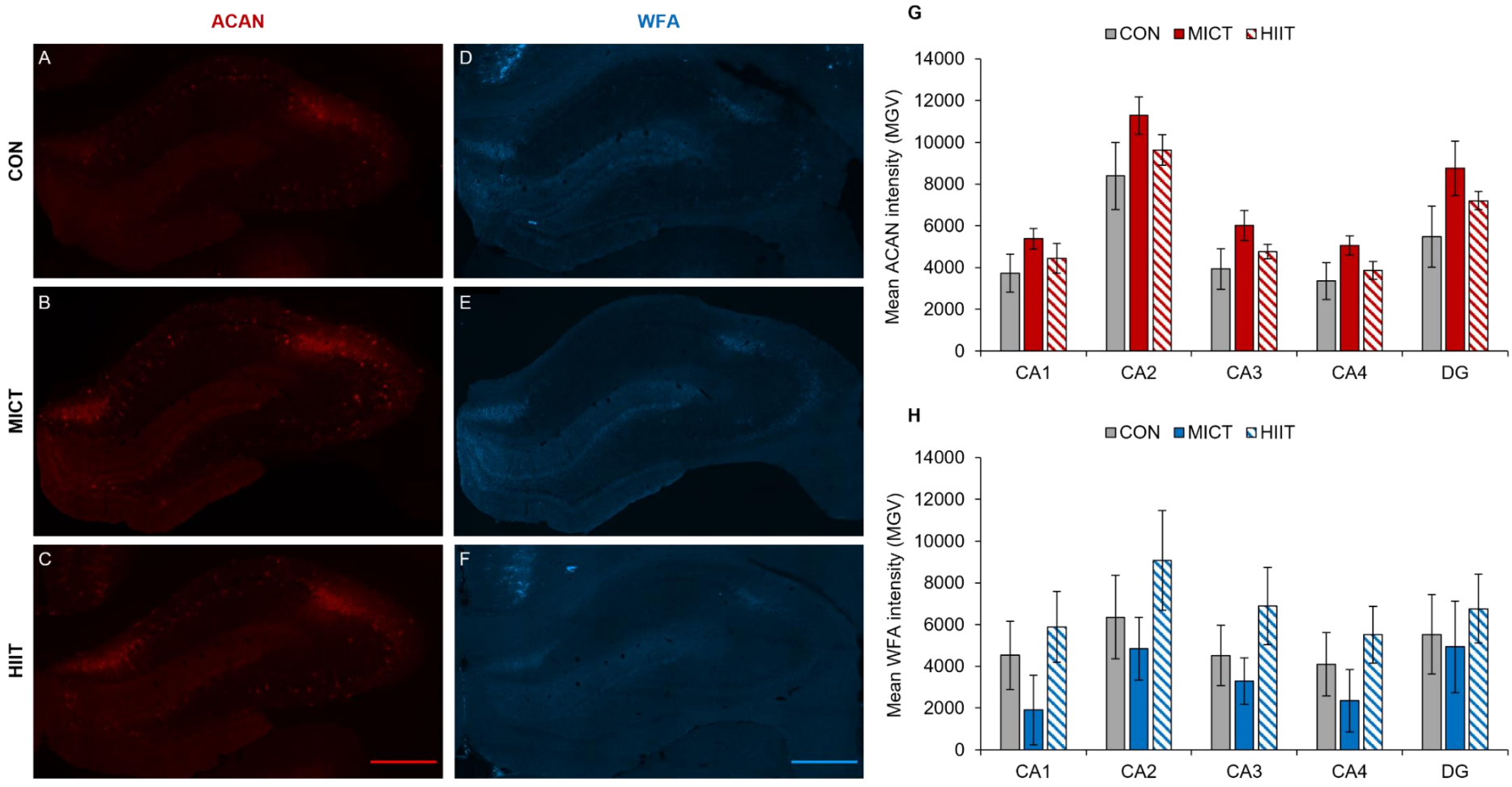

Figure 4.6. Exercise training does not alter aggrecan or WFA staining intensity in the hippocampus.

A-C. Hippocampal tile scans stained for aggrecan core protein (ACAN). D-F. Hippocampal tile scans stained for *Wisteria floribunda agglutinin* (WFA) that labels glycosaminoglycan chains of chondroitin sulphate proteoglycans. Scale bars: 200 µm. CON: sedentary control, MICT: moderate intensity continuous training, HIIT: high intensity interval training. G. Mean aggrecan staining intensity in hippocampal regions following exercise training. H. Mean WFA staining intensity in hippocampal regions following exercise training. Staining intensity was measured using mean gray value (MGV) in ImageJ that was normalised by subtracting the background staining of negative control tissue. There were no statistically significant differences in mean aggrecan or WFA staining following six weeks of either MICT or HIIT in the male Wistar hippocampus. Bars represent mean staining intensity ± SEM, $n=3$. Statistical significance determined using Kruskal Wallis H tests, alpha level $p<0.05$. DG: dentate gyrus.

However, MICT showed a trend for increased aggrecan staining intensity in the CA4 region (CON: 3352 ± 1530 MGV; MICT: 5063 ± 808 MGV; HIIT: 3866 ± 739 MGV; H(2)=5.600 p=0.061). Additionally, in every hippocampal region, aggrecan staining intensity was the highest in the MICT group, followed by HIIT, and then the sedentary control group (Figure 4.6). In contrast, MICT resulted in the lowest WFA intensity out of each experimental group, whilst HIIT trained animals displayed the highest WFA intensity, in every hippocampal region (Figure 4.6). As the staining intensity patterns were consistent in each hippocampal region following both exercise training protocols, it is possible that these widespread changes in the hippocampus have biological relevance despite lacking statistical significance.

Table 4.2. Aggrecan and WFA staining intensity following exercise training in the hippocampus.

		Mean staining intensity (MGV)			
		CON (SD)	MICT (SD)	HIIT (SD)	Kruskal-Wallis H
ACAN					
	CA1	3726 (1560)	5380 (845)	4438 (1238)	H(2)=1.867 p=0.393
	CA2	8394 (2788)	11286 (1542)	9640 (1269)	H(2)=1.867 p=0.393
	CA3	3933 (1679)	6017 (1246)	4770 (597)	H(2)=3.467 p=0.177
	CA4	3352 (1530)	5063 (808)	3866 (739)	H(2)=5.600 p=0.061
	DG	5479 (2536)	8757 (2248)	7209 (759)	H(2)=2.756 p=0.252
WFA					
	CA1	4530 (2822)	1906 (2893)	5881 (2943)	H(2)=1.867 p=0.393
	CA2	6359 (3466)	4847 (2608)	9073 (4143)	H(2)=1.867 p=0.393
	CA3	4525 (2511)	3296 (1913)	6893 (3209)	H(2)=1.867 p=0.393
	CA4	4101 (2629)	2350 (2601)	5512 (2370)	H(2)=1.422 p=0.491
	DG	5524 (3293)	4934 (3805)	6763 (2866)	H(2)=1.867 p=0.393

MGV – mean gray value, CON – sedentary control, MICT – moderate intensity continuous training, HIIT – high intensity interval training, SD – standard deviation, ACAN – Aggrecan, WFA – *Wisteria floribunda agglutinin. n=3.*

4.4.2 Exercise training increased the number of PNNs that only expressed aggrecan in the hippocampus.

For each hippocampal region, the total number of PNNs was calculated as the sum of PNNs that express aggrecan only, WFA only, or both aggrecan and WFA together. Each PNN was only counted once. Exercise training did not have an effect on the total number of PNNs in each hippocampal region (Table 4.3).

Table 4.3. Total PNN counts following exercise training in the hippocampus.

Total PNN count (PNN/mm^2)				
	CON (SD)	MICT (SD)	HIIT (SD)	ANOVA
CA1	0.343 (0.056)	0.283 (0.061)	0.299 (0.096)	F(2,6) = 0.530 p=0.614
CA2	0.163 (0.025)	0.160 (0.022)	0.139 (0.030)	F(2,6) = 0.732 p=0.520
CA3	0.221 (0.062)	0.226 (0.037)	0.195 (0.036)	F(2,6) = 0.362 p=0.711
CA3 (Pyramidal)	0.256 (0.029)	0.227 (0.096)	0.247 (0.065)	F(2,6) = 0.174 p=0.844
CA4	0.573 (0.060)	0.578 (0.032)	0.508 (0.108)	F(2,6) = 0.842 p=0.476
DG	0.247 (0.054)	0.207 (0.038)	0.217 (0.069)	F(2,6) = 0.416 p=0.677

PNN – Perineuronal net, mm – millimetre, CON – sedentary control, MICT – moderate intensity continuous training, HIIT – high intensity interval training, SD – standard deviation, DG – dentate gyrus. *n=3*.

To assess whether exercise altered PNN composition, PNN counts were conducted for three different phenotypes depending on whether PNNs expressed: a) both aggrecan and WFA (ACAN+ WFA+), b) aggrecan only (ACAN+ WFA-), or c) WFA only (ACAN- WFA+). The CA2 region displayed diffuse staining of aggrecan and WFA in the pyramidal layer, making it difficult to count individual PNNs (Figure 4.5). Therefore, in the CA2 region, individual PNNs were only counted in the stratum oriens and stratum radiatum hippocampal layers. Similarly, the pyramidal layer of the CA3 region displayed diffuse WFA staining (Figure 4.5 B). However, individual aggrecan-only PNNs could be identified in the CA3 pyramidal layer (Figure 4.5 A). Therefore, all three

phenotypes of PNNs were counted in the stratum oriens and stratum radiatum layers within the CA3 region (labelled in PNN count figures as ‘CA3’), whilst the pyramidal layer was counted separately, labelled as ‘CA3 (Pyramidal)’. See Figure 4.7 for a diagram of hippocampal layers. In the pyramidal layer of CA3, individual WFA-only PNNs could not be distinguished, thus in this region, aggrecan-only PNNs were counted, and then were checked to see if they colocalised with WFA staining. This resulted in only two phenotypes being counted in the CA3 pyramidal layer: ACAN+ WFA+ and ACAN+ WFA-.

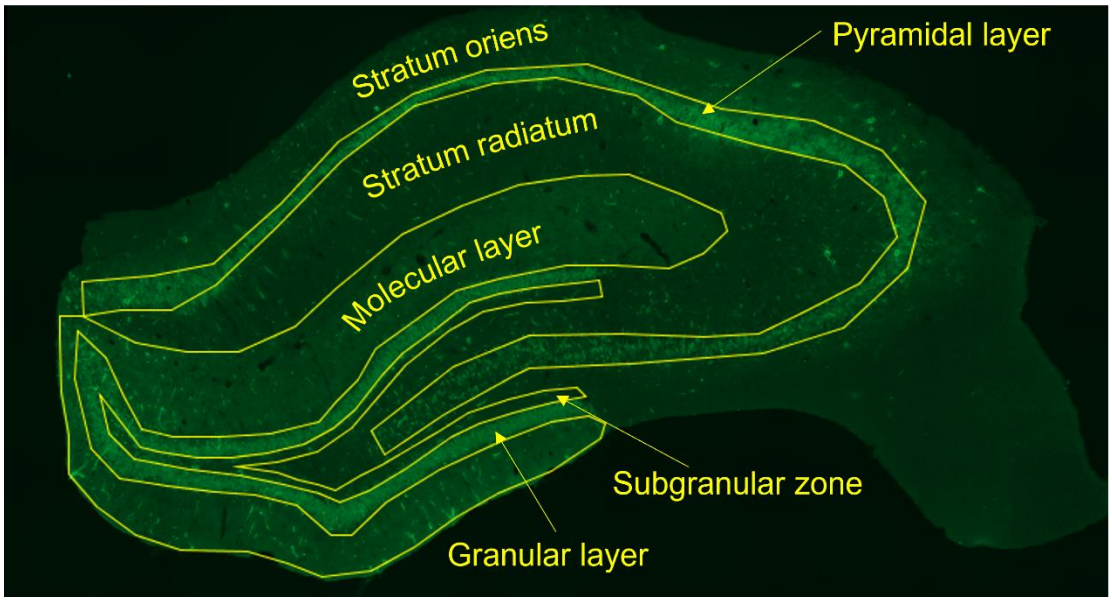

Figure 4.7 Layers of the hippocampus.

Tissue stained with NeuN to visualise hippocampal cell layers. Hippocampal layers defined from images in the online histological library, Brain Development Maps (Altman and Bayer, 2021).

MICT resulted in a statistically significant increase in the number of PNNs that expressed aggrecan only in the CA1 (Figure 4.8) (CON: 0.0076 ± 0.0018 PNNs/mm^2; MICT: 0.0310 ± 0.0037 PNNs/mm^2, p=0.043; HIIT: 0.0076 ± 0.0022 PNNs/mm^2, p=1; H(2)=6.3, p=0.043), CA3 (CON: 0.0294 ± 0.0126 PNNs/mm^2; MICT: 0.0571 ± 0.0070 PNNs/mm^2, p=0.043; HIIT: 0.0288 ± 0.0085 PNNs/mm^2,

p=1; H(2)=6.3, p=0.043), and CA3 pyramidal regions (CON: 0.0010 ± 0.0005 PNNs/mm^2; MICT: 0.0139 ± 0.0049 PNNs/mm^2, p=0.043; HIIT: 0.0041 ± 0.0026 PNNs/mm^2, p=1; H(2)=6.3, p=0.043) (Figure 4.9). Additionally, both MICT and HIIT significantly increased the number of aggrecan only PNNs in the CA4 region (CON: 0.0052 ± 0.0006 PNNs/mm^2; MICT: 0.0250 ± 0.0041 PNNs/mm^2, p=0.043; HIIT: 0.0160 ± 0.0035 PNNs/mm^2, p=0.043; H(2)=6.3, p=0.043). The increase in aggrecan only PNNs was accompanied with a significant reduction in PNNs expressing aggrecan and WFA by both exercise groups in the CA3 region (CON: 0.1223 ± 0.0033 PNNs/mm^2; MICT: 0.0917 ± 0.0101 PNNs/mm^2, p=0.043; HIIT: 0.1038 ± 0.0050 PNNs/mm^2, p=0.043; H(2)=6.3, p=0.043), and by HIIT in the CA4 region (CON: 0.3358 ± 0.0129 PNNs/mm^2; MICT: 0.2637 ± 0.0324 PNNs/mm^2, p=1; HIIT: 0.2780 ± 0.0063 PNNs/mm^2, p=0.043; H(2)=6.3, p=0.043). There was a similar pattern for exercise training to reduce the number of ACAN+ WFA+ PNNs in other hippocampal regions, though not statistically significant.

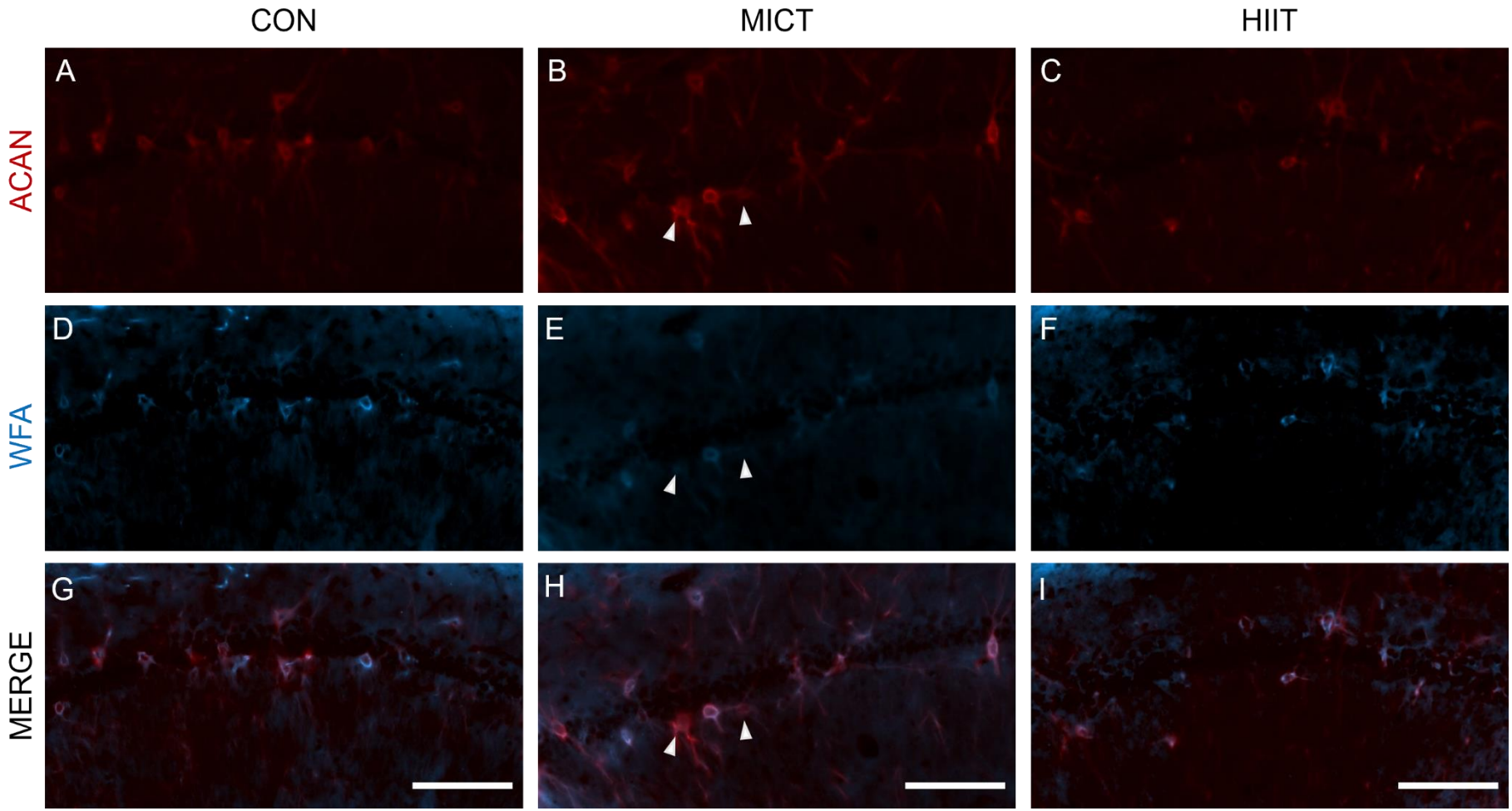

Figure 4.8. Perineuronal nets in the hippocampal CA1 region.

A-C. PNNs expressing aggrecan. D-F. PNNs expression WFA. G-I. Merge of PNNs expressing aggrecan and WFA. White arrowheads indicate PNNs that express aggrecan without WFA following MICT. Scale bars: 50 μm.

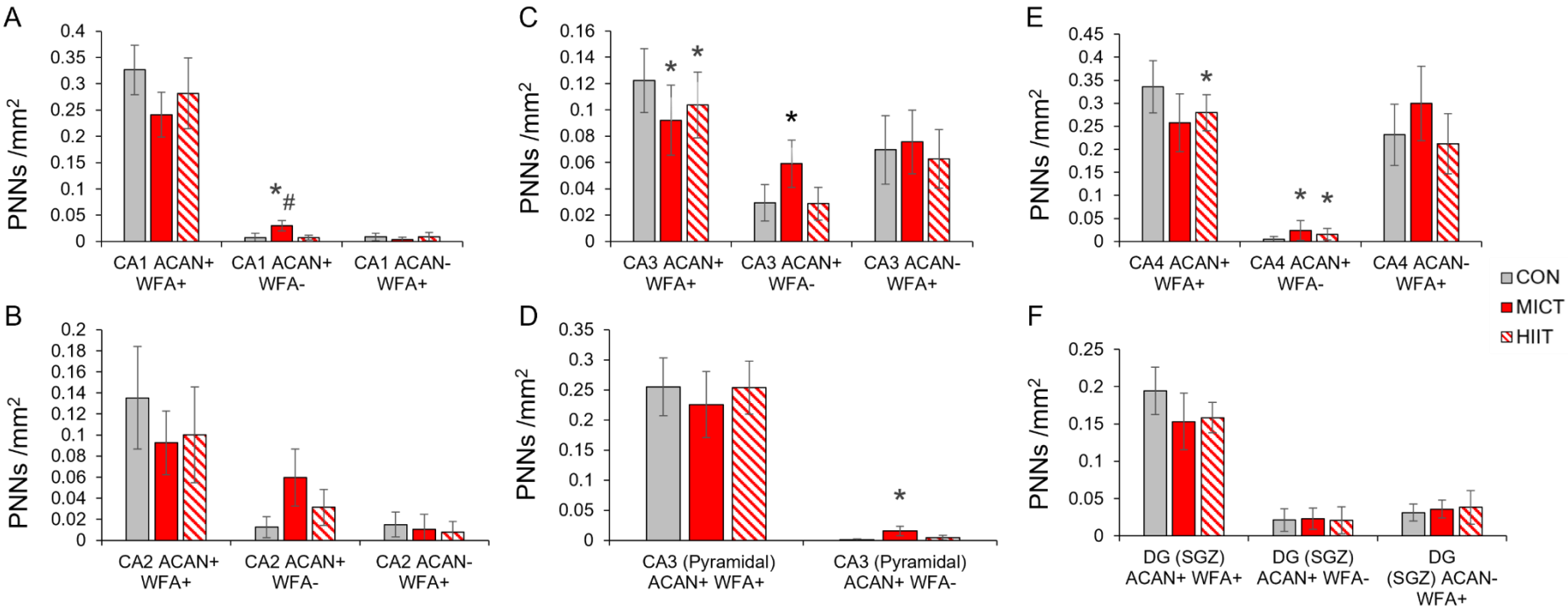

Figure 4.9. Exercise increases the number of PNNs expressing only aggrecan in the hippocampus.

PNNs were classified as one of three different phenotypes: expressing aggrecan and WFA (ACAN+ WFA+), expressing aggrecan only (ACAN+ WFA-), or expressing WFA only (ACAN- WFA+) in adult male Wistar rats following six weeks of MICT or HIIT on a motorised treadmill. PNN counts were conducted for the following hippocampal regions: A. CA1 B. CA2 C. CA3 D. CA3 pyramidal layer E. CA4 F. Subgranular zone (SGZ) of the dentate gyrus (DG). Bars represent mean PNN count ± SEM, *n*=3. Statistical significance was determined using Kruskal-Wallis H and Dunn's multiple comparison tests with the Bonferroni correction.*p<0.05 in comparison to the sedentary control group. #p<0.05 in comparison to the HIIT group. PNN – perineuronal net, CON – sedentary control, MICT – moderate intensity continuous training, HIIT – high intensity interval training.

The frequency of PNNs expressing each phenotype were also calculated as a percentage of the total PNNs observed within each hippocampal region. MICT induces a shift towards a higher proportion of total PNNs expressing only aggrecan and not WFA in the CA1 (χ^2 = 11.16 p=0.025), CA2 (χ^2 = 23.72 p<0.0001) and CA3 pyramidal regions (χ^2 = 7.19 p=0.027) (Figure 4.10). The dentate gyrus was the only hippocampal region that was resistant to changes in either PNN number or frequency.

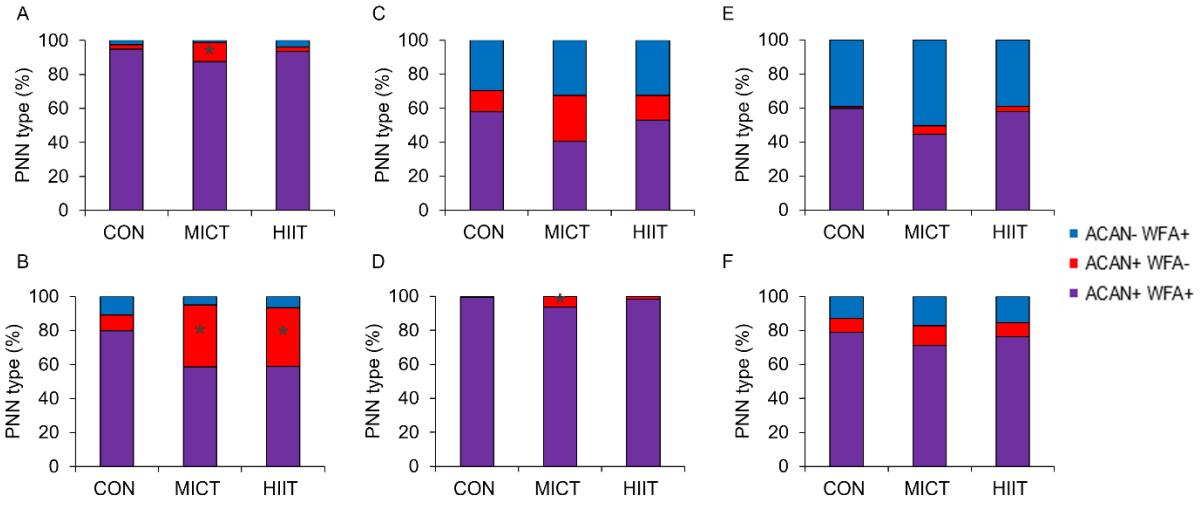

Figure 4.10. MICT increases the proportion of PNNs expressing only aggrecan in the hippocampus.

PNNs were classified as one of three different phenotypes: expressing aggrecan and WFA (ACAN+ WFA+), expressing aggrecan only (ACAN+ WFA-), or expressing WFA only (ACAN- WFA+) in adult male Wistar rats following six weeks of MICT or HIIT. The frequency of PNNs in each phenotype was analysed using Chi-square tests (*p<0.05) for the following hippocampal regions: A. CA1 B. CA2 C. CA3 D. CA3 pyramidal layer E. CA4 F. Subgranular zone of the dentate gyrus. Bars represent mean percentage of PNNs, n=3. PNN – perineuronal net, CON – sedentary control, MICT – moderate intensity continuous training, HIIT – high intensity interval training.

4.4.3 Exercise training does not alter PNN thickness in the hippocampus.

Previous research has demonstrated that six weeks of voluntary wheel running reduced the thickness of WFA+ PNNs in the hippocampal CA1, CA3, and dentate

gyrus regions (Smith *et al.*, 2015). However, in the present study, six weeks of treadmill training did not affect the thickness of aggrecan positive or WFA positive PNNs in the hippocampus (H(2) <2.22, p>0.329, and H(2) <3.6, p>0.165, respectively) (Figure 4.11).

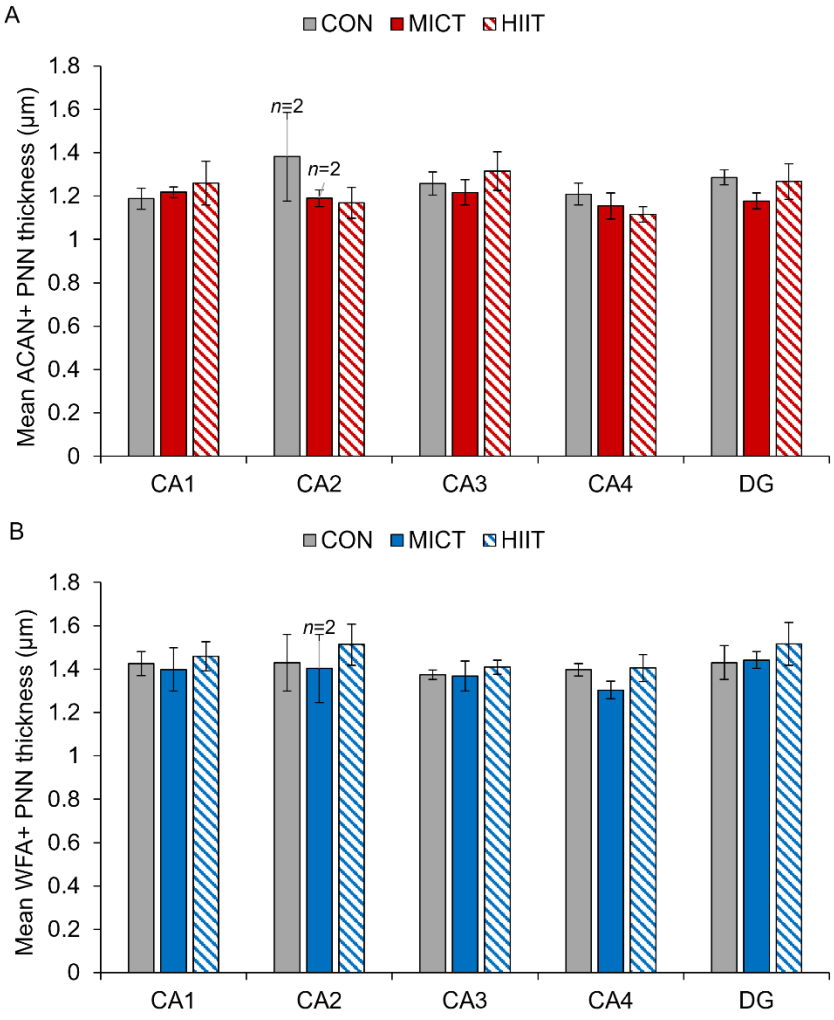

Figure 4.11. Hippocampal PNN thickness is comparable between sedentary and trained animals.

PNN thickness was calculated throughout the CA regions and dentate gyrus (DG) of the hippocampus in male Wistar rats following six weeks of exercise training (MICT or HIIT). A. Presents the thickness of PNNs expressing aggrecan. B. Presents the thickness of PNNs expressing WFA. Bars represent mean PNN thickness ± SEM, *n*=3 unless otherwise stated. Statistical analyses were performed with Kruskal-Wallis H tests, alpha level p<0.05. PNN – perineuronal net, CON – sedentary control, MICT – moderate intensity continuous training, HIIT – high intensity interval training.

4.4.4 HIIT increased hippocampal *Chst8* expression.

Whether CS-GAG chains exert an inhibitory or permissive effect on plasticity is dependent on patterns in CS-GAG sulphation (Wang *et al.*, 2008; Lin *et al.*, 2011). To assess whether exercise impacted CS-GAG sulphation in the hippocampus, RT-qPCR was used to determine the gene expression of six chondroitin sulfotransferases: *Chst3*, *Chst8*, *Chst11*, *Chst12*, *Chst13*, and *Chst15*. The mRNA expression of *Chst3, Chst12*, and *Chst13* was too low to be analysed. HIIT significantly upregulated the expression of *Chst8* in the hippocampus, which adds the inhibitory C4 sulphation to GalNAc residues (MICT: 0.484 ± 0.635 Log2 FC, p=0.924; HIIT: 1.419 ± 0.704 Log2 FC, p=0.034 F(2,9)=5.189, p=0.032) (Figure 4.12). There was no statistically significant difference in the expression of *Chst11* (MICT: 0.376 ± 0.675 Log2 FC, p=1; HIIT: 0.659 ± 0.913 Log2 FC, p=0.594; F(2,9)=0.972, p=0.415) or *Chst15* (MICT: 0.139 ± 0.504 Log2 FC, p=1; HIIT: 0.436 ± 0.545 Log2 FC, p=0.789; F(2,9)=0.733, p=0.507) in either exercise group.

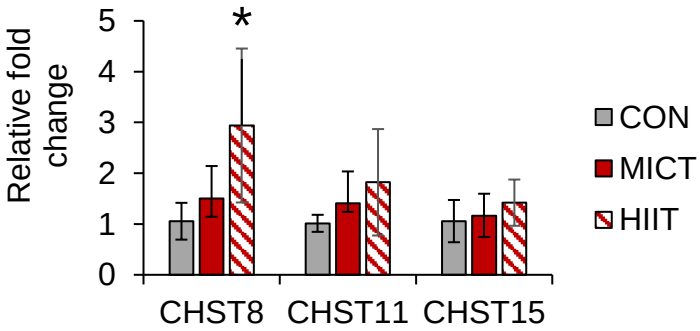

Figure 4.12. HIIT upregulates hippocampal *Chst8* expression.

Gene expression data presented as relative fold change to sedentary controls Statistical significance determined using a one way ANOVA and Bonferroni correction for multiple comparisons, * p<0.05 when compared to sedentary control, *n*=4. MICT – Moderate intensity continuous training, HIIT – High intensity interval training. Bars represent mean relative fold change ± SEM.

4.4.5 Exercise training did not affect PNNs in the primary motor cortex.

In Chapter 3, the mRNA expression of aggrecan was not modulated by exercise training in cortical tissue. However, as PNNs are abundantly expressed in the primary motor cortex, this study also investigated whether the protein expression of aggrecan, and the expression of CS-GAGs labelled by WFA was susceptible to change following MICT and HIIT. The mean staining intensity of aggrecan (CON: 4007.61 ± 1193.98 MGV; MICT: 4548.20 ± 2093.86 MGV; HIIT: 4922.58 ± 949.07 MGV; H(2)=0.409, p=0.815) and WFA (CON: 3600.26 ± 901.97 MGV; MICT: 3224.19 ± 518.31 MGV; HIIT: 2391.20 ± 468.58 MGV; H(2)=2.227, p=0.328) was comparable between all three experimental groups in the motor cortex. Furthermore, exercise training did not affect the number of aggrecan and WFA positive, aggrecan only, or WFA only PNNs in the motor cortex (Table 4.4).

Table 4.4. PNN counts in motor cortex of male Wistar rats following exercise training.

	Mean PNN count (PNNs/mm^2)			
	CON (SD)	MICT (SD)	HIIT (SD)	ANOVA
ACAN+ WFA+	0.589 (0.068)	0.591 (0.082)	0.575 (0.145)	F(2,7)=0.020 p=0.980
ACAN+ WFA-	0.123 (0.061)	0.102 (0.013)	0.159 (0.129)	F(2,7)=0.353 p=0.715
ACAN- WFA+	0.271 (0.258)	0.227 (0.017)	0.150 (0.059)	F(2,7)=0.640 p=0.556
Total PNN count	0.982 (0.359)	0.920 (0.092)	0.924 (0.234)	F(2,7)=0.122 p=0.887

PNN – perineuronal net, CON – sedentary control (*n*=3), MICT – moderate intensity continuous training (*n*=3), HIIT – high intensity interval training (*n*=4), ACAN – aggrecan, WFA – *Wisteria floribunda agglutinin.*

4.5 Discussion

Previous research has shown that six weeks of voluntary wheel running reduced the number and thickness of PNNs in the hippocampus (Smith *et al.*, 2015). Additionally, Chapter 3 demonstrated that MICT and HIIT downregulated the mRNA expression of aggrecan, a main component of PNNs, in the hippocampus. This is the first study to investigate the role of treadmill training on aggrecan and WFA positive PNNs in the CNS. PNNs were visualised using an antibody against the aggrecan core protein, and CS-GAG chains were labelled with the lectin WFA. In the hippocampus, MICT increased the proportion of PNNs that expressed aggrecan and lacked WFA, without altering the total PNN counts. This suggests that MICT may be modulating CS-GAG chains within PNNs in the hippocampus, which may facilitate neural plasticity.

4.5.1 PNNs in the hippocampus following exercise training.

In contrast to (Smith *et al.*, 2015), the present study did not observe any changes in the total number of PNNs or PNN thickness following six weeks of treadmill training in the hippocampus. Although, when further looking into PNN composition, MICT and HIIT significantly reduced the number of PNNs that expressed both aggrecan and WFA in the CA3 region of the hippocampus. In the (Smith *et al.*, 2015) paper, PNNs were visualised using only WFA following six weeks of voluntary wheel running. Following MICT, the staining intensity of WFA was shown to be lower than sedentary controls in all hippocampal regions, although not statistically significant. The daily distance ran by the rats in this study was approximately 600 m, whereas rats ran up to 8.76 km in the voluntary wheel running wheel paradigm utilised in (Smith *et al.*, 2015). It is possible that higher

volumes of exercise training are required to induce more widespread reductions in WFA-positive PNNs in the hippocampus.

Although the total number of PNNs remained unchanged following exercise training, MICT increased the number of PNNs expressing only aggrecan in the CA1, CA3, and CA4 regions. Aggrecan-positive PNNs that lack WFA expression have previously been observed in the hippocampus, somatosensory cortex and spinal cord (Ueno *et al.*, 2017; Yamada and Jinno, 2017; Irvine and Kwok, 2018). The antibody against aggrecan labels the CSPG core protein, and WFA labels the GalNAc residue of CS-GAG chains (Brückner *et al.*, 1996). Therefore, it is possible that MICT reduces the number of CS-GAG chains attached to aggrecan core proteins in hippocampal PNNs. In the CA3 region, the increase in aggrecan-positive PNNs coincided with a significant decrease in the number of PNNs expressing both aggrecan and WFA, suggesting that MICT induces a transition in PNN composition. The shift in PNN composition was also reflected in PNN frequencies as the proportion of PNNs expressing only aggrecan increased in response to MICT in the CA1, CA2, and CA3 regions. The inhibitory nature of aggrecan is dependent on chondroitin sulphate (Hering *et al.*, 2020). Thus, a reduction in CS-GAG expression within aggrecan positive PNNs may provide a more permissive environment for plasticity in the hippocampus.

However, it remains to be questioned whether CS-GAGs are indeed being modulated by exercise training, or whether WFA binding with CS-GAGs is being interrupted. The overexpression of 6-O-sulphation of GalNAc residues in CS-GAGs has been documented to reduce WFA expression whilst maintaining protein levels of aggrecan (Miyata *et al.*, 2012). As WFA binds to GalNAc sugars

in CS-GAG chains, it is possible that sulphation of these same sugars may interrupt WFA binding. Further research is required to determine the exact epitope where WFA binds to GalNAc, and whether this is conditional to specific sulphation patterns.

The bacterial enzyme Chondroitinase ABC cleaves CS-GAG chains from CSPGs in PNNs, and also degrades CS-GAGs in the loose extracellular matrix (Sorg *et al.*, 2016). This extensive attenuation of CS-GAGs in the perirhinal cortex enhanced object recognition memory in healthy rodents and Alzheimer's models (Romberg *et al.*, 2013; Yang *et al.*, 2015). The hippocampus is another brain region involved in object recognition memory (Broadbent *et al.*, 2010). It will be noteworthy to investigate whether the more subtle exercise-induced modulation of CS-GAGs observed in this study is associated with enhanced object recognition memory.

4.5.2 CS-GAG sulphation following exercise training.

The inhibitory nature of PNNs can also be attenuated without degrading CS-GAG chains. The degree of neural plasticity can be controlled by manipulating the sulphation patterns of GalNAc residues in CS-GAG chains, with C4S restricting, and C6S promoting plasticity (Wang *et al.*, 2008; Lin *et al.*, 2011; Miyata *et al.*, 2012). Overexpressing *Chst3* to enhance C6S alleviated memory deficits in aged mice (Yang *et al.*, 2021). As mentioned previously, C6S overexpression has been reported to reduce WFA expression whilst protein levels of aggrecan were unaltered (Miyata *et al.*, 2012). As MICT increased the number of aggrecan-positive PNNs that lacked WFA labelling, this study sought to investigate CS-GAG sulphation in the hippocampus following exercise training. RT-qPCR was

used to determine the expression of genes that are involved in adding the permissive sulphation at the C6 position of GalNAc (*Chst3),* the inhibitory sulphation at the C4 position of GalNAc (*Chst8, Chst11, Chst12, and Chst13),* and which add double sulphation at both C4 and C6 of GalNAc (*Chst15).* Unfortunately, expression of *Chst3* was too low in the tissue samples to be analysed within this study, and thus it was not possible to investigate whether 6-O-sulphation was associated with a higher number of PNNs lacking WFA.

However, HIIT significantly upregulated the mRNA expression of *Chst8* in the hippocampus. There were fewer PNN adaptations in HIIT trained animals in comparison to the MICT group, which could be due to the inhibitory action of *Chst8*. Alterations in gene expression do not always translate to changes in protein levels. Therefore, a more conclusive method of analysing CS-GAG sulphation, such as liquid chromatography-mass spectrometry, may be more useful for determining sulphation patterns of CS-GAGs following exercise training (Alonge *et al.*, 2019).

4.5.3 PNNs in the motor cortex following exercise training.

This is the first study to explore the role of exercise training on PNN expression in the motor cortex. The staining intensity of aggrecan and WFA, and the total and phenotypic PNN counts were comparable between sedentary controls and trained animals. In Chapter 3, gene expression of RhoA/ROCK pathway components were also resistant to change in the cortex, suggesting that the motor cortex is not susceptible to exercise-induced plasticity. In support of this, enhanced expression of BDNF, a known facilitator of neural plasticity, was

observed in the hippocampus whilst not in the cortex following voluntary wheel running (Neeper *et al.*, 1996).

4.5.4 Conclusions

This study provides a novel insight into how treadmill training alters PNN composition in the CNS. MICT induced a shift towards a higher proportion of PNNs that express only aggrecan without WFA in the hippocampus. This suggests that MICT may modulate the expression of CS-GAG chains in hippocampal PNNs. As the hippocampal region is related to learning and memory, it would be beneficial to investigate whether the exercise-induced changes in PNN composition are associated with memory improvements.

Chapter 5 The effect of exercise and hippocampal *Chst11* overexpression on object recognition memory.

5.1 Introduction

Both exercise training and the enzymatic/transgenic ablation of PNNs have been documented to improve object recognition memory (O'Callaghan, Ohle and Kelly, 2007; Bechara and Kelly, 2013; Romberg *et al.*, 2013; Rowlands *et al.*, 2018). In the hippocampus, exercise training in the form of voluntary wheel running reduced the number of PNNs (Smith *et al.*, 2015), and treadmill training induced a shift towards more PNNs expressing aggrecan core protein without labelled CS-GAG chains (Chapter 4). However, it is not yet known whether the exercise-induced modulation of PNNs is involved in improving hippocampal-related memory.

Studies implicating PNNs in object recognition memory often completely remove PNNs, either by using the bacterial enzyme chondroitinase ABC that degrades CSPGs, or by genetic knockout of aggrecan or the link protein CTRL1 that both prevent PNN formation (Romberg *et al.*, 2013; Rowlands *et al.*, 2018). However, manipulating CS-GAG sulphation via overexpressing the chondroitin 6-sulfotransferase (*Chst3*) rescued deficits in object recognition memory in aged mice (Yang *et al.*, 2021). It will be noteworthy to determine whether the more subtle modulation of CS-GAGs whilst maintaining intact aggrecan-positive PNN structure following treadmill training (as observed in Chapter 4) leads to improvements in object recognition memory.

There is currently no experimental model suitable for testing whether there is a causal relationship between the exercise-induced modulation of CS-GAGs and improved object recognition memory. MICT was not shown to change the overall number of PNNs, therefore we sought to target CS-GAG chains to make them

more inhibitory and to impair object recognition memory. As enhancing C6S with *Chst3* overexpression promoted plasticity and improved object recognition memory, it was expected that overexpressing the inhibitory C4S sulphation pattern on CS-GAGs would have the opposing effect of impairing object recognition memory. Therefore, this study intended to use the chondroitin 4-sulfotransferase, *Chst11,* to investigate whether exercise-induced CS-GAG modulation played a causal role in object recognition memory. In Chapter 4, MICT induced a shift towards a higher proportion of PNNs expressing aggrecan without WFA labelling, suggesting that CS-GAG expression had been reduced. As CS-GAGs will be targeted by *Chst11* to increase the inhibitory sulphation pattern, the exercise-induced modulation of hippocampal CS-GAGs may attenuate memory deficits produced by *Chst11* overexpression.

5.2 Aims

This chapter aimed to establish whether the exercise-induced modulation of CS-GAG expression within hippocampal PNNs lead to improvements in object recognition memory. To achieve this, an experimental model was developed to upregulate C4S sulphation of CS-GAG GalNAc residues using hippocampal injections of AAV1-PGK-CHST11. It was hypothesised that the overexpression of *Chst11* would upregulate hippocampal C4S and impair novel object recognition memory. This model was then used to investigate whether the modulation of CS-GAGs induced by exercise training was causally linked with improved object recognition memory performance. It was hypothesised that exercise training (MICT) would modulate CS-GAG chains that contained the inhibitory C4-sulphation, and therefore attenuate memory-impairments induced by *Chst11* overexpression.

5.3 Methods

5.3.1 Study overview

32 male Wistar rats (200-250 g) received stereotaxic hippocampal injections to overexpress either *GFP* or *Chst11.* Each group was further split into an exercise (MICT) or sedentary group for six weeks. MICT was conducted once a day, five days a week, for six weeks (see General Methods Section 2.2 for in-depth MICT protocol). Experimental groups were: Sedentary+GFP; Exercise+GFP; Sedentary+Chst11; and Exercise+Chst11 (*n*=8). After the six-week training period, novel object recognition tests took place to assess memory outcomes (timeline in Figure 5.1). CNS tissue was collected following the final day of behavioural testing.

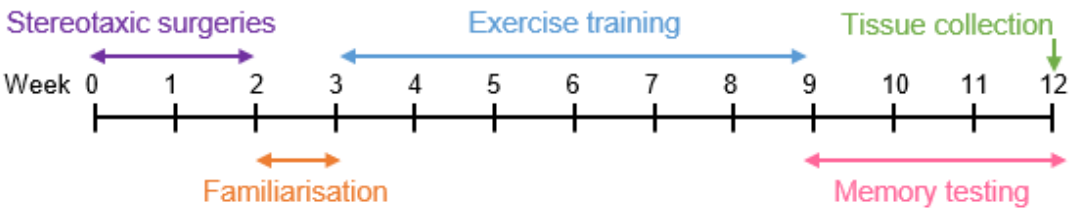

Figure 5.1. Study timeline for experiments in Chapter 5.

Adult male Wistar rats received hippocampal injections to over express either GFP or Chst11. Half of each group remained sedentary whilst the other half completed a six-week moderate intensity training protocol (once a day, 5 days a week, for six weeks). Memory testing (novel object recognition) was performed after the training regime. Novel object preference was measured following three hour and 24 hour time delays. Two behavioural trials were conducted for each timepoint with 48 hours rest between each behavioural trial. CNS tissue was collected 24 hours after the last day of behavioural testing.

5.3.2 Stereotaxic surgeries (Overexpressing *Chst11*)

Animals were anaesthetised using isoflurane (5 % in O_2 for induction and 2.5 % in O_2 for maintenance). The dorsal surface of the head was shaved and sterilised (50% iodine, 50% ethanol solution), and eye lubricant (Lubrithal) was applied. Animals were placed on a homeothermic heat pad (Harvard Apparatus Homoeothermic Monitoring System; Harvard Apparatus, Massachusetts, USA) and were secured in a stereotaxic frame throughout the surgery.

A skin incision was made on the midline of the head and connective tissues were pushed away with a cotton bud to expose landmarks of the skull. Bone wax was applied to the skull to suppress bone bleeding. The head was aligned so that Bregma and Lambda were within 1 mm of each other. Bilateral craniotomy windows (approximately 3.5 x 3 mm) were drilled using 1 mm round-headed drill bits and a dental drill (Saeshin Dental STRONG 90 Micro motor with 102S Hand piece 35,000 RPM; Saeshin Precision Co., Daegu, Korea). Skin retractors were used to keep the craniotomy windows clear. Six x 0.5 µL injections (3 each hemisphere into CA1, CA2, and CA3- total virus volume 3 µL per rat) of either AAV1-PGK-GFP or AAV1-PGK-CHST11 (Vigene Biosciences, Maryland, USA) were injected into the dorsal hippocampus (see Table 5.1 and Figure 5.1 for coordinates). The AAV1-PGK-CHST11 virus also contained FLAG and His tags to aid visualisation in future immunohistochemistry experiments (AAV1-PGK-Chst11v1-FLAG-His). The 0.5 µL of virus was injected over two minutes (250 nL/min) using a 5 µL Hamilton Syringe (26 gauge needle) and a UMP3 Microinjection Syringe Pump with Micro4 controller (WPI Instruments, Florida, USA). The needle was left in position for two minutes to allow residual AAV to be

absorbed before being slowly withdrawn. After the final injection the skin was sutured close with non-absorbable suture. Pain relief (Vetergesic Buprenorphine; 0.015 mg/kg; Henry Schein Animal Health, Dumfries, UK) and antibiotics (Baytril enrofloxacin; 2.5 mg/kg; Henry Schein Animal Health, Dumfries, UK) were administered by subcutaneous injection before removal from anaesthesia and for three days following surgery.

Table 5.1. Hippocampal injection coordinates.

	Left hemisphere			Right hemisphere		
Axis	CA3	CA2	CA1	CA1	CA2	CA3
AP	-0.33	-0.33	-0.33	-0.33	-0.33	-0.33
ML	-0.35	-0.3	-0.2	0.2	0.3	0.35
DV	-0.36	-0.3	-0.26	-0.26	-0.3	-0.36

AP: Anterior-posterior; ML: Medial-lateral: DV: Dorsal-ventral. All coordinates given in cm from Bregma (zero).

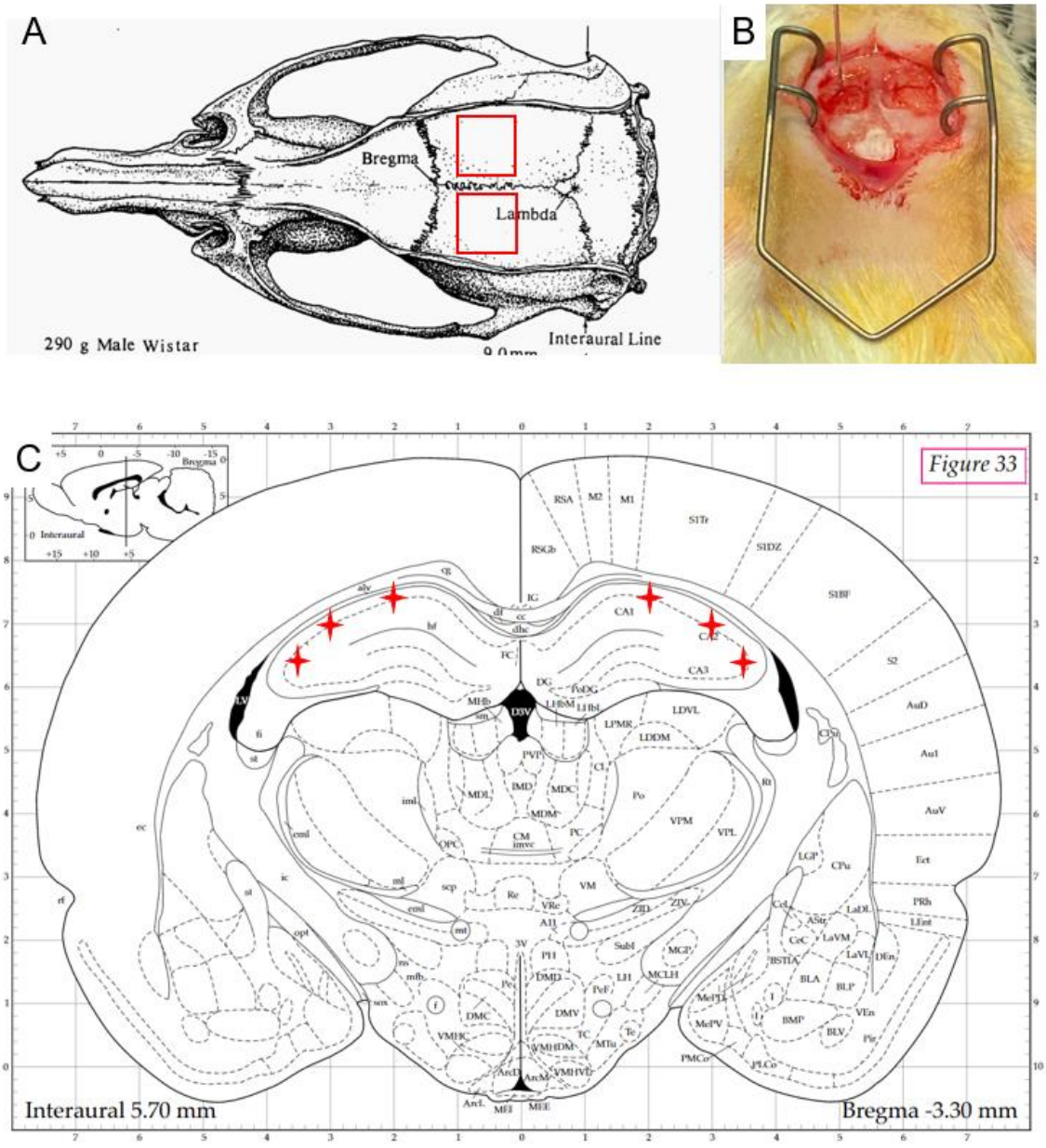

Figure 5.2. Stereotaxic hippocampal injections.

A. Red boxes indicate approximately where the ~3.5 x 3 mm craniotomy windows were drilled in relation to the skull landmarks. B. A stereotaxic surgery image showing the skin retractors keeping the craniotomies clear whilst the Hamilton needle is injected. C. The red stars mark the location of the six 0.5 µL injections of virus into the hippocampal CA1, CA2, and CA3 regions. A and C modified from the Rat Brain Atlas (Paxinos and Watson, 2013).

5.3.2.1 Confirmation of stereotaxic hippocampal injection location.

Brain tissue was prepared and immunohistochemically stained as described in Section 4.3.3. Hippocampal sections (Bregma -3.30 mm) from animals injected with AAV1-PGK-GFP were stained with a primary GFP antibody raised in mouse (9F9.F9, 1:500, Rockland) to visualise the overexpression of GFP induced by the hippocampal injections, and co-stained with biotin-conjugated *Wisteria floribunda agglutinin* (WFA) (#L1766, 1:300, Sigma) to label PNNs. The secondary antibodies used were donkey anti-mouse (1:1000, Alexa Fluor® 488, Invitrogen) and streptavidin (1:250, Pacific Blue™, Invitrogen). Hippocampal tile scans were imaged at 20X magnification on an Axio Scan Z1 slide scanner (Zeiss, UK).

5.3.3 *Chst11* overexpression – exercise protocol

Animals that received hippocampal injections of either AAV1-PGK-GFP or AAV1-PGK-CHST11 were randomly allocated into four experimental groups: Sedentary with GFP (Sed-GFP); Exercise with GFP (Ex-GFP); Sedentary with Chst11 (Sed-Chst11); and Exercise with Chst11 (Ex-Chst11) (n=8/group). The exercise groups performed the MICT protocol as described in Section 2.3.3. As some animals refused to run on the treadmill in this study, exercise compliance was measured as the mean percentage of training sessions that the animals complied with the exercise protocol.

5.3.4 Physiological assessments

Body mass (g) was measured before each training session throughout the six-week training period. Body mass change throughout the training period was calculated from the first to last training day (Equation 3.1). Estimated total work was calculated as outlined in Section 3.3.2.3.

5.3.5 Novel object recognition

5.3.5.1 Apparatus construction

A Y-shaped apparatus was constructed with 10 mm matt white foam PVC (Cut to size, Sheet Plastics, UK) using dimensions from (Winters *et al.*, 2004) (Figure 5.3).

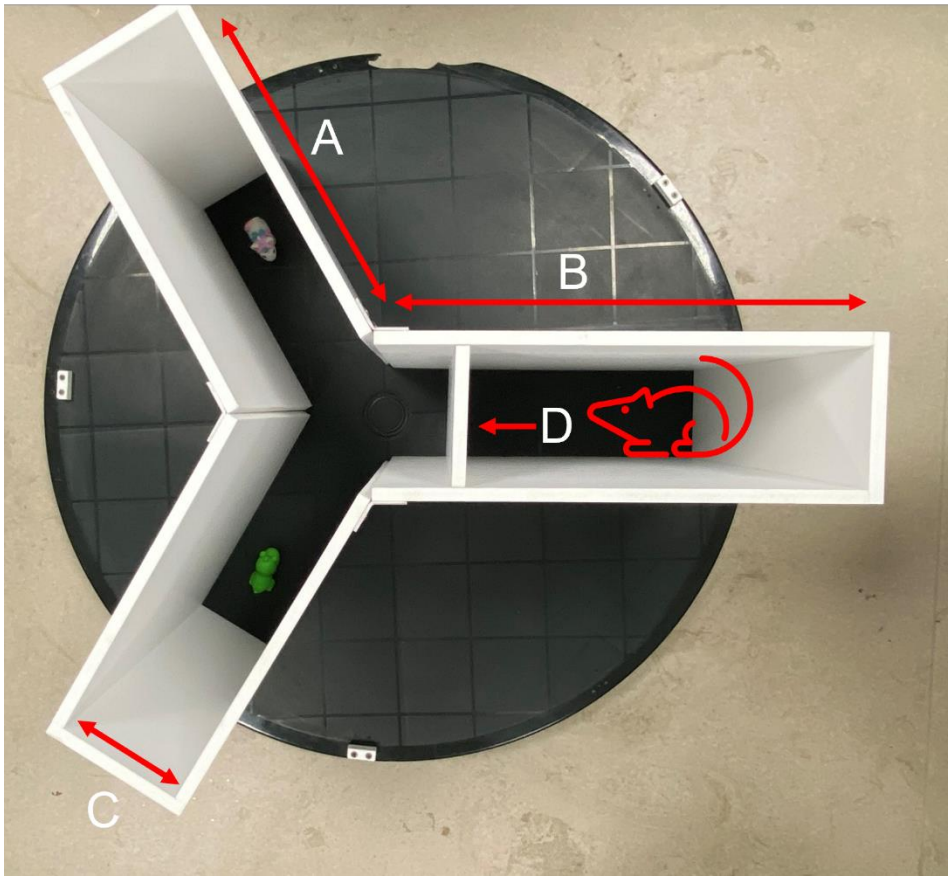

Figure 5.3. Y-shaped apparatus for novel object recognition tests.

The Y-shaped apparatus for rats was constructed using 10 mm matt white foam PVC. All panels of the apparatus were 40 cm high. Panel A for the two arms containing objects measured 27 cm in length. Panel B for the long arm where the rat starts the experiment measured 35 cm. Panel C for the end of each three arms measured 12 cm in length so that the internal width of the arm measured 10 cm. Panel D measured 10 cm in length so that it could be slotted in the longer arm as a guillotine door. Dimensions used from (Winters *et al.*, 2004).

5.3.5.2 Behavioural testing

Novel object recognition experiments were performed as outlined in (Romberg *et al.*, 2013). One arm of the Y-shaped apparatus was closed off by a guillotine door where the rats were placed at the start of the experiments. The other two shorter arms contained objects which the rat could explore once the guillotine door was opened. All rats were familiarised to the Y-shaped apparatus that contained treats (mini marshmallows) in the shorter arms for five minutes over two consecutive days. In the sample phase of the experiments two identical objects were placed in the short arms which rats could explore for five minutes (Figure 5.4 A-D). Following a delay of either three or 24 hours, the rats returned to the apparatus for the choice phase. In the choice phase the rats explored two new objects for three minutes: one identical to the sample object pair, and one completely novel object (Figure 5.4 E-H). The objects were held in place with white tack. Between each trial the objects and the apparatus were cleaned with fragrance free detergent (Citop Zero) to remove olfactory cues. The rats received two trials at each different delay timepoint (four trials in total) with 48 hours rest in between each trial. A different set of object pairings were used for each of the four trials. Four different random orders of objects were used throughout the experiments. The choice phase was recorded using a camcorder and tripod above the Y-shaped apparatus.

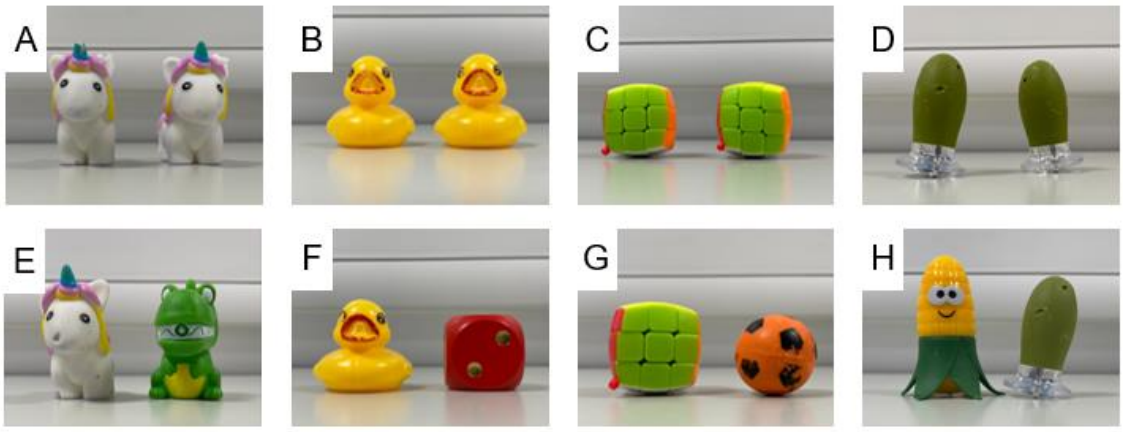

Figure 5.4. Object pairs used in novel object recognition tests.

A-D. Identical object pairings used in the five minute sample phase. E-H. Novel object pairings used in the three minute choice phase.

5.3.5.3 Video analysis

The time that rats explored the familiar and novel objects in the choice phase was timed using the Multiple Stopwatches function in the XNote Stopwatch software for desktop (Figure 5.5) (http://www.xnotestopwatch.com/). The timers were controlled by the keyboard and results were exported directly to Excel documents. Object exploration was timed when the rat was directly looking at/sniffing the object. Exploration was not timed if the rat looked away, stood above/on top of the object, or was sniffing/nibbling the white tack.

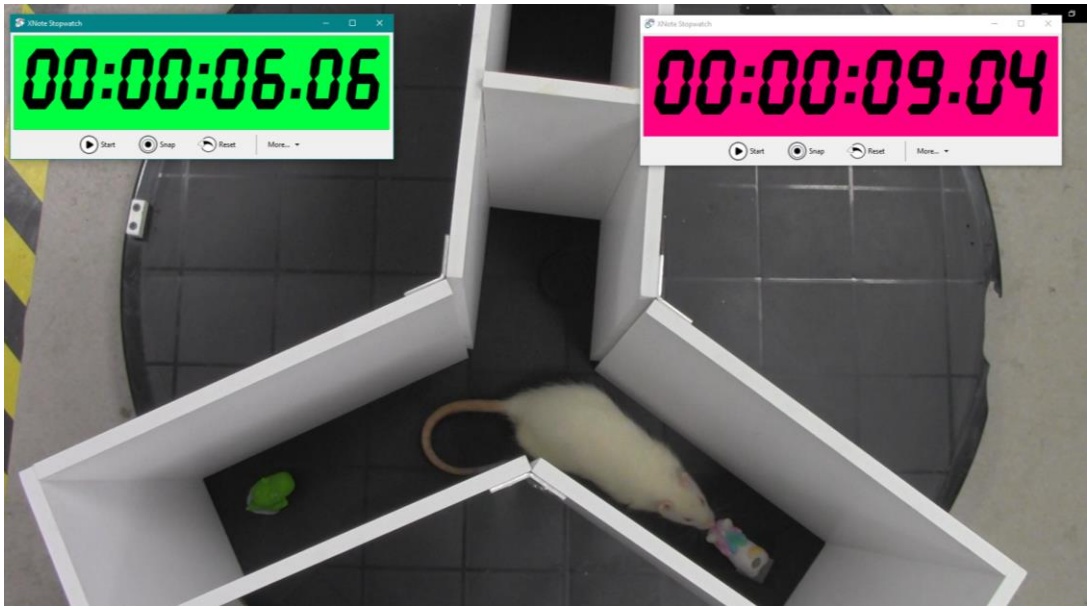

Figure 5.5. Novel object recognition video analysis.

Video screenshot of the choice phase being analysed with XNote Multiple Stopwatches. Green timer: familiar object – unicorn; Pink timer: novel object – dinosaur.

Equation 5.1. Discrimination index.

$$Discrimination\ index = \frac{(Time\ exploring\ novel\ object - Time\ exploring\ familiar\ object)}{(Time\ exploring\ novel\ object + Time\ exploring\ familiar\ object)}$$

The discrimination index was calculated using Equation 5.1. The discrimination index was calculated for one minute of video footage from the choice phase. The discrimination index gives a score between -1 and 1. A positive score shows that more time was spent exploring the novel object. Whereas a negative score shows that more time was spent exploring the familiar object. Rodents are expected to remember that they have already seen the familiar object and spend more time

exploring the novel object. Thus, rats with memory impairments would be expected to have lower discrimination indices.

5.3.6 Tissue collection

24 hours after the final day of behavioural testing, animals were overdosed with an intraperitoneal injection of sodium pentobarbital (200 mg/kg) to induce deep anaesthesia. Once the blink and pedal reflexes were absent tissue was collected in the following ways. Half of the rats from each experimental group were decapitated and fresh dissection of the brain and spinal cord were performed rapidly. The hippocampus, cortex (directly above the hippocampus), cerebellum, striatum, and lumbar region of the spinal cord were snap frozen in Eppendorfs using liquid nitrogen and later stored at −80°C. The other half of the rats from each experimental group were transcardially perfused (Gage, Kipke and Shain, 2012) with sodium phosphate buffer (1 M PB), followed by 4% paraformaldehyde (PFA), and a final rinse with 1 M PB. Brains were dissected out and post-fixed in 4% PFA overnight at 4°C. The tissue was then cryoprotected in a 30% sucrose solution with 1 M PB and stored at 4°C. Fixed brain tissue was collected for future immunohistochemistry experiments. Fresh CNS tissue was collected for future CS-GAG quantification experiments.

5.3.7 Statistical analysis and experimental design

Data are presented as means ± standard deviation (SD) unless otherwise specified. The alpha level was set at 0.05 and statistical significance was denoted in figures with an asterisk (*$p<0.05$). If other symbols were used they were noted in the figure captions. All statistical analysis was performed in IBM SPSS software

version 26 (IBM, USA). Shapiro-Wilk tests determined normality prior to conducting statistical tests.

5.3.7.1 Exercise and physiological assessments

Body mass data are presented as the mean ± SEM (bar chart). Independent t-tests were performed to compare the change in body mass throughout the six-week training period between the exercise groups and their sedentary controls (Ex-GFP vs. Sed-GFP; Ex-Chst11 vs. Sed-Chst11). Exercise compliance data are presented as mean percentage of sessions that the animals complied with the exercise protocol (stacked bar chart). Differences in exercise compliance were analysed with a Chi-Squared test (χ^2). All group sizes were n=8.

5.3.7.2 Novel object recognition

For behavioural analysis all group sizes were n=8. Data in bar charts are presented as the mean ± SEM. A mixed mode ANOVA was used to investigate the interaction between experimental groups and the time delay of behavioural testing, followed up by paired t tests to analyse differences in the discrimination index between the 3 and 24 hour time delays for each experimental group. A one-way ANOVA compared differences in the discrimination index between groups followed by Bonferroni post hoc tests. The percentage of trials with preference for the novel object was compared between groups using with a Chi-Squared test (χ^2) and presented in stacked bar charts.

5.4 Results

5.4.1 Confirmed location of stereotaxic hippocampal injections.

Hippocampal sections from animals injected with AAV1-PGK-GFP displayed immunoreactivity against GFP in the CA1, CA2, and CA3 regions of the hippocampus (Figure 5.6). This confirmed that the stereotaxic injection protocol was successful in delivering on-target AAV injections to the hippocampus.

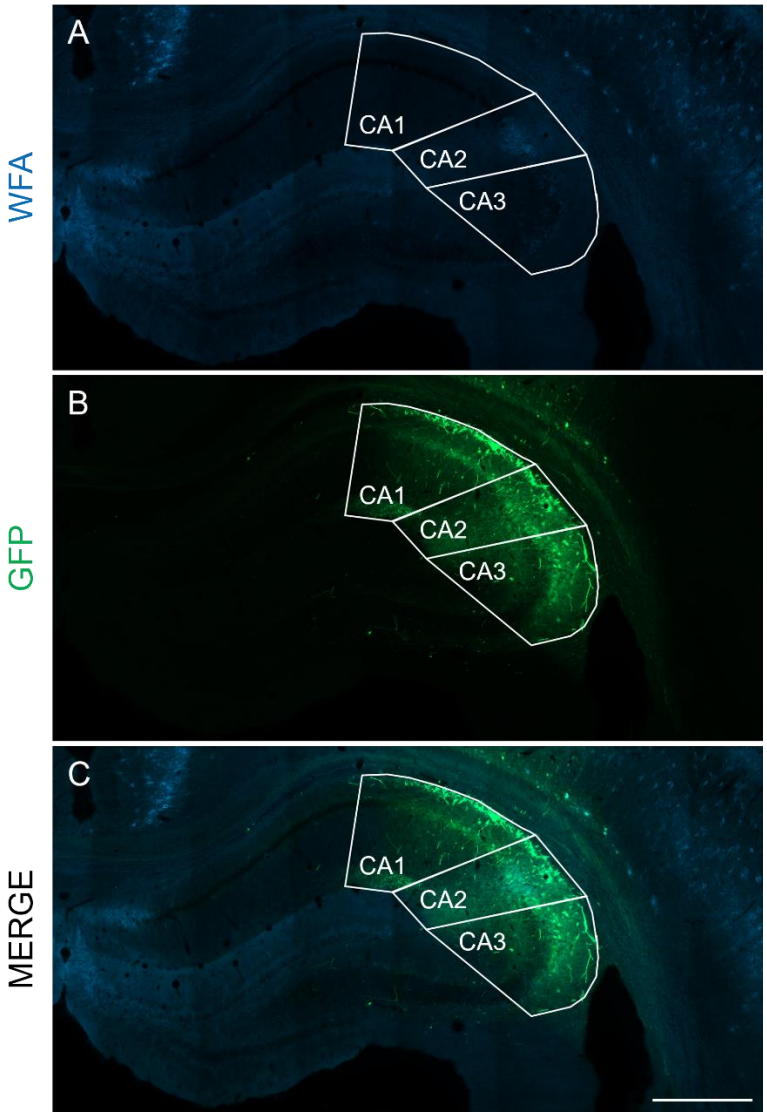

Figure 5.6. GFP expression in the hippocampus following AAV1-PGK-GFP injections.

A hippocampal tile scan stained for GFP (green) and *Wisteria floribunda agglutinin* (blue) to visualise GFP expression and PNNs, respectively, in an animal injected with AAV1-PGK-GFP. Animals received six 0.5 µL hippocampal injections (three each hemisphere) of AAV1-PGK-GFP targeting the CA1, CA2, and CA3 regions. GFP (green) was expressed in the CA1, CA2, and CA3 regions, confirming the on-target delivery of AAV into the hippocampus. Scale bar: 200 µm. Hippocampal section: Bregma -3.30 mm.

5.4.2 Hippocampal *Chst11* overexpression reduced exercise training compliance.

The percentage of training sessions in which animals complied with the MICT protocol was significantly reduced in animals that received AAV injections to overexpress *Chst11* in the hippocampus compared to animals that had GFP overexpression (Ex-Chst11: 58 %, Ex-GFP: 81 %, χ^2= 24.67, p<0.00001) (Figure 5.7). This suggests that hippocampal *Chst11* expression induced behavioural changes and reduced the animals' will to complete forced exercise.

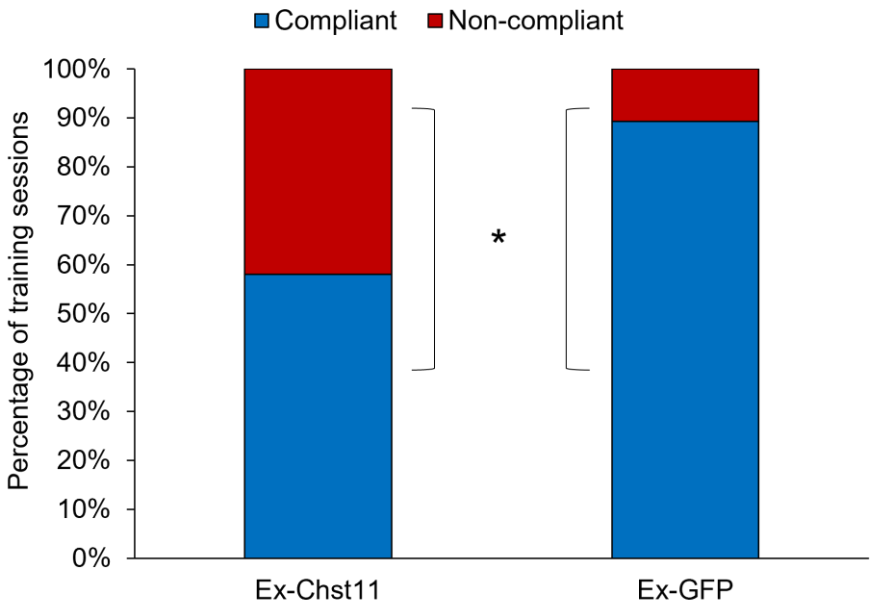

Figure 5.7. *Chst11* overexpression in the hippocampus reduced treadmill training compliance.

Exercise compliance was reduced in male Wistar rats that received hippocampal injections of AAV1-PGK-CHST11 in comparison to AAV1-PGK-GFP. Stacked bars present the mean percentage of training sessions in which animals were compliant or non-compliant with the moderate intensity continuous training (MICT) protocol over six weeks. Exercise compliance was calculated as the percentage of training sessions that the animals complied with the protocol. Non-compliance was recorded when the animals refused to run on the treadmill. Statistical significance was determined using a Chi-square test (*p<0.05). *n*=8. Ex – exercise (MICT protocol), Chst11 - Carbohydrate (chondroitin 4) sulfotransferase 11, GFP – green fluorescent protein.

Similar to previous exercise cohorts in this thesis, the trained animals that received the control GFP injections (Ex-GFP) gained less body mass following six weeks of MICT than their sedentary controls (Sed-GFP) (Ex-GFP: 52.13 ± 12.17 g; Sed-GFP: 73.50 ± 25.32 g, $t(14)= 2.152$, $p= 0.049$) (Figure 5.8). However, the change in body mass of trained animals that received hippocampal *Chst11* injections (Ex-Chst11) was comparable to their sedentary controls (Sed-Chst11) (Ex-Chst11: 65.88 ± 19.21 g; Sed-Chst11: 76.00 ± 14.452 g, $t(14)= 1.191$, $p= 0.253$). This is likely a reflection of the reduced willingness to exercise observed in animals with *Chst11* overexpression, thus resulting in lower energy expenditure. Using the percentage of compliant training sessions, the total distance performed by each training group was estimated. Throughout the study, Ex-GFP animals were collectively estimated to run 14.952 km, whereas Ex-Chst11 animals were estimated to run a total of 9.744 km.

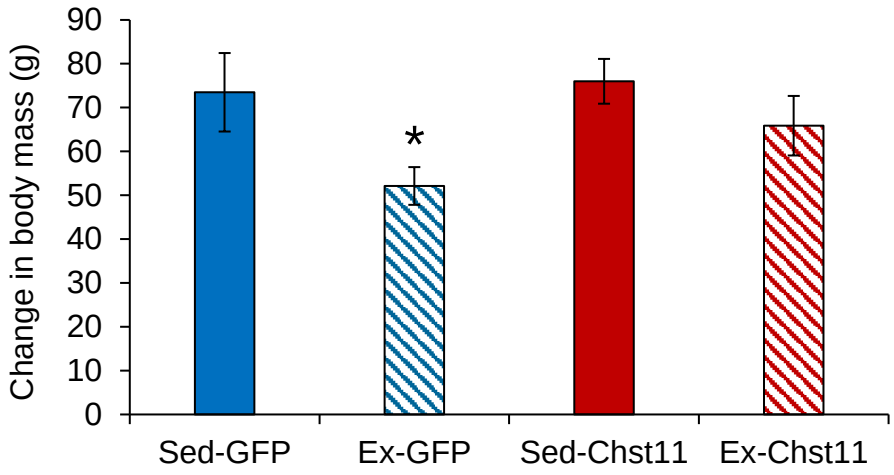

Figure 5.8. Change in body mass throughout six weeks of MICT.

Exercised male Wistar rats that received hippocampal GFP injections gained less body mass during six weeks of training than their sedentary controls, whilst change in body mass was comparable between trained and sedentary *Chst11* animals. Change in body mass was calculated between training day one and training day 30. Bars represent mean change in body mass ± SEM. *p<0.05 compared to corresponding sedentary control. Sed – sedentary; GFP – green fluorescent protein, Ex – exercise (moderate intensity continuous training); Chst11 - Carbohydrate (chondroitin 4) sulfotransferase 11. *n*=8. Statistical significance determined using independent t-tests between exercise groups and their corresponding sedentary control.

5.4.3 Hippocampal *Chst11* overexpression impaired object recognition memory after 3 hours.

Novel object recognition tests were conducted following six weeks of MICT. Rats were exposed to two identical objects in a Y-maze, removed from the apparatus for either a three hour or 24 hour delay, and then exposed to a new object pairing containing one familiar object and one novel object. Based on the innate curiosity of rats, the rats should recognise the familiar object and spend more time exploring the novel object. The exploration times of the familiar and novel objects were used to calculate the discrimination index which ranged between -1 and 1.

A positive value indicated novel object preference, whereas a negative value showed that the animal spent more time exploring the familiar object.

At the three hour delay, animals with hippocampal *Chst11* overexpression (Sed-Chst11 and Ex-Chst11) showed statistically significant reductions in the discrimination index than Ex-GFP animals (Ex-GFP: 0.541 ± 0.141 discrimination index; Sed-Chst11: 0.213 ± 0.249 discrimination index, p=0.044; Ex-Chst11: 0.200 ± 0.264 discrimination index, p=0.034; F(3,28)=5.092, p=0.006) (Figure 5.9). There were no statistically significant differences in the discrimination index between experimental groups at the 24 hour delay (Sed-GFP: 0.281 ± 0.328 discrimination index; Sed-Chst11: 0.221 ± 0.421 discrimination index; Ex-GFP: 0.362 ± 0.335 discrimination index; Ex-Chst11: 0.401 ± 0.286 discrimination index; F(3,28)=0.436, p=0.729).

A mixed mode ANOVA showed a trend in the interaction between experimental groupings and time points (F(3,28)=2.374, p=0.091). Therefore, paired t tests were performed to compare the differences in the discrimination index between the three and 24 hour delays for each experimental group. Memory performance was comparable between Sed-GFP and Ex-GFP animals at both the three and 24 hour time delays, with both groups showing a non-statistically significant reduction in discrimination index at 24 hours compared to three hours (Sed-GFP: 3 hours 0.495 ± 0.233 discrimination index, 24 hours 0.281 ± 0.328 discrimination index, t(7)=2.196 p=0.064; and Ex-GFP: 3 hours 0.541 ± 0.141 discrimination index, 24 hours 0.362 ± 0.335 discrimination index, t(7)=1.294 p=0.237) (Figure 5.9). When focusing on the groups that received hippocampal *Chst11* injections, both Sed-Chst11 and Ex-Chst11 showed comparable impairments in object

memory at the three hour time delay. After 24 hours, there was no change in the discrimination index of Sed-Chst11 animals in comparison to the three hour time point (Sed-Chst11: 3 hours 0.213 ± 0.249 discrimination index, 24 hours 0.221 ± 0.421 discrimination index, $t(7)=-0.052$ $p=0.960$). However, Ex-Chst11 animals showed a trend for object recognition memory improvements after 24 hours compared to the three hour delay (Ex-Chst11: 3 hours 0.200 ± 0.264 discrimination index, 24 hours 0.401 ± 0.286 discrimination index, $t(7)=-2.038$ $p=0.081$). This suggests that MICT was able to override the memory impairments induced by *Chst11* at the latter timepoint.

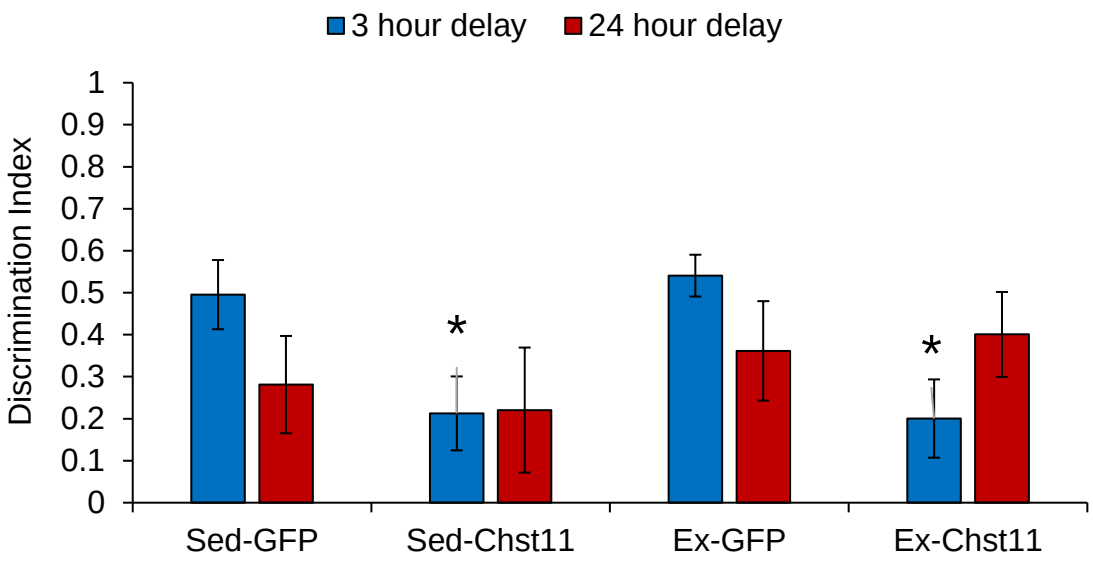

Figure 5.9. Hippocampal Chst11 overexpression impaired object recognition memory.

Novel object recognition memory was impaired in male Wistar rats that received hippocampal injections of AAV1-PGK-CHST11 at the 3 hour time delay. * - $p<0.05$ in comparison to Ex-GFP. Bars represent the mean discrimination index ± SEM. n-8. Statistically significant differences in the discrimination index between each experimental group were analysed using one way ANOVAs and Bonferroni post hoc tests for the three hour and 24 hour time delays. A mixed mode ANOVA showed that there was a trend for an interaction between the experimental groups and time delays ($F(3,28)=2.374$, $p=0.091$). To further investigate this interaction, paired t tests were used to compare the discrimination index between the 3 hour and 24 hour time delays. The Ex-Chst11 group showed a trend for exercise training to alleviate memory impairments induced by Chst11 in the 24 hour time point compared to three hours (Ex-Chst11: 3 hours 0.200 ± 0.264 discrimination index, 24 hours 0.401 ± 0.286 discrimination index, $t(7)=-2.038$ $p=0.081$). Sed – sedentary; GFP – green fluorescent protein, Ex – exercise (moderate intensity continuous training); Chst11 - Carbohydrate (chondroitin 4) sulfotransferase 11.

5.4.4 Exercise training increased novel object preference after 24 hours.

In addition to the discrimination index, the percentages of trials in which animals spent more time with the familiar or novel objects were calculated. Similar to the discrimination index, at the three hour delay there was a reduction in novel object preference in the Sed-Chst11 and Ex-Chst11 groups in comparison to animals overexpressing GFP (χ^2= 39.17, p<0.00001) (Figure 5.10). At the 24 hour time delay, both exercise groups (Ex-GFP and Ex-Chst11) demonstrated a higher proportion of trials with novel object preference than the sedentary animals (Sed-GFP and Sed-Chst11) (χ^2= 11.68, p=0.009).

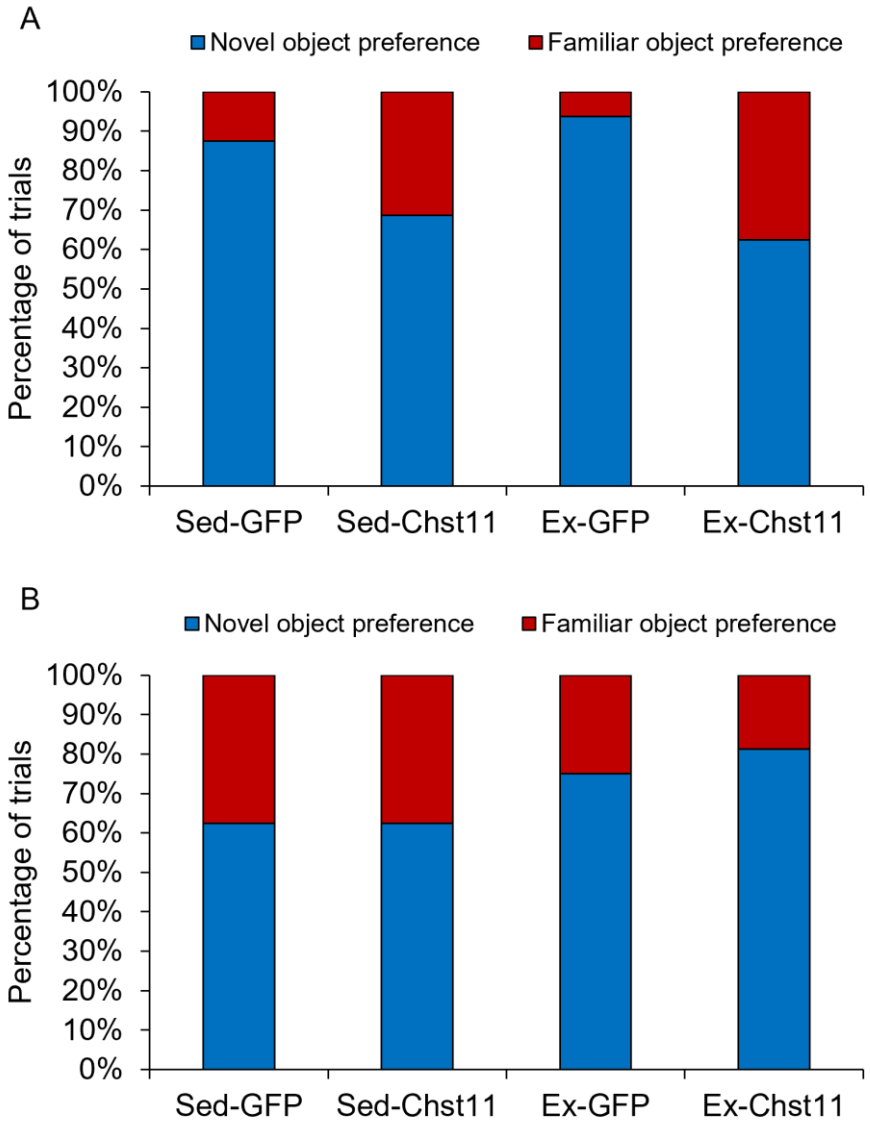

Figure 5.10. Exercise training reduced familiar object preference in *Chst11* animals.

Stacked bars present the mean percentage of training sessions in which animals preferred either the novel or familiar objects following delays of either 3 hours (A) or 24 hours (B). Preference for the familiar object increased in male Wistar rats that received hippocampal injections of AAV1-PGK-CHST11 compared to AAV1-PGK-GFP at the 3 hour time delay. Following 24 hours, rats that received *Chst11* and exercise training had reduced preference for the familiar object. The percentage of trials with preference for the novel and familiar objects were compared between groups with a Chi-Squared test (χ^2) *n*=8. Sed – sedentary; GFP – green fluorescent protein, Ex – exercise (moderate intensity continuous training); Chst11 - Carbohydrate (chondroitin 4) sulfotransferase 11.

5.5 Discussion

Sulphation patterns of chondroitin sulphate influence plasticity in the CNS (Miyata *et al.*, 2012). The increase in C4S:C6S ratio observed in aged rodents wass associated with impaired object recognition memory (Yang et al., 2021). Here, an AAV1 vector expressing *Chst11* was injected into the hippocampus in order to upregulate C4S, thus increasing the ratio of C4S:C6S. This is the first known study to induce expression of *Chst11* in the rodent CNS. The hippocampal *Chst11* injections were intended to impair object recognition memory to provide an experimental control group to assess whether exercise-induced CS-GAG modulation improved memory. This study demonstrated that hippocampal *Chst11* overexpression impaired memory performance in the three hour time delay of novel object recognition testing. This supports the notion that patterns of CS-GAG sulphation play an important role in controlling memory in the hippocampus. Secondly, this is the first study to investigate whether exercise training improves object recognition memory via modulating hippocampal CS-GAGs. Although exercise training had no statistically significant effect on the discrimination index, exercise increased the proportion of 24 hour delay trials during object recognition testing in which rats showed preference for the novel object compared to the familiar object. This suggests that whist hippocampal *Chst11* overexpression impaired short-term memory (three hours delay), exercise training can attenuate the decline observed in object recognition memory between the three and 24 hour timepoints.

5.5.1 Hippocampal *Chst11* overexpression impairs object recognition memory.

The broad degradation of CS-GAGs in PNNs and extracellular matrix, and the specific removal of PNNs have been shown to improve object recognition memory (Romberg *et al.*, 2013; Rowlands *et al.*, 2018). This study demonstrates that biochemically manipulating PNNs via CS-GAG sulphation also has the capacity to impact object recognition memory. Hippocampal injections of AAV1-PGK-CHST11 impaired object recognition memory in both sedentary and MICT adult rats. Further supporting the role of C4S in memory impairment, an antibody blocking C4S attenuated memory deficits in a tauopathy mouse model (Yang *et al.*, 2017).

Whilst *Chst11* expression and C4S is inhibitory to neuronal plasticity, the sulfotransferase *Chst3* and C6S promote plasticity in the CNS (Miyata *et al.*, 2012; Foscarin *et al.*, 2017; Yang *et al.*, 2021). An AAV expressing *Chst3* in the perirhinal cortex ameliorated age-related impairments in object recognition memory (Yang *et al.*, 2021). Additionally, transgenic overexpression of *Chst3* prevented the development of object recognition memory impairments in aged mice (Yang *et al.*, 2021). The opposing action of *Chst11* and *Chst3* supports that PNN function is dependent upon CS-GAG sulphation patterns, which play a key role in regulating cognition.

Increased *Chst3* expression reversed the age-related decline in the number of inhibitory synapses (stained with gephyrin) on parvalbumin-positive neurons and normalised the increased parvalbumin expression in the perirhinal cortex of aged mice (Yang *et al.*, 2021). As aged rodents display high C4S:C6S ratio and a

decreased number of inhibitory synapses on parvalbumin-positive neurons, it is expected that the hippocampal *Chst11* injections (which increase C4S) would also reduce the number of inhibitory synapses on parvalbumin-positive interneurons in hippocampal networks. PNNs surround inhibitory interneurons in the hippocampus, in which they regulate pyramidal cells (Yamada and Jinno, 2015; van't Spijker and Kwok, 2017). PNNs are also observed to enwrap excitatory pyramidal neurons in the CA2 region, preventing plasticity of excitatory synapses (Carstens *et al.*, 2016). Synapses surrounded by PNNs are stabilised and PNNs are known to hinder synaptic formation (Sorg *et al.*, 2016; van't Spijker and Kwok, 2017). Increases in C4S:C6S ratios make PNNs more inhibitory (Foscarin *et al.*, 2017), potentially making it harder for new connections to get through the lattice-like PNN structure and further preventing the formation of new synapses. Synaptic plasticity underpins memory formation (Takeuchi, Duszkiewicz and Morris, 2014), therefore, the memory deficits observed following *Chst11* overexpression may be due to reductions in synaptic connectivity in the hippocampus. This is biologically plausible as the application of synthetic chondroitin sulphate with a high C4S:C6S ratio reduced synaptic transmission in the CA1 and dentate gyrus regions of hippocampal slices (Albiñana *et al.*, 2015). Tissue collected from this study is currently being processed to address whether the *Chst11* injections and MICT altered synaptic connectivity in the hippocampus. Unfortunately, the start of the study in this chapter was delayed by over a year due to COVID restrictions, thus making it impossible to complete the immunohistochemistry experiments in time for thesis submission.

Overall this study has confirmed that overexpression of *Chst11* in the male rat hippocampus impaired object recognition memory. The overexpression of *Chst11* can therefore be used as a suitable experimental control for investigating whether CS-GAG modulation is involved in activity-driven plasticity and hippocampal-related memory improvements. Further investigations are required to explore the therapeutic potential of neutralising C4S to improve cognition and remediate age-related memory impairments.

5.5.2 Behavioural changes following hippocampal *Chst11* overexpression.

In addition to impaired memory, behavioural changes were observed in rats that received *Chst11* injections in the hippocampus. There was a higher proportion of *Chst11* rats that completely refused to run on the motorised treadmill in comparison to rats that received hippocampal GFP injections. Furthermore, some *Chst11* rats displayed extreme distressed and vocal behaviour whilst attempting to escape from the treadmill, behaviour which was not observed in other exercise cohorts. GFP injected rats were placid, whereas *Chst11* rats were observed to chew through and escape from their carry boxes, and bite the experimenter. Hippocampal lesions have been demonstrated to increase locomotion and hyperactivity in rats (van Praag, Dreyfus and Black, 1994). It is possible that the six stereotaxic hippocampal injections may have induced hyperactivity, however, as all rats in this study received hippocampal injections it is expected that the distressed behaviour observed was due to the overexpression of *Chst11.* Although behavioural distress was observed, it is important to note that animals did not display any visual signs of clinical distress such as pain or abnormal

respiration, grooming, motor posture, or appetite (National Research Council Committee (US), 2008; Sotocinal *et al.*, 2011). However, pain was not assessed experimentally and should be considered for future experiments overexpressing hippocampal *Chst11.* Possible behavioural tests to investigate hyperalgesia and neuropathic pain include Randall-Selitto paw pressure and von Frey tests (Chaplan *et al.*, 1994; Santos-Nogueira *et al.*, 2012).

Behavioural changes following *Chst11* injections were observed by the experimenter. Although this is not quantitative data, it does suggest that the upregulation of C4S in hippocampal PNNs may contribute to alterations in mood or emotion. Although beyond the scope of this study, the hippocampus has been implicated in psychiatric and mood disorders such as depression, schizophrenia, anxiety and bipolar disorder (Campbell and MacQueen, 2004; Revest *et al.*, 2009; Femenía *et al.*, 2012; Cao *et al.*, 2017; Lieberman *et al.*, 2018), and interacts with the amygdala which is associated with fear and emotion (Yang and Wang, 2017). Increases in C4S immunoreactivity have been observed in post-mortem hippocampal tissue from schizophrenia patients (Yukawa *et al.*, 2018). Moreover, post-mortem samples have shown a reduction of C6S in the amygdala from patients with schizophrenia and bipolar disorder (Pantazopoulos *et al.*, 2015). Together with the behavioural observations in this study, these results suggest that hippocampal CS-GAG sulphation patterns may play a role in the pathophysiology of psychiatric or mood disorders. The hippocampal injections overexpressing *Chst11* may have had an effect on the amygdala due to its proximity and connection to the hippocampus. Tissue collected in this study will be used in immunohistochemistry experiments to determine whether

hippocampal *Chst11* also affects the expression of PNNs and structural plasticity in the amygdala. More research is warranted to elucidate the behavioural effect of hippocampal *Chst11* overexpression. It is possible that C4S could be a therapeutic target for the treatment of mood and psychiatric disorders.

5.5.3 MICT improved object recognition memory after 24 hours.

Treadmill training has been documented to improve object recognition memory in healthy adult rats (O'Callaghan, Ohle and Kelly, 2007; Bechara and Kelly, 2013). In Chapter 4, MICT was shown to increase the proportion of PNNs that express only aggrecan without CS-GAG labelling in the hippocampus. To investigate whether the exercise-induced CS-GAG modulation was involved in memory improvements, six weeks of MICT was implemented following hippocampal *Chst11* injections that impair object recognition memory via upregulating the inhibitory sulphation of CS-GAGs. The hippocampal *Chst11* injections impaired object recognition memory in both sedentary and trained animals at the three hour delay. At the three hour time delay, MICT was not shown to improve object recognition memory in animals that received either GFP control injections or *Chst11* overexpression. The memory impairments induced by *Chst11* remained comparable between three and 24 hours in sedentary animals. However, there was a trend of a higher discrimination index in the Ex-Chst11 group at 24 hours compared to the three hour time delay. Additionally, MICT showed a statistically significant increase in the proportion of trials in the 24 hour delay which demonstrated a preference for the novel object in both the Ex-GFP and Ex-Chst11 groups. These results show that MICT is capable of attenuating memory deficits induced by hippocampal C4S sulphation at the 24 hour delay,

supporting a causal role of exercise-induced CS-GAG modulation in improved object recognition memory.

The MICT protocol adopted in this study involved a relatively low volume of daily exercise (33 minutes/day). Other treadmill paradigms utilising low daily exercise volumes (28 and 30 minutes/day) have also been reported to not produce statistically significant improvements in novel object recognition tests in healthy animals (Cefis *et al.*, 2019; Constans *et al.*, 2021). Whereas, longer durations of treadmill training sessions (one hour/day for seven days) have been documented to enhance object recognition memory (O'Callaghan, Ohle and Kelly, 2007; Bechara and Kelly, 2013). These results indicate that daily training volume is an important factor for enhancing object recognition memory in healthy rodents.

Animals used in this thesis and the aforementioned studies were young adult rats. Data presented in Figure 4A shows that animals in the control group (Sed-GFP) showed preference for the novel object in around 90% of trials at the three hour time delay, which does not leave much room for improvement. It is possible that exercise training has a more potent impact on improving object recognition memory in aged rodents, or models of Alzheimer's disease in which cognitive decline has already manifested. Aged rats (19-26 months old) displayed impaired object recognition memory in comparison to young adult rats (three to four months old) (Luparini *et al.*, 2000; Terry, Kutiyanawalla and Pillai, 2011). Moderate intensity treadmill training has been documented to improve object recognition memory in 32 month old rats, but not 24 month old rats (Téglás *et al.*, 2019). The overexpression of *Chst3* improved object recognition memory in 20 month old mice, whilst having no effect on young mice (6 months old) (Yang *et*

al., 2021) This further supports that the success of interventions to improve object recognition memory is age-dependent. Additionally, treadmill exercise with low daily training volume (30 - 40 minutes) normalised object recognition memory impairments in a rat model of Alzheimer's disease (Farzi *et al.*, 2019; Dare *et al.*, 2020).

In summary, MICT may have a more profound effect on object recognition memory in aged rats or in neurological conditions such as Alzheimer's disease where cognitive decline has developed. It is yet to be investigated whether the exercise-induced modulation of PNNs or CS-GAGs plays a role in ameliorating memory impairments in aged or Alzheimer's rodent models. Exploring this avenue may further elucidate therapeutic mechanisms of exercise training that are advantageous for managing cognitive decline.

5.5.4 Future work

Following behavioural testing, fresh and fixed brain tissue was collected to investigate structural hippocampal plasticity following MICT and *Chst11* overexpression. To further establish whether exercise training modulates CS-GAGs in the hippocampus, quantitative CS-GAG extraction experiments will be performed on fresh hippocampal samples. These experiments will also provide a novel insight into whether *Chst11* expression also alters the overall number of CS-GAGs in the hippocampus, or if CS-GAG numbers remain the same and only sulphation is manipulated.

The overexpression of *Chst11* is expected to make PNNs more inhibitory and restrict plasticity. Additionally, MICT is expected to modulate CS-GAGs and promote plasticity. Therefore, it will be beneficial to investigate excitatory and

inhibitory connectivity in PNNs of different hippocampal regions. To do this, fixed cryosections will be immunohistochemically stained for PNNs, excitatory synapses (HOMER antibody), and inhibitory synapses (gephyrin antibody).

5.5.5 Conclusions

Overall, this study suggests that the overexpression of *Chst11* impairs object recognition memory. However, immunohistochemistry experiments are required to confirm the spread of the virus and investigate C4S expression alongside structural changes in order to link hippocampal *Chst11* expression with impaired object recognition memory. MICT showed a positive effect of exercise training on memory with increased preference for the novel object after 24 hours. Furthermore, MICT rescued memory impairments associated with *Chst11* after 24 hours that remained unchanged from the three hour time point in sedentary animals. These results support that exercise-induced plasticity is not only dependent on mechanisms related to the upregulation of neurotrophic factors such as BDNF, and that the regulation of inhibitory molecules via exercise training may also play a critical role in how exercise effects the brain.

Chapter 6 General discussion

6.1 Summary of key findings

The aim of this thesis was to explore whether exercise training moderated the expression of inhibitory molecules that restrict CNS plasticity. Primary investigations demonstrated that treadmill training in the form of MICT modulated aggrecan expression, altered the biochemical composition of PNNs, and alleviated memory deficits induced by overexpression of *Chst11* in the hippocampus. Figure 6.1 depicts a proposed mechanism for how *Chst11* and MICT alter the biochemical structure of PNNs and impact novel object recognition memory. This thesis has provided a novel insight into how exercise training modulates the restriction of plasticity in the CNS of adult rats.

6.2 Exercise modulates PNN composition and improves novel object preference.

This is the first study to show that aggrecan mRNA and PNN composition can be regulated by treadmill training. It is well documented that exercise promotes plasticity by enhancing neurotrophic factors such as BDNF (Gómez-Pinilla *et al.*, 2002; Vaynman, Ying and Gómez-Pinilla, 2004; Griffin *et al.*, 2009; Lee *et al.*, 2012; Bechara and Kelly, 2013; Freitas *et al.*, 2018; Liu and Nusslock, 2018; Pietrelli *et al.*, 2018). This thesis supports the notion that exercise has a dual effect in the CNS, and also has the capacity to modulate molecules that are known to restrict plasticity.

In the hippocampus, the total number of PNNs was not altered by exercise training. However, it has been suggested that changes in memory are dependent on the biochemical composition of PNNs, rather than the overall number of PNN-bearing neurons (Yang *et al.*, 2021). Here, MICT was observed to increase the

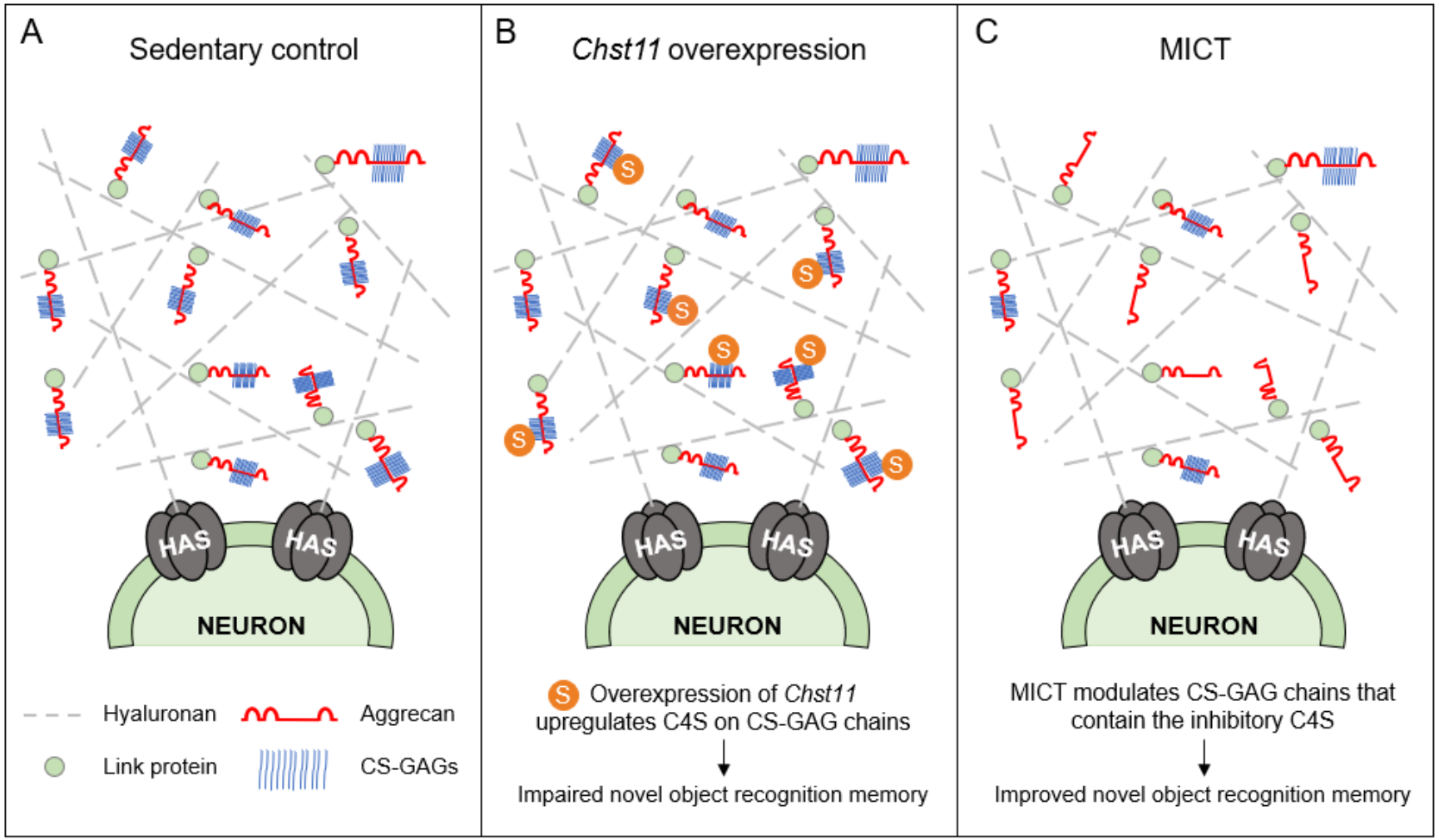

Figure 6.1. A proposed mechanism for how *Chst11* and MICT impact novel object recognition memory.

A. Depicts a simplified structure of a perineuronal net (PNN) under the normal physiological conditions used within this thesis (sedentary control animals). Hyaluronan synthase produces a hyaluronan back bone in which chondroitin sulphate proteoglycans (CSPGs), such as aggrecan, can bind to via link proteins. Chondroitin sulphate – glycosaminoglycan chains (CS-GAGs) are covalently attached to serine residues within the CSPG core protein. Other PNN components such as different lecticans and tenascins were omitted from the PNN schematic to clearly focus on the main candidates within this thesis, aggrecan (red) and CS-GAGs (blue).

B. Within this thesis, the overexpression of the chondroitin 4-sulfotransferase, *Chst11,* in the hippocampus was shown to impair novel object recognition performance. The *Chst11* gene is known to upregulate sulphation at position C4 on CS-GAGs (known as C4S – depicted as the orange circle containing a white 'S'). C4S is known to be inhibitory to neural plasticity, and thus, an upregulation of C4S may impede the synaptic changes that are required to sustain memory formation.

C. Six weeks of moderate intensity continuous training (MICT – once a day, five days a week, for six weeks) was shown to induce a shift towards a higher number of PNNs within the hippocampus that were labelled for aggrecan without CS-GAGs. Furthermore, MICT was demonstrated to improve preference for the novel object within novel object recognition tests. As CS-GAGs contain the inhibitory C4S, a reduction in the number of CS-GAGs in the hippocampus may create a more permissive environment for synaptic formation and synaptic changes to occur that may facilitate memory formation. Therefore, the modulation of hippocampal CS-GAGs induced by MICT may attenuate memory deficits associated with *Chst11.*

Note that this schematic has been created specifically within the context of this thesis. Further experiments are required to determine whether Chst11 overexpression upregulates the expression of hippocampal C4S, and whether Chst11 and MICT result in synaptic changes within the hippocampus that are associated with changes in novel object recognition memory performance.

proportion of PNNs expressing aggrecan and not WFA, suggesting that exercise training modulated the expression of CS-GAGs in hippocampal PNNs. CS-GAGs are implicated in learning and memory as their degradation with chondroitinase ABC has been demonstrated to improve learning acquisition, object recognition memory, and fear extinction (Gogolla *et al.*, 2009; Romberg *et al.*, 2013; Carulli *et al.*, 2020). Chondroitinase ABC results in the widespread digestion of CSPGs in the extracellular matrix and degrades PNNs. In comparison, MICT induced a subtle modulation of CS-GAGs whilst PNN integrity was maintained. Therefore, this study aimed to determine whether the more subtle modulation of CS-GAGs following MICT played a causal role in improving object recognition memory.

AAV1-PGK-CHST3 has previously been used to increase C6S (the plasticity promoting CS-GAG sulphation) in the perirhinal cortex of mice, and was observed to enhance object recognition memory (Yang *et al.*, 2021). Therefore, this study injected AAV1-PGK-CHST11, intending to make PNNs more inhibitory by upregulating C4S of CS-GAGs. It was expected that the overexpression of hippocampal *Chst11* would impair object recognition memory, and that MICT would modulate CS-GAG chains that contain the inhibitory C4S to attenuate the memory deficits. The hippocampal injections overexpressing *Chst11* were associated with impaired performance in object recognition tests. It is already known that PNNs in the perirhinal cortex are involved in object recognition memory (Romberg *et al.*, 2013; Yang *et al.*, 2021). However, this study demonstrated for the first time that hippocampal PNNs may also play a role in object recognition memory. There was a trend for MICT to improve novel object discrimination between the 3 and 24 hour delays in animals that received *Chst11*

injections suggesting that exercise training alleviates memory impairment induced by C4S of CS-GAGs. Further supporting this, MICT increased the proportion of trials in which animals displayed preference for the novel rather than familiar object in *Chst11* treated animals. These are encouraging results to support that CS-GAG modulation is a mechanism in which exercise training improves object recognition memory.

6.3 Does CS-GAG modulation reorganise synaptic circuitry?

Tissue is currently being processed to assess whether the exercise-induced modulation of CS-GAGs promoted synaptic reorganisation and whether this was associated with object recognition memory performance. Unfortunately due to COVID related lab restrictions, this work could not be included in the thesis.

Chondroitinase ABC has been shown to increase the number of inhibitory synapses, and decrease excitatory terminals around PNN bearing neurons in the deep cerebellar nuclei (Carulli *et al.*, 2020). Similar to removing CSPGs, rendering them less inhibitory by overexpressing *Chst3* in the perirhinal cortex also increased the number of inhibitory synapses on parvalbumin-positive neurons (Yang *et al.*, 2021). In contrast, application of chondroitinase ABC to hippocampal cultured neurons reduced the excitatory input to inhibitory neurons, and reduced the number of inhibitory synapses to both excitatory and inhibitory neurons (Dzyubenko *et al.*, 2021). This was supported as *in vivo* application of chondroitinase ABC in the cortex reduced the density of inhibitory synapses in fast-spiking interneurons (Dzyubenko *et al.*, 2021). These results demonstrate that chondroitinase ABC, and thus CSPGs, distinctly affect synaptic organisation in different neuronal populations. Therefore, it will be noteworthy to elucidate the

organisation of circuitry in the hippocampus following both the exercise-induced modulation of CS-GAGs, and the overexpression of *Chst11* to further characterise the role of hippocampal PNNs in object recognition memory.

It is possible that the overexpression of *Chst11* will have the opposite effect of *Chst3*, and reduce the number of inhibitory synapses around parvalbumin positive interneurons in the hippocampus. Hippocampal parvalbumin interneurons form synaptic connections on the soma, axon initial segment, and distal dendrites that can reduce activity of pyramidal cells (Hu, Gan and Jonas, 2014). Both fast-spiking interneurons and pyramidal cells are surrounded by PNNs in the hippocampus (Carstens *et al.*, 2016; Yamada and Jinno, 2017), and thus the synaptic connections upon both types of neurons may be altered following CS-GAG modulation. However, seven days of chondroitinase ABC treatment reduced the excitatory synaptic transmission, and increased inhibitory synaptic transmission of fast-spiking interneurons in the hippocampal CA2 region, whilst no changes in synaptic transmission were observed in CA2 pyramidal cells (Hayani, Song and Dityatev, 2018). Therefore, it is expected that the modulation of CS-GAGs will have a more potent effect on the synaptic organisation of hippocampal interneurons compared to pyramidal neurons.

6.3.1 Does MICT enhance synaptic formation?

It is expected that the exercised-induced modulation of CS-GAGs will make hippocampal PNNs less inhibitory, and facilitate synaptic formation. Exercise training has been documented to increase the expression of synapsin I, a synaptic protein associated with GABAergic synapses, in the rodent hippocampus (Vaynman, Ying and Gómez-Pinilla, 2004). As discussed

previously, the number of inhibitory synapses was increased following the degradation of CS-GAGs using chondroitinase ABC (Carulli *et al.*, 2020). Though, it is yet to be directly investigated whether the modulation of CS-GAGs is an underlying mechanism of exercise-induced hippocampal synaptogenesis.

This thesis also observed that exercise training reduced the expression of *NgR2* in the hippocampus. This further supports that exercise enhances synaptic formation as NgR2 is known to restrict the number of hippocampal synapses (Wills *et al.*, 2012). Additionally, MICT reduced the hippocampal expression of several RhoA/ROCK pathway components including: *Acan, OMGp, NgR2, NgR3, GNA13, ROCK2, Limk1, and Crmp2*. The RhoA/ROCK pathway plays a role in restricting plasticity of dendritic spines, in which postsynaptic sites are located (Spence and Soderling, 2015; Runge, Cardoso and de Chevigny, 2020). Thus, the combined effect of downregulated gene expression within the RhoA/ROCK pathway may enhance plasticity of dendritic spines, creating more target sites for the formation of new synapses in the hippocampus. CSPGs are known to bind to the receptors that activate the RhoA/ROCK pathway including NgR1, NgR3, and PTPRS (Dickendesher *et al.*, 2012). Chondroitinase ABC, that degrades CSPGs, was observed to increase dendritic spine motility in the visual cortex (De Vivo *et al.*, 2013). It is possible that the reduced activation of the RhoA/ROCK pathway dovetails with modulation of CS-GAGs observed following MICT to facilitate synaptic reorganisation.

The remaining tissue from the final study in this thesis will be used to investigate the excitatory/inhibitory synaptic organisation in hippocampal PNNs from MICT and *Chst11* animals. This will help determine whether exercise-induced CS-GAG

modulation is causally linked with improved object recognition memory. These findings will help elucidate the mechanisms underlying both exercise-dependent memory improvements, and C4S-dependent memory impairments, which will be advantageous for preventing or treating cognitive decline.

6.4 Exercise training does not regulate components of the RhoA/ROCK pathway in the cortex and lumbar regions.

The gene expression of many components within the RhoA/ROCK pathway were downregulated in the hippocampus following exercise training. However, the cortex and lumbar regions were much less susceptible to exercise-induced changes in the expression of RhoA/ROCK pathway genes. Within the cerebral cortex, exercise training has also been shown to not alter BDNF mRNA (Neeper *et al.*, 1996) and BDNF protein (Serra *et al.*, 2019), whilst hippocampal BDNF levels were increased. However, cortical neurons in the latter study demonstrated increased dendritic length, number of dendritic bifurcations, and number of dendritic ends following exercise training, despite a lack of enhanced cortical BDNF expression (Serra *et al.*, 2019). These results suggest that the enhanced dendritic complexity in the cortex following exercise training is independent of BDNF and the regulation of RhoA/ROCK pathway components. It is possible that exercise training regulates other mechanisms involved in dendritic plasticity within the cerebral cortex that were not analysed in this thesis. For example, reelin is an extracellular matrix glycoprotein that enhances dendritic growth, and Wnt family glycoproteins enhance dendritic complexity (Arikkath, 2012). Exercise training has been shown to upregulate Wnt/β-catenin signalling in the hippocampus and the cerebral cortex (Bayod *et al.*, 2014; Fang *et al.*, 2017; Chen

et al., 2020). Additionally, reelin expression was upregulated in the hippocampus following exercise training (Seo *et al.*, 2013; Baek, Ji and Lee, 2014), however, it is not yet known whether exercise training regulates cortical reelin expression.

This thesis showed that there were no statistically significant gene expression changes within the RhoA/ROCK pathway in lumbar tissue following exercise training. The lumbar region of the spinal cord contains motor neurons that are the last point of CNS control over motor output of the hindlimbs (Borrell *et al.*, 2016). In the CNS of non-injured animals, the neuronal circuitry controlling motor output may already be optimised and thus not require any structural plasticity. In support of this, voluntary wheel running was shown to enhance the thickness of PNNs in the lumbar spinal cord (Smith *et al.*, 2015), potentially further stabilising the existing synaptic connections of motor neurons. Aggrecan is a major CSPG expressed in motor neurons (Irvine and Kwok, 2018). In this thesis, aggrecan mRNA expression was shown to be slightly upregulated in lumbar tissue following exercise training compared to sedentary animals (CON: 1, MICT relative fold change 1.29, HIIT relative fold change 1.18). Although not statistically significant, the increase in lumbar aggrecan mRNA expression supports the theory that exercise training may be stabilising synapses of motor neurons.

6.5 MICT induces greater alterations in hippocampal PNN composition than HIIT.

Previous research has demonstrated that HIIT is superior to MICT for enhancing BDNF and GDNF protein levels in the rat hippocampus, despite the HIIT protocol having a lower duration and total distance than MICT (Afzalpour *et al.*, 2015). Another study that work-matched MICT and HIIT also showed that HIIT enhanced

the expression of hippocampal VEGF, PGC-1α (which stimulates mitochondrial biogenesis), and Trk-B to a greater extent that MICT (Constans *et al.*, 2021). Similarly, this thesis reported that HIIT resulted in a greater reduction of aggrecan mRNA than MICT in the hippocampus. However, MICT resulted in more widespread changes in hippocampal PNN composition than HIIT. Although HIIT enhances a number of growth factors for neural plasticity to a greater extent than MICT, low-moderate exercise intensities have been shown to be favourable for improving memory performance (Inoue, Hanaoka, *et al.*, 2015; Wu *et al.*, 2020). This thesis supports this as the MICT-induced modulation of CS-GAGs had a positive effect on recognition memory. The fewer adaptations in hippocampal PNNs following HIIT in comparison to MICT may be explained by the elevated hippocampal *Chst8* expression observed in HIIT animals. *Chst8*, a GalNAc 4-0 sulfotransferase, enhances C4S in CS-GAGs which is associated with lower levels of plasticity. Furthermore, PNNs are known to protect neurons from oxidative stress (Morawski *et al.*, 2004; Cabungcal *et al.*, 2013). In comparison to MICT, HIIT was shown to increase the hippocampal levels of hydrogen peroxide (H_2O_2), a marker of oxidative stress (Afzalpour *et al.*, 2015). Therefore, PNNs in the hippocampus of HIIT trained rats may be more resistant to change as a protective mechanism against oxidative stress.

In this thesis, MICT and HIIT were matched for duration, distance, and estimated work, thus the parameters that differed between the two groups were the nature of exercise (continuous vs. interval) and the intensity of exercise. Lower intensity treadmill training has previously been documented to be beneficial for improving spatial memory in a rodent stroke model in comparison to higher-intensity

treadmill training (Shih, Yang and Wang, 2013). Further comparisons of intensity in continuous treadmill training have shown that high intensity exercise elevated the stress hormone corticosterone in plasma, which was associated with lower levels of neurogenesis than observed after moderate intensity exercise (Inoue, Okamoto, *et al.*, 2015). Inoue *et al.,* (2015) also showed that moderate (below lactate threshold) and intense (above lactate threshold) exercise training resulted in different transcriptomic profiles in hippocampal tissue. The transcriptomic profile of intense exercise training was associated with an excessive inflammatory response which was expected to negatively regulate neural plasticity and explain the lower levels of hippocampal neurogenesis (Inoue, Okamoto, *et al.*, 2015).

Lactate was once considered to be a mere waste-product of glycolysis during exercise, however, exercise-derived lactate can cross the blood brain barrier and is now thought to enhance exercise-mediated plasticity (Huang *et al.*, 2021). In the CNS, astrocytes also produce lactate that is used as an energy source to sustain memory processes (Alberini *et al.*, 2018). Voluntary wheel running has been shown to increase hippocampal levels of lactate in mice, and lactate was shown to improve spatial memory (El Hayek *et al.*, 2019). However, it is not known whether that voluntary wheel running paradigm included exercise below or above the lactate threshold. The lactate threshold is the point where there is a non-linear increase blood lactate concentration (Ghosh, 2004), when lactate is produced faster than the body can remove it. The effect of lactate on PNNs has not yet been investigated. Although, it is expected that the HIIT protocol used in this thesis would produce more lactate than MICT, and thus it would be

noteworthy to investigate whether intensity-dependent lactate production is involved in the regulation of PNN composition.

HIIT is an attractive exercise paradigm for many people due to the lower durations of exercise required to promote physiological adaptations, and the incorporation of rest intervals. However, HIIT is associated with high injury prevalence (Rynecki *et al.*, 2019). Additionally, HIIT induces rapid elevation of systemic blood pressure which can lead to disruption of the blood brain barrier, and predisposition to strokes (Lucas *et al.*, 2015). Thus, the implementation of HIIT in older adults and clinical populations may be more suitable in rehabilitation settings which can screen for cardiovascular problems and deliver rapid medical attention if needed. MICT may be an easier and safer exercise paradigm to prescribe to older adults and patients with neurological conditions, and therefore MICT may be more feasible for widespread clinical implementation than HIIT for improving memory impairments.

6.6 Future perspectives

Within this thesis, treadmill training with low daily training volume was implemented as this form of exercise is more easily achievable for humans than the long distance running associated with voluntary wheel running paradigms. Although voluntary wheel running and larger training volumes showed greater changes in the reduction in number and thickness of PNNs (Smith *et al.*, 2015), this thesis established that low volume MICT modulated PNN composition in the hippocampus without altering the overall number of PNNs. These studies, alongside others, provide evidence that exercise-induced neural plasticity e.g. neurotrophic and inhibitory factor expression, object recognition memory

performance, and PNN modulation are volume-dependent (Neeper *et al.*, 1996; Gómez-Pinilla *et al.*, 2002; Ghiani *et al.*, 2007; O'Callaghan, Ohle and Kelly, 2007; Chytrova, Ying and Gomez-Pinilla, 2008; Bechara and Kelly, 2013; Smith *et al.*, 2015; Cefis *et al.*, 2019; Constans *et al.*, 2021). There is a large difference in the daily distances ran in this study (approximately 600 m) in comparison to distances ran in voluntary running wheel studies that demonstrated the reduction of PNN number and thickness in the hippocampus (up to 8.76 km) (Smith *et al.*, 2015). From a therapeutic perspective, it would be valuable to determine a profile of what PNN modifications are induced by different volumes of exercise, and establish the minimum volume of exercise required to induce functional plasticity and behavioural changes.

In addition to the work conducted by Smith *et al.,* (2015), this thesis has corroborated that PNNs are susceptible to exercise-induced modification. Current methods of manipulating PNNs to study their role in memory include the use of the bacterial enzyme chondroitinase ABC which is invasive (Romberg *et al.*, 2013), and transgenic knockout models that are not translatable to human treatment (Romberg *et al.*, 2013; Rowlands *et al.*, 2018). Exercise training poses a non-invasive and clinically relevant intervention in comparison to other current methods of PNN modulation. The observations that PNNs can be modulated by exercise can be extended to investigate whether exercise training has therapeutic value in neurological conditions that display PNN abnormalities, such as Alzheimer's disease, schizophrenia, epilepsy, CNS injuries, and strokes (Wen *et al.*, 2018). Additionally, the potential of exercise to regulate PNN expression and composition may be beneficial in the aged CNS in which higher ratios of C4S:C6S

make PNNs more inhibitory and are associated with memory impairments (Foscarin *et al.*, 2017; Yang *et al.*, 2021).

Further supporting the role of C4S in memory impairment, this thesis confirmed that the overexpression of *Chst11* in the hippocampus of healthy rats impaired object recognition memory. This adds to the growing body of literature demonstrating that PNN function, and thus the level of plasticity control, is dependent on the sulphation patterns of CS-GAG chains (Miyata *et al.*, 2012; Foscarin *et al.*, 2017; Yang *et al.*, 2017, 2021). There is limited evidence to support that using an antibody to block C4S alleviates memory deficits within a tauopathy model of Alzheimer's disease (Yang *et al.*, 2017). Together these studies highlight that C4S and *Chst11* are potential therapeutic candidates for neurological conditions that involve cognitive impairment.

6.7 Conclusions

This was the first study to assess the role of treadmill training on the expression of molecules that restrict neural plasticity in the CNS. The initial exploratory study identified that the mRNA expression of the CSPG aggrecan was downregulated in the hippocampus following MICT and HIIT. This finding highlighted aggrecan as a novel candidate in exercise-induced plasticity. Subsequently, MICT altered the composition of hippocampal PNNs with a transition towards more PNNs expressing aggrecan core protein without labelled CS-GAG chains. The overexpression of *Chst11* in the hippocampus impaired short-term object recognition memory, although future experiments are needed to establish whether this was associated with an upregulation of C4S and changes in synaptic connectivity. MICT enhanced object recognition memory in animals that received

Chst11 treatment after 24 hours, supporting that the exercise-induced modulation of CS-GAGs counteracts the inhibitory action of *Chst11.*

This study provides evidence that exercise training is a non-invasive method of manipulating aggrecan expression and PNN composition in the CNS, with the potential to attenuate memory deficits. These results have biological significance as current methods of manipulating PNNs such as chondroitinase ABC and transgenic knockout models are invasive and not translatable to human treatment. Furthermore, MICT is a cost-effective lifestyle intervention that can be performed anywhere without the cost of specialised equipment or gym membership. Therefore, MICT has great therapeutic potential for treating conditions that are characterised by cognitive decline e.g. in elderly populations or Alzheimer's disease, or for conditions that are associated with PNN abnormalities.

This body of work supports the notion that exercise training has a dual effect in the CNS. It is well known that exercise training upregulates neurotrophic factors that promote plasticity, and this thesis demonstrates that exercise training also modulates the restriction of plasticity exerted by PNNs. Previous research implementing exercise to enhance plasticity may have been reporting only one half of the story. Thus, incorporating the analysis of inhibitory modulators of plasticity into these interventions may provide a more complete understanding of exercise-induced plasticity.

Overall, the contents of this thesis have provided a novel insight into how treadmill training potentially enhances plasticity through the modulation of PNNs. More research is required to optimise the dose of exercise required to induce the level

of PNN modulation for the best functional benefit. Future investigations can build upon this to determine whether the exercise-induced modulation of PNNs or CS-GAGs can be harnessed to improve memory in conditions which cognitive decline is a debilitating symptom.

Appendix A $\dot{V}O_{2\ max}$ tests

i. Respirometry system used for $\dot{V}O2$ max tests

For all $\dot{V}O_{2\ max}$ tests, air was extracted from the chamber at 15 $L.min^{-1}$ by a vacuum pump (model DOA-P504-BN, GAST Manufacturing Inc., MI, USA), controlled by a mass flow controller (MFC-2, Sable Systems International Inc., NV, USA), through a mass flow control valve (840 Side-Trak Mass Flow Controller; Sierra Instruments Inc., CA, USA), and into an open syringe barrel (Figure_A.1). Air was subsampled from the barrel at 200 $mL.min^{-1}$ and passed through a Drierite column to remove water, before entering a custom made differential O_2 analyser based on a zirconia sensor. The analyser measured the difference in O_2 content between chamber air, and outside air that was drawn in at 200 $mL.min^{-1}$, dried (Drierite), and CO_2 scrubbed (soda lime). The air sample then passed through a CO_2 analyser (ADC-225-MK3, Analytical Development Company, UK). Outputs were converted by PowerLab and recorded in LabChart (ADInstruments Inc., CO, USA). The analysers were calibrated before each $\dot{V}O_{2\ max}$ test using a speciality gas mixture of 20% O_2 and 1% CO_2 (BOC Gases, UK) and outside air scrubbed of CO_2 (20.95% O_2 and 0% CO_2).

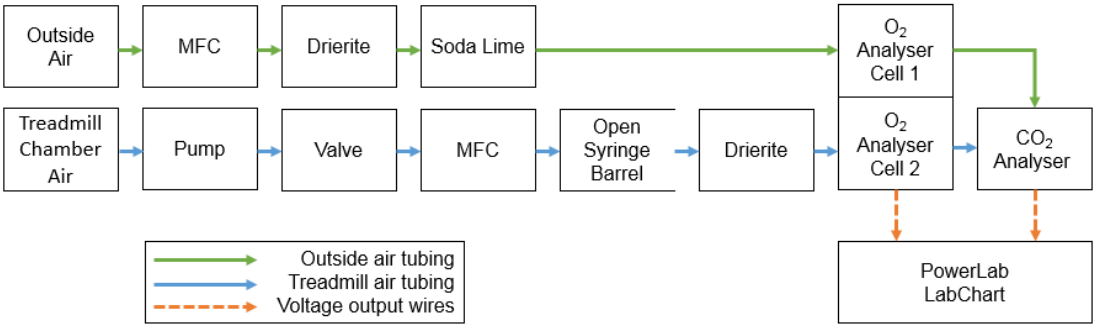

Figure_ A.1 Schematic diagram of the respirometry system

The coloured full-line arrows represent the air flow through components of the respirometry system. The dashed lines represent electrical wires in which the voltage output is converted from analogue to digital. MFC: mass flow controller.

ii. Respirometry data analysis

Respirometry data was analysed using IGOR Pro (version 6.2.2.2, WaveMetrics, USA). The calibration values set in LabChart transferred to the IGOR software (ΔCO_2: 0-1%, ΔO_2: 0-0.95%) (Figure A.2 A). The extraction flow rate (FR) was adjusted to read 15 $L.min^{-1}$ (Figure A.2 B). In future experiments, a two-point calibration will be used to calibrate extraction flow rate. As the air sample is analysed sequentially, there is a time offset between the O_2 and CO_2 traces as can be seen in Figure A.2 C. The number of data points between two identical peaks in the O_2 and CO_2 traces was calculated. The number of data points in the offset was removed from the start of the CO_2 trace to align the traces, and removed from the end of the O_2 trace to match the trace lengths. Figure A.2 D displays the aligned traces. The corrected flow rate (FR_c) was calculated using Equation A.1 (Lighton, 2008).

Equation_ A.1 Corrected flow rate (FR_c)

$$FR_c = FR\ (BP - WVP)/BP$$

where BP is ambient barometric pressure and WVP is the partial pressure of water vapour in the airflow. The rate of CO_2 production ($\dot{V}CO_2$, ml.min^{-1}) and O_2 consumption ($\dot{V}O_2$, ml.min^{-1}) was calculated using Equation A.2 and Equation A.3, respectively (Lighton, 2008).

Equation_ A.2 Rate of CO_2 production ($\dot{V}CO_2$)

$$\dot{V}_{CO_2} = \frac{FR_c\left[\left(F_{ECO_2} - F_{ICO_2}\right) + F_{ICO_2}\left(F_{IO_2} - F_{EO_2}\right)\right]}{\left(1 + F_{ICO_2}\right)}$$

Equation_ A.3 Rate of O_2 uptake ($\dot{V}O_2$)

$$\dot{V}_{O_2} = \frac{FR_c\left[\left(F_{IO_2} - F_{EO_2}\right) - F_{IO_2}\left(F_{ECO_2} - F_{ICO_2}\right)\right]}{\left(1 - F_{IO_2}\right)}$$

where F_{ICO_2} is the fractional CO_2 content of air entering the treadmill chamber, F_{ECO_2} is the fractional CO_2 content of air leaving the treadmill chamber, F_{IO_2} is the fractional O_2 content of air entering the treadmill chamber and F_{EO_2} is the fractional O_2 content of air leaving the treadmill chamber. $\dot{V}CO_2$ and $\dot{V}O_2$ traces are displayed in Figure 6E. The respiratory exchange ratio (RER) (Figure A.2 F) was calculated using Equation A.4.

Equation_ A.4 Respiratory exchange ratio (RER)

$$RER = \frac{\dot{V}_{CO_2}}{\dot{V}_{O_2}}$$

A RER less than or equal to one indicates that the exercise is aerobic, whereas a RER greater than one indicates that exercise is anaerobic.

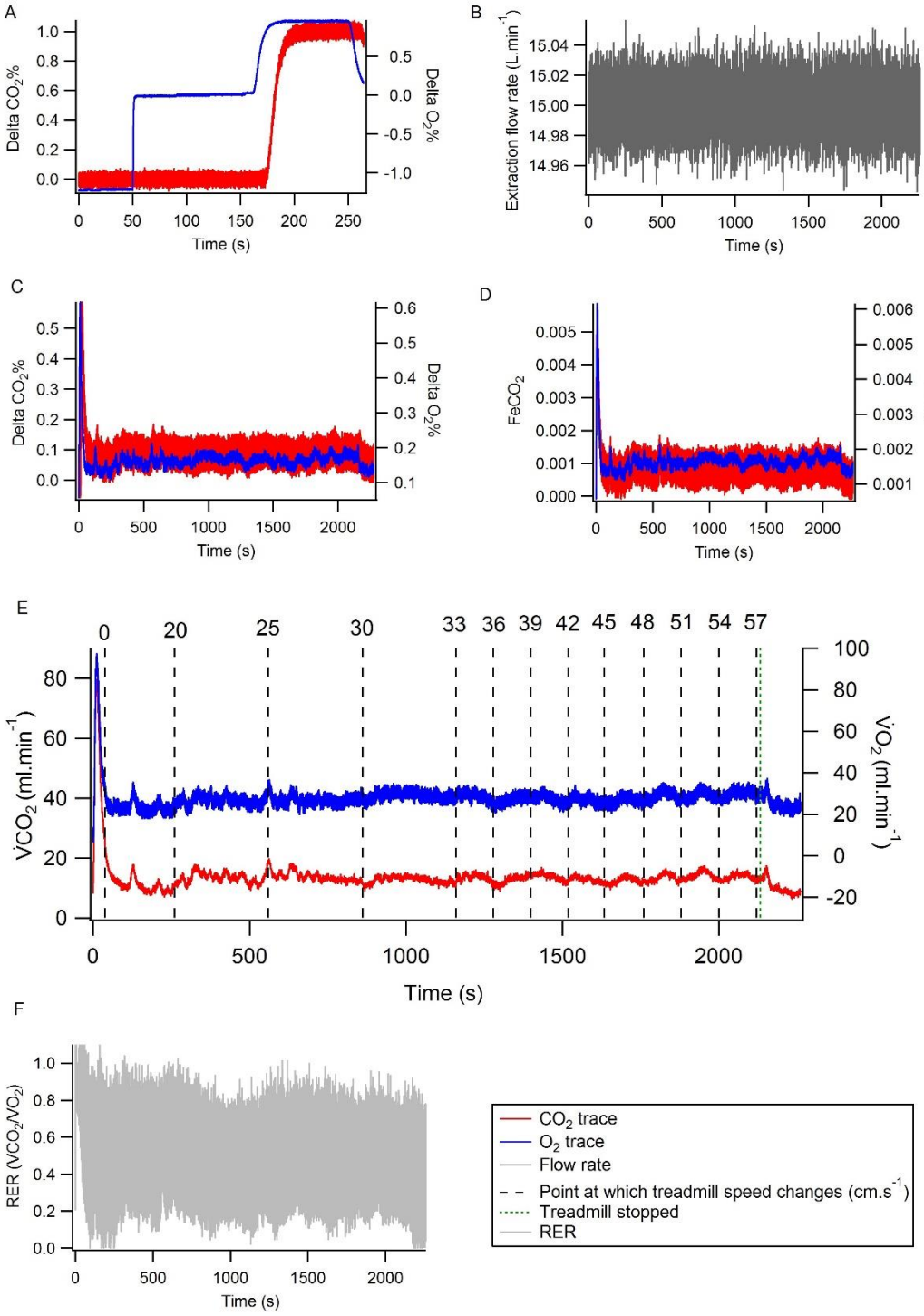

Figure_ A.2 Respirometry data analysis.

Stages of respirometry data analysis conducted in IGOR Pro. (A) Calibration gas traces. (B) Adjusted extraction flow rate. (C) O_2 and CO_2 traces containing a time offset. (D) Aligned O_2 and CO_2 traces (time offset removed). (E) The rate of O_2 consumption ($\dot{V}O_2$) and CO_2 production ($\dot{V}CO_2$) throughout a $\dot{V}O_{2\,max}$ test. (F) The respiratory exchange ratio (RER) throughout a $\dot{V}O_{2\,max}$ test.

Appendix B Macro scripts for immunohistochemistry

iii. Macro script for hippocampal regions of interest.

The following macro script was written in Fiji software for ImageJ (Schindelin et al., 2012). 12 hippocampal ROIs were manually drawn with the polygon tool on multichannel TIFF files (stained for NeuN, aggrecan, and WFA (Figure B.1). This script automated the process of renaming them with the image ID and saving them in a zip folder that could then be used in future analysis. This ensured that all analysis was completed in the exact same hippocampal regions. The script would also export a reference jpeg image of the ROIs (Figure B.1).

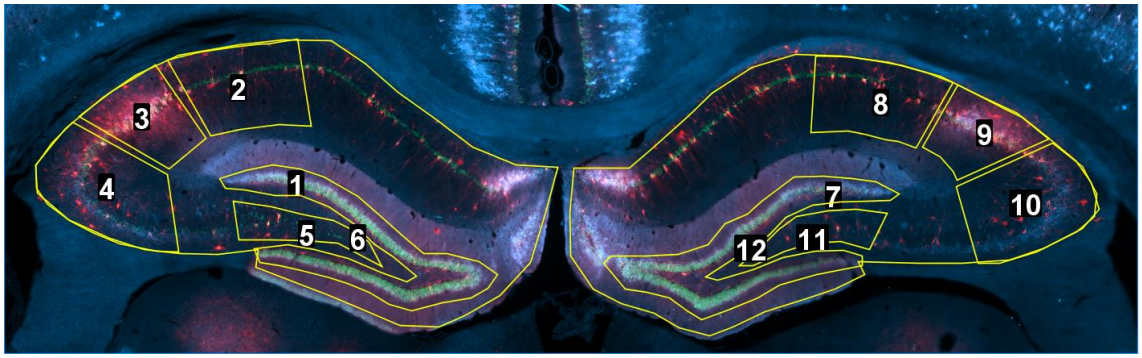

Figure_ B.1 Hippocampal regions of interest.

Hippocampal regions of interest manually drawn using ImageJ. 1 – Left total hippocampus (the number label is in the middle of the whole outlined region); 2 – Left CA1; 3 – Left CA2; 4 – Left CA3; 5 – Left CA4; 6 – Left dentate gyrus; 7 - Right total hippocampus (the number label is in the middle of the whole outlined region); 8 – Right CA1; 9 – Right CA2; 10 – Right CA3; 11 – Right CA4; 12 – Right dentate gyrus. Regions outlined using Figure 33 (Bregma -3.30 mm) in the Rat Brain Atlas (Paxinos and Watson, 2013).

Macro script

```
ROIoutput = getDirectory("Select Folder");
ROIREFERENCEoutput = getDirectory("Select Folder");
reference="_ROIReference.jpg";
//Get title of file
        currentFile=getTitle();
        filename=substring(currentFile,0)
run("ROI Manager...");
```

```
roiManager("Show All");
setTool("polygon");
waitForUser("Waiting for user to draw a polygon...");
roiManager("Add");
roiManager("Select", 0);
roiManager("Rename", filename+ "1Left_TotalHC");
setTool("polygon");
waitForUser("Waiting for user to draw a polygon...");
roiManager("Add");
roiManager("Select", 1);
roiManager("Rename", filename+ "2Left_CA1");
setTool("polygon");
waitForUser("Waiting for user to draw a polygon...");
roiManager("Add");
roiManager("Select", 2);
roiManager("Rename", filename+ "3Left_CA2");
setTool("polygon");
waitForUser("Waiting for user to draw a polygon...");
roiManager("Add");
roiManager("Select", 3);
roiManager("Rename", filename+ "4Left_CA3");
setTool("polygon");
waitForUser("Waiting for user to draw a polygon...");
roiManager("Add");
roiManager("Select", 4);
roiManager("Rename", filename+ "5Left_CA4");
setTool("polygon");
waitForUser("Waiting for user to draw a polygon...");
roiManager("Add");
roiManager("Select", 5);
roiManager("Rename", filename+ "6Left_DG");
setTool("polygon");
waitForUser("Waiting for user to draw a polygon...");
roiManager("Add");
```

```
roiManager("Select", 6);
roiManager("Rename", filename+ "7Right_TotalHC");
setTool("polygon");
waitForUser("Waiting for user to draw a polygon...");
roiManager("Add");
roiManager("Select", 7);
roiManager("Rename", filename+ "8Right_CA1");
setTool("polygon");
waitForUser("Waiting for user to draw a polygon...");
roiManager("Add");
roiManager("Select", 8);
roiManager("Rename", filename+ "9Right_CA2");
setTool("polygon");
waitForUser("Waiting for user to draw a polygon...");
roiManager("Add");
roiManager("Select", 9);
roiManager("Rename", filename+ "10Right_CA3");
setTool("polygon");
waitForUser("Waiting for user to draw a polygon...");
roiManager("Add");
roiManager("Select", 10);
roiManager("Rename", filename+ "10Right_CA4");
setTool("polygon");
waitForUser("Waiting for user to draw a polygon...");
roiManager("Add");
roiManager("Select", 11);
roiManager("Rename", filename+ "10Right_DG");
roiManager("Save", ROIoutput+ filename+ ".zip");
run("From ROI Manager");
run("Labels...", "color=white font=72 show draw");
saveAs("Jpeg", ROIREFERENCEoutput+ filename+  reference);
```

iv. Macro script for splitting channels

A macro script was used for the batch processing of splitting TIFF files into the individual channels (NeuN, aggrecan, WFA). The images from the aggrecan and WFA channels were saved to separate folders ready for staining intensity analysis.

Macro script

```
input = getDirectory("Select Folder");

WFAoutput = getDirectory("Select Folder");

Aggrecanoutput = getDirectory("Select Folder");

list = getFileList(input);

//check length of list of files

print(list.length)

for (i = 0; i < list.length; i++)

	{

	setBatchMode(true);

	open(input+list[i]);

	//Get title of file

	currentFile=getTitle();

	//Split channels

	run("Split Channels");

	//Assign titles of split channels to new variables

	NeuN = "C2-"+currentFile;

	WFA = "C1-"+currentFile;

	Aggrecan = "C3-"+currentFile;

	//Variable check

	print(Aggrecan);

	print(WFA);

	print(NeuN);

	//find length of current file and - ".czi"

	currentFilelength=lengthOf(currentFile);
```

```
print(currentFilelength);
filename=substring(currentFile,0, currentFilelength-4);
selectWindow(Aggrecan);
//Save as TIFF
saveAs("Tiff", Aggrecanoutput+filename+ "-aggrecan.tif");
selectWindow(WFA);
saveAs("Tiff", WFAoutput+filename+ "-WFA.tif");
run("Close All");
setBatchMode(false);
}
```

v. Macro script for aggrecan staining intensity

Single channel images stained with aggrecan were opened in ImageJ. This script waits for the user to identify the zip folder of ROIs for the opened image, then automatically measures the mean gray value for each ROI and exports the results in an excel file. This script also saves a reference image of the ROIs on the aggrecan image in case any regions had to be excluded from future data analysis.

Macro script

```
RESULTSoutput = getDirectory("Select Folder");
ROIREFERENCEoutput = getDirectory("Select Folder");
results="_AggrecanIntensity.csv";
reference="_ROIReference.jpg";
//Get title of file
    currentFile=getTitle();
    filename=substring(currentFile,0)
run("ROI Manager...");
waitForUser("Waiting for user to open ROI zip...");
roiManager("Select", 0);
run("Measure");
roiManager("Select", 1);
run("Measure");
roiManager("Select", 2);
```

```
run("Measure");
roiManager("Select", 3);
run("Measure");
roiManager("Select", 4);
run("Measure");
roiManager("Select", 5);
run("Measure");
roiManager("Select", 6);
run("Measure");
roiManager("Select", 7);
run("Measure");
roiManager("Select", 8);
run("Measure");
roiManager("Select", 9);
run("Measure");
roiManager("Select", 10);
run("Measure");
roiManager("Select", 11);
run("Measure");
saveAs("Results", RESULTSoutput+ filename+ results);
run("From ROI Manager");
run("Labels...", "color=white font=72 show draw");
saveAs("Jpeg", ROIREFERENCEoutput+ filename+  reference);
waitForUser("Waiting for user to copy results...");
```

vi. Macro script for WFA staining intensity

Same as above script but for WFA instead of aggrecan.

Single channel images stained with WFA were opened in ImageJ. This script waits for the user to identify the zip folder of ROIs for the opened image, then automatically measures the mean gray value for each ROI and exports the results in an excel file. This script also saves a reference image of the ROIs on the WFA image in case any regions had to be excluded from future data analysis.

Macro script

```
RESULTSoutput = getDirectory("Select Folder");
ROIREFERENCEoutput = getDirectory("Select Folder");
results="_WFAIntensity.csv";
reference="_ROIReference.jpg";
//Get title of file
	currentFile=getTitle();
	filename=substring(currentFile,0)
run("ROI Manager...");
waitForUser("Waiting for user to open ROI zip...");
roiManager("Select", 0);
run("Measure");
roiManager("Select", 1);
run("Measure");
roiManager("Select", 2);
run("Measure");
roiManager("Select", 3);
run("Measure");
roiManager("Select", 4);
run("Measure");
roiManager("Select", 5);
run("Measure");
roiManager("Select", 6);
run("Measure");
roiManager("Select", 7);
run("Measure");
roiManager("Select", 8);
run("Measure");
roiManager("Select", 9);
run("Measure");
roiManager("Select", 10);
run("Measure");
roiManager("Select", 11);
run("Measure");
saveAs("Results", RESULTSoutput+ filename+ results);
```

```
run("From ROI Manager");
run("Labels...", "color=white font=72 show draw");
saveAs("Jpeg", ROIREFERENCEoutput+ filename+  reference);
waitForUser("Waiting for user to copy results...");
```

References

Abel, J.L. and Rissman, E.F. (2013) 'Running-induced epigenetic and gene expression changes in the adolescent brain', *International journal of developmental neuroscience : the official journal of the International Society for Developmental Neuroscience*, 31(6), p. 382. doi:10.1016/J.IJDEVNEU.2012.11.002.

Afzalpour, M.E., Chadorneshin, H.T., Foadoddini, M. and Eivari, H.A. (2015) 'Comparing interval and continuous exercise training regimens on neurotrophic factors in rat brain', *Physiology and Behavior*, 147, pp. 78–83. doi:10.1016/j.physbeh.2015.04.012.

Akbik, F., Cafferty, W.B.J. and Strittmatter, S.M. (2012) 'Myelin associated inhibitors: A link between injury-induced and experience-dependent plasticity', *Experimental Neurology*. NIH Public Access, pp. 43–52. doi:10.1016/j.expneurol.2011.06.006.

Al-Shammari, A.A., Kissane, R.W.P., Holbek, S., Mackey, A.L., Andersen, T.R., Gaffney, E.A., Kjaer, M. and Egginton, S. (2018) 'Integrated method for quantitative morphometry and oxygen transport modeling in striated muscle', *Journal of Applied Physiology*, 126(3), pp. 544–557. doi:10.1152/JAPPLPHYSIOL.00170.2018.

Alberini, C.M., Cruz, E., Descalzi, G., Bessières, B. and Gao, V. (2018) 'Astrocyte glycogen and lactate: New insights into learning and memory mechanisms', *Glia*, 66(6), pp. 1244–1262. doi:10.1002/GLIA.23250.

Albiñana, E., Gutierrez-Luengo, J., Hernández-Juarez, N., Baraibar, A.M., Montell, E., Vergés, J., García, A.G. and Hernández-Guijo, J.M. (2015) 'Chondroitin sulfate induces depression of synaptic transmission and modulation of neuronal plasticity in rat hippocampal slices', *Neural Plasticity*, 2015. doi:10.1155/2015/463854.

Alonge, K.M., Logsdon, A.F., Murphree, T.A., Banks, W.A., Dirk Keene, C., Scott Edgar, J., Whittington, D., Schwartz, M.W. and Guttman, M. (2019) 'Quantitative analysis of chondroitin sulfate disaccharides from human and rodent fixed brain tissue by electrospray ionization-tandem mass spectrometry', *Glycobiology*, 29(12), p. 847. doi:10.1093/GLYCOB/CWZ060.

Alpár, A., Gärtner, U., Härtig, W. and Brückner, G. (2006) 'Distribution of pyramidal cells associated with perineuronal nets in the neocortex of rat', *Brain Research*, 1120(1), pp. 13–22. doi:10.1016/J.BRAINRES.2006.08.069.

Altman, J. and Bayer, S.A. (2021) *Brain Development: histological materials of the developing rat brain*. Available at: https://braindevelopmentmaps.org/ (Accessed: 30 December 2021).

Amano, M., Nakayama, M. and Kaibuchi, K. (2010) 'Rho-kinase/ROCK: A key regulator of the cytoskeleton and cell polarity', *Cytoskeleton*. Wiley-Blackwell, pp. 545–554. doi:10.1002/cm.20472.

Ang, E.T., Dawe, G.S., Wong, P.T.H., Moochhala, S. and Ng, Y.K. (2006) 'Alterations in spatial learning and memory after forced exercise', *Brain Research*, 1113(1), pp. 186–193. doi:10.1016/J.BRAINRES.2006.07.023.

Arikkath, J. (2012) 'Molecular mechanisms of dendrite morphogenesis', *Frontiers in Cellular Neuroscience*, 0(DEC), p. 61. doi:10.3389/FNCEL.2012.00061/BIBTEX.

Aspberg, A., Miura, R., Bourdoulous, S., Shimonaka, M., Heinegård, D., Schachner, M., Ruoslahti, E. and Yamaguchi, Y.U. (1997) 'The C-type lectin domains of lecticans, a family of aggregating chondroitin sulfate proteoglycans, bind tenascin-R by protein– protein interactions independent of carbohydrate moiety', *Proceedings of the National Academy of Sciences*, 94(19), pp. 10116–10121. doi:10.1073/PNAS.94.19.10116.

Baek, S.-S., Ji, E.-S. and Lee, M.-H. (2014) 'Effects of treadmill exercise on spatial learning memory and upregulation of reelin signaling pathway in autistic rats', *The FASEB Journal*, 28(S1), p. 884.29. doi:10.1096/FASEBJ.28.1_SUPPLEMENT.884.29.

Baig, S., Wilcock, G.K. and Love, S. (2005) 'Loss of perineuronal net N-acetylgalactosamine in Alzheimer's disease', *Acta Neuropathologica*, 110(4), pp. 393–401. doi:10.1007/S00401-005-1060-2/FIGURES/6.

Baldwin, K.T. and Giger, R.J. (2015) 'Insights into the physiological role of CNS regeneration inhibitors', *Frontiers in Molecular Neuroscience*, 8(June), p. 23. doi:10.3389/fnmol.2015.00023.

Banerjee, S.B., Gutzeit, V.A., Baman, J., Aoued, H.S., Doshi, N.K., Liu, R.C. and Ressler, K.J. (2017) 'Perineuronal nets in the adult sensory cortex are necessary for fear learning', *Neuron*, 95(1), pp. 169–179. doi:10.1016/J.NEURON.2017.06.007.

Barton, W.A., Liu, B.P., Tzvetkova, D., Jeffrey, P.D., Fournier, A.E., Sah, D., Cate, R., Strittmatter, S.M. and Nikolov, D.B. (2003) 'Structure and axon outgrowth inhibitor binding of the Nogo-66 receptor and related proteins', *The EMBO Journal*, 22(13), p. 3291. doi:10.1093/EMBOJ/CDG325.

Bashaw, G.J. and Klein, R. (2010) 'Signaling from axon guidance receptors', *Cold Spring Harbor perspectives in biology*. Cold Spring Harbor Laboratory Press, pp. 1941–1942. doi:10.1101/cshperspect.a001941.

Bayod, S., Menella, I., Sanchez-Roige, S., Lalanza, J.F., Escorihuela, R.M., Camins, A., Pallàs, M. and Canudas, A.M. (2014) 'Wnt pathway regulation by long-term moderate exercise in rat hippocampus', *Brain Research*, 1543, pp. 38–48. doi:10.1016/J.BRAINRES.2013.10.048.

Bechara, R.G. and Kelly, á M. (2013) 'Exercise improves object recognition memory and induces BDNF expression and cell proliferation in cognitively enriched rats', *Behavioural Brain Research*, 245, pp. 96–100. doi:10.1016/J.BBR.2013.02.018.

Bednarczyk, M.R., Aumont, A., Décary, S., Bergeron, R. and Fernandes, K.J.L. (2009) 'Prolonged voluntary wheel-running stimulates neural precursors in the hippocampus and forebrain of adult CD1 mice', *Hippocampus*, 19(10), pp. 913–

927. doi:10.1002/HIPO.20621.

Benson, M.D., Romero, M.I., Lush, M.E., Lu, R.Q., Henkemeyer, M. and Parada, L.F. (2005) 'Ephrin-B3 is a myelin-based inhibitor of neurite outgrowth', *Proceedings of the National Academy of Sciences of the United States of America*, 102(30), p. 10694. doi:10.1073/PNAS.0504021102.

Berchtold, N.C., Chinn, G., Chou, M., Kesslak, J.P. and Cotman, C.W. (2005) 'Exercise primes a molecular memory for brain-derived neurotrophic factor protein induction in the rat hippocampus', *Neuroscience*, 133(3), pp. 853–861. doi:10.1016/J.NEUROSCIENCE.2005.03.026.

Bishop, D.J., Granata, C. and Eynon, N. (2014) 'Can we optimise the exercise training prescription to maximise improvements in mitochondria function and content?', *Biochimica et Biophysica Acta (BBA) - General Subjects*, 1840(4), pp. 1266–1275. doi:10.1016/J.BBAGEN.2013.10.012.

Black, J.E., Isaacs, K.R., Anderson, B.J., Alcantara, A.A. and Greenough, W.T. (1990) 'Learning causes synaptogenesis, whereas motor activity causes angiogenesis, in cerebellar cortex of adult rats', *Proceedings of the National Academy of Sciences of the United States of America*, 87(14), pp. 5568–5572. doi:10.1073/PNAS.87.14.5568.

Blosa, M., Bursch, C., Weigel, S., Holzer, M., Jäger, C., Janke, C., Matthews, R.T., Arendt, T. and Morawski, M. (2016) 'Reorganization of synaptic connections and perineuronal nets in the deep cerebellar nuclei of purkinje cell degeneration mutant mice', *Neural plasticity*, 2016. doi:10.1155/2016/2828536.

Boghdadi, A.G., Teo, L. and Bourne, J.A. (2018) 'The involvement of the myelin-associated inhibitors and their receptors in CNS plasticity and injury', *Molecular Neurobiology*. Humana Press Inc., pp. 1831–1846. doi:10.1007/s12035-017-0433-6.

Van Der Borght, K., Kóbor-Nyakas, D.É., Klauke, K., Eggen, B.J.L., Nyakas, C., Van Der Zee, E.A. and Meerlo, P. (2009) 'Physical exercise leads to rapid adaptations in hippocampal vasculature: temporal dynamics and relationship to cell proliferation and neurogenesis', *Hippocampus*, 19(10), pp. 928–936. doi:10.1002/HIPO.20545.

Borisoff, J.F., Chan, C.C.M., Hiebert, G.W., Oschipok, L., Robertson, G.S., Zamboni, R., Steeves, J.D. and Tetzlaff, W. (2003) 'Suppression of Rho-kinase activity promotes axonal growth on inhibitory CNS substrates', *Molecular and Cellular Neuroscience*, 22(3), pp. 405–416. doi:10.1016/S1044-7431(02)00032-5.

Borrell, J.A., Frost, S.B., Peterson, J. and Nudo, R.J. (2016) 'A 3D map of the hindlimb motor representation in the lumbar spinal cord in Sprague Dawley rats', *Journal of Neural Engineering*, 14(1), p. 016007. doi:10.1088/1741-2552/14/1/016007.

Borrie, S.C., Sartori, S.B., Lehmann, J., Sah, A., Singewald, N. and Bandtlow, C.E. (2014) 'Loss of Nogo receptor homolog NgR2 alters spine morphology of CA1 neurons and emotionality in adult mice', *Frontiers in Behavioral Neuroscience*, 8(MAY). doi:10.3389/fnbeh.2014.00175.

Bosiacki, M., Gąssowska-Dobrowolska, M., Kojder, K., Fabiańska, M., Jeżewski, D., Gutowska, I. and Lubkowska, A. (2019) 'Perineuronal nets and their role in synaptic homeostasis', *International journal of molecular sciences*, 20(17). doi:10.3390/IJMS20174108.

Bradbury, E., Moon, L., Popat, R., King, V., Bennett, G., Patel, P., Fawcett, J. and McMahon, S. (2002) 'Chondroitinase ABC promotes functional recovery after spinal cord injury', *Nature*, 416(6881), pp. 636–640. doi:10.1038/416636A.

Bradbury, E.J. and Carter, L.M. (2011) 'Manipulating the glial scar: Chondroitinase ABC as a therapy for spinal cord injury', *Brain Research Bulletin*, 84(4–5), pp. 306–316. doi:10.1016/J.BRAINRESBULL.2010.06.015.

Broadbent, N.J., Gaskin, S., Squire, L.R. and Clark, R.E. (2010) 'Object recognition memory and the rodent hippocampus', *Learning and Memory*, 17(1), pp. 794–800. doi:10.1101/lm.1650110.

Broadbent, N.J., Squire, L.R. and Clark, R.E. (2004) 'Spatial memory, recognition memory, and the hippocampus', *Proceedings of the National Academy of Sciences*, 101(40), pp. 14515–14520. doi:10.1073/PNAS.0406344101.

Brockett, A.T., LaMarca, E.A. and Gould, E. (2015) 'Physical exercise enhances cognitive flexibility as well as astrocytic and synaptic markers in the medial prefrontal cortex', *PLoS ONE*, 10(5). doi:10.1371/JOURNAL.PONE.0124859.

Brückner, G., Bringmann, A., Köppe, G., Härtig, W. and Brauer, K. (1996) 'In vivo and in vitro labelling of perineuronal nets in rat brain', *Brain research*, 720(1–2), pp. 84–92. doi:10.1016/0006-8993(96)00152-7.

Brückner, G., Hausen, D., Härtig, W., Drlicek, M., Arendt, T. and Brauer, K. (1999) 'Cortical areas abundant in extracellular matrix chondroitin sulphate proteoglycans are less affected by cytoskeletal changes in Alzheimer's disease', *Neuroscience*, 92(3), pp. 791–805. doi:10.1016/S0306-4522(99)00071-8.

Bucher, E.A., Collins, J.M., King, A.E., Vickers, J.C. and Kirkcaldie, M.T.K. (2021) 'Coherence and cognition in the cortex: the fundamental role of parvalbumin, myelin, and the perineuronal net', *Brain structure & function*, 226(7), pp. 2041–2055. doi:10.1007/S00429-021-02327-3.

Bustin, S.A., Benes, V., Garson, J.A., Hellemans, J., Huggett, J., Kubista, M., Mueller, R., Nolan, T., Pfaffl, M.W., Shipley, G.L., Vandesompele, J. and Wittwer, C.T. (2009) 'The MIQE guidelines: Minimum information for publication of quantitative real-time PCR experiments', *Clinical Chemistry*, 55(4), pp. 611–622. doi:10.1373/clinchem.2008.112797.

Bye, N., Christie, K.J., Turbic, A., Basrai, H.S. and Turnley, A.M. (2016) 'Rho kinase inhibition following traumatic brain injury in mice promotes functional improvement and acute neuron survival but has little effect on neurogenesis, glial responses or neuroinflammation', *Experimental neurology*, 279, pp. 86–95. doi:10.1016/J.EXPNEUROL.2016.02.012.

Cabungcal, J.H., Steullet, P., Morishita, H., Kraftsik, R., Cuenod, M., Hensch, T.K. and Do, K.Q. (2013) 'Perineuronal nets protect fast-spiking interneurons

against oxidative stress', *Proceedings of the National Academy of Sciences of the United States of America*, 110(22), pp. 9130–9135. doi:10.1073/PNAS.1300454110/-/DCSUPPLEMENTAL.

Cafferty, W., Duffy, P., Huebner, E. and Strittmatter, S. (2010) 'MAG and OMgp synergize with Nogo-A to restrict axonal growth and neurological recovery after spinal cord trauma', *The Journal of neuroscience : the official journal of the Society for Neuroscience*, 30(20), pp. 6825–6837. doi:10.1523/JNEUROSCI.6239-09.2010.

Cafferty, W.B.J., Yang, S.H., Duffy, P.J., Li, S. and Strittmatter, S.M. (2007) 'Functional axonal regeneration through astrocytic scar genetically modified to digest chondroitin sulfate proteoglycans', *Journal of Neuroscience*, 27(9), pp. 2176–2185. doi:10.1523/JNEUROSCI.5176-06.2007.

Calabrese, E.J. (2004) 'Hormesis: a revolution in toxicology, risk assessment and medicine', *EMBO reports*, 5(S1), pp. S37–S40. doi:10.1038/SJ.EMBOR.7400222.

Calvo, P., Pastor, A. and De La Cruz, R. (2018) 'Vascular endothelial growth factor: an essential neurotrophic factor for motoneurons?', *Neural Regeneration Research*, 13(7), p. 1181. doi:10.4103/1673-5374.235024.

Campbell, S. and MacQueen, G. (2004) 'The role of the hippocampus in the pathophysiology of major depression', *Journal of Psychiatry and Neuroscience*, 29(6), p. 417. Available at: /pmc/articles/PMC524959/ (Accessed: 17 December 2021).

Cao, B., Passos, I.C., Mwangi, B., Amaral-Silva, H., Tannous, J., Wu, M.J., Zunta-Soares, G.B. and Soares, J.C. (2017) 'Hippocampal subfield volumes in mood disorders', *Molecular Psychiatry*, 22(9), pp. 1352–1358. doi:10.1038/mp.2016.262.

Carek, P.J., Laibstain, S.E. and Carek, S.M. (2011) 'Exercise for the treatment of depression and anxiety', *International journal of psychiatry in medicine*, 41(1), pp. 15–28. doi:10.2190/PM.41.1.C.

Carstens, K.E., Phillips, M.L., Pozzo-Miller, L., Weinberg, R.J. and Dudek, S.M. (2016) 'Perineuronal nets suppress plasticity of excitatory synapses on CA2 pyramidal neurons', *Journal of Neuroscience*, 36(23), pp. 6312–6320. doi:10.1523/JNEUROSCI.0245-16.2016.

Carter, B.C. and Bean, B.P. (2009) 'Sodium entry during action potentials of mammalian central neurons: incomplete inactivation and reduced metabolic efficiency in fast-spiking neurons', *Neuron*, 64(6), p. 898. doi:10.1016/J.NEURON.2009.12.011.

Carulli, D., Broersen, R., de Winter, F., Muir, E.M., Meškovic, M., de Waal, M., de Vries, S., Boele, H.J., Canto, C.B., de Zeeuw, C.I. and Verhaagen, J. (2020) 'Cerebellar plasticity and associative memories are controlled by perineuronal nets', *Proceedings of the National Academy of Sciences of the United States of America*, 117(12), pp. 6855–6865. doi:10.1073/pnas.1916163117.

Carulli, D., Pizzorusso, T., Kwok, J.C.F., Putignano, E., Poli, A., Forostyak, S., Andrews, M.R., Deepa, S.S., Glant, T.T. and Fawcett, J.W. (2010) 'Animals

lacking link protein have attenuated perineuronal nets and persistent plasticity', *Brain*, 133(8), pp. 2331–2347. doi:10.1093/BRAIN/AWQ145.

Carulli, D., Rhodes, K.E., Brown, D.J., Bonnert, T.P., Pollack, S.J., Oliver, K., Strata, P. and Fawcett, J.W. (2006) 'Composition of perineuronal nets in the adult rat cerebellum and the cellular origin of their components', *The Journal of comparative neurology*, 494(4), pp. 559–577. doi:10.1002/CNE.20822.

Carulli, D. and Verhaagen, J. (2021) 'Molecular sciences an extracellular perspective on CNS maturation: Perineuronal nets and the control of plasticity', *International Journal of Molecular Sciences*, 22(5), p. 2434. doi:10.3390/ijms22052434.

Cassilhas, R.C., Lee, K.S., Fernandes, J., Oliveira, M.G.M., Tufik, S., Meeusen, R. and De Mello, M.T. (2012) 'Spatial memory is improved by aerobic and resistance exercise through divergent molecular mechanisms', *Neuroscience*, 202, pp. 309–317. doi:10.1016/J.NEUROSCIENCE.2011.11.029.

Cassilhas, R.C., Tufik, S. and de Mello, M.T. (2015) 'Physical exercise, neuroplasticity, spatial learning and memory', *Cellular and Molecular Life Sciences 2015 73:5*, 73(5), pp. 975–983. doi:10.1007/S00018-015-2102-0.

Cefis, M., Prigent-Tessier, A., Quirié, A., Pernet, N., Marie, C. and Garnier, P. (2019) 'The effect of exercise on memory and BDNF signaling is dependent on intensity', *Brain Structure and Function 2019 224:6*, 224(6), pp. 1975–1985. doi:10.1007/S00429-019-01889-7.

Cetinkaya, C., Sisman, A.R., Kiray, M., Camsari, U.M., Gencoglu, C., Baykara, B., Aksu, I. and Uysal, N. (2013) 'Positive effects of aerobic exercise on learning and memory functioning, which correlate with hippocampal IGF-1 increase in adolescent rats', *Neuroscience Letters*, 549, pp. 177–181. doi:10.1016/J.NEULET.2013.06.012.

Chan, C.C.M., Khodarahmi, K., Liu, J., Sutherland, D., Oschipok, L.W., Steeves, J.D. and Tetzlaff, W. (2005) 'Dose-dependent beneficial and detrimental effects of ROCK inhibitor Y27632 on axonal sprouting and functional recovery after rat spinal cord injury', *Experimental Neurology*, 196(2), pp. 352–364. doi:10.1016/J.EXPNEUROL.2005.08.011.

Chang, S. and Cao, Y. (2021) 'The ROCK inhibitor Y-27632 ameliorates blood-spinal cord barrier disruption by reducing tight junction protein degradation via the MYPT1-MLC2 pathway after spinal cord injury in rats', *Brain Research*, 1773, p. 147684. doi:10.1016/J.BRAINRES.2021.147684.

Chaplan, S.R., Bach, F.W., Pogrel, J.W., Chung, J.M. and Yaksh, T.L. (1994) 'Quantitative assessment of tactile allodynia in the rat paw', *Journal of Neuroscience Methods*, 53(1), pp. 55–63. doi:10.1016/0165-0270(94)90144-9.

Chen, D., Zhang, Y., Zhang, M., Chang, J., Zeng, Z., Kou, X. and Chen, N. (2020) 'Exercise attenuates brain aging by rescuing down-regulated Wnt/β-Catenin signaling in aged rats', *Frontiers in Aging Neuroscience*, 12. doi:10.3389/FNAGI.2020.00105.

Chen, K., Marsh, B.C., Cowan, M., Al'Joboori, Y.D., Gigout, S., Smith, C.C., Messenger, N., Gamper, N., Schwab, M.E. and Ichiyama, R.M. (2017)

‘Sequential therapy of anti-Nogo-A antibody treatment and treadmill training leads to cumulative improvements after spinal cord injury in rats’, *Experimental neurology*, 292, pp. 135–144. doi:10.1016/J.EXPNEUROL.2017.03.012.

Chen, Y., Rex, C.S., Rice, C.J., Dubé, C.M., Gall, C.M., Lynch, G. and Barama, T.Z. (2010) ‘Correlated memory defects and hippocampal dendritic spine loss after acute stress involve corticotropin-releasing hormone signaling’, *Proceedings of the National Academy of Sciences*, 107(29), pp. 13123–13128. doi:10.1073/PNAS.1003825107.

Chytrova, G., Ying, Z. and Gomez-Pinilla, F. (2008) ‘Exercise normalizes levels of MAG and Nogo-A growth inhibitors after brain trauma’, *European Journal of Neuroscience*, 27(1), pp. 1–11. doi:10.1111/j.1460-9568.2007.05982.x.

Clark, P.J., Brzezinska, W.J., Puchalski, E.K., Krone, D.A. and Rhodes, J.S. (2009) ‘Functional analysis of neurovascular adaptations to exercise in the dentate gyrus of young adult mice associated with cognitive gain’, *Hippocampus*, 19(10), pp. 937–950. doi:10.1002/HIPO.20543.

Constans, A., Pin-Barre, C., Molinari, F., Temprado, J.J., Brioche, T., Pellegrino, C. and Laurin, J. (2021) ‘High-intensity interval training is superior to moderate intensity training on aerobic capacity in rats: Impact on hippocampal plasticity markers’, *Behavioural Brain Research*, 398, p. 112977. doi:10.1016/J.BBR.2020.112977.

Cooper, C., Moon, H.Y. and Van Praag, H. (2018) ‘On the run for hippocampal plasticity’, *Cold Spring Harbor Perspectives in Medicine*, 8(4). doi:10.1101/cshperspect.a029736.

Cotman, C.W., Berchtold, N.C. and Christie, L.A. (2007) ‘Exercise builds brain health: key roles of growth factor cascades and inflammation’, *Trends in neurosciences*, 30(9), pp. 464–472. doi:10.1016/J.TINS.2007.06.011.

Cramer, S. *et al.* (2011) ‘Harnessing neuroplasticity for clinical applications’, *Brain*. Oxford Academic, pp. 1591–1609. doi:10.1093/brain/awr039.

Crocker, P.R., Paulson, J.C. and Varki, A. (2007) ‘Siglecs and their roles in the immune system’, *Nature Reviews Immunology*, 7(4), pp. 255–266. doi:10.1038/nri2056.

Dare, L.R., Garcia, A., Soares, C.B., Lopes, L., Neves, B.H.S., Dias, D. V. and Mello-Carpes, P.B. (2020) ‘The reversal of memory deficits in an Alzheimer’s disease model using physical and cognitive exercise’, *Frontiers in Behavioral Neuroscience*, 14. doi:10.3389/FNBEH.2020.00152.

Dauth, S., Grevesse, T., Pantazopoulos, H., Campbell, P.H., Maoz, B.M., Berretta, S. and Parker, K.K. (2016) ‘Extracellular matrix protein expression is brain region dependent’, *Journal of Comparative Neurology*, 524(7), pp. 1309–1336. doi:10.1002/CNE.23965.

Day, J.M., Olin, A.I., Murdoch, A.D., Canfield, A., Sasaki, T., Timpl, R., Hardingham, T.E. and Aspberg, A. (2004) ‘Alternative splicing in the aggrecan G3 domain influences binding interactions with tenascin-C and other extracellular matrix proteins’, *The Journal of biological chemistry*, 279(13), pp. 12511–12518. doi:10.1074/JBC.M400242200.

Deepa, S.S., Carulli, D., Galtrey, C., Rhodes, K., Fukuda, J., Mikami, T., Sugahara, K. and Fawcett, J.W. (2006) 'Composition of perineuronal net extracellular matrix in rat brain: A different disaccharide composition for the net-associated proteoglycans', *Journal of Biological Chemistry*, 281(26), pp. 17789–17800. doi:10.1074/JBC.M600544200.

Dergham, P., Ellezam, B., Essagian, C., Avedissian, H., Lubell, W.D. and McKerracher, L. (2002) 'Rho signaling pathway targeted to promote spinal cord repair', *Journal of Neuroscience*, 22(15), pp. 6570–6577. doi:10.1523/JNEUROSCI.22-15-06570.2002.

Dhikav, V. and Anand, K. (2012) 'Hippocampus in health and disease: An overview', *Annals of Indian Academy of Neurology*, 15(4), p. 239. doi:10.4103/0972-2327.104323.

Dickendesher, T.L., Baldwin, K.T., Mironova, Y.A., Koriyama, Y., Raiker, S.J., Askew, K.L., Wood, A., Geoffroy, C.G., Zheng, B., Liepmann, C.D., Katagiri, Y., Benowitz, L.I., Geller, H.M. and Giger, R.J. (2012) 'NgR1 and NgR3 are receptors for chondroitin sulfate proteoglycans', *Nature Neuroscience*, 15(5), pp. 703–712. doi:10.1038/nn.3070.

Domeniconi, M., Cao, Z., Spencer, T., Sivasankaran, R., Wang, K., Nikulina, E., Kimura, N., Cai, H., Deng, K., Gao, Y., He, Z. and Filbin, M. (2002) 'Myelin-associated glycoprotein interacts with the Nogo66 receptor to inhibit neurite outgrowth', *Neuron*, 35(2), pp. 283–290. doi:10.1016/S0896-6273(02)00770-5.

Doncheva, N.T., Morris, J.H., Gorodkin, J. and Jensen, L.J. (2019) 'Cytoscape StringApp: Network analysis and visualization of proteomics data', *Journal of Proteome Research*, 18(2), pp. 623–632. doi:10.1021/acs.jproteome.8b00702.

Dostes, S., Dubreucq, S., Ladevèze, E., Marsicano, G., Abrous, D.N., Chaouloff, F. and Koehl, M. (2016) 'Running per se stimulates the dendritic arbor of newborn dentate granule cells in mouse hippocampus in a duration-dependent manner', *Hippocampus*, 26(3), pp. 282–288. doi:10.1002/HIPO.22551.

Duncan, J.A., Foster, R. and Kwok, J.C.F. (2019) 'The potential of memory enhancement through modulation of perineuronal nets', *British Journal of Pharmacology*, 176(18), pp. 3611–3621. doi:10.1111/BPH.14672.

Dupret, D., Revest, J.M., Koehl, M., Ichas, F., De Giorgi, F., Costet, P., Abrous, D.N. and Piazza, P.V. (2008) 'Spatial relational memory requires hippocampal adult neurogenesis', *PloS one*, 3(4). doi:10.1371/JOURNAL.PONE.0001959.

Dzyubenko, E., Fleischer, M., Manrique-Castano, D., Borbor, M., Kleinschnitz, C., Faissner, A. and Hermann, D.M. (2021) 'Inhibitory control in neuronal networks relies on the extracellular matrix integrity', *Cellular and Molecular Life Sciences*, 78(14), p. 5647. doi:10.1007/S00018-021-03861-3.

Eadie, B.D., Redila, V.A. and Christie, B.R. (2005) 'Voluntary exercise alters the cytoarchitecture of the adult dentate gyrus by increasing cellular proliferation, dendritic complexity, and spine density', *The Journal of comparative neurology*, 486(1), pp. 39–47. doi:10.1002/CNE.20493.

Eigentler, A. (2020) 'Oroboros instruments high-resolution respirometry

oroboros protocols enzymes laboratory protocol: Citrate synthase a mitochondrial marker enzyme', *Mitochondrial Physiology Network*, 17(04), pp. 1–12. Available at: http://wiki.oroboros.at/index.php/MiPNet17.04_CitrateSynthasewww.mitofit.org (Accessed: 25 October 2021).

Ekstrand, J., Hellsten, J. and Tingström, A. (2008) 'Environmental enrichment, exercise and corticosterone affect endothelial cell proliferation in adult rat hippocampus and prefrontal cortex', *Neuroscience letters*, 442(3), pp. 203–207. doi:10.1016/J.NEULET.2008.06.085.

Fagiolini, M., Pizzorusso, T., Berardi, N., Domenici, L. and Maffei, L. (1994) 'Functional postnatal development of the rat primary visual cortex and the role of visual experience: Dark rearing and monocular deprivation', *Vision Research*, 34(6), pp. 709–720. doi:10.1016/0042-6989(94)90210-0.

Fang, G., Zhao, J., Zhang, L., LI, P., LI, L., Yang, X. and YU, T. (2017) 'Effects of aerobic exercise on Wnt/β-Catenin pathway in the cerebral cortex and hippocampus of rats', *Chinese Journal of Sports Medicine*, 36(9), pp. 765–772. doi:10.3969/J.ISSN.1000-6710.2017.09.004.

Fanselow, M.S. and Dong, H.-W. (2010) 'Are the dorsal and ventral hippocampus functionally distinct structures?', *Neuron*, 65(1), p. 7. doi:10.1016/j.neuron.2009.11.031.

Farenia, R., Lesmana, R., Uchida, K., Iwasaki, T., Koibuchi, N. and Shimokawa, N. (2019) 'Changes in biomarker levels and myofiber constitution in rat soleus muscle at different exercise intensities', *Molecular and cellular biochemistry*, 458(1–2), pp. 79–87. doi:10.1007/S11010-019-03532-9.

Farmer, J., Zhao, X., Van Praag, H., Wodtke, K., Gage, F.H. and Christie, B.R. (2004) 'Effects of voluntary exercise on synaptic plasticity and gene expression in the dentate gyrus of adult male sprague–dawley rats in vivo', *Neuroscience*, 124(1), pp. 71–79. doi:10.1016/J.NEUROSCIENCE.2003.09.029.

Farzi, M.A., Sadigh-Eteghad, S., Ebrahimi, K. and Talebi, M. (2019) 'Exercise improves recognition memory and acetylcholinesterase activity in the beta amyloid-induced rat model of Alzheimer's disease', *Annals of Neurosciences*, 25(3), p. 121. doi:10.1159/000488580.

Fawcett, J.W., Oohashi, T. and Pizzorusso, T. (2019) 'The roles of perineuronal nets and the perinodal extracellular matrix in neuronal function', *Nature Reviews Neuroscience 2019 20:8*, 20(8), pp. 451–465. doi:10.1038/s41583-019-0196-3.

Femenía, T., Gómez-Galán, M., Lindskog, M. and Magara, S. (2012) 'Dysfunctional hippocampal activity affects emotion and cognition in mood disorders', *Brain Research*, 1476, pp. 58–70. doi:10.1016/J.BRAINRES.2012.03.053.

Ferreira, A.F.B., Real, C.C., Rodrigues, A.C., Alves, A.S. and Britto, L.R.G. (2011) 'Short-term, moderate exercise is capable of inducing structural, bdnf-independent hippocampal plasticity', *Brain Research*, 1425, pp. 111–122. doi:10.1016/J.BRAINRES.2011.10.004.

Fischer, D., Petkova, V., Thanos, S. and Benowitz, L.I. (2004) 'Switching

mature retinal ganglion cells to a robust growth state in vivo: Gene expression and synergy with RhoA inactivation', *The Journal of Neuroscience*, 24(40), p. 8726. doi:10.1523/JNEUROSCI.2774-04.2004.

Foscarin, S., Raha-Chowdhury, R., Fawcett, J.W. and Kwok, J.C.F. (2017) 'Brain ageing changes proteoglycan sulfation, rendering perineuronal nets more inhibitory', *Aging*, 9(6), pp. 1607–1622. doi:10.18632/AGING.101256.

Fouad, K., Dietz, V. and Schwab, M.E. (2001) 'Improving axonal growth and functional recovery after experimental spinal cord injury by neutralizing myelin associated inhibitors', *Brain Research Reviews*, 36(2–3), pp. 204–212. doi:10.1016/S0165-0173(01)00096-0.

Fowke, T.M., Karunasinghe, R.N., Bai, J.Z., Jordan, S., Gunn, A.J. and Dean, J.M. (2017) 'Hyaluronan synthesis by developing cortical neurons in vitro', *Scientific reports*, 7. doi:10.1038/SREP44135.

Freeman, J.H. and Steinmetz, A.B. (2011) 'Neural circuitry and plasticity mechanisms underlying delay eyeblink conditioning', *Learning & Memory*, 18(10), p. 666. doi:10.1101/LM.2023011.

Freitas, D.A., Rocha-Vieira, E., Soares, B.A., Nonato, L.F., Fonseca, S.R., Martins, J.B., Mendonça, V.A., Lacerda, A.C., Massensini, A.R., Poortamns, J.R., Meeusen, R. and Leite, H.R. (2018) 'High intensity interval training modulates hippocampal oxidative stress, BDNF and inflammatory mediators in rats', *Physiology and Behavior*, 184, pp. 6–11. doi:10.1016/j.physbeh.2017.10.027.

Frischknecht, R., Heine, M., Perrais, D., Seidenbecher, C.I., Choquet, D. and Gundelfinger, E.D. (2009) 'Brain extracellular matrix affects AMPA receptor lateral mobility and short-term synaptic plasticity', *Nature neuroscience*, 12(7), pp. 897–904. doi:10.1038/NN.2338.

Frischknecht, R. and Seidenbecher, C.I. (2008) 'The crosstalk of hyaluronan-based extracellular matrix and synapses', *Neuron Glia Biology*, 4(3), pp. 249–257. doi:10.1017/S1740925X09990226.

Fu, P. cai, Tang, R. hua, Wan, Y., Xie, M. jie, Wang, W., Luo, X. and Yu, Z. yuan (2016) 'ROCK inhibition with fasudil promotes early functional recovery of spinal cord injury in rats by enhancing microglia phagocytosis', *Journal of Huazhong University of Science and Technology. Medical sciences* , 36(1), pp. 31–36. doi:10.1007/S11596-016-1537-3.

Fujita, Y. and Yamashita, T. (2014) 'Axon growth inhibition by RhoA/ROCK in the central nervous system', *Frontiers in Neuroscience*. Frontiers Research Foundation, p. 338. doi:10.3389/fnins.2014.00338.

Gage, G.J., Kipke, D.R. and Shain, W. (2012) 'Whole animal perfusion fixation for rodents', *Journal of Visualized Experiments : JoVE*, (65), p. 3564. doi:10.3791/3564.

Gallo, M., MacLean, I., Tyreman, N., B Martins, K.J., Syrotuik, D., Gordon, T. and Putman, C.T. (2008) 'Adaptive responses to creatine loading and exercise in fast-twitch rat skeletal muscle', *Am J Physiol Regul Integr Comp Physiol*, 294, pp. 1319–1328. doi:10.1152/ajpregu.00631.2007.-We.

Galtrey, C.M. and Fawcett, J.W. (2007) ‘The role of chondroitin sulfate proteoglycans in regeneration and plasticity in the central nervous system’, *Brain research reviews*, 54(1), pp. 1–18. doi:10.1016/J.BRAINRESREV.2006.09.006.

Galtrey, C.M., Kwok, J.C.F., Carulli, D., Rhodes, K.E. and Fawcett, J.W. (2008) ‘Distribution and synthesis of extracellular matrix proteoglycans, hyaluronan, link proteins and tenascin-R in the rat spinal cord’, *The European journal of neuroscience*, 27(6), pp. 1373–1390. doi:10.1111/J.1460-9568.2008.06108.X.

Galván, A. (2010) ‘Neural plasticity of development and learning’, *Human Brain Mapping*, 31(6), pp. 879–890. doi:10.1002/HBM.21029.

Ghiani, C.A., Ying, Z., De Vellis, J. and Gomez-Pinilla, F. (2007) ‘Exercise decreases myelin-associated glycoprotein expression in the spinal cord and positively modulates neuronal growth’, *GLIA*, 55(9), pp. 966–975. doi:10.1002/glia.20521.

Ghiselli, G. (2017) ‘Drug-mediated regulation of glycosaminoglycan biosynthesis’, *Medicinal research reviews*, 37(5), pp. 1051–1094. doi:10.1002/MED.21429.

Ghosh, A.K. (2004) ‘Anaerobic threshold: Its concept and role in endurance sport’, *The Malaysian Journal of Medical Sciences : MJMS*, 11(1), p. 24. Available at: /pmc/articles/PMC3438148/ (Accessed: 1 January 2022).

Giamanco, K.A., Morawski, M. and Matthews, R.T. (2010) ‘Perineuronal net formation and structure in aggrecan knockout mice’, *Neuroscience*, 170(4), pp. 1314–1327. doi:10.1016/J.NEUROSCIENCE.2010.08.032.

Giger, R.J., Hollis, E.R. and Tuszynski, M.H. (2010) ‘Guidance molecules in axon regeneration’, *Cold Spring Harbor perspectives in biology*. Cold Spring Harb Perspect Biol. doi:10.1101/cshperspect.a001867.

Gogolla, N., Caroni, P., Lüthi, A. and Herry, C. (2009) ‘Perineuronal nets protect fear memories from erasure’, *Science*, 325(5945), pp. 1258–1261. doi:10.1126/science.1174146.

Gomez-Pinilla, F., Vaynman, S. and Ying, Z. (2008) ‘Brain-derived neurotrophic factor functions as a metabotrophin to mediate the effects of exercise on cognition’, *The European journal of neuroscience*, 28(11), pp. 2278–2287. doi:10.1111/J.1460-9568.2008.06524.X.

Gómez-Pinilla, F., Ying, Z., Roy, R.R., Molteni, R. and Reggie Edgerton, V. (2002) ‘Voluntary exercise induces a BDNF-mediated mechanism that promotes neuroplasticity’, *Journal of Neurophysiology*, 88(5), pp. 2187–2195. doi:10.1152/jn.00152.2002.

Griffin, E., Bechara, R., Birch, A. and Kelly, A. (2009) ‘Exercise enhances hippocampal-dependent learning in the rat: evidence for a BDNF-related mechanism’, *Hippocampus*, 19(10), pp. 973–980. doi:10.1002/HIPO.20631.

Härtig, W., Brauer, K. and Brückner, G. (1992) ‘Wisteria floribunda agglutinin-labelled nets surround parvalbumin-containing neurons’, *Neuroreport*, 3(10), pp. 869–872. doi:10.1097/00001756-199210000-00012.

Härtig, W., Derouiche, A., Welt, K., Brauer, K., Grosche, J., Mäder, M., Reichenbach, A. and Brückner, G. (1999) 'Cortical neurons immunoreactive for the potassium channel Kv3.1b subunit are predominantly surrounded by perineuronal nets presumed as a buffering system for cations', *Brain Research*, 842(1), pp. 15–29. doi:10.1016/S0006-8993(99)01784-9.

Hayani, H., Song, I. and Dityatev, A. (2018) 'Increased excitability and reduced excitatory synaptic input into fast-spiking CA2 interneurons after enzymatic attenuation of extracellular matrix', *Frontiers in Cellular Neuroscience*, 12, p. 149. doi:10.3389/FNCEL.2018.00149/BIBTEX.

El Hayek, L., Khalifeh, M., Zibara, V., Abi Assaad, R., Emmanuel, N., Karnib, N., El-Ghandour, R., Nasrallah, P., Bilen, M., Ibrahim, P., Younes, J., Abou Haidar, E., Barmo, N., Jabre, V., Stephan, J.S. and Sleiman, S.F. (2019) 'Lactate mediates the effects of exercise on learning and memory through SIRT1-dependent activation of hippocampal brain-derived neurotrophic factor (BDNF))', *The Journal of neuroscience* , 39(13), pp. 2369–2382. doi:10.1523/JNEUROSCI.1661-18.2019.

Heberle, H., Meirelles, V.G., da Silva, F.R., Telles, G.P. and Minghim, R. (2015) 'InteractiVenn: A web-based tool for the analysis of sets through Venn diagrams', *BMC Bioinformatics*, 16(1). doi:10.1186/s12859-015-0611-3.

Hensch, T.K. (2004) 'Critical period regulation', *Annual Review of Neuroscience*, 27, pp. 549–579. doi:10.1146/ANNUREV.NEURO.27.070203.144327.

Hering, T.M., Beller, J.A., Calulot, C.M. and Snow, D.M. (2020) 'Contributions of Chondroitin Sulfate, Keratan Sulfate and N-linked Oligosaccharides to Inhibition of Neurite Outgrowth by Aggrecan', *Biology*, 9(2), p. 29. doi:10.3390/biology9020029.

Hirokawa, T., Zou, Y., Kurihara, Y., Jiang, Z., Sakakibara, Y., Ito, H., Funakoshi, K., Kawahara, N., Goshima, Y., Strittmatter, S.M. and Takei, K. (2017) 'Regulation of axonal regeneration by the level of function of the endogenous Nogo receptor antagonist LOTUS', *Scientific Reports 2017 7:1*, 7(1), pp. 1–9. doi:10.1038/s41598-017-12449-6.

Hirono, M., Watanabe, S., Karube, F., Fujiyama, F., Kawahara, S., Nagao, S., Yanagawa, Y. and Misonou, H. (2018) 'Perineuronal nets in the deep cerebellar nuclei regulate GABAergic transmission and delay eyeblink conditioning', *The Journal of neuroscience : the official journal of the Society for Neuroscience*, 38(27), pp. 6130–6144. doi:10.1523/JNEUROSCI.3238-17.2018.

Hori, M., Nakamachi, T., Shibato, J., Rakwal, R., Shioda, S. and Numazawa, S. (2015) 'Unraveling the specific ischemic core and penumbra transcriptome in the permanent middle cerebral artery occlusion mouse model brain treated with the neuropeptide PACAP38', *Microarrays*, 4(1), pp. 2–24. doi:10.3390/microarrays4010002.

Hu, H., Gan, J. and Jonas, P. (2014) 'Fast-spiking, parvalbumin^{+} GABAergic interneurons: from cellular design to microcircuit function', *Science (New York, N.Y.)*, 345(6196). doi:10.1126/SCIENCE.1255263.

Huang, E.J. and Reichardt, L.F. (2001) ‘Neurotrophins: Roles in neuronal development and function’, *Annual review of neuroscience*, 24, p. 677. doi:10.1146/ANNUREV.NEURO.24.1.677.

Huang, Z., Zhang, Y., Zhou, R., Yang, L. and Pan, H. (2021) ‘Lactate as potential mediators for exercise-induced positive effects on neuroplasticity and cerebrovascular plasticity’, *Frontiers in Physiology*, 12, p. 1006. doi:10.3389/FPHYS.2021.656455/BIBTEX.

Hübener, M. and Bonhoeffer, T. (2014) ‘Neuronal plasticity: Beyond the critical period’, *Cell*, 159(4), pp. 727–737. doi:10.1016/J.CELL.2014.10.035.

Hynds, D.L. and Snow, D.M. (1999) ‘Neurite outgrowth inhibition by chondroitin sulfate proteoglycan: Stalling/stopping exceeds turning in human neuroblastoma growth cones’, *Experimental Neurology*, 160(1), pp. 244–255. doi:10.1006/EXNR.1999.7212.

Ichiyama, R.M., Gilbert, A.B., Waldrop, T.G. and Iwamoto, G.A. (2002) ‘Changes in the exercise activation of diencephalic and brainstem cardiorespiratory areas after training’, *Brain research*, 947(2), pp. 225–233. doi:10.1016/S0006-8993(02)02929-3.

Inashima, S., Matsunaga, S., Yasuda, T. and Wada, M. (2003) ‘Effect of endurance training and acute exercise on sarcoplasmic reticulum function in rat fast- and slow-twitch skeletal muscles’, *European journal of applied physiology*, 89(2), pp. 142–149. doi:10.1007/S00421-002-0763-5.

Inatani, M., Honjo, M., Otori, Y., Oohira, A., Kido, N., Tano, N., Honda, Y. and Tanihara, H. (2001) ‘Inhibitory effects of neurocan and phosphacan on neurite outgrowth from retinal ganglion cells in culture |’, *Investigative Ophthalmology & Visual Science* , 42, pp. 1930–1938. Available at: https://iovs.arvojournals.org/article.aspx?articleid=2200013 (Accessed: 6 May 2022).

Inoue, K., Hanaoka, Y., Nishijima, T., Okamoto, M., Chang, H., Saito, T. and Soya, H. (2015) ‘Long-term mild exercise training enhances hippocampus-dependent memory in rats’, *International journal of sports medicine*, 36(4), pp. 280–285. doi:10.1055/S-0034-1390465.

Inoue, K., Okamoto, M., Shibato, J., Lee, M.C., Matsui, T., Rakwal, R. and Soya, H. (2015) ‘Long-term mild, rather than intense, exercise enhances adult hippocampal neurogenesis and greatly changes the transcriptomic profile of the hippocampus’, *PloS one*, 10(6). doi:10.1371/JOURNAL.PONE.0128720.

Irvine, S.F. and Kwok, J.C.F. (2018) ‘Perineuronal nets in spinal motoneurones: Chondroitin sulphate proteoglycan around alpha motoneurones’, *International journal of molecular sciences*, 19(4). doi:10.3390/IJMS19041172.

Irving, E.A., Vinson, M., Rosin, C., Roberts, J.C., Chapman, D.M., Facci, L., Virley, D.J., Skaper, S.D., Burbidge, S.A., Walsh, F.S., Hunter, A.J. and Parsons, A.A. (2005) ‘Identification of neuroprotective properties of anti-MAG antibody: A novel approach for the treatment of stroke?’, *Journal of Cerebral Blood Flow and Metabolism*, 25(1), pp. 98–107. doi:10.1038/SJ.JCBFM.9600011.

Itano, N. and Kimata, K. (2002) ‘Mammalian hyaluronan synthases’, *IUBMB life*, 54(4), pp. 195–199. doi:10.1080/15216540214929.

Ito, Y., Oinuma, I., Katoh, H., Kaibuchi, K. and Negishi, M. (2006) ‘Sema4D/plexin-B1 activates GSK-3beta through R-Ras GAP activity, inducing growth cone collapse’, *EMBO reports*, 7(7), pp. 704–709. doi:10.1038/SJ.EMBOR.7400737.

Jessberger, S., Clark, R.E., Broadbent, N.J., Clemenson, G.D., Consiglio, A., Lie, D.C., Squire, L.R. and Gage, F.H. (2009) ‘Dentate gyrus-specific knockdown of adult neurogenesis impairs spatial and object recognition memory in adult rats’, *Learning & Memory*, 16(2), p. 147. doi:10.1101/LM.1172609.

Jiménez-Maldonado, A., Rentería, I., García-Suárez, P.C., Moncada-Jiménez, J. and Freire-Royes, L.F. (2018) ‘The impact of high-intensity interval training on brain derived neurotrophic factor in brain: A mini-review’, *Frontiers in Neuroscience*, 0(NOV), p. 839. doi:10.3389/FNINS.2018.00839.

Jones, L., Margolis, R. and Tuszynski, M. (2003) ‘The chondroitin sulfate proteoglycans neurocan, brevican, phosphacan, and versican are differentially regulated following spinal cord injury’, *Experimental neurology*, 182(2), pp. 399–411. doi:10.1016/S0014-4886(03)00087-6.

Kemi, O.J., Loennechen, J.P., Wisløff, U. and Ellingsen, Ø. (2002) ‘Intensity-controlled treadmill running in mice: cardiac and skeletal muscle hypertrophy’, *Journal of Applied Physiology*, 93(4), pp. 1301–1309. doi:10.1152/japplphysiol.00231.2002.

Kempf, A., Tews, B., Arzt, M.E., Weinmann, O., Obermair, F.J., Pernet, V., Zagrebelsky, M., Delekate, A., Iobbi, C., Zemmar, A., Ristic, Z., Gullo, M., Spies, P., Dodd, D., Gygax, D., Korte, M. and Schwab, M.E. (2014) ‘The sphingolipid receptor S1PR2 is a receptor for Nogo-A repressing synaptic plasticity’, *PLoS Biology*, 12(1), p. 1001763. doi:10.1371/JOURNAL.PBIO.1001763.

Kim, J.J. and Fanselow, M.S. (1992) ‘Modality-specific retrograde amnesia of fear’, *Science (New York, N.Y.)*, 256(5057), pp. 675–677. doi:10.1126/SCIENCE.1585183.

Kim, S.H., Kim, H.B., Jang, M.H., Lim, B.V., Kim, Y.J., Kim, Y.P., Kim, S.S., Kim, E.H. and Kim, C.J. (2002) ‘Treadmill exercise increases cell proliferation without altering of apoptosis in dentate gyrus of Sprague-Dawley rats’, *Life Sciences*, 71(11), pp. 1331–1340. doi:10.1016/S0024-3205(02)01849-0.

Kitagawa, H., Tsutsumi, K., Tone, Y. and Sugahara, K. (1997) ‘Developmental Regulation of the Sulfation Profile of Chondroitin Sulfate Chains in the Chicken Embryo Brain *’, *Journal of Biological Chemistry*, 272(50), pp. 31377–31381. doi:10.1074/JBC.272.50.31377.

Kleim, J.A., Cooper, N.R. and VandenBerg, P.M. (2002) ‘Exercise induces angiogenesis but does not alter movement representations within rat motor cortex’, *Brain research*, 934(1), pp. 1–6. doi:10.1016/S0006-8993(02)02239-4.

Kleim, J.A., Lussnig, E., Schwarz, E.R., Comery, T.A. and Greenough, W.T.

(1996) ‘Synaptogenesis and Fos expression in the motor cortex of the adult rat after motor skill learning’, *The Journal of neuroscience : the official journal of the Society for Neuroscience*, 16(14), pp. 4529–4535. doi:10.1523/JNEUROSCI.16-14-04529.1996.

Kleim, J.A., Vij, K., Ballard, D.H. and Greenough, W.T. (1997) ‘Learning-dependent synaptic modifications in the cerebellar cortex of the adult rat persist for at least four weeks’, *The Journal of neuroscience : the official journal of the Society for Neuroscience*, 17(2), pp. 717–721. doi:10.1523/JNEUROSCI.17-02-00717.1997.

Kobilo, T., Liu, Q.-R., Gandhi, K., Mughal, M., Shaham, Y. and Praag, H. van (2011) ‘Running is the neurogenic and neurotrophic stimulus in environmental enrichment’, *Learning & Memory*, 18(9), p. 605. doi:10.1101/LM.2283011.

Koch, J.C., Tatenhorst, L., Roser, A.E., Saal, K.A., Tönges, L. and Lingor, P. (2018) ‘ROCK inhibition in models of neurodegeneration and its potential for clinical translation’, *Pharmacology and Therapeutics*. Elsevier Inc., pp. 1–21. doi:10.1016/j.pharmthera.2018.03.008.

Koh, C., Pronin, S. and Hughes, M. (2018) ‘Chondroitinase ABC for neurological recovery after acute brain injury: systematic review and meta-analyses of preclinical studies’, *Brain injury*, 32(6), pp. 715–729. doi:10.1080/02699052.2018.1438665.

Kubo, H., Shibato, J., Saito, T., Ogawa, T., Rakwal, R. and Shioda, S. (2015) ‘Unraveling the rat intestine, spleen and liver genome-wide transcriptome after the oral administration of lavender oil by a two-color dye-swap DNA Microarray Approach’, *PLOS ONE*. Edited by F.J. Esteban, 10(7), p. e0129951. doi:10.1371/journal.pone.0129951.

Kubo, T., Yamaguchi, A., Iwata, N. and Yamashita, T. (2008) ‘The therapeutic effects of Rho-ROCK inhibitors on CNS disorders’, *Therapeutics and Clinical Risk Management*. Dove Press, pp. 605–615. doi:10.2147/tcrm.s2907.

Kullander, K., Croll, S.D., Zimmer, M., Pan, L., McClain, J., Hughes, V., Zabski, S., DeChiara, T.M., Klein, R., Yancopoulos, G.D. and Gale, N.W. (2001) ‘Ephrin-B3 is the midline barrier that prevents corticospinal tract axons from recrossing, allowing for unilateral motor control’, *Genes & Development*, 15(7), p. 877. doi:10.1101/GAD.868901.

Kurihara, Y. and Takei, K. (2015) ‘LOTUS, a potent blocker of nogo receptor-1 causing inhibition of axonal growth’, *Neural Regeneration Research*, 10(1), pp. 46–48. doi:10.4103/1673-5374.150652.

Kwok, J.C.F., Carulli, D. and Fawcett, J.W. (2010) ‘In vitro modeling of perineuronal nets: hyaluronan synthase and link protein are necessary for their formation and integrity’, *Journal of neurochemistry*, 114(5), pp. 1447–1459. doi:10.1111/J.1471-4159.2010.06878.X.

Kwok, J.C.F., Dick, G., Wang, D. and Fawcett, J.W. (2011) ‘Extracellular matrix and perineuronal nets in CNS repair’, *Developmental neurobiology*, 71(11), pp. 1073–1089. doi:10.1002/DNEU.20974.

Kwok, J.C.F., Warren, P. and Fawcett, J.W. (2012) ‘Chondroitin sulfate: A key

molecule in the brain matrix', *The International Journal of Biochemistry & Cell Biology*, 44(4), pp. 582–586. doi:10.1016/J.BIOCEL.2012.01.004.

De la Rosa, A., Olaso-Gonzalez, G., Arc-Chagnaud, C., Millan, F., Salvador-Pascual, A., García-Lucerga, C., Blasco-Lafarga, C., Garcia-Dominguez, E., Carretero, A., Correas, A.G., Viña, J. and Gomez-Cabrera, M.C. (2020) 'Physical exercise in the prevention and treatment of Alzheimer's disease', *Journal of sport and health science*, 9(5), pp. 394–404. doi:10.1016/J.JSHS.2020.01.004.

Lai, K.O. and Ip, N.Y. (2013) 'Structural plasticity of dendritic spines: The underlying mechanisms and its dysregulation in brain disorders', *Biochimica et Biophysica Acta - Molecular Basis of Disease*. Elsevier, pp. 2257–2263. doi:10.1016/j.bbadis.2013.08.012.

LeDoux, J.E. (2000) 'Emotion circuits in the brain', *Annual review of neuroscience*, 23, pp. 155–184. doi:10.1146/ANNUREV.NEURO.23.1.155.

Lee, J.K., Geoffroy, C.G., Chan, A.F., Tolentino, K.E., Crawford, M.J., Leal, M.A., Kang, B. and Zheng, B. (2010) 'Assessing spinal axon regeneration and sprouting in Nogo-, MAG-, and OMgp-deficient mice', *Neuron*, 66(5), pp. 663–670. doi:10.1016/J.NEURON.2010.05.002/ATTACHMENT/951340EE-3690-448E-B1AB-9F51FF4C2C6E/MMC1.PDF.

Lee, M.C., Okamoto, M., Liu, Y.F., Inoue, K., Matsui, T., Nogami, H. and Soya, H. (2012) 'Voluntary resistance running with short distance enhances spatial memory related to hippocampal BDNF signaling', *J Appl Physiol (1985)*, 113(8), pp. 1260–1266. doi:10.1152/JAPPLPHYSIOL.00869.2012.

Lehmann, M., Fournier, A., Selles-Navarro, I., Dergham, P., Sebok, A., Leclerc, N., Tigyi, G. and McKerracher, L. (1999) 'Inactivation of rho signaling pathway promotes CNS axon regeneration', *Journal of Neuroscience*, 19(17), pp. 7537–7547. doi:10.1523/JNEUROSCI.19-17-07537.1999.

Lensjø, K.K., Christensen, A.C., Tennøe, S., Fyhn, M. and Hafting, T. (2017) 'Differential expression and cell-type specificity of perineuronal nets in hippocampus, medial entorhinal cortex, and visual cortex examined in the rat and mouse', *eNeuro*, 4(3). doi:10.1523/ENEURO.0379-16.2017.

Lensjø, K.K., Lepperød, M.E., Dick, G., Hafting, T. and Fyhn, M. (2017) 'Removal of perineuronal nets unlocks juvenile plasticity through network mechanisms of decreased inhibition and increased gamma activity', *Journal of Neuroscience*, 37(5), pp. 1269–1283. doi:10.1523/JNEUROSCI.2504-16.2016.

Leuner, B. and Gould, E. (2010) 'Structural plasticity and hippocampal function', *Annual Review of Psychology*, 61, pp. 111–140. doi:10.1146/annurev.psych.093008.100359.

Lieberman, J.A., Girgis, R.R., Brucato, G., Moore, H., Provenzano, F., Kegeles, L., Javitt, D., Kantrowitz, J., Wall, M.M., Corcoran, C.M., Schobel, S.A. and Small, S.A. (2018) 'Hippocampal dysfunction in the pathophysiology of schizophrenia: a selective review and hypothesis for early detection and intervention', *Molecular Psychiatry 2018 23:8*, 23(8), pp. 1764–1772. doi:10.1038/mp.2017.249.

Liebscher, T., Schnell, L., Schnell, D., Scholl, J., Schneider, R., Gullo, M., Fouad, K., Mir, A., Rausch, M., Kindler, D., Hamers, F.P.T. and Schwab, M.E. (2005) 'Nogo-A antibody improves regeneration and locomotion of spinal cord–injured rats', *Annals of Neurology*, 58(5), pp. 706–719. doi:10.1002/ANA.20627.

Lighton, J.R.B. (2008) *Measuring metabolic rates : a manual for scientists*. Oxford University Press.

Lin, R., Rosahl, T., Whiting, P., Fawcett, J. and Kwok, J. (2011) '6-Sulphated chondroitins have a positive influence on axonal regeneration', *PloS one*, 6(7), p. 21499. doi:10.1371/JOURNAL.PONE.0021499.

Lin, T.W., Chen, S.J., Huang, T.Y., Chang, C.Y., Chuang, J.I., Wu, F. Sen, Kuo, Y.M. and Jen, C.J. (2012) 'Different types of exercise induce differential effects on neuronal adaptations and memory performance', *Neurobiology of learning and memory*, 97(1), pp. 140–147. doi:10.1016/J.NLM.2011.10.006.

Liu, B.P., Fournier, A., GrandPré, T. and Strittmatter, S.M. (2002) 'Myelin-Associated Glycoprotein as a functional ligand for the Nogo-66 receptor', *Science*, 297(5584), pp. 1190–1193. doi:10.1126/SCIENCE.1073031.

Liu, J., Gao, H. and Wang, X. (2015) 'The role of the Rho/ROCK signaling pathway in inhibiting axonal regeneration in the central nervous system', *Neural Regeneration Research*, 10(11), p. 1892. doi:10.4103/1673-5374.170325.

Liu, P.Z. and Nusslock, R. (2018) 'Exercise-mediated neurogenesis in the hippocampus via BDNF', *Frontiers in Neuroscience*. Frontiers Media S.A., p. 52. doi:10.3389/fnins.2018.00052.

Lucas, S.J.E., Cotter, J.D., Brassard, P. and Bailey, D.M. (2015) 'High-intensity interval exercise and cerebrovascular health: curiosity, cause, and consequence', *Journal of Cerebral Blood Flow & Metabolism*, 35(6), p. 902. doi:10.1038/JCBFM.2015.49.

Lueptow, L.M. (2017) 'Novel object recognition test for the investigation of learning and memory in mice', *Journal of Visualized Experiments : JoVE*, 2017(126), p. 55718. doi:10.3791/55718.

Luo, Y., Wu, X., Liu, S. and Li, K. (2011) 'Reactivation of visual cortical plasticity by NEP1-40 from early monocular deprivation in adult rats', *Neuroscience letters*, 494(3), pp. 196–201. doi:10.1016/J.NEULET.2011.03.011.

Luparini, M.R., Del Vecchio, A., Barillari, G., Magnani, M. and Prosdocimi, M. (2000) 'Cognitive impairment in old rats: a comparison of object displacement, object recognition and water maze', *Aging (Milan, Italy)*, 12(4), pp. 264–273. doi:10.1007/BF03339846.

Mabuchi, M., Murakami, S., Taguchi, T., Ohtsuka, A. and Murakami, T. (2001) 'Purkinje cells in the adult cat cerebellar cortex possess a perineuronal net of proteoglycans', *Archives of Histology and Cytology*, 64(2), pp. 203–209. doi:10.1679/AOHC.64.203.

Mahmmoud, R.R., Sase, S., Aher, Y.D., Sase, A., Gröger, M., Mokhtar, M., Höger, H. and Lubec, G. (2015) 'Spatial and working memory is linked to spine density and mushroom spines', *PLOS ONE*. Edited by G. Chapouthier, 10(10),

p. e0139739. doi:10.1371/journal.pone.0139739.

Maier, I., Ichiyama, R., Courtine, G., Schnell, L., Lavrov, I., Edgerton, V. and Schwab, M. (2009) 'Differential effects of anti-Nogo-A antibody treatment and treadmill training in rats with incomplete spinal cord injury', *Brain : a journal of neurology*, 132(Pt 6), pp. 1426–1440. doi:10.1093/BRAIN/AWP085.

Mateos-Aparicio, P. and Rodríguez-Moreno, A. (2019) 'The impact of studying brain plasticity', *Frontiers in Cellular Neuroscience*, 13, p. 66. doi:10.3389/FNCEL.2019.00066.

Matthews, R.T., Kelly, G.M., Zerillo, C.A., Gray, G., Tiemeyer, M. and Hockfield, S. (2002) 'Aggrecan glycoforms contribute to the molecular heterogeneity of perineuronal nets', *Journal of Neuroscience*, 22(17), pp. 7536–7547. doi:10.1523/jneurosci.22-17-07536.2002.

Mattson, M.P. (2008) 'Glutamate and neurotrophic factors in neuronal plasticity and disease', *Annals of the New York Academy of Sciences*, 1144, p. 97. doi:10.1196/ANNALS.1418.005.

McGee, A.W., Yang, Y., Fischer, Q.S., Daw, N.W. and Strittmatter, S.H. (2005) 'Experience-driven plasticity of visual cortex limited by myelin and nogo receptor', *Science (New York, N.Y.)*, 309(5744), p. 2222. doi:10.1126/SCIENCE.1114362.

McKeon, R.J., Jurynec, M.J. and Buck, C.R. (1999) 'The chondroitin sulfate proteoglycans neurocan and phosphacan are expressed by reactive astrocytes in the chronic CNS glial scar', *The Journal of Neuroscience*, 19(24), p. 10778. doi:10.1523/JNEUROSCI.19-24-10778.1999.

McKeon, R.J., Schreiber, R.C., Rudge, J.S. and Silver, J. (1991) 'Reduction of neurite outgrowth in a model of glial scarring following CNS injury is correlated with the expression of inhibitory molecules on reactive astrocytes', *The Journal of neuroscience : the official journal of the Society for Neuroscience*, 11(11), pp. 3398–3411. doi:10.1523/JNEUROSCI.11-11-03398.1991.

Mi, S., Lee, X., Shao, Z., Thill, G., Ji, B., Relton, J., Levesque, M., Allaire, N., Perrin, S., Sands, B., Crowell, T., Cate, R.L., McCoy, J.M. and Pepinsky, R.B. (2004) 'LINGO-1 is a component of the Nogo-66 receptor/p75 signaling complex', *Nature Neuroscience 2004 7:3*, 7(3), pp. 221–228. doi:10.1038/nn1188.

Mikami, T. and Kitagawa, H. (2013) 'Biosynthesis and function of chondroitin sulfate', *Biochimica et Biophysica Acta (BBA) - General Subjects*, 1830(10), pp. 4719–4733. doi:10.1016/J.BBAGEN.2013.06.006.

Mirzadeh, Z., Alonge, K.M., Cabrales, E., Herranz-Pérez, V., Scarlett, J.M., Brown, J.M., Hassouna, R., Matsen, M.E., Nguyen, H.T., Garcia-Verdugo, J.M., Zeltser, L.M. and Schwartz, M.W. (2019) 'Perineuronal net formation during the critical period for neuronal maturation in the hypothalamic arcuate nucleus', *Nature metabolism*, 1(2), pp. 212–221. doi:10.1038/S42255-018-0029-0.

Miyata, S., Komatsu, Y., Yoshimura, Y., Taya, C. and Kitagawa, H. (2012) 'Persistent cortical plasticity by upregulation of chondroitin 6-sulfation', *Nature neuroscience*, 15(3), pp. 414–422. doi:10.1038/NN.3023.

Monnier, P.P., Sierra, A., Schwab, J.M., Henke-Fahle, S. and Mueller, B.K. (2003) 'The Rho/ROCK pathway mediates neurite growth-inhibitory activity associated with the chondroitin sulfate proteoglycans of the CNS glial scar', *Molecular and Cellular Neuroscience*, 22(3), pp. 319–330. doi:10.1016/S1044-7431(02)00035-0.

Morawski, M., Brückner, M.K., Riederer, P., Brückner, G. and Arendt, T. (2004) 'Perineuronal nets potentially protect against oxidative stress', *Experimental neurology*, 188(2), pp. 309–315. doi:10.1016/J.EXPNEUROL.2004.04.017.

Morawski, M., Dityatev, A., Hartlage-Rübsamen, M., Blosa, M., Holzer, M., Flach, K., Pavlica, S., Dityateva, G., Dityateva, G., Brückner, G. and Schachner, M. (2014) 'Tenascin-R promotes assembly of the extracellular matrix of perineuronal nets via clustering of aggrecan', *Philosophical Transactions of the Royal Society B: Biological Sciences*, 369(1654). doi:10.1098/RSTB.2014.0046.

Moreau-Fauvarque, C., Kumanogoh, A., Camand, E., Jaillard, C., Barbin, G., Boquet, I., Love, C., Jones, Y., Kikutani, H., Lubetzki, C., Dusart, I. and Chédotal, A. (2003) 'The transmembrane semaphorin Sema4D/CD100, an inhibitor of axonal growth, is expressed on oligodendrocytes and upregulated after CNS lesion', *The Journal of neuroscience : the official journal of the Society for Neuroscience*, 23(27), pp. 9229–9239. doi:10.1523/JNEUROSCI.23-27-09229.2003.

Moser, M.B., Moser, E.I., Forrest, E., Andersen, P. and Morris, R.G. (1995) 'Spatial learning with a minislab in the dorsal hippocampus.', *Proceedings of the National Academy of Sciences of the United States of America*, 92(21), p. 9697. doi:10.1073/PNAS.92.21.9697.

Moser, M.B., Trommald, M. and Andersen, P. (1994) 'An increase in dendritic spine density on hippocampal CA1 pyramidal cells following spatial learning in adult rats suggests the formation of new synapses.', *Proceedings of the National Academy of Sciences of the United States of America*, 91(26), p. 12673. doi:10.1073/PNAS.91.26.12673.

Mueller, A., Davis, A., Carlson, S.S. and Robinson, F.R. (2014) 'N-Acetylgalactosamine positive perineuronal nets in the saccade-related-part of the cerebellar fastigial nucleus do not maintain saccade gain', *PLOS ONE*, 9(3), p. e86154. doi:10.1371/JOURNAL.PONE.0086154.

Mulherkar, S., Firozi, K., Huang, W., Uddin, M.D., Grill, R.J., Costa-Mattioli, M., Robertson, C. and Tolias, K.F. (2017) 'RhoA-ROCK inhibition reverses synaptic remodeling and motor and cognitive deficits caused by traumatic brain injury', *Scientific Reports*, 7(1), pp. 1–12. doi:10.1038/s41598-017-11113-3.

Mulherkar, S. and Tolias, K.F. (2020) 'RhoA-ROCK signaling as a therapeutic target in traumatic brain injury', *Cells*, 9(1), p. 245. doi:10.3390/cells9010245.

Naghibzadeh, M., Ranjbar, R., Tabandeh, M. and Habibi, A. (2019) 'Comparing the effect of high intensity interval training and continuous training on BDNF, GDNF and NGF in hippocampus of C57BL/6 male mice', *Journal of Shahid Sadoughi University of Medical Sciences* [Preprint]. doi:10.18502/SSU.V26I12.664.

National Research Council Committee (US) (2008) ‘Recognition and Assessment of Stress and Distress’, *The National Academies Press* [Preprint]. Available at: https://www.ncbi.nlm.nih.gov/books/NBK4033/ (Accessed: 17 December 2021).

Neeper, S.A., Gómez-Pinilla, F., Choi, J. and Cotman, C.W. (1996) ‘Physical activity increases mRNA for brain-derived neurotrophic factor and nerve growth factor in rat brain’, *Brain Research*, 726(1–2), pp. 49–56. doi:10.1016/0006-8993(96)00273-9.

Nelson, A.J., Juraska, J.M., Musch, T.I. and Iwamoto, G.A. (2005) ‘Neuroplastic adaptations to exercise: neuronal remodeling in cardiorespiratory and locomotor areas’, *Journal of applied physiology (Bethesda, Md. : 1985)*, 99(6), pp. 2312–2322. doi:10.1152/JAPPLPHYSIOL.00693.2005.

Nelson, A.J., Juraska, J.M., Ragan, B.G. and Iwamoto, G.A. (2010) ‘Effects of exercise training on dendritic morphology in the cardiorespiratory and locomotor centers of the mature rat brain’, *Journal of applied physiology (Bethesda, Md. : 1985)*, 108(6), pp. 1582–1590. doi:10.1152/JAPPLPHYSIOL.00137.2009.

Nishio, Y., Koda, M., Kitajo, K., Seto, M., Hata, K., Taniguchi, J., Moriya, H., Fujitani, M., Kubo, T. and Yamashita, T. (2006) ‘Delayed treatment with Rho-kinase inhibitor does not enhance axonal regeneration or functional recovery after spinal cord injury in rats’, *Experimental neurology*, 200(2), pp. 392–397. doi:10.1016/J.EXPNEUROL.2006.02.123.

Nokia, M.S., Lensu, S., Ahtiainen, J.P., Johansson, P.P., Koch, L.G., Britton, S.L. and Kainulainen, H. (2016) ‘Physical exercise increases adult hippocampal neurogenesis in male rats provided it is aerobic and sustained’, *The Journal of physiology*, 594(7), pp. 1855–1873. doi:10.1113/JP271552.

Nowicka, D., Soulsby, S., Skangiel-Kramska, J. and Glazewski, S. (2009) ‘Parvalbumin-containing neurons, perineuronal nets and experience-dependent plasticity in murine barrel cortex’, *The European journal of neuroscience*, 30(11), pp. 2053–2063. doi:10.1111/J.1460-9568.2009.06996.X.

O’Callaghan, R.M., Ohle, R. and Kelly, Á.M. (2007) ‘The effects of forced exercise on hippocampal plasticity in the rat: A comparison of LTP, spatial- and non-spatial learning’, *Behavioural Brain Research*, 176(2), pp. 362–366. doi:10.1016/J.BBR.2006.10.018.

Oberman, L. and Pascual-Leone, A. (2013) ‘Changes in plasticity across the lifespan: Cause of disease and target for intervention’, in *Progress in Brain Research*. Elsevier B.V., pp. 91–120. doi:10.1016/B978-0-444-63327-9.00016-3.

Oertle, T. and Schwab, M.E. (2003) ‘Nogo and its paRTNers’, *Trends in Cell Biology*, 13(4), pp. 187–194. doi:10.1016/S0962-8924(03)00035-7.

Ohtake, Y., Wong, D., Abdul-Muneer, P.M., Selzer, M.E. and Li, S. (2016) ‘Two PTP receptors mediate CSPG inhibition by convergent and divergent signaling pathways in neurons’, *Scientific Reports 2016 6:1*, 6(1), pp. 1–17. doi:10.1038/srep37152.

Oinuma, I., Ito, Y., Katoh, H. and Negishi, M. (2010) ‘Semaphorin 4D/Plexin-B1

stimulates PTEN activity through R-Ras GTPase-activating protein activity, inducing growth cone collapse in hippocampal neurons', *Journal of Biological Chemistry*, 285(36), pp. 28200–28209. doi:10.1074/JBC.M110.147546.

Okamoto, M., Mizuuchi, D., Omura, K., Lee, M., Oharazawa, A., Yook, J.S., Inoue, K. and Soya, H. (2021) 'High-intensity intermittent training enhances spatial memory and hippocampal neurogenesis associated with BDNF signaling in rats', *Cerebral Cortex*, 31(9), pp. 4386–4397. doi:10.1093/CERCOR/BHAB093.

Okaty, B.W., Miller, M.N., Sugino, K., Hempel, C.M. and Nelson, S.B. (2009) 'Transcriptional and electrophysiological maturation of neocortical fast-spiking GABAergic interneurons', *Journal of Neuroscience*, 29(21), pp. 7040–7052. doi:10.1523/JNEUROSCI.0105-09.2009.

Oliff, H.S., Berchtold, N.C., Isackson, P. and Cotman, C.W. (1998) 'Exercise-induced regulation of brain-derived neurotrophic factor (BDNF) transcripts in the rat hippocampus', *Molecular Brain Research*, 61(1–2), pp. 147–153. doi:10.1016/S0169-328X(98)00222-8.

Omotade, O.F., Pollitt, S.L. and Zheng, J.Q. (2017) 'Actin-based growth cone motility and guidance', *Molecular and Cellular Neuroscience*, 84, pp. 4–10. doi:10.1016/J.MCN.2017.03.001.

Oohira, A., Matsui, F. and Katoh-Semba, R. (1991) 'Inhibitory effects of brain chondroitin sulfate proteoglycans on neurite outgrowth from PC12D cells', *The Journal of Neuroscience*, 1(3), pp. 822–827.

Pantazopoulos, H., Markota, M., Jaquet, F., Ghosh, D., Wallin, A., Santos, A., Caterson, B. and Berretta, S. (2015) 'Aggrecan and chondroitin-6-sulfate abnormalities in schizophrenia and bipolar disorder: a postmortem study on the amygdala', *Translational Psychiatry*, 5(1), p. e496. doi:10.1038/TP.2014.128.

Park, J., Yiu, G., Kaneko, S., Wang, J., Chang, J., He, X., Garcia, K. and He, Z. (2005) 'A TNF receptor family member, TROY, is a coreceptor with Nogo receptor in mediating the inhibitory activity of myelin inhibitors', *Neuron*, 45(3), pp. 345–351. doi:10.1016/J.NEURON.2004.12.040.

Partida, E., Mironets, E., Hou, S. and Tom, V.J. (2016) 'Cardiovascular dysfunction following spinal cord injury', *Neural Regeneration Research*, 11(2), p. 189. doi:10.4103/1673-5374.177707.

Patten, A.R., Sickmann, H., Hryciw, B.N., Kucharsky, T., Parton, R., Kernick, A. and Christie, B.R. (2013) 'Long-term exercise is needed to enhance synaptic plasticity in the hippocampus', *Learning & memory (Cold Spring Harbor, N.Y.)*, 20(11), pp. 642–647. doi:10.1101/LM.030635.113.

Paxinos, G. and Watson, C. (2013) 'The rat brain in stereotaxic coordinates : Hard cover edition.', p. 466.

Pereira, A.C., Huddleston, D.E., Brickman, A.M., Sosunov, A.A., Hen, R., McKhann, G.M., Sloan, R., Gage, F.H., Brown, T.R. and Small, S.A. (2007) 'An in vivo correlate of exercise-induced neurogenesis in the adult dentate gyrus', *Proceedings of the National Academy of Sciences*, 104(13), pp. 5638–5643. doi:10.1073/PNAS.0611721104.

Piercy, K.L. and Troiano, R.P. (2018) ‘Physical activity guidelines for Americans from The US Department of Health and Human Services’, *Circulation. Cardiovascular quality and outcomes*, 11(11), p. e005263. doi:10.1161/CIRCOUTCOMES.118.005263.

Pietrelli, A., Matković, L., Vacotto, M., Lopez-Costa, J.J., Basso, N. and Brusco, A. (2018) ‘Aerobic exercise upregulates the BDNF-Serotonin systems and improves the cognitive function in rats’, *Neurobiology of Learning and Memory*, 155, pp. 528–542. doi:10.1016/J.NLM.2018.05.007.

Pignot, V., Hein, A.E., Barske, C., Wiessner, C., Walmsley, A.R., Kaupmann, K., Mayeur, H., Sommer, B., Mir, A.K. and Frentzel, S. (2003) ‘Characterization of two novel proteins, NgRH1 and NgRH2, structurally and biochemically homologous to the Nogo-66 receptor’, *Journal of Neurochemistry*, 85(3), pp. 717–728. doi:10.1046/j.1471-4159.2003.01710.x.

Pizzorusso, T., Medini, P., Berardi, N., Chierzi, S., Fawcett, J.W. and Maffei, L. (2002) ‘Reactivation of ocular dominance plasticity in the adult visual cortex’, *Science*, 298(5596), pp. 1248–1251. doi:10.1126/science.1072699.

Pothuizen, H., Zhang, W., Jongen-Rêlo, A., Feldon, J. and Yee, B. (2004) ‘Dissociation of function between the dorsal and the ventral hippocampus in spatial learning abilities of the rat: a within-subject, within-task comparison of reference and working spatial memory’, *The European journal of neuroscience*, 19(3), pp. 705–712. doi:10.1111/J.0953-816X.2004.03170.X.

Van Praag, H., Christie, B.R., Sejnowski, T.J. and Gage, F.H. (1999) ‘Running enhances neurogenesis, learning, and long-term potentiation in mice’, *Proceedings of the National Academy of Sciences of the United States of America*, 96(23), pp. 13427–13431. doi:10.1073/PNAS.96.23.13427.

van Praag, H., Dreyfus, C.F. and Black, I.B. (1994) ‘Dissociation of motor hyperactivity and spatial memory deficits by selective hippocampal lesions in the neonatal rat’, *Journal of cognitive neuroscience*, 6(4), pp. 321–331. doi:10.1162/JOCN.1994.6.4.321.

Price, M.J. and Trbovich, M. (2018) ‘Thermoregulation following spinal cord injury’, *Handbook of Clinical Neurology*, 157, pp. 799–820. doi:10.1016/B978-0-444-64074-1.00050-1.

Qin, F., Dong, Y., Wang, S., Xu, M., Wang, Z., Qu, C., Yang, Y. and Zhao, J. (2020) ‘Maximum oxygen consumption and quantification of exercise intensity in untrained male Wistar rats’, 10, p. 11520. doi:10.1038/s41598-020-68455-8.

Radahmadi, M., Hosseini, N. and Alaei, H. (2016) ‘Effect of exercise, exercise withdrawal, and continued regular exercise on excitability and long-term potentiation in the dentate gyrus of hippocampus’, *Brain research*, 1653, pp. 8–13. doi:10.1016/J.BRAINRES.2016.09.045.

Raiker, S.J., Lee, H., Baldwin, K.T., Duan, Y., Shrager, P. and Giger, R.J. (2010) ‘Oligodendrocyte-Myelin Glycoprotein and Nogo negatively regulate activity-dependent synaptic plasticity’, *Journal of Neuroscience*, 30(37), pp. 12432–12445. doi:10.1523/JNEUROSCI.0895-10.2010.

Revest, J.M., Dupret, D., Koehl, M., Funk-Reiter, C., Grosjean, N., Piazza, P. V.

and Abrous, D.N. (2009) ‘Adult hippocampal neurogenesis is involved in anxiety-related behaviors’, *Molecular Psychiatry 2009 14:10*, 14(10), pp. 959–967. doi:10.1038/mp.2009.15.

Romberg, C., Yang, S., Melani, R., Andrews, M.R., Horner, A.E., Spillantini, M.G., Bussey, T.J., Fawcett, J.W., Pizzorusso, T. and Saksida, L.M. (2013) ‘Depletion of perineuronal nets enhances recognition memory and long-term depression in the perirhinal cortex’, *Journal of Neuroscience*, 33(16), pp. 7057–7065. doi:10.1523/JNEUROSCI.6267-11.2013.

Roughley, P.J. and Mort, J.S. (2014) ‘The role of aggrecan in normal and osteoarthritic cartilage’, *Journal of Experimental Orthopaedics*, 1(1), pp. 1–11. doi:10.1186/S40634-014-0008-7.

Rowlands, D., Lensjø, K.K., Dinh, T., Yang, S., Andrews, M.R., Hafting, T., Fyhn, M., Fawcett, J.W. and Dick, G. (2018) ‘Aggrecan directs extracellular matrix-mediated neuronal plasticity’, *Journal of Neuroscience*, 38(47), pp. 10102–10113. doi:10.1523/JNEUROSCI.1122-18.2018.

Ruegsegger, G.N., Toedebusch, R.G., Childs, T.E., Grigsby, K.B. and Booth, F.W. (2017) ‘Loss of Cdk5 function in the nucleus accumbens decreases wheel running and may mediate age-related declines in voluntary physical activity’, *The Journal of Physiology*, 595(1), pp. 363–384. doi:10.1113/JP272489.

Runge, K., Cardoso, C. and de Chevigny, A. (2020) ‘Dendritic spine plasticity: function and mechanisms’, *Frontiers in Synaptic Neuroscience*, 12, p. 36. doi:10.3389/FNSYN.2020.00036/BIBTEX.

Russo-Neustadt, A.A., Alejandre, H., Garcia, C., Ivy, A.S. and Chen, M.J. (2004) ‘Hippocampal brain-derived neurotrophic factor expression following treatment with reboxetine, citalopram, and physical exercise’, *Neuropsychopharmacology*, 29, pp. 2189–2199. doi:10.1038/sj.npp.1300514.

Rynecki, N.D., Siracuse, B.L., Ippolito, J.A. and Beebe, K.S. (2019) ‘Injuries sustained during high intensity interval training: Are modern fitness trends contributing to increased injury rates?’, *Journal of Sports Medicine and Physical Fitness*, 59(7), pp. 1206–1212. doi:10.23736/S0022-4707.19.09407-6.

Sami, A., Selzer, M.E. and Li, S. (2020) ‘Advances in the signaling pathways downstream of glial-scar axon growth inhibitors’, *Frontiers in Cellular Neuroscience*. Frontiers Media S.A., p. 174. doi:10.3389/fncel.2020.00174.

Santos-Nogueira, E., Redondo Castro, E., Mancuso, R. and Navarro, X. (2012) ‘Randall-Selitto test: A new approach for the detection of neuropathic pain after spinal cord injury’, *Journal of Neurotrauma*, 29(5), p. 898. doi:10.1089/NEU.2010.1700.

Schindelin, J., Arganda-Carreras, I., Frise, E., Kaynig, V., Longair, M., Pietzsch, T., Preibisch, S., Rueden, C., Saalfeld, S., Schmid, B., Tinevez, J.-Y., White, D.J., Hartenstein, V., Eliceiri, K., Tomancak, P. and Cardona, A. (2012) ‘Fiji: an open-source platform for biological-image analysis’, *Nature Methods 2012 9:7*, 9(7), pp. 676–682. doi:10.1038/nmeth.2019.

Schluter, J.M. and Fitts, R.H. (1994) ‘Shortening velocity and ATPase activity of rat skeletal muscle fibers: effects of endurance exercise training’, *The American*

journal of physiology, 266(6 Pt 1). doi:10.1152/AJPCELL.1994.266.6.C1699.

Schmandke, Antonio, Schmandke, Andre and Schwab, M.E. (2014) 'Nogo-A: Multiple roles in CNS development, maintenance, and disease', *Neuroscientist*, 20(4), pp. 372–386. doi:10.1177/1073858413516800.

Schmidt, B., Roessler, C. and Schumann, J. (2018) 'Septic-induced microRNA expression modulations are linked to angiogenesis, vasomotion, and hypoxia-induced processes', in *Advances in Experimental Medicine and Biology*. Springer New York LLC, pp. 227–231. doi:10.1007/978-3-319-91287-5_36.

Schnaar, R.L. and Lopez, P.H.H. (2009) 'Myelin-associated glycoprotein and its axonal receptors', *Journal of Neuroscience Research*, 87(15), pp. 3267–3276. doi:10.1002/jnr.21992.

Schwab, M.E. (2010) 'Functions of Nogo proteins and their receptors in the nervous system', *Nature Publishing Group*, 11(12), pp. 799–811. doi:10.1038/nrn2936.

Scott, G.A., Terstege, D.J., Roebuck, A.J., Gorzo, K.A., Vu, A.P., Howland, J.G. and Epp, J.R. (2021) 'Adult neurogenesis mediates forgetting of multiple types of memory in the rat', *Molecular Brain*, 14(1), pp. 1–13. doi:10.1186/S13041-021-00808-4/FIGURES/4.

Seo, T.-B., Cho, H.-S., Shin, M.-S., Kim, C.-J., Ji, E.-S., Baek, S.-S., Seo, T.-B., Cho, H.-S., Shin, M.-S., Kim, C.-J., Ji, E.-S. and Baek, S.-S. (2013) 'Treadmill exercise improves behavioral outcomes and spatial learning memory through up-regulation of reelin signaling pathway in autistic rats', *Journal of Exercise Rehabilitation*, 9(2), pp. 220–229. doi:10.12965/JER.130003.

Serra, F.T., Carvalho, A.D., Araujo, B.H.S., Torres, L.B., Cardoso, F. dos S., Henrique, J.S., Placencia, E.V.D., Lent, R., Gomez-Pinilla, F., Arida, R.M. and Gomes da Silva, S. (2019) 'Early exercise induces long-lasting morphological changes in cortical and hippocampal neurons throughout of a sedentary period of rats', *Scientific Reports*, 9(1), pp. 1–11. doi:10.1038/s41598-019-50218-9.

Seymour, A., Andrews, E., Tsai, S., Markus, T., Bollnow, M., Brenneman, M., O'Brien, T., Castro, A., Schwab, M. and Kartje, G. (2005) 'Delayed treatment with monoclonal antibody IN-1 1 week after stroke results in recovery of function and corticorubral plasticity in adult rats', *Journal of cerebral blood flow and metabolism : official journal of the International Society of Cerebral Blood Flow and Metabolism*, 25(10), pp. 1366–1375. doi:10.1038/SJ.JCBFM.9600134.

Shamah, S.M., Lin, M.Z., Goldberg, J.L., Estrach, S., Sahin, M., Hu, L., Bazalakova, M., Neve, R.L., Corfas, G., Debant, A. and Greenberg, M.E. (2001) 'EphA receptors regulate growth cone dynamics through the novel guanine nucleotide exchange factor ephexin', *Cell*, 105(2), pp. 233–244. doi:10.1016/S0092-8674(01)00314-2.

Shannon, P., Markiel, A., Ozier, O., Baliga, N.S., Wang, J.T., Ramage, D., Amin, N., Schwikowski, B. and Ideker, T. (2003) 'Cytoscape: A software Environment for integrated models of biomolecular interaction networks', *Genome Research*, 13(11), pp. 2498–2504. doi:10.1101/gr.1239303.

Shi, W., Wei, X., Wang, X., Du, S., Liu, W., Song, J. and Wang, Y. (2019)

‘Perineuronal nets protect long-term memory by limiting activity-dependent inhibition from parvalbumin interneurons’, *Proceedings of the National Academy of Sciences of the United States of America*, 116(52), pp. 27063–27073. doi:10.1073/PNAS.1902680116/-/DCSUPPLEMENTAL.

Shih, P.C., Yang, Y.R. and Wang, R.Y. (2013) ‘Effects of exercise intensity on spatial memory performance and hippocampal synaptic plasticity in transient brain ischemic rats’, *PloS one*, 8(10). doi:10.1371/JOURNAL.PONE.0078163.

Sigal, Y.M., Bae, H., Bogart, L.J., Hensch, T.K. and Zhuang, X. (2019) ‘Structural maturation of cortical perineuronal nets and their perforating synapses revealed by superresolution imaging’, *Proceedings of the National Academy of Sciences of the United States of America*, 116(14), pp. 7071–7076. doi:10.1073/PNAS.1817222116/-/DCSUPPLEMENTAL.

Silva, S.G. da, Unsain, N., Mascó, D.H., Toscano-Silva, M., Amorim, H.A. de, Araújo, B.H.S., Simões, P.S.R., Naffah-Mazzacoratti, M. da G., Mortara, R.A., Scorza, F.A., Cavalheiro, E.A. and Arida, R.M. (2012) ‘Early exercise promotes positive hippocampal plasticity and improves spatial memory in the adult life of rats’, *Hippocampus*, 22(2), pp. 347–358. doi:10.1002/HIPO.20903.

Siu, P.M., Donley, D.A., Bryner, R.W. and Alway, S.E. (2003) ‘Citrate synthase expression and enzyme activity after endurance training in cardiac and skeletal muscles’, *Journal of applied physiology (Bethesda, Md. : 1985)*, 94(2), pp. 555–560. doi:10.1152/JAPPLPHYSIOL.00821.2002.

Smith, C.C., Mauricio, R., Nobre, L., Marsh, B., Wüst, R.C.I., Rossiter, H.B. and Ichiyama, R.M. (2015) ‘Differential regulation of perineuronal nets in the brain and spinal cord with exercise training’, *Brain Research Bulletin*, 111, pp. 20–26. doi:10.1016/j.brainresbull.2014.12.005.

Snow, D.M., Lemmon, V., Carrino, D.A., Caplan, A.I. and Silver, J. (1990) ‘Sulfated proteoglycans in astroglial barriers inhibit neurite outgrowth in vitro’, *Experimental neurology*, 109(1), pp. 111–130. doi:10.1016/S0014-4886(05)80013-5.

Sorg, B.A., Berretta, S., Blacktop, J.M., Fawcett, J.W., Kitagawa, H., Kwok, J.C.F. and Miquel, M. (2016) ‘Casting a wide net: Role of perineuronal nets in neural plasticity’, in *Journal of Neuroscience*. Society for Neuroscience, pp. 11459–11468. doi:10.1523/JNEUROSCI.2351-16.2016.

Sotocinal, S.G., Sorge, R.E., Zaloum, A., Tuttle, A.H., Martin, L.J., Wieskopf, J.S., Mapplebeck, J.C.S., Wei, P., Zhan, S., Zhang, S., McDougall, J.J., King, O.D. and Mogil, J.S. (2011) ‘The Rat Grimace Scale: a partially automated method for quantifying pain in the laboratory rat via facial expressions’, *Molecular pain*, 7. doi:10.1186/1744-8069-7-55.

Soya, H., Nakamura, T., Deocaris, C.C., Kimpara, A., Iimura, M., Fujikawa, T., Chang, H., McEwen, B.S. and Nishijima, T. (2007) ‘BDNF induction with mild exercise in the rat hippocampus’, *Biochemical and Biophysical Research Communications*, 358(4), pp. 961–967. doi:10.1016/J.BBRC.2007.04.173.

Spence, E.F. and Soderling, S.H. (2015) ‘Actin out: Regulation of the synaptic cytoskeleton published’, *J Biol Chem*, 290(48), pp. 28613–28622.

doi:10.1074/jbc.R115.655118.

Stankiewicz, T.R. and Linseman, D.A. (2014) ‘Rho family GTPases: Key players in neuronal development, neuronal survival, and neurodegeneration’, *Frontiers in Cellular Neuroscience*. Frontiers Media S.A. doi:10.3389/fncel.2014.00314.

Stehle, J.H., Sheng, Z., Hausmann, L., Bechstein, P., Weinmann, O., Hernesniemi, J., Neimat, J.S., Schwab, M.E. and Zemmar, A. (2021) ‘Exercise-induced Nogo-A influences rodent motor learning in a time-dependent manner’, *PLOS ONE*, 16(5), p. e0250743. doi:10.1371/JOURNAL.PONE.0250743.

Stoeckli, E.T. (2018) ‘Understanding axon guidance: Are we nearly there yet?’, *Development (Cambridge)*, 145(10). doi:10.1242/DEV.151415/48515.

Stranahan, A.M., Khalil, D. and Gould, E. (2007) ‘Running induces widespread structural alterations in the hippocampus and entorhinal cortex’, *Hippocampus*, 17(11), pp. 1017–1022. doi:10.1002/HIPO.20348.

Stuchlik, A. (2014) ‘Dynamic learning and memory, synaptic plasticity and neurogenesis: an update’, *Frontiers in Behavioral Neuroscience*, 0(APR), p. 106. doi:10.3389/FNBEH.2014.00106.

Su, W., Matsumoto, S., Sorg, B. and Sherman, L.S. (2019) ‘Distinct roles for hyaluronan in neural stem cell niches and perineuronal nets’, *Matrix Biology*, 78–79, pp. 272–283. doi:10.1016/J.MATBIO.2018.01.022.

Sumi, T., Imasaki, T., Aoki, M., Sakai, N., Nitta, E., Shirouzu, M. and Nitta, R. (2018) ‘Structural insights into the altering function of CRMP2 by phosphorylation’, *Cell Structure and Function*, 43(1), pp. 15–23. doi:10.1247/CSF.17025.

Swain, R.A., Harris, A.B., Wiener, E.C., Dutka, M. V., Morris, H.D., Theien, B.E., Konda, S., Engberg, K., Lauterbur, P.C. and Greenough, W.T. (2003) ‘Prolonged exercise induces angiogenesis and increases cerebral blood volume in primary motor cortex of the rat’, *Neuroscience*, 117(4), pp. 1037–1046. doi:10.1016/S0306-4522(02)00664-4.

Swiercz, J.M., Kuner, R., Behrens, J. and Offermanns, S. (2002) ‘Plexin-B1 directly interacts with PDZ-RhoGEF/LARG to regulate RhoA and growth cone morphology’, *Neuron*, 35(1), pp. 51–63. doi:10.1016/S0896-6273(02)00750-X.

Szklarczyk, D., Gable, A.L., Lyon, D., Junge, A., Wyder, S., Huerta-Cepas, J., Simonovic, M., Doncheva, N.T., Morris, J.H., Bork, P., Jensen, L.J. and Von Mering, C. (2019) ‘STRING v11: protein–protein association networks with increased coverage, supporting functional discovery in genome-wide experimental datasets’, *Nucleic Acids Research*, 47(D1), pp. D607–D613. doi:10.1093/NAR/GKY1131.

Takeuchi, T., Duszkiewicz, A.J. and Morris, R.G.M. (2014) ‘The synaptic plasticity and memory hypothesis: encoding, storage and persistence’, *Philosophical Transactions of the Royal Society B: Biological Sciences*, 369(1633). doi:10.1098/RSTB.2013.0288.

Tasaka, G.I., Negishi, M. and Oinuma, I. (2012) ‘Semaphorin 4D/Plexin-B1-Mediated M-Ras GAP activity regulates Actin-Based Dendrite remodeling

through lamellipodin', *Journal of Neuroscience*, 32(24), pp. 8293–8305. doi:10.1523/JNEUROSCI.0799-12.2012.

Téglás, T., Németh, Z., Koller, Á., Van der Zee, E.A., Luiten, P.G.M. and Nyakas, C. (2019) 'Effects of long-term moderate intensity exercise on ocgnitive behaviors and cholinergic forebrain in the aging rat', *Neuroscience*, 411, pp. 65–75. doi:10.1016/J.NEUROSCIENCE.2019.05.037.

Terry, A. V., Kutiyanawalla, A. and Pillai, A. (2011) 'Age-dependent alterations in nerve growth factor (NGF)-related proteins, sortilin, and learning and memory in rats', *Physiology & behavior*, 102(2), pp. 149–157. doi:10.1016/J.PHYSBEH.2010.11.005.

Thompson, E.H., Lensjø, K.K., Wigestrand, M.B., Malthe-Sørenssen, A., Hafting, T. and Fyhn, M. (2018) 'Removal of perineuronal nets disrupts recall of a remote fear memory', *Proceedings of the National Academy of Sciences of the United States of America*, 115(3), pp. 607–612. doi:10.1073/PNAS.1713530115/-/DCSUPPLEMENTAL.

Tong, L., Shen, H., Perreau, V.M., Balazs, R. and Cotman, C.W. (2001) 'Effects of exercise on gene-expression profile in the rat hippocampus', *Neurobiology of disease*, 8(6), pp. 1046–1056. doi:10.1006/NBDI.2001.0427.

Tsai, S., Papadopoulos, C., Schwab, M. and Kartje, G. (2011) 'Delayed anti-nogo-a therapy improves function after chronic stroke in adult rats', *Stroke*, 42(1), pp. 186–190. doi:10.1161/STROKEAHA.110.590083.

Ueno, H., Suemitsu, S., Okamoto, M., Matsumoto, Y. and Ishihara, T. (2017) 'Sensory experience-dependent formation of perineuronal nets and expression of Cat-315 immunoreactive components in the mouse somatosensory cortex', *Neuroscience*, 355, pp. 161–174. doi:10.1016/J.NEUROSCIENCE.2017.04.041.

van't Spijker, H.M. and Kwok, J.C.F. (2017) 'A sweet talk: The molecular systems of perineuronal nets in controlling neuronal communication', *Frontiers in Integrative Neuroscience*, 11. doi:10.3389/FNINT.2017.00033/FULL.

Vaynman, S., Ying, Z. and Gomez-Pinilla, F. (2004) 'Hippocampal BDNF mediates the efficacy of exercise on synaptic plasticity and cognition', *European Journal of Neuroscience*, 20(10), pp. 2580–2590. doi:10.1111/J.1460-9568.2004.03720.X.

Vaynman, S., Ying, Z. and Gómez-Pinilla, F. (2004) 'Exercise induces BDNF and synapsin I to specific hippocampal subfields', *Journal of Neuroscience Research*, 76(3), pp. 356–362. doi:10.1002/JNR.20077.

Venkatesh, K., Chivatakarn, O., Lee, H., Joshi, P.S., Kantor, D.B., Newman, B.A., Mage, R., Rader, C. and Giger, R.J. (2005) 'The Nogo-66 receptor Homolog NgR2 is a sialic acid-dependent receptor selective for Myelin-Associated Glycoprotein', *Journal of Neuroscience*, 25(4), pp. 808–822. doi:10.1523/JNEUROSCI.4464-04.2005.

Vigelsø, A., Andersen, N.B. and Dela, F. (2014) 'The relationship between skeletal muscle mitochondrial citrate synthase activity and whole body oxygen uptake adaptations in response to exercise training', *International Journal of*

Physiology, Pathophysiology and Pharmacology, 6(2), p. 84. Available at: /pmc/articles/PMC4106645/ (Accessed: 22 November 2021).

Vitellaro-Zuccarello, L., Bosisio, P., Mazzetti, S., Monti, C. and De Biasi, S. (2007) 'Differential expression of several molecules of the extracellular matrix in functionally and developmentally distinct regions of rat spinal cord', *Cell and Tissue Research*, 327(3), pp. 433–447. doi:10.1007/s00441-006-0289-y.

De Vivo, L., Landi, S., Panniello, M., Baroncelli, L., Chierzi, S., Mariotti, L., Spolidoro, M., Pizzorusso, T., Maffei, L. and Ratto, G.M. (2013) 'Extracellular matrix inhibits structural and functional plasticity of dendritic spines in the adult visual cortex', *Nature Communications 2013 4:1*, 4(1), pp. 1–10. doi:10.1038/ncomms2491.

Wang, F., Liang, Z., Hou, Q., Xing, S., Ling, L., He, M., Pei, Z. and Zeng, J. (2007) 'Nogo-A is involved in secondary axonal degeneration of thalamus in hypertensive rats with focal cortical infarction', *Neuroscience letters*, 417(3), pp. 255–260. doi:10.1016/J.NEULET.2007.02.080.

Wang, H., Katagiri, Y., McCann, T.E., Unsworth, E., Goldsmith, P., Yu, Z.X., Tan, F., Santiago, L., Mills, E.M., Wang, Y., Symes, A.J. and Geller, H.M. (2008) 'Chondroitin-4-sulfation negatively regulates axonal guidance and growth', *Journal of Cell Science*, 121(18), pp. 3083–3091. doi:10.1242/jcs.032649.

Wang, K., Koprivica, V., Kim, J., Sivasankaran, R., Guo, Y., Neve, R. and He, Z. (2002) 'Oligodendrocyte-myelin glycoprotein is a Nogo receptor ligand that inhibits neurite outgrowth', *Nature*, 417(6892), pp. 941–944. doi:10.1038/NATURE00867.

Wen, T.H., Binder, D.K., Ethell, I.M. and Razak, K.A. (2018) 'The perineuronal "safety" net? Perineuronal net abnormalities in neurological disorders', *Frontiers in Molecular Neuroscience*, 11, p. 270. doi:10.3389/FNMOL.2018.00270.

Wills, Z.P., Mandel-Brehm, C., Mardinly, A.R., Mccord, A.E., Giger, R.J. and Greenberg, M.E. (2012) 'The nogo receptor family restricts synapse number in the developing hippocampus', *Neuron*, 73(3), pp. 466–481. doi:10.1016/j.neuron.2011.11.029.

Winters, B.D., Forwood, S.E., Cowell, R.A., Saksida, L.M. and Bussey, T.J. (2004) 'Double dissociation between the effects of peri-postrhinal cortex and hippocampal lesions on tests of object recognition and spatial memory: heterogeneity of function within the temporal lobe', *The Journal of Neuroscience*, 24(26), pp. 5901–5908. doi:10.1523/JNEUROSCI.1346-04.2004.

Woolfrey, K.M. and Srivastava, D.P. (2016) 'Control of dendritic spine morphological and functional plasticity by small GTPases', *Neural Plasticity* [Preprint]. Hindawi Limited. doi:10.1155/2016/3025948.

Wu, Y., Deng, F., Wang, J., Liu, Y., Zhou, W., Qu, L. and Cheng, M. (2020) 'Intensity-dependent effects of consecutive treadmill exercise on spatial learning and memory through the p-CREB/BDNF/NMDAR signaling in hippocampus', *Behavioural Brain Research*, 386, p. 112599. doi:10.1016/J.BBR.2020.112599.

Xu, J., He, J., He, H., Peng, R. and Xi, J. (2017) 'Comparison of RNAi NgR and

NEP1-40 in acting on axonal regeneration after spinal cord injury in rat models', *Molecular neurobiology*, 54(10), pp. 8321–8331. doi:10.1007/S12035-016-0315-3.

Yamada, J. and Jinno, S. (2015) 'Subclass-specific formation of perineuronal nets around parvalbumin-expressing GABAergic neurons in Ammon's horn of the mouse hippocampus', *Journal of Comparative Neurology*, 523(5), pp. 790–804. doi:10.1002/CNE.23712/FORMAT/PDF.

Yamada, J. and Jinno, S. (2017) 'Molecular heterogeneity of aggrecan-based perineuronal nets around five subclasses of parvalbumin-expressing neurons in the mouse hippocampus', *The Journal of comparative neurology*, 525(5), pp. 1234–1249. doi:10.1002/CNE.24132.

Yamada, K. and Nabeshima, T. (2003) 'Brain-derived neurotrophic factor/TrkB signaling in memory processes', *Journal of pharmacological sciences*, 91(4), pp. 267–270. doi:10.1254/JPHS.91.267.

Yamaguchi, Y. (2000) 'Lecticans: Organizers of the brain extracellular matrix', *Cellular and Molecular Life Sciences*, 57(2), pp. 276–289. doi:10.1007/PL00000690.

Yang, S., Cacquevel, M., Saksida, L.M., Bussey, T.J., Schneider, B.L., Aebischer, P., Melani, R., Pizzorusso, T., Fawcett, J.W. and Spillantini, M.G. (2015) 'Perineuronal net digestion with chondroitinase restores memory in mice with tau pathology', *Experimental Neurology*, 265, pp. 48–58. doi:10.1016/J.EXPNEUROL.2014.11.013.

Yang, S., Gigout, S., Molinaro, A., Naito-Matsui, Y., Hilton, S., Foscarin, S., Nieuwenhuis, B., Tan, C.L., Verhaagen, J., Pizzorusso, T., Saksida, L.M., Bussey, T.M., Kitagawa, H., Kwok, J.C.F. and Fawcett, J.W. (2021) 'Chondroitin 6-sulphate is required for neuroplasticity and memory in ageing', *Molecular Psychiatry 2021*, pp. 1–11. doi:10.1038/s41380-021-01208-9.

Yang, S., Hilton, S., Alves, J.N., Saksida, L.M., Bussey, T., Matthews, R.T., Kitagawa, H., Spillantini, M.G., Kwok, J.C.F. and Fawcett, J.W. (2017) 'Antibody recognizing 4-sulfated chondroitin sulfate proteoglycans restores memory in tauopathy-induced neurodegeneration', *Neurobiology of aging*, 59, pp. 197–209. doi:10.1016/J.NEUROBIOLAGING.2017.08.002.

Yang, Y. and Wang, J.Z. (2017) 'From structure to behavior in basolateral amygdala-hippocampus circuits', *Frontiers in Neural Circuits*, 11. doi:10.3389/FNCIR.2017.00086.

Yook, J.S., Shibato, J., Rakwal, R. and Soya, H. (2016) 'DNA microarray-based experimental strategy for trustworthy expression profiling of the hippocampal genes by astaxanthin supplementation in adult mouse', *Genomics Data*, 7, pp. 32–37. doi:10.1016/j.gdata.2015.11.001.

Yukawa, T. *et al.* (2018) 'Pathological alterations of chondroitin sulfate moiety in postmortem hippocampus of patients with schizophrenia', *Psychiatry research*, 270, pp. 940–946. doi:10.1016/J.PSYCHRES.2018.10.062.

Zhang, Q.W., Deng, X.X., Sun, X., Xu, J.X. and Sun, F.Y. (2013) 'Exercise promotes axon regeneration of newborn striatonigral and corticonigral projection

neurons in rats after ischemic stroke', *PLoS ONE*, 8(11). doi:10.1371/journal.pone.0080139.